Barrett's Oesophagus - studies of novel optical diagnostic tools and minimally invasive therapies

Jason Mark Dunn

A thesis submitted for the degree of Doctor of Philosophy (Ph.D.)

2011

National Medical Laser Centre

Department of Surgery

University College London

For Katherine and Olivia

In loving memory of my parents,

June and Henry

STATEMENT OF ORIGINALITY

I, Jason Mark Dunn, confirm that the work presented in this thesis is my own. Any contribution made to the research by colleagues, with whom I have worked at UCL or elsewhere during my candidature, is fully acknowledged. Specifically in Chapter 9 section 1, patients enrolled into the PDT trial before October 2007 were treated by my predecessor, Dr GD Mackenzie, and have been reported on in a previous interim analysis.

I declare that this is a true copy of my thesis, including any final revisions, as approved by my thesis committee and the Graduate Studies office, and that this thesis has not been submitted for a higher degree to any other University or Institution.

Abstract

Dysplasia arising in Barrett's oesophagus (BO) confers risk of progression to oesophageal adenocarcinoma (OAC), but it is variable and confounded by sampling error and diagnostic inter-observer variability. There is a need for biomarkers to accurately define risk and guide surveillance and treatment strategies. Oesophagectomy is the preferred treatment of high grade dysplasia (HGD), although this has been challenged by the emergence of endoscopic therapy.

This thesis has shown image cytometric DNA ploidy analysis (ICDA) is accurate when compared to flow cytometry. In a multi centre biomarker validation study, ICDA predicted cancer risk in non dysplastic BO. ICDA also predicted relapse following photodynamic therapy (PDT).

Nucleotyping (NT) is an imaging technique that evaluates textural changes of nuclei, which correlate with chromatin content and organisation. In this thesis NT was demonstrated to yield additional diagnostic information over ICDA alone, and the combination was highly accurate for dysplasia classification.

In an experiment evaluating replication licensing factors in OAC, those representing the S-G2-M phases of the cell cycle correlated with aneuploidy. Polo like kinase 1 upregulation had the strongest correlation, the first time this has been shown in BO.

Elastic scattering spectroscopy detected DNA ploidy abnormalities with equal accuracy using a standard or near infra-red enhanced spectrometer. In a prospective *in vivo* surveillance study, fewer biopsies were taken without a change in the diagnostic yield for dysplasia. A field carcinogenesis effect was also demonstrated, independent of both dysplasia and DNA ploidy abnormalities.

Finally, in a randomised control trial of PDT for HGD, patients with BO less than 7cm had significantly higher efficacy and better tolerability with ALA than photofrin. Radiofrequency ablation was shown to be a safe and effective rescue therapy for patients that failed PDT.

In summary these studies advance our understanding of biomedical optics for the risk stratification and treatment of Barrett's oesophagus.

Table of Contents

List of Figures

List of Tables

List of Abbreviations

4D-ELF	4-Dimensional Elastic Light-Scattering Fingerprinting	**IOD**	Integrated Optical Density
a/LCI	Angle resolved Low Coherence Interferometry	**IQR**	Inter Quartile Range
AFI	Autofluorescence Imaging	**ITT**	Intention To Treat
AFS	Autofluorescence Spectroscopy	**LEBS**	Low-coherence Enhanced Backscattering Spectroscopy
AGA	American Society of Gastroenterology	**LDA**	Liner Discrimant Analysis
ALA	5-aminolaevulinic acid	**LGD**	Low Grade Dysplasia
ALT	Alanine transaminase	**LI**	Labelling Index
APC	Argon Plasma Coagulation	**LIFE**	Light Induced Fluorescence Endoscopy
AUC	Area Under Curve	**LOH**	Loss Of Heterozygosity
BMI	Body Mass Index	**LSS**	Light Scattering Spectrosopy
BO	Barrett's Oesophagus	**MAb**	Monoclonal Antibody
BSG	British Society of Gastroenterology	**MBDB**	Methylene Blue Directed Biopsy
CCD	Charge Coupled Device	**Mcm**	Mini Chromosome Maintenance Protein
CCR	Correct Classification Rate	**MHz**	Mega Herz
CE	Conformite Europeene	**MPEC**	Multipolar Electrocoagulation
CI	Confidence Interval	**mTHPC**	m-tetrahydroxyphenyl chlorin
CIN	Chromosomal Instability	**NAD(P)H**	nicotinamide adenine dinucleotide phosphate
CLE	Confocal Laser Endomicroscopy	**NBI**	Narrow Band Imaging
CLO	Columnar Lined Oesophagus	**Nd:YAG**	Neodymium-doped Yttrium Aluminium Garnet
COX	Cyclo-oxygenase	**NICE**	National Institute For Clinical Excellence
CV	Coefficient of Variance	**NF-kB**	Nuclear Factor kappa B
DI	DNA Index	**NPV**	Negative Predictive Value
DNA	Deoxyribonucleic acid	**NSAID**	Non-Steroidal Anti-Inflammatory Drug

EIBS	Early increase in blood supply	**NT**	Nucleotyping
ELISA	Enzyme-linked immunosorbent assay	**OAC**	Oesophageal Adenocarcinoma
EMR	Endoscopic Mucosal Resection	**OCT**	Optical Coherence Tomography
ESD	Endoscopic Submucosal Dissection	**OFDI**	Optical Frequency Domain Imaging
ESS	Elastic Scattering Spectroscopy	**OR**	Odds Ratio
ETMI	Endoscopic Trimodal Imaging	**PBS**	Phosphate Buffered Saline
EUS	Endoscopic Ultrasound	**PCA**	Principal Component Analysis
FC	Flow Cytometry	**PCR**	Polymerase Chain Reaction
FFPE	Formalin Fixed Paraffin Embedded	**PDT**	Photodynamic Therapy
FISH	Fluorescence insitu hybridization	**PLK**	Polo Like Kinase
FTIR	Fourier transform infrared	**PPI**	Proton Pump Inhibitor
GI	Gastro-intestinal	**PPV**	Positive Predictive Value
GLCM	Grey Level Co-occurrence Matrix	**QALY**	Quality Adjusted Life Year
GLEM	Grey Level Entropy Matrix	**RCT**	Randomised Controlled Trial
GOJ	Gastro-oesophageal junction	**REC**	Research Ethics Committee
GORD	Gastro-oesophageal reflux disease	**RFA**	Radiofrequency Ablation
HD	High Definition	**RLF**	DNA Replication Licensing Factor
HER-2	Human Epidermal growth factor Receptor 2	**RNA**	Ribonucleic acid
HGD	High Grade Dysplasia	**ROC**	Receiver Operator Curve
HR	Hazard Ratio	**RR**	Relative Risk
ICDA	Image cytometric DNA ploidy analysis	**SIM**	Specialised Intestinal Metaplasia
IHC	Immunohistochemistry	**TEM**	Transmission Electron Micrograph
IMC	Intramucosal cancer	**UV**	Ultraviolet
IND	Indefinite for dysplasia	**WLE**	White Light Endoscopy

Acknowledgements

Firstly I would to thank my supervisors, Laurence Lovat and Steve Bown. I have learnt so much under their tutorage and they have inspired me to continue an academic career. They have both given a lot of time and energy to help me bring three years of research to fruition, and hopefully Steve can now retire happy that one more got through!

In the histopathology department Marco Novelli, 'the third supervisor', has had a major influence on the content of this thesis and the direction my research has taken. I will miss our meetings in his office discussing the finer points of molecular biology and road bikes. Thank you to Dahmane, a brilliant 'green fingered' scientist who has helped me in the understanding and practical execution of the majority of laboratory methods in this thesis.

This work would not have been possible without a great deal of collaboration. Thank you to Havard Danielsen and the team at Oslo University, Peter Rabinovitch for ensuring such a pleasant and rewarding time in his laboratory in Seattle, Stuart McDonald for teaching me laser capture microdissection and for the use of facilities at LRI and the MRC study group, in particular Rebecca Fitzgerald.

At the Laser centre I would like to thank Martin Austwick, Sandy Mosse, Ying Zhu and Yan Jiao, all of whom had a major role in the PDT and ESS projects. Warm thanks go to Sarah Green and Faith Hanstater for their tireless help with all things administrative. A big thank you to Sally Thorpe who has been a great help to me throughout my time at UCL, both in my clinical research work and personally. Thanks also to Matthew Banks and Louise Langmead for clinical support.

My biggest thank you is for my family, Katherine and Olivia. When I first started this journey Olivia was not born, and her arrival changed everything. She is the happy smile after a bad day, a cuddle after a failed experiment, a big kiss after a rejected paper. She puts everything in perspective. None of that would be possible without my darling wife Katherine, who keeps everything together. This thesis is for both of you.

Chapter 1 –
Barrett’s columnar lined oesophagus

Chapter 1 Barrett's columnar lined oesophagus

1.1 Barrett's oesophagus and adenocarcinoma of the oesophagus

Adenocarcinoma of the oesophagus is a deadly disease with a 5 year survival of less than 15%.[Polednak, 2003] Its incidence is increasing rapidly in the West with a 350% increase in the USA over the last 20 years [Devesa et al., 1998], and a similar increase in the U.K.[Reed, 1991;Steevens et al., 2010] Data from the U.S.A National Cancer Institute estimates that the incidence of oesophageal cancer in the general population (all races, both sexes, all ages) is approximately 5 per 100,000. Cancer statistics from Thames Registry show this rate to be higher in England and Wales, 12.8 per 100,000 in men and 5.7 per 100,000 in women.[Newnham et al., 2003]. The most striking rise is in Scotland, with an estimated percentage change in incidence rates from 1977 to 1996 of 140%. [Brewster et al., 2000] Patients are often not candidates for surgery due to late presentation and death is usually caused by malnutrition due to dysphagia and pneumonia.

Barrett's oesophagus (BO) is a change in the oesophageal epithelium in which any portion of the normal squamous lining has been replaced by a metaplastic columnar epithelium which is visible macroscopically by endoscopy. This condition is of great importance as it represents a pre-invasive precursor lesion to oesophageal adenocarcinoma (OAC). It is thought that 64-86% of all adenocarcinomas arise in Barrett's oesophagus.[Hamilton et al., 1988;Cameron et al., 1995] A recent systematic review of 47 studies of patients undergoing surveillance endoscopy for BO showed that the overall attributable risk of adenocarcinoma was 6.1 cases per 1,000 person-years (0.61 percent per year).[Yousef et al., 2008] A UK based study of 1,677 patients demonstrated a similar attributable risk of 4.4 per 1,000 person-years. [Solaymani-Dodaran et al., 2005] Overall the incidence of OAC for patients with BO appears to be increased 30-100 fold above that for the general population.[Sharma et al., 2009a;Solaymani-Dodaran et al., 2005] The prevalence of BO is estimated at 1.6% of the general population,[Ronkainen et al., 2005] and it is found in approximately 10% of

patients with gastro-oesophageal reflux disease or heartburn and up to 20% of patients undergoing endoscopy for oesophagitis.

1.2 History of Barrett's oesophagus

In 1950 Norman Barrett, a British surgeon, described the columnar lined oesophagus that now bears his name. The disorder had, however, been described 50 years previously by a Boston pathologist named Tileston who described patients with peptic ulcer of the oesophagus and noted 'the close resemblance of the mucous membrane about the ulcer to that normally found in the stomach'.[Tileston, 1906] Later investigators, including Barrett himself, argued that the ulcerated columnar line segment was not oesophagus at all, rather a tubular segment of stomach that had been pulled up into the chest due to a congenitally short squamous oesophagus.

It was Bosher and Taylor, in 1951, who first described the intestinal type goblet cells in a columnar lined oesophagus 'but no parietal cells', which we now refer to as specialised intestinal metaplasia (SIM).[Bosher and Taylor, 1951] Two years later Allison and Johnstone linked the association of gastro-oesophageal reflux disease (GORD) and columnar lined oesophagus (CLO).[Allison and Johnstone, 1953] Barrett agreed that the columnar lined organ was oesophagus and suggested the condition be called lower oesophagus lined by columnar epithelium. He also recognised the association with hiatal hernia and severe reflux oesophagitis, though maintained the condition was congenital.[Barrett, 1957] By the 1970s it was clear that CLO was associated with severe GORD. [Naef et al., 1975;Borrie and Goldwater, 1976]

1.3 Risk of Barrett's oesophagus and cancer progression - Epidemiological studies

It has been shown that SIM arising in BO is a risk factor for progression to cancer, though this risk varies. The effectiveness of surveillance programmes on risk reduction is often called into question when assessing cost-effectiveness and overall affect on cancer mortality, as the overall mortality rates of patients with BO from other causes is said to be similar to the general population. Evidence from large scale epidemiological studies that attempt to quantify risk is, however, conflicting.

In 1989 van deer Even and colleagues reported on 166 patients with BO and over 4.4 years of follow up, and found that survival was not different to an age and sex matched population.[Van, V et al., 1989] These data have since been re-evaluated, with a mean follow up of 9.3 years, and an excess mortality of 50% was reported when compared with those of an age and sex matched control population.[van der et al., 1996] Eckardt *et al.* reported that the estimated 10 year survival of patients with long segment BO was similar to that of the general population.[Eckardt et al., 2001] None of these studies was population based.

Perhaps the largest population based study is from the Northern Ireland Barrett's Oesophagus Registry (NIBR), an ethnically similar group (Caucasian) with low rates of emigration reducing loss to follow up.[Murray et al., 2003] Between 1993 and 1999, 4955 oesophageal biopsies (from 2969 patients) met criteria for BO, defined as the presence of columnar metaplasia in the oesophagus irrespective of whether Barrett's mucosa was reported. The mean follow up was 3.7 years (range 1 to 8), with 11 068 person years of follow up. Oesophageal cancer rates were 0.26% a year overall, and 0.4% a year for patients with SIM. The malignancy rate in men was 2.5 times that in women. Men older then 70 with SIM had an increased incidence of cancer, greater than 1% per year, but 2/3 of cancers occurred in the group aged less than 70.

An interesting study by Sontag and colleagues [Sontag et al., 1985] reported an increased incidence of colonic tumours in patients with BO, leading to the often versed view that a patient with BO is more likely to die from colorectal cancer than OAC. More recent studies have refuted this view and have found that there is no association between colorectal tumours and BO.[Cook et al., 2007;Murray et al., 2003;Laitakari et al., 1995]

1.3.1 Sex distribution

Several studies have shown that the rate of progression to OAC is significantly higher in men and occurs at an earlier age. In an analysis of 5317 BO patients, as part of the UK Barrett's Oesophagus Registry (UKBOR), Caygill *et al.* reported a mean age at diagnosis of 62 years in males and 67.5 years in females. Rates of OAC showed a similar trend,

mean ages at diagnosis being 64.7 years in males and 74.0 years in females.[Caygill et al., 2004] Murray *et al.* showed males were on average younger than females at diagnosis of BO: 58.2 years versus 63.9 years ($p<0.001$).[Anderson et al., 2003] The annual rate of diagnosis of BO between 1993 and 1999 in this study was 4 per 1000 males and 2 per 1000 females.

A more recent study by McColl's group in Scotland has demonstrated a lag time for the development of OAC between males and females.[Derakhshan et al., 2009] The crude incidence rate of intestinal subtype upper GI adenocarcinoma was higher in males, at 23.86 per 100,000 person-years, versus females, at 9.00 per 100,000 person-years, resulting in an male: female ratio of 2.65. The gender effect expressed as male: female incidence ratio varied with age: 3.41 at age less than 50, rising to 7.86 at age 50–59 years, with a progressive decrease with a minimum of 2.29 at age group 80 years and over. In contrast, the male: female ratio of diffuse subtype cancer was 0.89 at age less than 50 and did not show any significant changes with increasing age. Using curve fitting the authors concluded that the gender phenomenon is due to the development of the intestinal subtype of cancer being delayed by 17.3 years in females. It is unclear why this is. The authors argue that the delay is occurring at age less than 55 years, which makes it likely to be related to an endogenous protective effect associated with the reproductive years in the female. The female sex hormone oestrogen is known to suppress the inflammatory response and cytokine production in certain tissues and might be exerting similar effects in the upper GI tract. In addition, females have lower body iron stores during their reproductive years and this might modify the degree of DNA damage arising from chronic inflammation.

1.3.2 Reflux symptoms

There have been few population based studies on the interaction between reflux symptoms and cancer progression. Perhaps the largest was from Sweden, with information on 1349 patients with a history of gastro-oesophageal reflux collected in personal interviews. [Lagergren et al., 1999a] From this group 189 had OAC, 262 had adenocarcinoma of the cardia, 167 patients had oesophageal squamous-cell carcinoma and 820 were control subjects from the general population. Among persons with

recurrent symptoms of reflux, as compared with persons without such symptoms, the odds ratios were 7.7 (95% CI, 5.3 to 11.4) for OAC. This risk increased with the duration and severity of symptoms. Subjects with severe reflux symptoms of more than 20 years had an odds ratio for OAC of 43.5 (95% CI, 18.3 to 103.5) as compared with asymptomatic persons. The risk of oesophageal squamous-cell carcinoma was not associated with reflux (odds ratio, 1.1; 95% CI, 0.7 to 1.9). These data were adjusted for tobacco smoking, body-mass index and other possible confounders, though none had a serious influence on the risk estimates.

1.3.3 Obesity

Obesity (defined by the World Health Organisation as a body mass index (BMI) >30) has been found to be a risk factor for OAC in several epidemiological case control studies.[Lagergren et al., 1999b;Chow et al., 1998;MacInnis et al., 2006;Hampel et al., 2005;Merry et al., 2007] In other case control studies, however, no association was found between BMI and the risk of either adenocarcinoma of the oesophagus or the gastric cardia.[Corley et al., 2007] These studies are limited by confounding bias due to a significant association between high BMI and symptoms of GORD. Compared with those with a BMI < 25, the risk of reflux is increased among severely obese (BMI > 35) men (OR = 3.3; 95% CI 2.4-4.7) and women (OR = 6.3; 95% CI 4.9–8.0).[Nilsson et al., 2003] More recent large scale population based studies strongly indicate that there is a true and dose dependent association between increasing BMI and risk of OAC, independent of reflux.[Lagergren, 2005;Jacobson et al., 2009]

1.3.4 Length of Barrett's segment

To avoid the problems of false positive diagnosis, investigators in the early 1980s established arbitrary criteria for the length of the columnar lined oesophagus. In a study on risk of progression by Skinner *et al* only patients with more than 3cm BO were included,[Skinner et al., 1983] and this has now come to be accepted as long segment BO (LSBO), with ≤3cm as short segment BO (SSBO). But are there any differences between the two groups? Both were predominantly white male and middle aged as described earlier. The duration of reflux symptoms has been shown to be greater in patients with LSBO compared to SSBO.[Oberg et al., 1999] It also appears that the pathophysiological

abnormalities seen in patients with SSBO falls somewhere between LSBO and uncomplicated GORD. Loughney *et al* found that lower oesophageal sphincter pressure was lower in SSBO than controls, but higher than LSBO.[Loughney et al., 1998] Distal acid exposure time for SSBO was also somewhere between controls and LSBO.

Weston *et al* reported significant differences in the prevalence of both dysplasia and OAC between SSBO and LSBO, 8.1% *versus* 24.4% for dysplasia and 0% *versus* 15.4% for OAC.[Weston et al., 1997] A comprehensive prospective study of 889 consecutive patients undergoing endoscopy by Hirota *et al.,* separated subjects into 4 groups; reference/control group; patients having intestinal metaplasia of the cardia; SSBO ;LSBO.[Hirota et al., 1999] The prevalence of dysplasia and cancer together was significantly different between the four patient subgroups, 0%, 6.4%, 10%, and 31%, respectively.

The term ultra short segment BO (USSBO) has been defined as specialised intestinal metaplasia at the GOJ, when there is less than 1cm of circumferential columnar lined mucosa. This diagnosis is controversial, because it is indistinguishable from IM of the Cardia, which differs in aetiology, pathogenesis, natural history and importantly, neoplastic potential. [Morales et al., 2000;Sharma et al., 2000;Csendes et al., 2002] IM of the cardia is also common, occurring in 9-36% of patients with GORD. [Spechler et al., 1994;Goldstein, 2000] The pattern of cytokeratin 7 and cytokeratin 20 staining has been postulated to help differentiate the two conditions.[Ormsby et al., 2000] This CK7/20 staining pattern consists of diffuse strong CK7 staining of the surface and glandular epithelium, and weak staining of columnar epithelium by CK20. Other investigators have, however, failed to consistently reproduce these findings.[Glickman et al., 2005;Mohammed et al., 2002] One interesting study suggested that the combination of MUC 1 and MUC 6 staining was 90% specific for detection of goblet cells related to BO rather than goblet cells from IM of the Cardia. [Glickman et al., 2003] There remains controversy about taking biopsies from below the GOJ to look for IM of the cardia, as this may lead to the incorrect labelling of a patient as having BO, with subsequent impact on the patients' life including lifelong surveillance, difficulty in obtaining insurance and

associated worry regarding risk of cancer progression. Accurate documentation of the endoscopic appearances of the columnar lined oesophagus is therefore vitally important in establishing a reliable diagnosis.

Prague C & M Criteria

To further accurately document the nature of Barrett's CLO the International Working Group for Classification of Oesophagitis (IWGCO) developed the Prague C&M criteria.[Sharma et al., 2006c] This scoring system is based on the circumferential (C value, in cm) and the maximal extent (M value, in cm) of BO above the gastro-oesophageal junction (GOJ). For example, if BO was circumferential for 2 cm above the GOJ and the maximal extent of non-circumferential BO was 5 cm (i.e., with 3 cm of BO "tongues") above the GOJ, this would be recorded as C2M5. The consensus group in this study decided that 'true islands of squamous and columnar mucosa should not influence the measurement of extent of BO and that only segments of contiguous BO are measured'. The proposed scoring system was validated in a study using 29 digital recordings of endoscopies. Internal validation yielded a high reliability coefficient value for agreement on the presence of BO >1 cm (r =0.72).

The diagnostic criteria for BO have evolved over the past century and will continue to do so as researchers and pathologists debate the relative merits of classification according to pathology and endoscopic findings. Other markers of risk stratification are necessary to reduce variation in the approach to the management of patients with Barrett's oesophagus.

1.4 The importance of Specialised Intestinal Metaplasia

Metaplasia is the replacement of one tissue by another in two different ways – either by a switch of developmental commitment (so called true metaplasia) or by colonisation with cells of a different origin.[Slack, 1986] They arise in epithelial renewal tissues when there is chronic tissue regeneration occasioned by trauma, infection or abnormal stimulation. Different theories have been proposed for the origin of metaplasia in BO: proximal migration of the gastric cardia; re-differentiation of the squamous epithelium

and colonisation of cells from the oesophageal gland ducts.[Leedham et al., 2008] The histogenesis of BO remains unknown.

The histological features of CLO demonstrate a multitude of different cellular types - the characteristic intestinal mucosa, cardiac type mucosa and fundic type mucosa. Intestinal type epithelium or specialised SIM is the most common type encountered in BO.[Flejou and Svrcek, 2007] Morphologically, it frequently shows a villiform pattern. The epithelium is composed mainly of goblet cells interspersed between intermediate mucous cells, both in the surface and glandular epithelium. (See figure 1.1)

Figure 1.1 Haemotoxylin and eosin stain of specialized intestinal metaplasia
(courtesy of Professor Novelli)

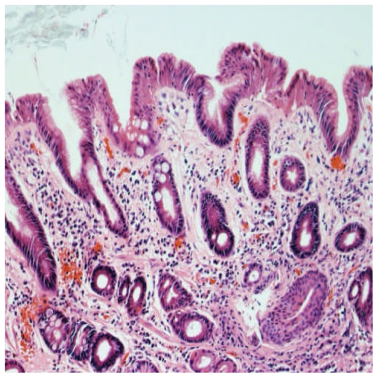

By the late 1980s it became apparent that SIM was the specific epithelial type that predisposes to OAC.[Reid et al., 1988] Indeed, the American College of Gastroenterology has published guidelines that propose 'Barrett's oesophagus is a change in the oesophageal epithelium that can be recognised at endoscopy and is confirmed to have SIM by biopsy'. The insistence that intestinal metaplasia with goblet cells is necessary to establish the diagnosis of BO is not a view shared by UK pathologists or gastroenterologists, who suggest that SIM may be present but just 'missed' by the sampling error of random biopsies. In a study evaluating 1646 biopsies from 125 patients with long segment BO, 8 biopsies was the minimum required for the reliable detection of goblet cells in BO, with a yield in 68% of endoscopies, in contrast to 35% if only 4 were taken.[Harrison et al., 2007] Adherence to four quadrant 2cm biopsy sampling has been demonstrated to be poor in clinical practice, as demonstrated by a review of the 2245 BO

surveillance cases from the CARIS database, with adherence rate of 51%.[Abrams et al., 2009] Non-adherence was associated with significantly decreased dysplasia detection with an OR = 0.53, 95% CI 0.35-0.82.

There is increasing evidence that CLO in the absence of goblet cells has at least the same neoplastic potential as SIM and should be included in the Barrett's population. A UK study demonstrated no significant difference in the future cancer risk of 712 patients followed up for a median of 12 years irrespective of the presence of SIM. The adenocarcinoma rates were 4.5% (17/379) in the group with SIM and 3.6% (11/309) in the group with CLO only.[Kelty et al., 2007] A chromosomal analysis study of non-dysplastic BO (NDBO) demonstrated chromosomal gains were more frequent in CLO in the absence of goblet cells than in SIM. [Chaves et al., 2007] In a separate study DNA content abnormalities were shown to occur with equal frequency and extent in metaplastic columnar epithelium of the oesophagus without goblet cells compared with metaplastic columnar epithelium with goblet cells. [Liu et al., 2009b] The recent BSG guidelines therefore suggest an alternative proposal to replace the term Barrett's oesophagus with CLO, and classify according to the presence or absence of intestinal metaplasia. [Watson et al., 2007]

1.5 Metaplasia-Dysplasia-Carcinoma Sequence

Barrett's adenocarcinoma develops through a multistep process with progressive worsening of a precursor lesion called 'dysplasia'. Dysplasia is a purely morphological term, and has been defined by *Riddell et al.* as 'an unequivocal neoplastic epithelium strictly confined within the basement membrane of the gland from which it arises'.[Riddell et al., 1983] Although this definition was initially proposed for premalignant changes which can develop in inflammatory bowel disease, it has been progressively extended to the entire gastrointestinal tract, including BO.[Schmidt et al., 1985] There are two types of classification system; a three tiered system grading dysplasia mild, moderate or severe; the more commonly used modified Vienna classification system, as shown below in Figure 1.2.[Schlemper et al., 2000b;Schlemper et al., 2000a] The three-tiered classification, although still in use in some centres, is

obsolete because it creates more intra- and inter-observer variability than the Vienna classification.[Flejou and Svrcek, 2007]

Figure 1.2 Modified Vienna classification

Category 1	No neoplasia
Category 2	Indefinite for neoplasia
Category 3	Low-grade adenoma/dysplasia
Category 4	High-grade neoplasia
4.1	High-grade adenoma/dysplasia
4.2	Noninvasive carcinoma (carcinoma in situ)
4.3	Suspicion for invasive carcinoma
4.4	Intramucosal carcinoma
Category 5	Submucosal invasive carcinoma (carcinoma with invasion of the submucosa or deeper)

1.5.1 High grade dysplasia

High grade dysplasia (HGD) is characterised by architectural changes which include increased budding, branching, and crowding, villiform surface configuration, and the presence of intraluminal bridges or papillae. Cytological features of HGD include marked nuclear pleomorphism (i.e., variation in nuclear size and shape), loss of polarity (i.e., loss of normal nuclear orientation, in which the long axis of the nucleus is perpendicular to the basement membrane and basally oriented), and full-thickness nuclear stratification. (see figure 1.3) Mitotic figures, especially atypical ones, are often present and may involve the surface epithelium. [Bellizzi and Odze, 2010]

Figure 1.3 Haemotoxylin and eosin stain of high grade dysplasia

(Courtesy of Professor Novelli- Left x100, right x400)

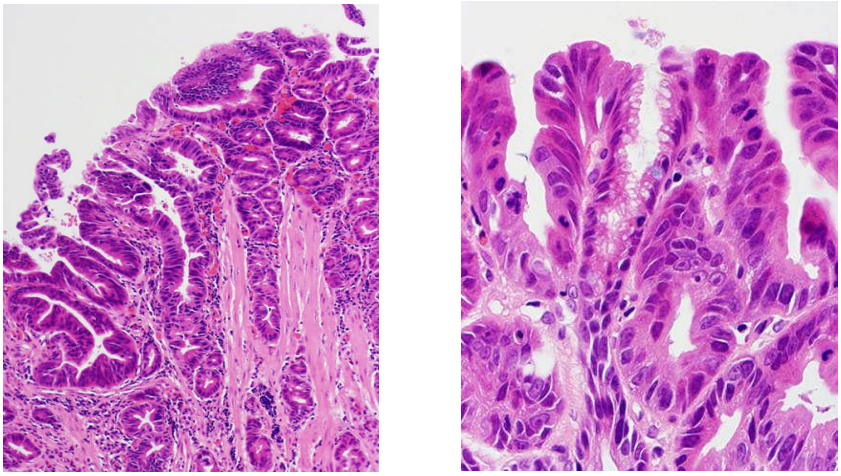

HGD is at present the most robust routinely used clinical marker of cancer progression in BO; its presence confers a 16-59% risk of developing cancer within 5 years of the diagnosis of HGD.[Montgomery et al., 2001;Schnell et al., 2001;Reid et al., 2000b;Buttar et al., 2001b] It is likely that the figures of 59% reported by Reid *et al* and 56% by Buttar *et al* are more representative of the actual risk. The lower figure of 16% in Schnell's study may be related to several observations -

a) The biopsy protocol of Reid and colleagues was every 1cm vs. every 2cm by Schnell and colleagues
b) Four of the patients with HGD on first endoscopy who were found to have invasive cancer during the first year of surveillance were excluded from further analysis
c) The patient group is different from others reported. It included both prevalent and inception cohorts with no description of HGD extent.

It is generally accepted that a diagnosis of HGD is an indication for treatment.[Playford, 2006] The conventional therapy for HGD in BO is oesophagectomy due to the high risk of developing cancer and the belief that up to 40% of patients may already harbour occult cancer in the Barrett's segment.[Fernando et al., 2002] The BSG guidelines recommend that 'all columnar-lined oesophagus should be resected. Extensive lymphadenectomy is not necessary, if there is no invasive cancer. Referral to a specialist oesophageal surgeon and centre is important: the mortality of the procedure must be less than 5%.' These recommendations are for patients deemed to have a low operative risk.

For those with high operative risk the BSG recommends minimally invasive endoscopic therapy. Several minimally invasive ablative treatments for BO have been studied, and shown to be effective in eradicating HGD and reducing the risk of progression to cancer. Two randomised controlled trials (RCT) have demonstrated a reduction in cancer risk, from 28 to 13% at 5 years follow up using photofrin photodynamic therapy (PDT) [Overholt et al., 2005] and 9% to 2% at 1 year follow up using radiofrequency ablation (RFA).[Shaheen et al., 2009a] This has led to the approval of photofrin PDT and RFA by the National Institute of Clinical Excellence in the UK (in 2006 and 2010 respectively)

for the treatment of HGD arising in BO. Since the BSG guidelines were published there has been a paradigm shift in the use of these minimally invasive therapies for HGD, and the question of whether they should be offered to all patients with HGD, as a first line treatment, is the subject of great debate.

1.5.2 Low grade dysplasia

Low grade dysplasia (LGD) is characterized by crypts with relative preservation of simple glandular architecture. Epithelial cell nuclei are oval or elongated and generally retain polarity. The nuclei are hyperchromatic with mild irregularity of nuclear membrane contour. Nuclear stratification is present and usually occupies the lower half of the thickness of the epithelium; full-thickness stratification is not present (see figure 1.4). Other features include mucin depletion, decreased number of goblet cells, and increased epithelial mitotic figures. Importantly, there is lack of maturation at the surface such that these changes are present on surface epithelium.

Figure 1.4 Haemotoxylin and eosin stain of low grade dysplasia

(Courtesy of Professor Novelli – the sharp cut off between normal and atypia favours dysplasia)

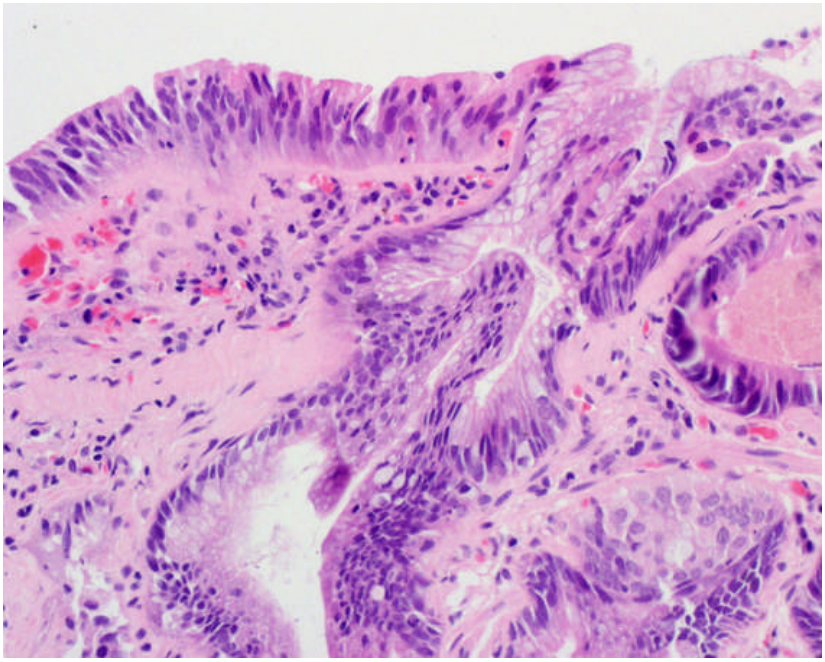

Less is known about the natural history of LGD, with risk of progression to cancer varying between 0.6-13.4% per patient year in surveillance cohorts (see table 1.1).[Reid et al., 2000b;Weston et al., 2001;Skacel et al., 2000;Sharma et al., 2006b;Lim et al., 2007;Gatenby et al., 2009;Wani et al., 2009;Curvers et al., 2010] This compares to 0.3-0.6% for NDBO.[Sharma et al., 2006b;Wani et al., 2009] One of the explanations could be the high degree of interobserver variability in establishing this diagnosis between pathologists.[Kerkhof et al., 2007;Lovat et al., 2006] Skacel *et al*. reported that when two or more histopathologists agree on a diagnosis of LGD, the risk of HGD/OAC progression increases.[Skacel et al., 2000] Seven out of 43 patients developed neoplasia with a single pathologist reporting LGD, if two agreed the risk rose to 41% (7/17) and if all three agreed there was an 80% risk (4/5). These conclusions were drawn from a relatively small number of patients with LGD.

Table 1.1 Risk of developing cancer/high grade dysplasia per patient year with low grade dysplasia

Study	Number patients	Risk of cancer	Risk of HGD	Comments
Reid[Reid et al., 2000b]	43	2.4%		Increased risk with aneuploidy
Weston[Weston et al., 2001]	54	3%		
Skacel [Skacel et al., 2000]	43	3.7%	12.9%	
Sharma [Sharma et al., 2006b]	156	0.6%		
Lim [Lim et al., 2007]	34	3.4%		
Gatenby [Gatenby et al., 2009]	217	2.7%	4.6%	Reduced to 1.4% & 2.2% when prevalent cases excluded
Wani [Wani et al., 2009]	611	1.7%		(meta-analysis)
Curvers [Curvers et al.,2010] (downstaged)	92	0.49%		Unclear how many were prevalent HGD/OAC
Curvers (consensus)	19	13.4%		

A recent study by Curvers *et al* confirms the importance of consensus diagnosis for the management of LGD.[Curvers et al., 2010] Biopsies from 147 patients with LGD diagnosed at a local hospital were reviewed by two expert GI pathologists. After review 85% of the patients were downstaged to non-dysplastic BO (NDBO) or indefinite for dysplasia. In only 15% of the patients was the initial diagnosis confirmed as LGD. After a mean 51 months follow up, patients with a consensus diagnosis of LGD had a higher incidence rate of HGD or OAC than those downstaged to NDBO (13.4% vs 0.49% per patient per year). These findings need validation in larger prospective studies.

The uncertainty of the risk of cancer has led to great debate about the advantages and disadvantages of treating low grade dysplasia, particularly with the advent of minimally invasive endoscopic therapies. There is an argument that ablation of LGD is more cost effective than surveillance, with models demonstrating a 65% reduction in progression if complete reversal of dysplasia (CR-D) is achieved in 28%.[Inadomi et al., 2009] A noteworthy feature of LGD that is not included in these models is the phenomenon of regression. This is demonstrated in the recent RCT of RFA versus a sham procedure, when 23% of patients achieved spontaneous regression of low grade dysplasia in the control group.[Shaheen et al., 2009a] This is most likely related to sampling error, the interobserver variability among pathologists, misdiagnosis, removal of the dysplastic focus by biopsy, and perhaps even true regression of the dysplastic area. At the present time the BSG recommends that a diagnosis of LGD should warrant close follow-up, with endoscopy every six months.[Playford, 2006] This approach has been shown to increase detection of HGD/OAC in a registry setting.[Ramus et al., 2009]

1.6 Screening and surveillance

1.6.1 Screening

The most recent guidelines from the American College of Gastroenterology advise upper gastrointestinal (UGI) endoscopy for patients with longstanding GORD for the detection of BO, although a recent update states that screening for BO remains controversial because of the lack of documented impact on mortality from adenocarcinoma.[Wang and

Sampliner, 2008] Conversely, the BSG guidelines suggest that 'endoscopic screening of patients with chronic heartburn to detect columnar lined esophagus cannot be recommended, due to a lack of directly applicable studies'.

A contributing factor to the difficulty of applying UGI endoscopy as a screening tool is the lack of an easily identifiable patient group. Although GORD is thought to be essential to the pathogenesis of BO, there is a lack of evidence that symptomatic GORD is predictive of BO incidence. In a study of 300 patients referred for colonoscopy, the prevalence of BO and associated GORD symptoms was evaluated.[Ward et al., 2006] Overall 106/300 patients (35%) reported GORD symptoms. BO was present in 50 of the 300 patients (16.7%) and there was no significant difference in GORD symptoms, 21/50 were symptomatic and 29/50 asymptomatic.

Another study evaluated patients who had a diagnosis of erosive reflux disease at baseline endoscopy and followed them up to ascertain subsequent incidence of BO.[Modiano and Gerson, 2009] Of 102 patients identified 9 developed BO, and all nine had severe oesophagitis of Savary-Miller grade 4 (erosive lesion[s] complicated by ulceration or stricture) at their baseline endoscopy. These patients were referred for dysphagia (n=3) or upper GI bleeding (n=6). None of the patients who were referred for initial endoscopic assessment due to reflux symptoms developed BO after a mean follow up of 25 months.

A study by the same group evaluated 515 GORD patients (412 with no erosive disease on endoscopy, 103 with oesophagitis) and 169 BO patients.[Stoltey et al., 2007] None of the 412 GORD patients with non-erosive reflux disease developed BO over a mean follow-up time of 3.4 ± 2.2 years. In the group with oesophagitis 5/103 developed subsequent BO. In the BO group no patient had a normal endoscopy at baseline.

These studies present two interesting observations. The first is the presence of severe oesophagitis, in particular grade 4 disease that provokes spontaneous GI bleed, is a significant risk factor for subsequent BO, either because the severity of mucosal damage

is more likely to heal by metaplastic columnar epithelium or because the columnar epithelium is already present but not visualised. The second observation, that symptomatic GORD without erosive disease (non erosive reflux disease) is not predictive of future BO incidence, is interesting although follow up was short, and confounding variables such as smoking status or PPI usage were not addressed in a multivariate analysis.

Even if a patient group that were at high risk of BO could be identified, the cost of endoscopy based screening techniques and patient acceptability limit the feasibility of screening. This has led to the assessment of new technologies for screening that are applicable to an outpatient clinic setting

Unsedated transnasal endoscopy

With the introduction of high-quality, small-caliber endoscopes with an outer diameter of less than 6 mm, the use of unsedated UGI endoscopy as a screening tool has recently become feasible. This technique can be carried out in an outpatient setting, removes the need for sedation and has been shown to be acceptable to patients undergoing surveillance.[Murata et al., 2007] Several types of transnasal endoscope are available with four-directional or two-directional angulation of the tip. When biopsies are taken, the availability of four-way angulation has been shown to decrease examination time while not significantly altering tolerability.[Tatsumi et al., 2008] Paediatric biopsy forceps are necessary due to the smaller size of the working channel, which limits the size of biopsy taken. In a small comparative study of 32 patients however, there was no significant difference between the histological diagnosis of IM or dysplasia between the two techniques, despite the smaller biopsy size.[Saeian et al., 2002]

In a feasibility study, Jobe *et al* evaluated unsedated small-calibre UGI endoscopy and conventional endoscopy in a randomised crossover design. Of 121 patients who were referred for either screening of reflux symptoms or surveillance, 26% had BO using conventional endoscopy vs. 30% using unsedated endoscopy (p=0.50). The level of agreement between the two approaches was "moderate" (kappa value = 0.59) and

diagnostic yield for LGD was similar, though only one patient had HGD. The majority of patients (71%) preferred unsedated small-calibre endoscopy. However, despite the advantages of this technique, availability has not been shown to increase the referral pattern for screening.[Atkinson et al., 2008] At present the use of this promising screening tool remains in a research setting.

Wireless capsule endoscopy

Given Imaging were the first to introduce wireless capsule endoscopy (WCE) (M2A, Given Imaging Ltd, Yoqneam, Israel), a device that has revolutionised imaging of the small bowel. Soon after this a capsule designed for oesophageal use was released, the latest model being PillCam ESO2. The ESO capsules differs from the small bowel capsule in having viewing heads at both ends of the capsule, which can obtain a total of 18 frames per second, as opposed to 4 frames per second with the M2A capsule. To slow oesophageal transit and maximise image capture time, the protocol generally involves swallowing the capsule recumbent in the right lateral position aided by taking sips of water through a straw.

Studies on the utility of WCE as a screening tool for BO have followed. Lin *et al.* evaluated 90 patients, 66 screening patients with GORD and 24 surveillance patients with BO, using WCE with PillCam ESO capsule.[Lin et al., 2007] This study demonstrated a moderate sensitivity and specificity for the detection of BO, 67% and 84% respectively. The average number of frames in which all four quadrants were visible and the presence of bubbles were significant factors in missing the diagnosis of BO. In a similar study by Sharma *et al.*, a total of 94 patients (41 screening patients with GORD symptoms and 53 known BO under surveillance) had screening with Pillcam ESO.[Sharma et al., 2008] The sensitivity and specificity were again moderate, 78 and 75% respectively. A recent meta-analysis that evaluated nine studies, comprising a total of 618 patients, demonstrated a pooled sensitivity and specificity of WCE for the diagnosis of BO were 77 and 86 % respectively.[Bhardwaj et al., 2009] WCE was found to be safe and had a high rate of patient preference.

A major drawback for the use of WCE is the rapid transit time through the oesophagus which may lead to inadequate imaging of the oesophageal mucosa and GOJ. A new approach of string-capsule endoscopy (SCE) using the M2A capsule has been piloted in a feasibility study of 50 patients with BO.[Ramirez et al., 2005] Strings were attached to the capsule allowing operator dependent control of the probe and acquisition of multiple images around the region of interest at the squamo-columnar junction. All patients were correctly diagnosed by WCE (mean Barrett's length of 4.47 cm), confirmed by subsequent UGI endoscopy. The procedure was safe and better tolerated by patients than UGI endoscopy using a simple questionnaire. In addition the probe could be disinfected allowing for multiple uses.

The same group of investigators subsequently conducted a prospective blinded study of 100 consecutive patients with GORD symptoms who were referred for screening of BO.[Ramirez et al., 2008] In the study, 46 patients had endoscopic evidence of BO and 27 were confirmed by presence of SIM (21 with short segment, six with long segment). The sensitivity, specificity and observed accuracy of SCE for BO when using endoscopic diagnosis as the criterion standard, was again moderate at 78%, 83% and 84% respectively. Of the 16 patients misclassified 10 were false negatives, all of whom had SSBO at UGI endoscopy.

Other approaches to externally control the capsule by creating a locomotion or propulsion mechanism include external magnets, electrostimulation, hydrojets, shape memory alloy coils, and Micro-Electro-Mechanical Systems (MEMS) based modular actuators.[Sharma, 2009] A major disadvantage of using WCE, is the inability to collect tissue samples. Although pilot studies have demonstrated the feasibility of performing mucosal biopsies using a spring loaded Crosby capsule, no trials have been published to date.

In summary, WCE has many inherent advantages over endoscopy as a screening tool because it is minimally invasive, safe, well tolerated by patients and it can be carried out in a nurse led clinic setting. Despite these advantages, on current evidence the diagnostic

accuracy of WCE is not sufficiently high to warrant use as a primary screening tool, and the inability to collect tissue samples make this impractical for Barrett's surveillance. Further technological advances in the design of WCE that can allow for fluid aspiration, brushings for cytology, multimodal spectroscopic imaging and immunological cancer recognition may address these limitations.

Capsule sponge

A non-endoscopic capsule sponge device for screening in BO has been recently developed in the UK. This was first tested in the Transkei region of South Africa in the 1980s for the screening of squamous dysplasia.[Jaskiewicz et al., 1987] The device consists of a polyurethane sponge, contained within a gelatin capsule, which is attached to a string. The capsule is swallowed and dissolves within the stomach after 3–5 min. The sponge can then be retrieved by pulling on the string. In a pilot study of 92 patients (40 BO, 52 controls) the sponge was found to be acceptable and safe.[Lao-Sirieix et al., 2007] The group evaluated mcm2 (a cell cycle marker of proliferation) on cytological nuclear monolayers and showed a sensitivity and specificity for BO of 67%. In a follow up study DNA microarray analysis was undertaken after paraffin embedding of the cytology specimens and serial sectioning.[Lao-Sirieix et al., 2009] Trefoil factor 3 (TFF3) was identified as the most promising candidate marker for the presence of IM arising in BO, with a sensitivity of 78% and specificity of 94%. A prospective cohort study of 504 patients was published recently.[Kadri et al., 2010] The sponge was swallowed by 99% of patients and no serious adverse events occurred. The prevalence of Barrett's oesophagus in this cohort (defined as presence of ≥1cm of CLO with IM) was 3%. The sensitivity of the sponge using TFF3 for the detection of BO was 73.3% (95% CI, 44.9%-92.2%). For a cut off of ≥2 cm sensitivity increased to 90.0% (95% CI, 55.5%-99.7%). These initial results are promising and warrant further study.

1.6.2 Surveillance

The rationale of surveillance is the detection of OAC at an early stage when the prognosis is much more favourable,[Wang and Sampliner, 2008;Playford, 2006] although there is only partial scientific validation to support this view and the value of surveillance is still subject to considerable debate. A four quadrant biopsy protocol (the 'Seattle'

protocol) consisting of jumbo forceps biopsies from every 2cm of columnar mucosa, was first proposed for surveillance of patients with BO in 1993,[Levine et al., 1993] and national guidelines of many countries recommend this protocol every 2-3 years as standard. There are some observational data to suggest that patients enrolled in surveillance programmes have OAC detected at an earlier stage than non surveillance detected cancers, with subsequent improved survival.[Corley et al., 2002;Dulai, 2002;Incarbone et al., 2002] A recent report from the UKBOR cohort on 817 patients, demonstrated a large proportion of dysplastic disease (>90%) was detected on specific surveillance endoscopies, though variation in surveillance practice for BO was observed throughout the UK.[Ramus et al., 2009] A study by Abela *et al.* showed that there was a 13 fold increase in detection of prevalent dysplasia between patients who underwent four quadrant biopsies every 2cm (median biopsy number; 16) compared to those who had non-systematic biopsies (median biopsy number; 4). [Abela et al., 2008]

Decision analytic models have suggested that BO surveillance every two years costs less than £25,000/ life-year saved.[Inadomi et al., 2003;Sonnenberg et al., 2002] Contradictory evidence was presented in a recent model completed by PenTAG, who found that surveillance was not cost-effective, with a cost/QALY of approximately £125,000.[Somerville et al., 2008] Cost effectiveness analysis of surveillance programmes are dependent on the prevalence of BO, incremental detection rate of dysplasia by endoscopic surveillance and the risk of progression to cancer. As the risk of progression and prevalence rates are extracted form observational studies and therefore represent moderate grade evidence, this in turn makes cost effective models difficult to interpret. This has led to the conception of a large UK based multi centre randomised controlled trial, designed to answer the question of whether surveillance is worthwhile in BO (Barrett's Oesophagus surveillance study or BOSS). This study is now open to enrolment with the aim of randomising 2500 patients in a 1:1 ratio to either 2 yearly surveillance endoscopy or on demand endoscopy as symptoms dictate. The results of this trial will be eagerly awaited.

1.7 Risk stratification - biomarkers to predict disease progression

Dysplasia is an imperfect marker for assessing cancer risk in patients with BO, and therefore decision making strategies based on histology, such as treatment and surveillance intervals, are by extension also flawed and consequently have little impact on oesophageal cancer rates. Molecular biomarkers that may more accurately predict cancer progression are needed for improved risk assessment.[Reid et al., 2003] A perfect biomarker would be accurate, robust, reproducible in different tissues and inexpensive. Moreover when the abnormality was reversed then this would lead to a reduction in cancer risk.

The Early Detection Research Network of the National Cancer Institute has defined five phases of biomarker development and these are summarised below in table 1.2 [Pepe et al., 2001]. There are several key mechanisms for cancer development that can be potentially exploited for use as biomarkers, and a summary of those most comprehensively studied in Barrett's OAC will follow.

Table 1.2 Stages of biomarker development

Phase 1	Preclinical/Exploratory	The identification of potentially useful markers
Phase 2	Clinical Assay and Validation	Clinical Assay detects established disease
Phase 3	Retrospective Longitudinal	Biomarker detects disease early before it becomes clinical & a positive test is defined
Phase 4	Prospective Screening	Extent and characteristics of disease detected by the test and false positive rate identified
Phase 5	Cancer Control	Impact of screening on reducing the burden of disease on the population is quantified

1.7.1 Genomic Instability

The acquisition of genomic instability is a crucial feature in tumor development and there are at least 3 distinct pathways: chromosomal instability (CIN), microsatellite instability, and gene promoter hypermethylation.[Pino and Chung, 2010] There is a growing body of evidence that the majority of OACs arising in BO occur in association with CIN, which is characterized by widespread imbalances in chromosome number (aneuploidy/tetraploidy) and loss of heterozygosity. These karyotypic abnormalities are often associated with the accumulation of mutations in specific tumour suppressor genes and oncogenes that activate cancer initiation and progression. Whether CIN creates the fertile ground for the accumulation of these mutations, or vice versa, remains one of the great unanswered questions in cancer research.

P53 tumour suppressor gene

The p53 gene (also known as TP53) is situated on the short arm of chromosome 17 and encodes for a protein containing 393 amino acids, known as protein 53 (p53). Cellular p53 is a transcription factor that regulates the cell cycle and apoptosis and has been described as 'the guardian of the genome'.[Lane, 1992] When DNA damage occurs and p53 is functioning correctly, it leads to cell-cycle arrest to allow for DNA repair or apoptosis if the damage is excessive. P53 gene mutations are found in over 50% of tumours making this the most frequently mutated gene in human cancer. P53 mutations are present in 50%-70% of OAC (depending on the number of exons included in each study) and are generally mis-sense mutations. Their presence is associated with poor differentiation, a worse overall prognosis and increased disease recurrence.[Casson et al., 1998;Ribeiro, Jr. et al., 1998] Abnormalities of p53 are relatively early events in neoplastic progression in BO, and have been shown to develop in diploid cells prior to aneuploidy. [Galipeau et al., 1999;Blount et al., 1994]

The gold standard for measurement of p53 mutations is gene sequencing, although until recently this was expensive and not widely available. TP53 mutation can also be measured by immunohistochemistry (IHC), a relatively simple technique that is widely available in pathology laboratories, and has led to much interest for its role as a potential

biomarker in BO. In a recent case control study of 54 BO patients, 27 of whom progressed to HGD/OAC and 27 non-progressors, moderate p53 overexpression was associated with a significantly increased risk of progression with a HR of 6.5 (95% CI, 2.5-17.1).[Sikkema et al., 2009] These findings concur with a previous case–control study of 29 patients who progressed to OAC and 6 who progressed to HGD, when TP53 expression was associated with an increased risk of progression (OR = 11.7, 95% CI: 1.93 - 71.4). [Murray et al., 2006] In this study only 32% cases were TP53 positive at baseline, possibly due to underestimation of p53 mutations that do not lead to TP53 accumulation (such as frameshift mutations). TP53 IHC is also associated with inter laboratory variability and is less specific than gene sequencing.[Alsner et al., 2008] These problems make it unlikely to be used as a single platform biomarker in BO.

Loss of heterozygosity (LOH)

Loss of heterozygosity (LOH) refers to the loss of a chromosome segment after a faulty cell division, and hence the loss of the functioning genes in that lost chromosomal segment, for example p53 at the short arm (p) of chromosome 17 (17pLOH). In BO, both 17pLOH and 9p LOH (p16 gene) have shown promise as potential biomarkers to predict cancer progression. In a prospective cohort study of 256 patients, 54 patients had biopsies demonstrating 17pLOH and 202 patients had biopsies demonstrating two 17p alleles. [Reid et al., 2001] There was a significantly higher 3-year cumulative incidence of cancer in patients with 17pLOH (38% vs. 3.3%). In a subset analysis of patients who had NDBO, IND or LGD, 17pLOH was a significant predictor of progression to HGD (RR = 3.6; 95% CI = 1.3 - 10). In a further analysis of 59 patients with HGD at baseline, 17pLOH remained a significant predictor of progression to cancer at 3 years (RR = 3.0; 95% CI = 1.1 - 8.2). In these studies, 17pLOH was detected in flow cytometry-purified cells, isolated from fresh frozen tissues, which then underwent whole-genome amplification by PCR followed by genotypic analyses for LOH, techniques which are quite labor-intensive. Copy number analysis by FISH, using both FFPE tissue and cytology specimens, has been explored as an alternative technique with an equivalent specificity, but only 66% sensitivity compared to the PCR method.[Wongsurawat et al., 2006]

DNA ploidy abnormalities

Aneuploidy, defined as abnormal DNA content of the nucleus of a cell, is one of the most frequent characteristics of cancer cells that occurs in approximately 90% of solid tumours.[Weaver and Cleveland, 2006] It was Boveri, in 1914, who first hypothesised that aneuploid cells are the progenitors of tumours.[Boveri, 2008] Since then aneuploidy has been shown to have diverse effects on cell metabolism, proliferation, and immortalisation.[Williams et al., 2008] The failure of mitosis has been implicated as the major contributor to aneuploidy and chromosomal instability. The major cell cycle control mechanism that acts during mitosis is the mitotic checkpoint, also known as the spindle assembly checkpoint. The mitotic checkpoint prevents chromosome mis-segregation and aneuploidy by inhibiting the irreversible transition to anaphase until all of the replicated chromosomes have made productive attachments to spindle microtubules.[Weaver and Cleveland, 2006] Mitotic checkpoint errors, mis-segregation events (when a kinetochore attaches to both spindle poles) and spindle assembly errors producing a single spindle pole have all been reported to produce aneuploid cells. Exit from mitosis without attempting cytokinesis (or with a failed cytokinesis) produces tetraploid cells containing two centrosomes.

A large number of gene products contribute to the mitotic checkpoint response and mutations of these genes has been linked to aneuploidy, including but not limited to MAD 1 and 2, BUB1, BUBR 1 and BRCA 1&2. A study in Barrett's oesophagus has implicated HSP27, though MAD2 and BUB 1 were not correlated with aneuploidy on FISH probes for chromosomes 4 and 8.[Doak et al., 2004] Allelic loss of APC (adenomatosis polyposis coli) tumour suppressor gene and/or loss of APC protein expression has also been shown to occur early in the metaplasia-dysplasia-carcinoma sequence.[Bektas, 2000]

Supporting evidence for aneuploidy as a causative agent in cancer is its increased prevalence in pre-neoplastic tissue. FISH analysis from brush cytology specimens of gastric mucosa has shown incremental aneuploidy levels at chromosome 1 during histological progression to gastric cancer.[Williams et al., 2009] Indeed, aneuploidy is

found in cervical,[Ried et al., 1999] head and neck [Ai et al., 2001] and colonic intra-epithelial neoplasia.[Cardoso et al., 2006] In BO, aneuploidy at chromosomes 4 and 8 has been shown to be an early event in carcinogenesis, as have aneuploidy at chromosomes 7 and 17.[Doak et al., 2003;Chaves et al., 2007] Loss of the Y chromosome is commonly seen in males at the transformation of LGD to HGD.[Cestari et al., 2007] Translation of these individual chromosomal abnormalities into a clinically useful biomarker has not yet been realised.

DNA ploidy abnormalities (aneuploidy/tetraploidy), which can be measured by flow cytometry (FC), are a measure of DNA content across the whole genome rather than individual chromosomes. DNA ploidy abnormalities have been evaluated in prospective trials of patients with BO, representing phase 4 biomarker development.[Reid et al., 2000b;Reid et al., 2001;Rabinovitch et al., 2001;Galipeau et al., 2007] A landmark study by the Reid group at the University of Washington demonstrated that patients who had both HGD and aneuploidy or tetraploidy had a five year cancer risk of 66%, compared to 42% with HGD alone and 28% with DNA ploidy abnormalities alone. Patients who had no cytometric abnormality (diploid) and did not have HGD had a five year cancer risk of zero.[Reid et al., 2000b]

The same group went on to evaluate the role of a chromosomal instability panel, combining 9pLOH, 17pLOH and DNA ploidy abnormalities. [Galipeau et al., 2007]The combination of all three was a better predictor of progression to OAC than any one biomarker alone (RR = 38.7; 95% CI = 10.8–138.5; $p<0.001$). Unfortunately these markers are not used in most centres, as they require a combination of platforms that would be difficult to perform outside of specialist research centres. DNA content flow cytometry particularly is associated with inter laboratory variability, quality control issues and significant set up and running costs.[Reid et al., 1992;Alanen et al., 1989] New single platform techniques to measure chromosomal instability, such as SnP and gene chip arrays [Paulson et al., 2009], are being developed that may provide rapid throughput of FFPE material, but there accuracy and cost implications for surveillance programmes remains unclear.

1.7.2 Epigenetic changes

Epigenetic changes are another causative mechanism for genomic instability. These may be global changes such as hypomethylation or hypermethylation of DNA, changes in the histones which make up the chromatin, as well as gene specific effects.

Gene promoter Hypermethylation

Methylation of DNA cytosine residues in the gene promoter region is a common gene silencing mechanism that has been shown to occur early in tumorigenesis, and assessment of promoter methylation at CpG islands provides a novel group of potential biomarkers. Promoter methylation of specific genes BNC 2 and CDKN2A (both 9p) has been shown to occur in large areas of contiguous Barrett's epithelium early in progression to adenocarcinoma.[Sato and Meltzer, 2005] Kuester *et al.* explored the promoter hypermethylation and protein expression of the pro-apoptotic death-associated protein kinase (DAPK) in BO, and demonstrated that DAPK inactivation by promoter hypermethylation is an early event in Barrett's carcinogenesis, suggesting that DAPK might play a role in the development and progression of OAC.[Kuester et al., 2007] In a retrospective case control study, Schulmann *et al* demonstrated methylation arrays of RUNX2, HPP1 and p16 can predict progression to either HGD or adenocarcinoma in biopsies of NDBO and LGD.[Schulmann et al., 2005] The same group then applied a panel of eight methylation biomarkers in a retrospective, multicentre, double-blind validation study.[Jin et al., 2009] Using this panel progression to HGD/OAC over 2 years was associated with a high sensitivity of 90% but a low specificity of 61%.

At present the techniques for determining the methylation status of promoters are relatively complex, although higher throughput methods are being developed using pyrosequencing technology rather than the more commonly used methylation-specific PCR.[Peng et al., 2009] Validation of these techniques by gene expression at the transcript and protein level is required.

Gene expression arrays

The application of gene chip methods to the study of gene expression is a major technological advance, as only a single or several gene expressions need to be observed

for each test. This allows for high throughput identification of differentially expressed genes and the construction of differential expression profiles. The adoption of these techniques by research laboratories has been paralleled by a plethora of studies that have applied this technology for Barrett's metaplasia and adenocarcinoma, although the majority may be classed in the discovery phase. More recently there is interest in the utility of these platforms to assess Barrett's histogenesis and predict disease progression.

Initial discovery studies focused on analysing the clustering of genes by comparing different histological subtypes. Greenawalt *et al*. reported on cDNA microarrays to compare the gene expression profiles of 25 sections from BO and 38 from adenocarcinoma.[Greenawalt et al., 2007] Differentially expressed genes were identified between each of the tissue types. Comparison of gene ontologies and gene expression profiles identified gene profiles specific to OAC and BO, representing digestion, hydrolase, and transcription factor genes. A further study evaluated 51 RNAs hybridized to cDNA microarrays, comprising 24 patients with normal oesophagus, 18 with BO and 9 with OAC.[Wang et al., 2006] The expression pattern of BO was statistically more similar to OAC than to normal oesophagus, not withstanding the known histological differences between the two. The authors suggested that changes modulated at the molecular biologic level supervene earlier than histological changes, and that BO is an early intermediate stage in the process of OAC. El-Serag *et al.* found that BO gene expression clustered most closely with that of the gastric antrum and least closely with that of squamous oesophagus.[El-Serag et al., 2006] The expression of genes involved in the negative regulation of apoptosis and the inflammatory response were significantly lower in BO compared to squamous oesophagus.

These approaches offer valuable insight to the pathogenesis of BO. Translation beyond experimental work into the clinical setting may be difficult however, as they are not amenable to standard immunodiagnostic methods such as immunohistochemistry (solid tissues) or ELISA (biological fluids).

1.8 Chemoprevention for Barrett's oesophagus

Chemoprevention, the use of pharmacological techniques to reduce cancer risk, is an intense area of research interest in BO. GORD is thought to be essential for BO development and may have a role in initiating and promoting tumour development. The refluxate contains numerous noxious substances including acid, bile, pancreatic enzymes, ingested food and metabolites, which can cause acute and chronic inflammation and oxidative stress. An ideal treatment strategy for patients with BO, therefore, may be a treatment that prevented reflux and associated inflammatory change with resultant decreased progression to cancer. Consequently potential targets that have been identified for chemoprevention include acid suppression with proton pump inhibitors (PPI), bile salt manipulation and cyclo-oxegenase (COX) inhibitors.

1.8.1 Proton pump Inhibitors

The hypothesis that PPIs may reduce neoplastic progression in BO by reduction of GORD and inflammation is intuitive, yet the evidence from laboratory studies is somewhat conflicting. There is evidence that PPIs have advantageous effects on cellular proliferation,[Ouatu-Lascar et al., 1999] cell cycle control and DNA stability.[Umansky et al., 2001] Other studies have demonstrated that PPI usage, by reducing acid exposure, may increase the relative concentration of bile acid in the refluxate, leading to increased proliferation.[Kaur et al., 2000]

The majority of clinical studies on the use of PPI in BO are retrospective cohort design, with a lack of randomised controlled data and use of surrogate end points for cancer risk. A recent Australian study of 502 cancer-free BO patients reported that patients not on PPIs at the time of diagnosis were 3.4 times more likely to have higher-risk endoscopic features (e.g., ulceration, nodularity, or stricture) or LGD than patients who were on a PPI at the time of diagnosis.[Hillman et al., 2008] The same group previously reported that patients who delayed starting PPIs by 2 years or more after BO diagnosis had a subsequent five- to 20-fold increased risk for development of HGD or OAC compared with patients who started shortly after their diagnosis. [Hillman et al., 2004] In a US study of 236 patients followed for 5 years, use of a PPI after the diagnosis of BO was

independently associated with a four-fold decreased risk for development of dysplasia.[El-Serag et al., 2004] In the UK the Aspirin Esomeprazole Chemoprevention Trial (AspECT) is a large multi centre randomised controlled trial with a two by- two design, to determine the effects of high- and low-dose PPI therapy with and without low-dose aspirin. This study has recently finished recruiting 2500 patients and results are due in 2013.

A major concern regarding the long term use of PPIs is the secondary increase in serum gastrin. Increased gastrin expression has been shown to increase risk of dysplasia and cancer in Barrett's oesophagus in several studies.[Wang et al., 2010;Jansen et al., 1990] Gastrin is known to increase COX-2 expression [Abdalla et al., 2004] and induce proliferation by activation of the cholecystokinin 2 receptor.[Haigh et al., 2003;Harris et al., 2004;Obszynska et al., 2010] These experiments are complicated by the variable expression of CCKR in oesophageal tissue and the physiological effects of subtle variations in gastrin concentration. Studies using gastrin antagonists in patients with BO may soon be available for Phase II/III testing.[Jankowski et al., 2010] The risk of PPI induced hypergastrinaemia, in the presence and absence of COX-2 suppression, may be answered from the results of the AspECT trial.

Long term PPI use is also associated with side effects. *Clostridium difficile* infections have been shown to be significantly increased in patients taking long term acid suppression in 3 separate studies, and the incidence seems to be dose related. [Dial et al., 2005;Howell et al., 2010] [Linsky et al., 2010] PPI use has also been found to be associated with a small but significant increased risk of gastroenteritis,[Garcia Rodriguez et al., 2007] pulmonary infections and hip fractures,[Targownik et al., 2008;Yang et al., 2006] which was independent of bone mineral density.[Targownik et al., 2010] Although the effect is moderate, this could amount to a significant morbidity if these drugs were to be used on a large population. In light of the current evidence the BSG guidelines suggest that routine use of high-dose PPI therapy, beyond that needed for symptom relief and mucosal healing, is not recommended.

1.8.2 Bile salt manipulation

One of the major constituents of the refluxate, after acid, is bile and it has been shown that up to up to a third of patients on PPI therapy will continue to reflux bile salts. [Caldwell et al., 1995;Sontag, 1990] Bile salts can produce injury over a wide range of pH and chronic injury is dependent on the acid dissociation properties of the bile salt. Taurine-conjugated bile salts, for example, cause chronic mucosal injury when the esophageal reflux is acidic (pH 4), whereas unconjugated bile salts cause mucosal injury when the pH is neutral or alkaline.[Nehra et al., 1999] These properties are important as long-term use of PPIs, in addition to increasing the pH of the lower oesophagus, can cause bacterial colonisation of the upper gut which deconjugates bile salts.[Theisen et al., 2000] In a laboratory model, brief exposure of BO cells to bile salts, in the absence of acid, led to increased proliferation; however, a combination of bile salts and acid together inhibited cell proliferation.[Kaur and Triadafilopoulos, 2002]

Bile salts may play a role in both the initiation of tumour development and promotion of growth. Bile salts have been shown to induce DNA damage in a dose dependent but non-linear fashion.[Jenkins et al., 2007;Jenkins et al., 2008] In addition, bile salts alter cell kinetics so as to enable cells that have sustained DNA damage to resist apoptosis via activation of the NF-κB pathway.[Hormi-Carver et al., 2009] The DNA damage caused by bile salts appears to be mediated by reactive oxygen species, which may lead to the potential use of antioxidants for chemoprevention in BO.[Jenkins et al., 2007] At the present time no clinical studies of bile salt manipulation or antioxidants have been undertaken.

1.8.3 COX-2 inhibitors

COX-2 is an inducible enzyme that synthesizes prostaglandins from arachidonic acid, and has been found to be increasingly over-expressed along the metaplastic pathway to OAC. [Moons et al., 2007;Ferguson et al., 2008] Potential chemopreventative agents that block COX- 2 include aspirin, non-steroidal anti-inflammatory drugs (NSAIDs) or the more specific selective COX-2 inhibitors.

Celecoxib, a selective COX-2 inhibitor, has been studied in a phase 2b, multicentre, double-blind randomised placebo-controlled study called the Chemoprevention for Barrett's Esophagus Trial (CBET).[Heath et al., 2007] In this study 100 patients with LGD or HGD were randomised to either 48 weeks of treatment with 200mg celecoxib or placebo. No significant change in the proportion of biopsy samples with dysplasia or cancer was observed between the two treatment groups. Furthermore COX-2 expression and prostaglandin E2 levels were unaltered, suggesting that the dose of celecoxib was inadequate. A higher dose of celecoxib may not be feasible, however, due to the associated risk of cardiovascular complications. A trial of celecoxib for colon cancer prevention, found that long-term (33 months) use of higher doses (400 and 800 mg daily) demonstrated an increased cardiovascular risk compared with placebo.[Bertagnolli et al., 2006] A recent meta-analysis demonstrated an increased cardiovascular risk for celecoxib that was dose dependent, noted at daily doses of 400 mg or greater.[Kearney et al., 2006]

Non selective COX-2 inhibition with aspirin or NSAIDs is an alternative strategy for chemoprevention. The protective effect of long term aspirin or NSAID use on the risk of progression to OAC has been consistently shown in retrospective cohort and case-control studies.[Anderson et al., 2006;Farrow et al., 1998;Abnet et al., 2009;Duan et al., 2008;Sadeghi et al., 2008] A meta-analysis of observational studies evaluating both aspirin and NSAIDs suggests a protective effect for OAC, although aspirin was shown to be more effective.[Corley et al., 2003]

A study from the Reid group has shown that regular users of aspirin or other NSAIDs had a strong and significant decreased risk of progression to cancer, especially in high-risk individuals with multiple chromosomal instability markers (79% vs. 30% 10 year cumulative cancer incidence). [Galipeau et al., 2007] The inhibition of COX-2 by these agents may therefore represent a useful chemoprevention strategy that may reduce the incidence of OAC in patients at low/medium risk of progression. The safety and efficacy of this treatment strategy needs to be validated in clinical trials and at the present time there is insufficient data for chemoprevention with low dose aspirin for BO.

1.9 Summary

The effective diagnosis and treatment of BO is intrinsically linked with the goal of reduction in the incidence of oesophageal cancer. Although the relationship between BO and reflux, male gender (and to a lesser extent obesity) has been established from epidemiological a studies, a clearly defined at risk group has not been characterised. Non-endoscopic tools for population based screening have yet to reach the clinic.

Once BO is diagnosed the risk of cancer progression is highly variable. Although high grade dysplasia is the best current biomarker of cancer risk, it is often occult and may already be associated with early cancer. LGD and SIM are sub-optimal for risk assessment associated with inter-observer variability, sampling error and regression. Endoscopic surveillance programmes based on these criteria are not cost effective and their value in reducing cancer mortality is the subject of considerable debate. Evidence for chemoprevention strategies for NDBO comes mainly from cohort studies and randomised control trial data is awaited. The recommended treatment strategy for HGD in BO remains surgery, associated with significant morbidity and mortality.

Continued research in BO is needed to solve these problems. Better risk stratification may be achieved by biomarkers, such as genomic instability measured by DNA ploidy and LOH status, yet these have not been translated from the bench to the bedside. Better imaging is being explored to allow the endoscopist to target biopsy and decrease mis-diagnosis, and to enable morphological diagnosis in real time by interrogation of tissue at a cellular level. Better staging and treatment may be achieved with the advent of minimally invasive endoscopic therapy, which has been shown to reduce cancer progression in RCT. These three areas are central to the quantification and reduction of cancer risk for patients with BO.

Chapter 2
Imaging techniques for surveillance of Barrett's oesophagus

Chapter 2 Imaging techniques for surveillance of Barrett's oesophagus

2.1 Introduction

The rationale for endoscopic surveillance in patients with BO is to detect progression to cancer and to allow early intervention when the disease is curable. At least three studies have shown that surveillance appears to allow the detection of cancers at an earlier stage with improved cure rates or survival rates as a consequence.[Corley et al., 2002;Wright et al., 1996;Incarbone et al., 2002] The development of effective minimally invasive treatments to prevent OAC makes detection of future cancer risk an increasingly important goal. Currently the most important identifiable risk factor for cancer progression is dysplasia, although the development of biomarkers of genetic abnormalities is emerging to better quantify an individuals risk of cancer progression.

One limitation of all these risk factors is sampling error. White light endoscopy is not sensitive enough to detect HGD so typically the endoscopic diagnosis of BO and neoplasia arising from within a BO segment is dependent on random biopsies. The standard approach is to take one biopsy in every quadrant of the Barrett's segment every 1-2 cm and send for histopathological review.[Reid et al., 1988;Reid et al., 2000a] Even the most rigorous biopsy protocols including those using jumbo biopsy forceps survey less than 1% of the oesophageal mucosa and still miss up to one third of cases with HGD or early cancer.[Kara et al., 2005a;Kara et al., 2005c;Reid et al., 2000a;Falk et al., 1999] Because of the focal and patchy nature of intestinal metaplasia and neoplasia, novel endoscopic approaches aimed at improving current screening and surveillance strategies have been explored.

An ideal targeted surveillance technique would have the following properties

a) Ability to differentiate low and high risk areas of tissue rapidly in vivo
b) Compatible with current White light endoscopy systems
c) Minimal need for interpretation of results by endoscopist, thereby reducing inter-observer variability
d) Cost effective

e) Reduction in number of biopsies taken, and hence reduction in time of procedure and histopathology costs

The following is a summary of novel optical diagnostic tools in for BO.

2.2 White Light Endoscopy

Conventional standard definition (SD) videoendoscopes are equipped with charged-coupled device (CCD) chips that produce an image signal built up from 100,000 to 300,000 individual pixels. This technical feature, also referred to as pixel density, is important because it relates to image resolution and hence the ability to discriminate two closely approximated points. The higher the pixel density, the higher the image resolution, the more likely minute lesions will be discriminated and detected. Recent advances are the introduction of high definition (HD) endoscopes, which produce signal images with resolutions that range from 850,000 pixels to 1.25 million (Hd+ I-scan system, Pentax). The addition of HD monitors has improved resolution, from 640 pixels wide x 480 lines with SD monitors (approximately 300,000 pixels) to 1920 pixels wide x 1080 lines with HD (2.07 million pixels). To produce a true high definition image each component of the system (endoscope CCD chip, processor, monitor and cables) must be HD compatible and ideally match formats so the image may be displayed in 'native resolution', i.e without digital enhancement.

Magnification endoscopy is a relatively simple technique that enlarges the video image, usually using a movable lens controlled by the endoscopist to vary the degree of magnification. Optical zoom obtains a closer image of the target while retaining image resolution, whereas digital zoom simply moves the image closer on the display resulting in a decreased image resolution. Magnification has also seen significant improvements from 30-35x optical zoom with standard endoscopes to 150 x optical zoom with newer HD zoom endoscopes. The majority of studies on magnification endoscopy have combined its use with chromoendsocopy or Narrow band Imaging (NBI), and description of these technologies will follow below. The clinical value of HD endoscopes to improve detection of dysplasia is yet to be evaluated.

2.3 Use of dyes and chromophores

The use of chromoendoscopy in the GI tract was first described in 1977,[Tada et al., 1977] and involves the topical application of stains or pigments to improve characterization of the surface epithelium during endoscopy. There are three main types of stains that are used: absorptive stains (methylene blue, Lugol's solution, also referred to as vital staining) resulting in selective uptake, contrast stains (indigo carmine, acetic acid) resulting in enhancement of mucosal surface pattern, and reactive stains such as congo red or phenol red.[Canto, 1999] Most of the staining methods are inexpensive and rather simple as they do not require any additional technical equipment, except for a special spraying catheter. A tabulated summary of stains and their principles, taken from U Peitz *et al* is shown in Figure 2.5.[Peitz and Malfertheiner, 2002]

Figure 2.5 Stains and their principles

Principle of staining	Stain	Concentration	Structures stained	Color
Absorptive	Lugol's solution	0.5–3%, mostly 1%	Glycogen-containing nonkeratinized squamous epithelium	Brown, black
	Methylene blue	0.1–1%, mostly 0.5%	Absorptive intestinal and colonic epithelium, specialized intestinal metaplasia of the esophagus (Barrett's mucosa)	Blue
	Cresyl violet	0.2%	Gastric or colonic neoplasia	Violet
	Crystal violet	0.05%	Intestinal metaplasia, neoplasia	Violet
	Toluidine blue	1%	Nuclear DNA, neoplasia	Blue
Contrast	Indigo carmine	0.1–0.5%, mostly 0.4%	Foveolae, crypts, folds	Blue-violet
Reactive	Congo red	0.3–0.5%	Gastric secretions	Red at neutral or alkaline pH, dark-blue or black at acidic pH
	Phenol red	0.1%	Gastric secretions	Yellow at neutral or acidic pH, red at alkaline pH

2.3.1 Vital staining

Lugol's iodine

Lugol's iodine has been commonly used in the diagnosis of squamous dysplasia of the oesophagus although its use was first described by Schiller in 1932 to aid the diagnosis of cervical neoplasia. It is a brown liquid composed of iodine and potassium iodide, used at

concentrations ranging from 0.5 to 3%, mostly 1%. The normal squamous cell epithelium stains in a homogeneously brown colour, as the iodine is taken up by glycogen in nonkeratinized squamous epithelial cells. Unhealthy squamous tissue loses glycogen and these lesions do not pick up stain, referred to as unstained lesions (USLs), see figure 2.6. In the high-risk region of Linxian, China, the test increased the sensitivity for squamous cell oesophageal cancer from 62% to 96%.[Dawsey et al., 1998] Studies in BO are limited to a single study which was unable to distinguish between metaplastic Barrett's epithelium and inflammatory/erosive lesions in squamous cell epithelium at the GOJ.[Witt et al., 1994]

Figure 2.6 Lugol's iodine staining of squamous dysplasia

Left Nodule at 11o'clock and surface change from 1 to 5 o'clock.
Right After Lugol's iodine these areas are unstained. Biopsy confirmed HGD

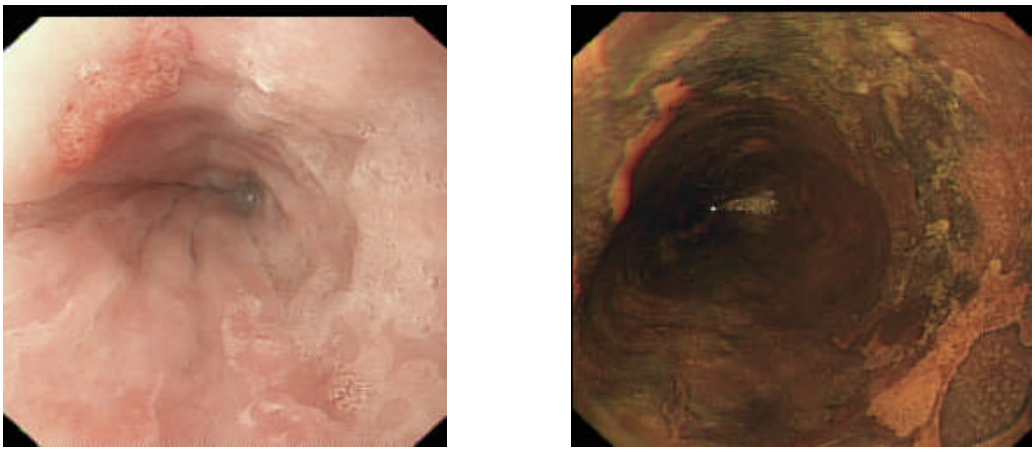

Methylene Blue

Unlike Lugol's solution, methylene blue, a thiazin dye, has been shown to selectively stain specialised intestinal metaplasia, since it is specifically absorbed by goblet cells. The technique most commonly used involves application of a mucolytic agent, typically 16 ml of 10% solution of N-acetyl cysteine for each 5 cm of circumferential BO, sprayed on the surface using a washing catheter. Then 20 mls of a 0.5% solution of methylene blue is sprayed from distal to proximal for every 5 cm of columnar epithelium. Two

minutes after the application of methylene blue, approximately 120 to 300 ml of tap water is vigorously sprayed on the oesophageal mucosa to wash off excess dye. Positive staining is defined as the presence of blue stained mucosa that persists despite vigorous water irrigation.

Methylene Blue Directed Biopsy (MBDB) was first described in Barrett's oesophagus in a pilot study by Canto *et al.*[Canto et al., 1996] They assessed 14 patients with Barrett's oesophagus and 12 control patients. Methylene blue stained specialized columnar epithelium in 18 of the 26 patients, including those with intramucosal carcinoma (1), high-grade dysplasia (1), and indefinite/low-grade dysplasia (6). The overall sensitivity of methylene blue staining for the biopsy finding of specialized intestinal metaplasia was 95%. The same group then went on to a prospective, sequence randomized, trial of MBDB vs. standard surveillance endoscopy with 2cm four quadrant biopsy.[Canto et al., 2000] Forty one patients were studied with each procedure performed by separate endoscopists within an interval of 3 to 4 weeks. The average number of biopsies was significantly lower with MBDB than 2cm quadrantic biopsy but the MBDB staining added a mean of 7 minutes (range 2 to 12 minutes) to the endoscopy procedure. Dysplasia or cancer was diagnosed in significantly more biopsy specimens (12% vs. 6%, $p = 0.004$) and patients (44% vs. 28%, $p = 0.03$) by MBDB than by random biopsy technique.

The sensitivity of MBDB for detection of SIM was confirmed by Kiesslich *et al.* in a similar study of 73 patients.[Kiesslich et al., 2001] The specificity was lower at 68% and there were too few patients with dysplasia to draw any conclusions on the value of MBDB in differentiating dysplastic from non-dysplastic tissue. Gossner *et al.* studied a group of 86 patients with histologically proven HGD or early cancer that was not visible at conventional endoscopy.[Gossner et al., 2006] Subjects went on to repeat endoscopy with quadrantic biopsies followed by MBDB. More patients were diagnosed with dysplasia/cancer by MBDB (87%) than quadrantic biopsy (65%) but this did not reach statistical significance ($p=0.053$). HGD or early cancer was diagnosed in significantly more methylene blue-directed biopsies (80.9% versus 26.4%, $P<0.005$) and also

significantly more lesions could be identified in the methylene blue group (96/98; 98%) while in the random biopsies group only 58/98 lesions (59%) could be localised ($p<0.05$).

The utility of MBDB has been questioned in a recent meta-analysis of 8 studies on MBDB from 1980 to 2007.[Ngamruengphong et al., 2009] From a total of 251 patients no significant difference was found for the sensitivity for detection of SIM; the yield of MBDB was 75% versus 70% for four quadrant biopsies. When comparing detection of dysplasia (all grades, n = 450) there was also no significant difference between the two modalities; sensitivity of MBDB was 43% vs. 32% for four quadrant biopsies. Finally, there was no significance difference for the detection of HGD and OAC (n=405). Sensitivity was 26% for MBDB compared with a 19% for four quadrant biopsies.

Besides adding significant time to the endoscopic procedure, methylene blue staining is somewhat operator dependent. It is influenced by the washing technique used, as inadequate lavage after staining may cause false-positive staining of gastric surface cells. Inadequate exposure of the BO to the mucolytic agent and methylene blue may cause SIM to appear pink, resulting in a false positive indication of gastric mucosa. Interpretation of chromoendoscopic findings is also subject to considerable interobserver variability.[Meining et al., 2004] Finally, there is potential toxicity related to oxidative DNA damage to methylene blue-stained columnar epithelial cells when exposed to white light. An *in vivo* study of 15 patients with Barrett's oesophagus on matched biopsies taken before and after methylene blue staining demonstrated a significant increase in the amount of DNA damage, measured by strand breaks at alkali sensitive sites and FpG-sensitive sites.[Olliver et al., 2003] In conclusion, there is insufficient evidence to substantiate the routine use of methylene blue for the surveillance of Barrett's oesophagus.

Cresyl violet

Cresyl violet is a synthetic dye that readily binds to the acidic components of the neuronal cytoplasm, such as RNA-rich ribosomes, and is widely utilized to stain neuronal tissues. In gastroenterology, it is used an in vitro stain for histological identification of

Helicobacter pylori.[Burnett et al., 1987] Cresyl violet chromoendoscopy has been reported to enhance the mucosal pattern of early gastric cancer.[Furuta et al., 1985] In a recent prospective *in vivo* study of Confocal laser endomicroscopy in human colon, topical cresyl violet was used as an alternative contrast agent to fluorescein.[Goetz et al., 2009] Cresyl violet is advantageous as it allows direct nuclear visualization and does not need to be injected, thus averting the potential systemic side effects occasionally seen with fluorescein (adverse reactions/ skin discolouration). The sensitivity and specificity for the differentiation of non-neoplastic from neoplastic changes were 98% and 100%, respectively. There are no studies on the use of cresyl violet in Barrett's oesophagus to date.

Crystal violet

Crystal violet (gentian violet), not to be confused with cresyl violet, is a topical antimicrobial agent which binds to microbial DNA, and is commonly used as a stain for distinguishing Gram positive and Gram negative bacteria. It was first described as an aid to diagnosis of Barrett's oesophagus in 2 case series, both of which were biased by the use of methylene blue before application of the dye.[Amano et al., 2005;Amano et al., 2004] Yuki *et al.* followed this with a study of 1030 patients, without the addition of methylene blue.[Yuki et al., 2006] Using a simple classification system based on two classes of pit pattern (round /ovoid/regular or tubular/villous/irregular) dysplasia was identified with a sensitivity of 96.0%, specificity of 66% and accuracy rate of 67.4%. Criticism of the study design includes addition of acetic acid in a third of patients, with no sub-group analysis or direct comparison between the two techniques. The number of biopsies containing dysplasia was also very small (n=25/1115), and on average only 1 biopsy was taken per patient. This leads to questions of sampling error and the degree of dysplasia may have been underestimated.

Toluidine Blue

Toluidine blue is a basic absorptive stain which stains nuclei by binding to the nuclear DNA.[Canto, 1999] Cells with a high nuclear-to-cytoplasmic ratio, i.e a higher mitotic activity, absorb this stain more intensely. In 1987 Chobanian *et al*. reported on 58 patients a sensitivity of 98% and specificity of 80% for diagnosing BO, but could not

discriminate between grades of dysplasia.[Chobanian et al., 1987] Some concerns have been raised about potential side effects including vomiting, agranulocytosis, and methaemoglobinemia.[Canto, 1999]

2.3.2 Contrast staining

Acetic Acid Magnification chromoendoscopy

Although originally reported in GI endoscopy as an aid to detect small islands of residual Barrett's esophagus after ablation therapy,[Guelrud and Herrera, 1998] acetic acid has been used during colposcopy for over 40 years as an aid to detection of intra epithelial neoplasia of the cervix. Typically a solution freshly prepared from glacial acetic acid, 1%±3% dilution, with a pH 2.5±3.0, is used for *in vivo* application. When topically applied to multilayered squamous epithelium the acetic acid is progressively neutralized by mucus covering the epithelium and the underlying stroma and vascular network are protected.[Lambert et al., 2003] In single layered columnar lined oesophagus the acetic acid reversibly alters the barrier function of the epithelium and reaches the stroma and vascular network. This leads to swelling of the mucosal surface and enhancement of the surface architecture. There is also enhancement of vascular pattern due to congestion of the capillaries. Transient changes to the structure of cellular proteins may also occur.

All of the studies using acetic acid have combined magnification endoscopy to study the pit pattern of the mucosa. Classification is based on Guelrud's description of four typical pit patterns [Guelrud and Herrera, 1998]; gastric patterns (pattern I = pits with a regular and orderly arranged circular dots; pattern II = reticular pits that are circular or oval and are regular in shape and arrangement); SIM patterns (pattern III = fine villiform appearance with regular shape and arrangement; pattern IV = thick villous convoluted shape with a cerebriform appearance with regular shape and arrangement).

In the first prospective cohort study of 49 patients, sensitivity for specialized intestinal metaplasia was 97%, specificity was 89% and overall accuracy was 92%.[Guelrud et al., 2001] Using modified criteria, a second study of 67 patients demonstrated a sensitivity of 89%, specificity of 90% and diagnostic accuracy of 90%.[Toyoda et al., 2004] Reaud *et*

al. studied 28 patients with a type III or IV pattern with sensitivity for SIM of 96%, specificity of 43% and diagnostic accuracy of 75%.[Reaud et al., 2006]

One study, by Meining *et al.*, reported a low accuracy rate of 52% although due to the study design the co-registration of biopsy sites may have been inaccurate [Meining et al., 2004]. Finally in a randomised crossover trial of 76 BO patients, Hoffman *et al.* demonstrated a significantly higher diagnostic yield of targeted biopsy specimens after acetic acid high-magnification chromoendoscopy for BO than random biopsy (78% vs. 57%, respectively).[Hoffman et al., 2006] Furthermore, the number of biopsy specimens needed to diagnose specialized columnar epithelium could be decreased by about 56% if endoscopic biopsy was directed to Guelrud pit patterns III and IV. The overall diagnostic accuracy was 83%.

Although there is a growing body of evidence that magnification chromoendoscopy with acetic acid improves the diagnosis of SIM, evidence for improved diagnosis of dysplasia is currently lacking. The technique is advantageous as it is both safe and inexpensive. The Guelrud pit pattern classification has not been universally adopted in the studies presented and inter-user variability of pattern interpretation is unknown. In conclusion, more studies are necessary before this promising technique gains widespread use in Barrett's surveillance programmes.

Indigo Carmine

Indigo carmine is a combination of a blue plant dye and a red colouring agent which has been used extensively in the surveillance of colonic polyps,[Lee et al., 2003] and detection of dysplasia in ulcerative colitis.[Rutter et al., 2004] Sharma *et al*. investigated it use in patients with BO, by using magnifying endoscopy in conjunction with indigo carmine staining.[Sharma et al., 2003] Intestinal metaplasia was identified in 57 of 62 (97%) patients with ridged/villous pattern and in 2 of 12 (17%) with circular pattern. High-grade dysplasia was detected in 6 patients, all of whom had a distinct irregular/distorted pattern, whereas the appearances of low-grade dysplasia (18 patients) were similar to SIM.

2.4 Optical Imaging techniques

2.4.1 Narrow Band Imaging

NBI is a novel technique analogous to chromoendoscopy but without dyes – instead it is based on the optical phenomenon that the depth of light penetration into tissues depends on the wavelength; the shorter the wavelength, the more superficial the penetration (see figure 2.7). Using in scope filter systems to separate the spectral components into two narrow band widths – 415nm and 540nm (i.e blue and green)- the limited penetration of blue light into tissue results in preferential enhancement of the surface characteristics of the mucosa. Visualization of the vascular network overlying the mucosal surface is also improved as the 415nm light is absorbed by the capillary vessels at the surface epithelium, whereas the 540nm light is absorbed by the mucosal blood vessels.

Figure 2.7 Narrow Band Imaging

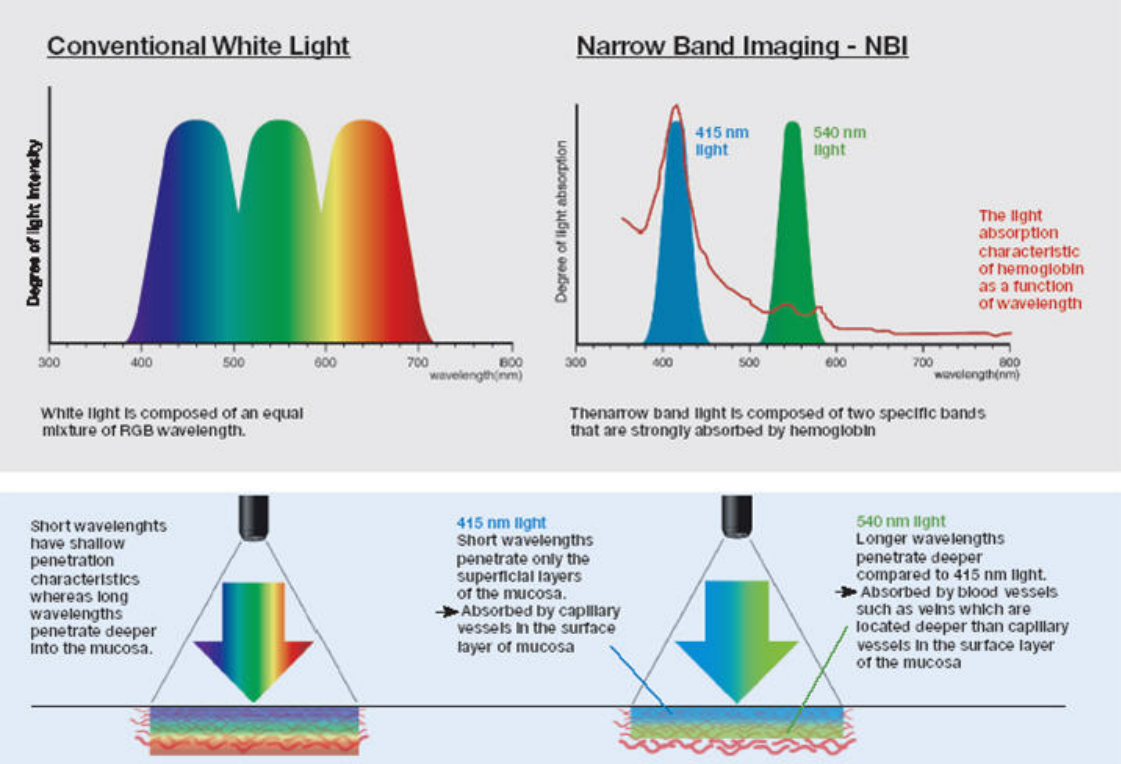

In a small study Hamamoto *et al.* compared magnifying endoscopy with and without NBI. Targeted biopsies obtained under NBI yielded SIM in 90%, compared to 40% under conventional WLE.[Hamamoto et al., 2004] Another small study compared chromoendoscopy to NBI (both in combination with high-resolution endoscopy) in 28 patients with known BO undergoing surveillance, 14 of whom had HGD.[Kara and Bergman, 2006] The sensitivity for HGD and IMC was 79% using a high-resolution endoscope alone. The addition of chromoendoscopy with indigo carmine or the addition of NBI led to slightly higher but not statistically different sensitivity of 93% and 86%, respectively. This group subsequently assessed images from 63 patients, 41 with HGD, taken using magnification endoscopy + NBI.[Kara and Bergman, 2006] Three factors were found to be important for differentiating HGD from non-dysplastic tissues: (1) irregular mucosal patterns; (2) irregular vascular patterns; and (3) the presence of abnormal blood vessels. In all areas with HGD (n = 48), at least one of these abnormalities was present; and in 85% of cases, two or more of these factors were detected.

Sharma *et al.* reported there results of magnification endoscopy + NBI on 51 patients (27 SSBO, 24 LSBO).[Sharma et al., 2006a] NBI images were graded according to mucosal pattern (ridge/villous, circular and irregular/distorted) and vascular pattern (normal and abnormal), and images were then correlated with histology in a prospective, blinded manner. The sensitivity for intestinal metaplasia within LSBO was 100%, and 71% for SSBO. All of the 7 patients with HGD had an abnormal vascular pattern.

Curvers *et al.* compared high-resolution white light endoscopy, indigo carmine chromoendoscopy, acetic acid chromoendoscopy, and NBI to determine the best technique for use in Barrett's oesophagus.[Curvers et al., 2008c] Images obtained were classified according to three criteria: regularity of mucosal pattern, regularity of vascular pattern, and presence of abnormal blood vessels. These images were then evaluated by 5 expert endoscopists with experience in advanced imaging technique and 7 endoscopists with no specific expertise in BO. In total, 22 areas were included in the evaluation; 8 areas with HGD/IMC, 1 area with LGD, 1 area IND, and 12 areas with nondysplastic

BO. Using a visual analogue score, all endoscopists subjectively scored overall image quality and vascular image quality of NBI as better than WLE. Importantly, the addition of all 3 enhancement techniques did not improve the yield of neoplasia over WLE. A second study by the same group, using the same criteria, found no significant difference in interobserver agreement between expert and non-expert endoscopists when NBI and WLE images were compared. [Curvers et al., 2008a]

In a prospective blinded tandem endoscopy study Wolfsen *et al.* evaluated 65 patients with BO undergoing surveillance endoscopy, 17 with HGD/IMC.[Wolfsen et al., 2008] In 12 patients (18%) a higher grade of histology (more advanced dysplasia) was detected using NBI compared with WLE. There were no patients in whom a finding of dysplasia was found via the standard resolution white light endoscopy with random biopsy approach that was not found via the high-resolution NBI approach. Interestingly of the 5 cases of HGD/IMC missed by SD endoscopy, 3 were found by HD endoscopy without NBI.

There is considerable user bias within studies of NBI, illustrated by a surveillance study of 400 patients undergoing colonoscopy for colonic polyps, randomised to either SD endoscopy or NBI.[Adler et al., 2008] Adenoma detection rates were significantly higher by NBI (26.5%) than SD colonoscopy (8%) in the first 100 patients studied ($p=0.02$). As consecutive groups of 100 patients were analysed however, the rate of adenoma detection by NBI remained stable but with SD colonoscopy increased steadily until being equivalent in the last 100 cases (25.5% versus 26.5%, $p=0.91$). The authors speculated that the increasing adenoma rate in the conventional group may have been caused by a training effect of better polyp recognition by NBI.

2.4.2 Autofluorescence endoscopy

Autofluorescence results when a tissue surface is illuminated by short wavelengths, either ultraviolet (UV 400 nm) or short visible light (400–550 nm). The resulting fluorescence is of a longer wavelength and emanates from tissue biomolecules (‘fluorophores’) that are distributed in varying concentrations in the different layers of the oesophagus. The dominant fluorescent layer is the submucosa, which contains highly green-fluorescing

connective tissues (collagen and elastin), while a weaker mucosal component arises from epithelium and lamina propria. Different excitation wavelengths activate different groups of fluorophores, each of which emits at different wavelengths.

This phenomenon was first utilised in Barrett's oesophagus using spectroscopic point measurements,[Panjehpour et al., 1996] and is described in more detail below. In brief, low collagen fluorescence and high NAD(P)H fluorescence characterise lesions with high grade dysplasia as opposed to non-dysplastic epithelia. Hence, with progression towards neoplasia one would typically observe a reduction in the intensity of green fluorescence, and a relative increase in red fluorescence.

The technology was then adapted for incorporation into video endoscopes. The early prototype LIFE (light induced fluorescence endoscopy) system (LIFE-GI; Xillix, Canada and Olympus, Japan) showed promise in uncontrolled clinical feasibility studies. Two studies reported an increased detection rate of HGD using this technique.[Haringsma et al., 2001;Niepsuj et al., 2003] A randomized, crossover, controlled study of LIFE with SD endoscopy gave more disappointing results.[Kara et al., 2005c] 15/50 patients had HGD or early cancer. The overall sensitivity was 85% for SD endoscopy and 69% for LIFE (p=0.69). The authors concluded that LIFE was not superior to SD video endoscopy.

This group went on to evaluate a new AF endoscopy system manufactured by Olympus (AFI).[Kara et al., 2005b] The AFI system incorporates an HD endoscope, with a separate CCD for video AFI. The authors reported objectively that images were clearer with AFI than LIFE. Of 60 patients evaluated, 22 had HGD/EC. Of these 15/22 were detected by WLE and four-quadrant biopsies and 21/22 were detected by targeted biopsies using AFI, an additional 7 patients missed by four-quadrant biopsies. Only 1/22 patients was missed by AFI, with HGD found on random biopsies.

An international study group went on to evaluate a newer Olympus system, Endoscopic tri-modal imaging (ETMI).[Curvers et al., 2008b] It incorporates a HD endoscope (with

an optical zoom capability), AFI and NBI. 84 patients were studied, 30 with HGD/OAC. 19/30 were detected by HD endoscopy. 24/30 were detected by targeted biopsies using AFI, with 7 additional patients detected by AFI alone. 3/30 patients were missed by AFI. The authors concluded that 'as none of the control areas with unsuspicious AFI showed HGD/OAC upon biopsy the negative-predictive value of AFI was high', but this failed to take into account the 10% of patients missed by targeted biopsy with AFI. The false positive rate of AFI was 81%. When NBI was used to evaluate the areas highlighted by AFI the false positive rate was reduced to 26%. This is encouraging but the problems with end user interpretation remain, as illustrated by the 3 lesions containing HGD/OAC (one detected by HD endoscopy, two with AFI) that were diagnosed as ''NBI unsuspicious'' after detailed inspection with NBI.

2.4.3 Endoscopic Ultrasound

Endoscopic ultrasonography (EUS) is established as the most accurate modality for the local staging of oesophageal neoplasms. Since the introduction of the first prototype 5MHz radial echoendoscopes in 1980,[DiMagno et al., 1980] the development and quality of EUS has significantly improved. Advances in the field include the introduction of high frequency ultrasound miniprobes (HFPUS) ranging from 20-30 MHz, which provide higher resolution at the expense of penetration depth. Despite these advances the resolution is limited to features with dimensions larger than 100 μm.

Several studies have looked at the potential role of EUS in the detection of dysplasia in Barrett's oesophagus. Srivastava *et al*. first described endosonography findings in BO in 1994 in a study involving 15 patients with BO (6 with dysplasia) and 13 controls.[Srivastava et al., 1994] Using a radial scanning echoendoscope, oesophageal wall images were taken at a frequency of 12 MHz along the oesophagus. The authors found that although there was significantly greater wall thickening in those with BO than controls, no statistically significant difference was found between dysplastic and non-dysplastic Barrett's oesophagus.

Adrain *et al*. evaluated 17 patients with biopsy-proved Barrett's metaplasia (defined as specialized intestinal metaplasia), 12 normal controls, and 10 patients with reflux oesophagitis.[Adrain et al., 1997] EUS was performed by using 20 MHz HFPUS. Barrett's metaplasia by HFPUS was defined as those in which the second (hypoechoic) layer of the oesophageal mucosa was thicker than the first (hyperechoic) layer. All 17 patients with BO as well as the 12 controls were appropriately identified, with a sensitivity of 100% and a specificity of 86%. The investigators concluded that HFPUS is a sensitive tool for the identification of Barrett's oesophagus, but could not identify patients with dysplasia. From the current published evidence therefore, EUS has no role in detecting dysplasia in BO.

2.4.4 Optical interferometry

Optical interferometry combines two or more light waves in an optical instrument in such a way that interference occurs between them. By measuring the cross-correlation between an electric field reflected from a target and a coherent replica of the original field, distances can be readily measured with a precision well below a single wavelength.

Optical Coherence Tomography

OCT is an emerging endoscopic imaging technique that is analogous to B-mode ultrasonography, but measures the intensity of back scattered light instead of sound using the principle of low-coherence optical interferometry. Real-time imaging rates of 4 frames per second have been demonstrated and resolution is in the range of 10-20 um, 10 times greater than conventional EUS. The high spatial resolution achieved by OCT is offset, however, by a limited sampling depth of 1–2 mm. Like EUS, scanning can be linear, transverse or radial. With linear scanning, the cross-sectional image has a higher pixel density and better transverse image resolution than radial scanning. OCT has the potential to detect changes in tissue morphology associated with disease pathogenesis and allows identification of microscopic features such as villi, glands, and crypts.[Herz et al., 2004]

Potential utilities in Barrett’s oesophagus are the accurate staging of depth of invasion by intramucosal cancers, and detection and grading of dysplasia. The potential of OCT for

diagnosing SIM has been demonstrated in prospective studies showing sensitivities ranging from 81% to 97% and specificities from 57% to 92%.[Poneros et al., 2001;Evans et al., 2007] In the larger of the 2 studies Poneros *et al* assessed 121 patients with 288 biopsy-correlated OCT images.[Poneros et al., 2001] SIM was characterized by (1) absence of the layered structure of normal squamous epithelium and the vertical "pit and crypt" morphology of gastric mucosa, (2) disorganized architecture with inhomogeneous tissue contrast and an irregular mucosal surface, and (3) presence of submucosal glands. These criteria were 100% sensitive and 93% specific for SIM when applied retrospectively and 97% sensitive and 92% specific when tested prospectively. OCT has recently been investigated for detecting dysplasia in Barrett's oesophagus, and promising results have been reported ranging from 54% to 83% with corresponding specificities of 72% to 75%. [Evans et al., 2006;Isenberg et al., 2005]

Ultra high-resolution (UHR) OCT is a recent advance which, in animal feasibility studies, resulted in a 5 μm axial resolution measured in air, corresponding to a resolution of 3.7 μm in rabbit oesophagus using linear scanning.[Herz et al., 2004] The same group then evaluated UHR OCT in 50 human subjects with BO, and demonstrated an 83% sensitivity for HGD and 97% for LGD [Chen et al., 2007]. One significant barrier inhibiting adoption of OCT is the focal, probe based, nature of imaging and the speed of image construction or frame rate.

Optical Frequency Domain Imaging (OFDI)

A variant of OCT, called Optical frequency domain imaging (OFDI), produces images that are identical to those obtained by OCT but at a rate of more than 100 frames per second.[Yun et al., 2006] In combination with a recently developed balloon-centred optical catheter, OFDI makes it possible to comprehensively image the entire distal oesophagus in a time that is acceptable for an endoscopic procedure (<2 minutes at 50 μm pitch). This device was first tested *in vivo* on pig oesophagus in a feasibility study.[Vakoc et al., 2007] This group have gone on to successfully assess this technique in 10 human subjects, although no direct correlation with histology was noted in this study.[Suter et al., 2008] Future uses of this device may include accurate staging of early

intramucosal cancers, and utility as an optical scanner for dysplasia. Multi–centre studies evaluating this promising new device are awaited.

Angle-resolved low-coherence interferometry (a/LCI)

Angle-resolved low coherence interferometry (a/LCI) is a probe based optical biopsy technique that obtains nuclear morphology measurements of epithelial tissues by combining optical coherence tomography with light scattering spectroscopy. In an ex vivo study 3 oesophagectomy specimens were examined using the a/LCI device.[Pyhtila et al., 2007] Comparison was made with sites of dysplastic BO and normal gastric epithelium. Both the nuclear density and the nuclear diameter were statistically different between the two groups, with increased nuclear diameter and decreased nuclear density measured in dysplastic BO. Although these data are encouraging the sample size was small (18 sites) and the device is yet to be tested *in vivo*.

2.4.5 Confocal Laser Endomicroscopy

Confocal laser endomicroscopy is a new endoscopic modality developed to obtain very high-resolution images of the mucosal layer of the GI tract. To create confocal images, a low-powered laser (an argon-ion laser that generates an excitation wavelength of 488 nm, blue laser light) is focused by an objective lens into a single point, within a fluorescent specimen, with subsequent detection of the fluorescence light reflected from the tissue through a pinhole. The laser light is focused at a selected depth in the tissue of interest and reflected light is then refocused onto the detection system by the same lens. The term confocal refers to the alignment of both illumination and collection systems in the same focal plane. Images generated are comparable with histological examination, which has led to the moniker of ‘virtual endomicroscopy’.

There are two types of commercially available device – either integrated endoscope technology (EG-3870CIK; Pentax, Tokyo, Japan) or probe based CLE (Cellvizio, Mauna Kea Technologies, Paris, France) inserted through the biopsy channel. Tissue fluorescence is achieved using contrast agents, such as intravenous fluorescein or topical acriflavin, tetracycline and cresyl violet through a spraying catheter. Intravenously

delivered fluorescein distributes throughout the extracellular matrix of the surface epithelium and lamina propria but does not stain cell nuclei. Fluorescein is usually administered within 5 minutes of imaging; however, the dose and timing of contrast administration have not been standardized. After the contrast administration, the tip of the confocal endomicroscope or miniprobe is positioned in gentle contact with the area of interest to obtain high-resolution confocal images. Accumulated images can be saved for postprocedural analysis.

The first prospective human trial evaluated confocal endomicroscopy during screening for colorectal cancer in 69 patients.[Kiesslich et al., 2004] The presence of neoplastic changes in colonic polyps was predicted with high accuracy (97.4% sensitivity, 99.4% specificity, 99.2%accuracy). Other studies of colonic polyps, gastric neoplasia, and squamous cell cancer of the oesophagus have demonstrated similar in vivo images comparable to histology.[Evans and Nishioka, 2005;Meining et al., 2007;Kakeji et al., 2006;Liu et al., 2009a]

Kiesslich *et al.* were the first to examine patients with Barrett's oesophagus by means of integrated endoscope based CLE system.[Kiesslich et al., 2006] The authors were able to achieve a high sensitivity both in the diagnosis of Barrett metaplasia and dysplasia (96.8% and 97.4% respectively). The probe based CLE system (pCLE) has been evaluated in a multi-centre study of 63 patients with BO undergoing surveillance endoscopy. SIM and dysplasia were diagnosed with 98% and 93% sensitivity and 94% and 98% specificity, respectively.[Pohl et al., 2008] Other studies have shown CLE can detect SIM and dysplasia in BO with similar accuracy.[Sharma and Bansal, 2006;Leung et al., 2009]

In a prospective randomised crossover trial 39 patients underwent CLE (using the integrated endoscope system) or SD endoscopy with four quadrant biopsies.[Dunbar et al., 2009] The order of the procedures was randomised and carried out at two different time points, 2- 6 weeks apart. The endoscopist was blinded to previous pathology and endoscopy reports, but was aware if the patient had been referred for evaluation of HGD

or routine surveillance. Of 13 patients with HGD, there was no significant difference in the sensitivity of each method (11/13 patients correctly identified by each method, 9/13 concordant cases). The diagnostic yield for neoplasia was significantly different between the two methods, 34% using CLE and 17% during SD endoscopy. Of the 26 patients in the non-dysplastic group there was an 86% reduction in the number of biopsies necessary vs. four quadrant biopsy. An interesting sub-analysis in the study evaluated the use of CLE for real time guided EMR. Two patients had EMR during their CLE procedures when the decision to perform EMR was based on CLE images of flat mucosa suggesting HGD. Both were confirmed as HGD histologically. A further 2 EMRs were performed at the end of SD endoscopy based on endoscopic appearances, which showed LGD and non-dysplastic BO only.

A prospective multi-centre cohort study has evaluated the utility of pCLE alone vs. four quadrant biopsies for the diagnosis of dysplasia.[Bajbouj et al., 2010] Precise matching of pCLE recordings to the biopsy site was enabled by marking with APC, and tissue was then sucked into an EMR cap. Diagnosis was made on site and after 3 months on review of films. In 68 patients undergoing surveillance the specificity for dysplasia was 95%, but sensitivity was very poor at only 12%. The authors concluded that due to its low PPV and sensitivity, pCLE may not replace standard biopsy techniques for the diagnosis of Barrett's esophagus and associated neoplasia.

The recently completed DON'T BIOPCE study, that utilized a newer probe with a resolution of 1.0 μm, has been presented in abstract form.[Sharma et al., 2010] This multicenter international randomized trial evaluated the incremental diagnostic yield of WLE, NBI and pCLE to target mucosal abnormalities and compared histology results with a standard random four quadrant 2cm biopsy protocol. Of the 856 total locations, 116 had biopsies showing HGD or OAC. The addition of pCLE gave a significantly improved diagnostic yield over both WLE and NBI. When pCLE was combined with pCLE and NBI all patients with high risk lesions were detected. If targeted and random four quadrant biopsies were only performed in patients with suspicious lesions on white light endoscopy, NBI or pCLE, 39% of biopsies would have been avoided without loss of

diagnostic yield. The authors concluded that pCLE has a significant impact on the detection of neoplasia in BO compared to white light endoscopy and NBI, and has the potential to make surveillance endoscopy a more cost effective strategy.

In summary the use of CLE has moved on rapidly in the last five years, with real time images equivalent to histological examination now achievable at endoscopy. The potential for the use of CLE to guide endoscopic therapy (by EMR or focal ablation) is interesting and requires larger clinical studies. The main drawback of CLE, like many other examiner-dependent modalities reviewed above, is end user interpretation. Histopathology training may be required for the adequate interpretation of the CLE images that are generated, and interobserver and intraobserver variability of this technique has not yet been adequately studied. The procedure is also time consuming and requires administration of off licence intravenous fluorescein dye for acceptable resolution. At present CLE is not suitable for widespread clinical use in Barrett's surveillance and remains a promising research tool.

2.5 Spectroscopy

All spectroscopic modalities (Scattering, Raman, absorption, fluorescence) analyse light-tissue interactions to yield diagnostic information about the structural and molecular composition of tissue. When light of a certain wavelength is used to stimulate tissue, distinct optical signals are produced. These "spectra" can then be correlated with histopathology and analysed to create algorithms for tissue classification and grading. Spectroscopy offers the potential for real-time endoscopic differentiation of neoplastic and normal mucosa, and has the additional advantage of dispensing with end user interpretation.

2.5.1 Scattering (Reflectance) Spectroscopy

Elastic & Light scattering spectroscopy

When tissue is interrogated by white light, typically delivered through a fibre, *elastic* scattering events occur that redirect incident photons without a change in wavelength (or energy). Elastic scattering (also known as diffuse reflectance) spectra, which may be

detected by a second collection fibre, are a measure of the behaviour of white light emerging from the tissue surface following these multiple elastic scattering events. These spectra may contain both multiply scattered photons (primarily from the stroma) and photons that have undergone single or few scattering events following their interaction with the epithelium. Incident photons are also sensitive to tissue absorbers, such as haemoglobin that reduce the intensity of the diffusely reflected light at particular wavelengths. ESS thus informs on the tissue morphology (predominantly scatter) and tissue biochemistry (predominantly absorption). The interpretation of these spectra, and how they correlate with the physical properties of pre-neoplastic and neoplastic tissue, is the subject of much interest.

Physical Correlation

ESS spectra relate to the wavelength-dependence and angular-probability of scattering efficiency of tissue micro-components. The sizes, indices of refraction and structures of the denser sub-cellular components (e.g., the nucleus, nucleolus, and mitochondria) are known to change upon transformation to premalignant or malignant conditions. Indeed, histopathologists use these nuclear changes to grade dysplasia, i.e. the sizes and shapes of nuclei and organelles, the ratio of nuclear to cellular volume (nuclear:cytoplasmic ratio) and clustering patterns (nuclear crowding).

Mourant *et al.* examined the influence of scatterer size in rat tumour cell lines and compared them with non-tumourigenic cells.[Mourant et al., 1998] An optical geometry of 400μm optical fibre and a 200μm collection fibre spaced 550μm away (centre-to-centre) was used. ESS measurements demonstrated a small but significant difference in optical properties between the two cell lines, with this difference in the scattering rather than the absorption properties of the cells. The authors postulated this was either due to the average size of a scattering particle being larger in cancer cell lines (i.e size of nuclei or mitochondria increase), or there could be a change in the number and distribution of scattering particles (i.e number of mitochondria increase). The same group went on to hypothesise that spectral signatures will be altered if the refractive index of the nucleus changes, due to an increase in the amount of DNA content.[Mourant et al., 2000] By

measuring DNA content by flow cytometry, DI was calculated for 2 different cell lines, and plotted against high angle scatter (between 110° and 140°). Cell suspensions with higher DI (analogous to aneuploidy) scattered more light than cell suspensions with smaller DI (analogous to diploid).

Backman *et al.* have reported on the correlation of tissue morphology with reflectance spectra using polarized light, which allows measurement of single scattering events, called light scattering spectroscopy (LSS).[Backman et al., 2000] LSS was evaluated on colonic cell lines and ex vivo colonic polyps, where the spectrum of the single backscattering events provided quantitative information about the epithelial-cell nuclei such as nuclear size, degree of pleomorphism, degree of hyperchromasia and amount of chromatin.[Gurjar et al., 2001]

Clinical Studies of ESS/LSS

The largest clinical *in vivo* study of scattering spectroscopy to date evaluated the value of ESS in discriminating dysplastic and non-dysplastic tissue in Barrett's oesophagus.[Lovat et al., 2006] A total of 181 matched biopsy sites from 81 patients, where histopathological consensus was reached, were analysed. There was good pathologist agreement in differentiating high grade dysplasia and cancer from other pathology (kappa = 0.72). Spectral data was analysed by LDA + PCA to form a model which was then tested by leave one out cross validation (jacknife analysis). Elastic scattering spectroscopy detected HGD or cancer with 92% sensitivity and 60% specificity. If used to target biopsies during endoscopy, the number of low risk biopsies taken would decrease by 60% with minimal loss of accuracy. ESS had a negative predictive value of 99.5% for high grade dysplasia or cancer.

There have been 2 clinical studies of LSS. The first, on 13 BO patients (76 biopsies, 4 HGD), found a sensitivity and specificity of 90%.[Wallace et al., 2000] The second study evaluated LSS with ESS and AFS as part of a putative 'tri-modal spectroscopy' system. 16 Barrett's patients (40 biopsies, 7 HGD) were studied and the sensitivity and specificity for differentiating HGD from non HGD BO was evaluated. LSS gave a sensitivity and

specificity of 100% and 91% respectively, ESS 86% and 100% respectively and AFS 100% and 97% respectively.[Georgakoudi et al., 2001] When all 3 modalities were combined the sensitivity and specificity were both reported as 100%, although as only 7 sites contained dysplasia, and multiple spectral parameters were evaluated, the possibility of statistical error by overfitting is high. Finally, a novel rotational scanner based on LSS has been recently described which has shown promising results in early clinical studies.[Qiu et al., 2010]

The Field effect – 4DELF and LEBS

Backman's group have gone on to develop two new approaches that are extensions of LSS, called 4-dimensional elastic light-scattering fingerprinting (4D-ELF) and low-coherence enhanced backscattering spectroscopy (LEBS). Both of these techniques may detect field changes in colon carcinogenesis - the proposition that the genetic/environmental milieu that results in neoplasia in one region should be detectable throughout the mucosa.[Kopelovich et al., 1999]

4D-ELF allows acquisition of light-scattering data in several dimensions; (1) wavelength of light; (2) the scattering angle; (3) azimuthal angle of scattering; and (4) polarization of scattered light.[Roy et al., 2004] These 4-dimensional fingerprints are sensitive to changes in tissue organisation, at scales ranging from tens of nanometres to microns. In a study of the azoxymethane-treated rat carcinogenesis model, changes in the spectral slope of ex vivo tissue from the distal colon were significantly decreased compared to a control as early as 2 weeks after carcinogen treatment, and continued to decrease over the 20 weeks of the experiment.

LEBS was evaluated in a similar study of azoxymethane-treated rats and the spectral slope was also shown to progressively decrease over a 6 week period.[Roy et al., 2006] LEBS was then assessed on ex vivo human tissue obtained from 63 patients. All were sampled from endoscopically normal colon, at least 5 cm away from any neoplastic lesion. In a post-hoc analysis there was a significant decrease in the spectral slope obtained from patients who harboured adenomas somewhere in their colon when

compared with those who were free of neoplasia ($P < 0.01$). The same group have recently published on a larger dataset of 219 patients.[Roy et al., 2009] For advanced adenomas, the LEBS marker had a sensitivity of 100%, specificity of 80%, and area under the receiver operator characteristic curve of 0.895. Rectal LEBS measurements were sensitive to lesions in both the distal and proximal colon, although the magnitude of alterations was greater in the distal colon.

In a landmark clinical study, both LEBS and 4D-ELF were able to detect pancreatic adenocarcinoma from optical measurements taken from the histologically normal duodenal periampullary mucosa.[Liu et al., 2007] In addition to changes in tissue organization, 4D-ELF also measures subtle changes in microvascular blood supply (so called early increase in blood supply or EIBS) that may inform on field carcinogenesis elsewhere.[Wali et al., 2005] A recent study using a simplified 4D-ELF probe supports this theory in colon cancer.[Gomes et al., 2009] Microvascular blood content was increased by 50% in the endoscopically normal rectal mucosa of patients harboring advanced adenomas when compared with neoplasia-free patients, irrespective of lesion location. Logistic regression using mucosal oxy-haemoglobin concentration and patient age resulted in a sensitivity of 83%, a specificity of 82%, and an area under the receiver operating characteristic curve of 0.88 for the detection of advanced adenomas.

The detection of field effect is the ‘golden goose’ for screening programmes, as it would allow the interrogation of apparently normal mucosa which is easily accessible in an outpatient clinic setting without the need for endoscopy (i.e. rectum for colon cancer or mouth for oesophageal cancer) and inform on the presence of early cancer downstream from the normal tissue. No studies have been undertaken on patients with BO to date. Further large scale clinical studies of these promising techniques are awaited.

2.5.2 Raman Spectroscopy

Raman spectroscopy provides molecular specific information about tissue based on the detection of *inelastically* scattered light. The Raman effect was first demonstrated in 1928.[Raman and Krishnan, 1998] Following tissue excitation by a laser, a small fraction

of the scattered light undergoes “wavelength shifts” relative to the excitation wavelength due to energy transfer between incident photons and tissue molecules. Recent developments in instrumentation have enabled its application in tissue to allow the objective identification of molecular markers associated with neoplastic progression.[Stone et al., 2004;Shetty et al., 2006]

In an proof of concept ex vivo study Raman spectra were measured on snap frozen biopsy samples from 44 patients.[Kendall et al., 2003] 87 samples were evaluated, 20 with HGD or adenocarcinoma in BO and a further 8 squamous HGD/cancer. A system was developed to provide an optimal configuration for the rapid acquisition of high-quality tissue Raman spectra output in conjunction with an argon ion pumped Ti : sapphire laser tuned to 830nm. Spectral data was analysed by LDA + PCA followed by jacknife analysis. There were 2 distinct training algorithms based on pathologist agreement – a consensus model (where all 3 pathologists agreed) and a majority model (2/3 agreed). Of note is that no specimens of LGD were included in the consensus model as all 3 pathologists could not reach agreement. The consensus model gave a 97% sensitivity and 99% specificity for squamous tissue, 84% and 98% for non-dysplastic BO, and 94% and 93% for dysplastic tissue. 72% were correctly classified in the majority model. Despite promising results ex vivo however, in vivo studies in BO are limited because readings take a comparatively long time to collect (around 5 seconds) and the oesophagus is a dynamic organ. In a single centre in vivo study of 65 patients, 26 out of 192 biopsy sites showed HGD or early cancer and Raman correctly identified these with a sensitivity 88% and specificity of 89%.[Song et al., 2005]

2.5.3 Absorption Spectroscopy

Fourier transform infra-red spectroscopy

Fourier transform infra-red (FTIR) spectroscopy probes the vibrational properties of amino acids and cofactors which are sensitive to minute structural changes.[Berthomieu and Hienerwadel, 2009] It is advantageous over Raman spectroscopy as FTIR produces large signals that are insensitive to tissue autofluorescence. In the first study of FTIR spectroscopy in BO, Wang *et al.* showed that DNA, protein, glycogen, and glycoprotein

comprise the principal sources of infrared absorption.[Wang et al., 2007] Using LDA with leave-one-out cross-validation on 98 ex vivo specimens from 32 patients, squamous mucosa could be distinguished from columnar mucosa (Barrett's and gastric) with a sensitivity and specificity of 100% and 97% respectively. Moreover, FTIR to detect dysplastic mucosa resulted in a sensitivity and specificity of 92% and 80% respectively. Dysplastic Barrett's mucosa was found to have a higher mean DNA content and greater average glycoprotein concentration than non-dysplastic Barrett's. This study was limited by its use of partially dehydrated tissue samples. Martin *et al.* commented that 'hydrated or *in vivo* samples are a problem for FTIR spectroscopy because the water peak obscures much of the useful information in the biomolecular range'.[Martin and Fullwood, 2007]

2.5.4 Fluorescence Spectroscopy

This is a point measurement, achieved by measuring tissue fluorescence generated by endogenous molecules (autofluorescence or AFS) or following administration of an exogenous agent (drug-enhanced fluorescence or DFS).

Autofluorescence Spectroscopy

Panjehpour *et al.* were the first to report the *in vivo* use of AFS in the oesophagus.[Panjehpour et al., 1996] 36 patients were studied using a laser induced fluorescence (LIF) system with an excitation wavelength of 410 nm, which corresponds to the excitation of flavins. Normal oesophagus could be distinguished from oesophageal cancer with a sensitivity of 100% and a specificity of 98%. Specificity however, dropped to 28% for the 56 biopsies that demonstrated focal HGD. Wang *et al.* studied AFS on 87 BO patients with a total of 326 collected biopsies. Sensitivity and specificity for detecting HGD was high at 95% and 80% respectively, although only 14 biopsies contained HGD.

Two studies have assessed the accuracy of diagnosis of dysplasia when the excitation wavelengths are in the near-ultraviolet (UV) range. With 330 nm excitation light, the major endogenous fluorophores contributing to tissue emission are collagen (absorption maximum 335 nm), NADH (absorption maximum 340 nm) and, to a much lesser degree,

flavins (absorption maximum 450 nm). Hence as several fluorophores are involved, more spectral information may be collected.

Bourg-Heckly *et al.* used various excitation ratios of different wavelengths to assess 18 patients with BO, 15 non-dysplastic and 3 HGD/IMC.[Bourg-Heckly et al., 2000] An excitation ratio of 390/550nm gave the best results, with a sensitivity of 86% and specificity of 95%. Another study had disappointing results using 337nm, with sensitivity of 74% and specificity of 67% for differentiating dysplastic and non-dysplastic Barrett's mucosa.[Pfefer et al., 2003] The authors of this study also evaluated time resolved fluorescence, with the hypothesis that using time or frequency domain techniques, changes in tissue constituents or factors such as pH or oxygenation may be evaluated. A previous study had successfully applied this technique in the colon for detection of adenomatous polyps, with subsequent increase in diagnostic accuracy.[Mycek et al., 1998] In the study on BO, however, no such improvement was noted.

Drug Induced Fluorescence Spectroscopy

Fluorescence can be enhanced by the addition of exogenous pro-drugs that induce endogenous photosensitiser. Aminolaevulinic acid is perhaps the best studied. Administration causes an increase in porphobilinogen deaminase levels and decreased ferrochelatase levels in the tissue which leads to greater production and retention of Protoporphyrin IX (PpIX) in neoplastic cells. Excitation by UV light from a xenon lamp (375–440 nm) causes emission of fluorescence signals which are stronger than AFS.

Clinical studies of drug-enhanced fluorescence spectroscopy have yet to demonstrate a significant diagnostic advantage over AFS. Brand *et al.* evaluated 93 biopsies from 20 patients with Barrett's oesophagus administered oral ALA (10 mg/kg).[Brand et al., 2002] DFS distinguished HGD from non-dysplastic mucosa with a sensitivity and specificity of 77% and 71%, respectively. Another study comparing different ratios also looked at Time-gated drug induced fluorescence.[Ortner et al., 2003] ALA was administered by topical application with a spray catheter during endoscopy. Patients then underwent repeat gastroscopy 1-2 hours later. Of 596 biopsy specimens taken only 141

reached consensus diagnosis by 3 pathologists. Of these only 9 specimens had HGD, with a further 41 samples displaying LGD. The sensitivity and specificity for detection of dysplasia was 76 and 63% respectively. In summary DFS has not been shown to be advantageous over AFS, and due to the problems of variable drug pharmacokinetics, adverse effects, costs, and regulatory approval, its use is unlikely to gain a wider application in Barrett's surveillance.

2.6 Summary

Several techniques for improved surveillance in BO have emerged over the past decade, and these are summarised in Table 2.3. The understanding of the physical correlation of spectroscopic data and tissue morphology continues to evolve. A correlation with genomic instability both at the site of biopsy and from a field effect has now been shown. In addition the recent introduction of both CLE and OCT, allows real time *in vivo* assessment at the cellular level. These advances in optical diagnostics may pave the way for a new strategy in Barrett's surveillance, whereby a multimodal approach would allow the endoscopist to accurately quantify an individual's risk of progression to cancer *in vivo*. Furthermore as endoscopic therapy for Barrett's dysplasia becomes more commonly employed as a first line treatment for dysplasia and early cancer in BO, so to will there be a need for accurate assessment of the mucosa, both prior to and after therapy. Indeed it may be possible for real time management decisions to be made at endoscopy, based on information from these modalities. Ultimately the adoption of these advanced optical techniques as standard practice will be based on ease of use, diagnostic accuracy and cost.

Table 2.3 Summary of optical diagnostic techniques in Barrett's Oesophagus

Technique	Description	Depth of interrogation	Advantages	Disadvantages
Dye sprays	Acetic acid, methylene blue	surface	Cheap and widely available	Limited evidence from single centres, user dependent, adds 5-10 mins to procedure time
Narrow Band Imaging	'Optical dye spray'	300-400μm	In scope technology, standard in most scopes	User bias, mainly epithelial changes
Autofluorescence Imaging	Endogenous tissue fluorescence	300-400μm	In scope technology, red flag field technique	High false positive rates, user bias
Optical Coherence Tomography	Optical analogue of EUS	1-2mm	Allows depth assessment (2mm), 10-20μm resolution	Slow spectral acquisition time, probe based
OFDI	High speed balloon based OCT	1-2mm	Similar to OCT but wide field can be scanned	Limited to single centre discovery studies, expensive
Confocal Laser Endomicroscopy	Probe or integrated virtual histology	100-300 μm	1-10μm resolution, fast acquisition time	Time consuming, off license iv fluorescein for acceptable resolution, pathology skills required, expensive
Raman spectroscopy	Laser based probe spectroscopy	100-200 μm	Highly accurate, detects molecular changes	Slow spectral acquisition, limited *in vivo* studies, expensive
Elastic Scattering Spectroscopy	White light based probe spectroscopy	10-30 μm	Cheap, detects molecular changes, no end user interpretation	Point measurement, complex statistical analysis, black box technology needs rigorous testing

Chapter 3
Ablative therapies for the treatment of dysplasia

Chapter 3 Ablative therapies for the treatment of dysplasia

3.1 Introduction

The principle of endoscopic therapy for BO is that the columnar lined oesophagus may be effectively removed and is replaced by squamous epithelium (squamous regeneration). This principle was first demonstrated in 1992 using Nd:YAG laser therapy, which has a depth of injury of 3-4mm.[Brandt and Kauvar, 1992] The last 20 years has seen a plethora of new endoscopic techniques and these have been evaluated in large cohort series and randomised controlled trials. These techniques can be broadly categorised into therapy that removes tissue for histological evaluation (Endoscopic resection) and those that do not (ablative therapies). The aim of this chapter is to review these techniques.

3.2 Ablative therapies

3.2.1 Photodynamic therapy

PDT is a field ablation technique that is potentially an effective lower risk alternative to oesophagectomy for the treatment of HGD in BO.[Overholt et al., 1999;Overholt et al., 2003] It is a two step non-thermal, photochemical process, which requires the interaction of a photosensitiser, light and oxygen. The first step is the administration of the chemical photosensitiser, which becomes concentrated in the abnormal target tissue. The majority of PDT photosensitisers possess a heterocyclic ring structure similar to that of either chlorophyll (chlorine-based photosensitisers) or haem (porphyrin-based photosensitisers). Most of the currently approved clinical photosensitisers belong to the porphyrin family.

The second step is the application of a visible light of appropriate wavelength and energy, which photo activates the porphyrin molecule, resulting in the production of a cytotoxic singlet oxygen, or superoxide that contributes to the destruction of the abnormal cells where it is concentrated. [Lofgren et al., 1995] The most commonly used PDT light sources are lasers as they produce high energy monochromatic light of a specific wavelength with a narrow bandwidth for a specific photosensitiser. KTP (neodymium:YAG laser directed through a potassium titanyl phosphate crystal) or copper

vapour pumped dye systems were the most widely used lasers for PDT prior to the approval of the portable, light-weight, and less expensive diode lasers (e.g., DIOMED 630 PDT; Diomed Inc.).[Huang, 2005]

There are many parameters that may be varied to obtain optimal conditions for photodynamic therapy including drug dose, light dose, energy delivered, wavelength of activating light and the time interval between photosensitiser administration and activation (drug-light dose interval). Hence, although there are many photosensitisers in development for the treatment of Barrett's oesophagus, only the first generation haematoporphyrin derivative Photofrin (porfimer sodium; Axcan Pharma Inc.) has received US Federal Drug Administration (FDA) and UK National Institute for Clinical Excellence (NICE) approval. Both Foscan (temoporfin, meta-tetrahydroxyphenylchlorin, mTHPC; Biolitec AG) and Levulan (5-aminolevulinic acid HCl; DUSA Pharmaceuticals Inc., New York, USA) have been investigated and the results of clinical trials are summarised below.

Photofrin

Photofrin is a hematoporphyrin derivative (HpD), a mixture of different porphyrins, and dihematoporphyrin ester (DHE). In the UK NICE approved photofrin PDT for treating HGD arising in BO in 2006. The drug is administered by intravenous injection, 3 days prior to therapy, at a dose of 2 mg/kg body weight. Photofrin is activated by 630nm laser light, typically by using a balloon based cylindrical fibre-optic diffuser (e.g. Wizard X-cell balloon) that is endoscopically placed in the oesophageal lumen, and inflated so as to hold position and flatten the oesophageal folds.[Panjehpour et al., 2000a] Photosensitivity lasts up to 3 months after drug delivery.

Clinical studies

Early studies of cohort series demonstrated encouraging results for ablation of BO, with reversal of HGD in 88-95%.[Overholt et al., 1999;Panjehpour et al., 2000b;Wang, 2000] A multicentre, international randomised controlled trial of 200 patients with high grade dysplasia in Barrett's oesophagus has confirmed the effectiveness of Photofrin PDT.[Overholt et al., 2005;Overholt et al., 2007] Patients were randomised in a 2:1 ratio

to either Photofrin PDT and a PPI (omeprazole), or PPI alone. Complete reversal of HGD (CR-HGD) at 1 year was achieved with Photofrin PDT in 71% vs. 30% in the control group ($p<0.001$). In the follow up evaluation at 5 years CR-HGD was 59% compared to 5% in the control arm.[Overholt et al., 2007] A significant decreased incidence of oesophageal adenocarcinoma (13% with Photofrin PDT, 28% with PPI alone) was reported as a secondary end point.

A retrospective study of 199 patients with HGD in BO has compared outcomes of Photofrin PDT versus surgery.[Prasad et al., 2007b] There was no significant difference in long term survival, with overall mortality 9% (11/129) for PDT and 8.5% (6/70) in the oesophagectomy group, over a median 5 year follow-up. None of the patients treated either with surgery or PDT died from oesophageal cancer. A more recent study from the same group, comparing outcomes for early intramucosal cancer with PDT plus endoscopic mucosal resection versus surgery, came to a similar conclusion.[Prasad et al., 2009]

Several studies have evaluated the cost-effectiveness of PDT, and all have found that photofrin PDT for high-grade dysplasia is cost-effective in terms of quality-adjusted life years, when compared to oesophagectomy.[Shaheen et al., 2004;Vij et al., 2004;Comay et al., 2007]

Adverse Events

Two common side effects of PDT using porfimer sodium are photosensitivity reactions and oesophageal strictures. Photosensitivity can occur up to 3 months after treatment and is reported in more than 60% of patients. This can lead to severe burns requiring hospital admission and patients are advised to undertake strict light precautions after therapy. In the RCT severity was graded as mild in 66%, moderate in 24% and severe in 1%.[Overholt et al., 2005]

As porfimer sodium affects the full thickess of the oesophageal wall, the associated oesophageal stricture rate is high; 22% with one treatment and rising to 50% with

multiple treatments.[Overholt et al., 1999;Overholt et al., 2003] Other adverse events include pleural effusions, atrial fibrillation, nausea and vomiting, and odynophagia.[Overholt et al., 1997] Overall adverse events affected 94% of patients in the randomised controlled trial. These complications significantly affect the acceptability of Photofrin PDT and, despite NICE approval, it is very rarely given.

5-aminolaevulinic acid (ALA)

Levulan (DUSA Pharmaceuticals Inc., New York, USA) is the chemically stable hydrochloride salt of 5-aminolaevulinic acid (ALA), a naturally occurring, 5-carbon aminoketone, carboxylic acid (Figure 3.8). It is a new drug that has come into prominence over the last decade for its potential use in the photodynamic therapy (PDT) of superficial, benign and malignant skin disorders. ALA is not a new chemical entity however. It is present in virtually all human cells as the first committed intermediate of the biochemical pathway resulting in haem synthesis in humans and chlorophyll in plants (Figure 3.9). It differs from other types of PDT in that it is not a preformed photosensitiser, but instead a metabolic precursor of the endogenously formed photosensitiser, protoporphyrin IX (PpIX). The human body is estimated to synthesise 350mg of ALA per day to support endogenous haem production.

The synthesis of ALA is normally tightly controlled by feedback inhibition of ALA synthetase, presumably by intracellular haem levels. ALA, when provided to the cell, bypasses this control point and enters the haem synthesis pathway, which results in the accumulation of PpIX.[Marcus et al., 1996] Free PpIX, unlike haem, does not appear to have intrinsic biological activity. However, PpIX is a potent natural photosensitiser, and irradiation of tissues that have been photosensitized, at sufficient dose rates and doses of light, can lead to significant photodynamic effects on cells, subcellular elements, and macromolecules via production of singlet oxygen.[Poh-Fitzpatrick, 1986]

Figure 3.8 Physical, chemical and pharmacological properties of 5 amino-laevulinic acid

$HOOCCH_2CH_2COCH_2NH_2 \cdot HCl$

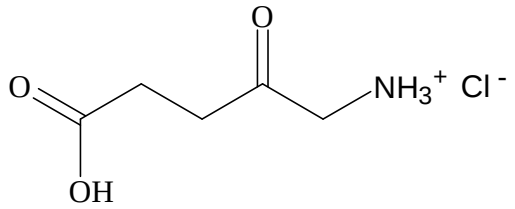

Levulan® (5-Aminolevulinic Acid Hydrochloride)

Physical Form: Odourless, white to off-white crystalline powder

Molecular Formula: $C_5H_9N0_3$ HCl

Molecular Weight: 167.59

Melting Point (Range): 151-156º C (Decomposition).

Solubilities: Very soluble in water. Slightly soluble in methanol and ethanol. Practically insoluble in chloroform, hexane and mineral oil.

pKa Value: 3.816

pH Value: (1:5 aqueous solution) 1.77

Degradation Product: Pyrazine 2, 5-dipropionic acid, formed by the auto condensation of 2 ALA molecules

Figure 3.9 Schematic diagram of haem synthesis

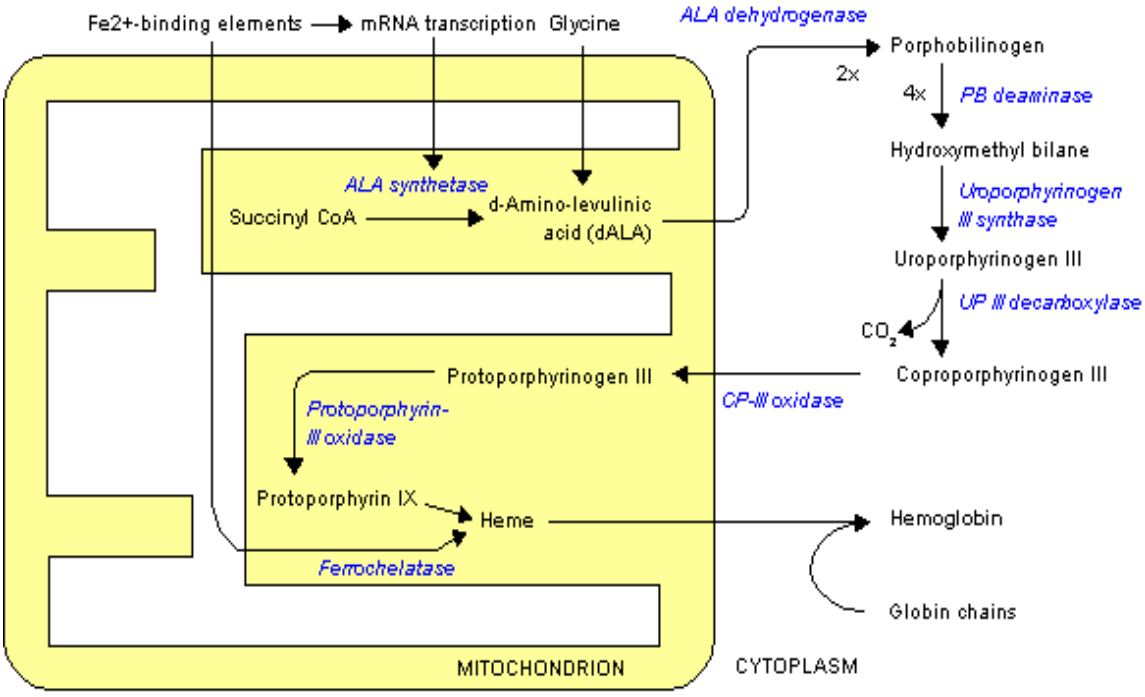

Clinical studies

The first study of PDT in the human gastrointestinal tract using 5 ALA induced PpIX as the photosensitising agent was published in 1995.[Regula et al., 1995] Eighteen patients with colorectal, duodenal and oesophageal tumours were studied. 30-60 mg/kg of ALA was given orally, and then biopsy specimens of tumour and adjacent normal mucosa were taken 1-72 hours later. These specimens were examined by quantitative fluorescence microscopy for assessment of sensitisation with PpIX. Ten patients were given a second dose of ALA a few weeks later and their tumours were treated with red laser light (628 nm). With 30 mg/kg ALA, the highest fluorescence values were detected in the duodenum and oesophagus, and the lowest in the large bowel. Doubling the ALA dose in patients with colorectal tumours gave PpIX fluorescence intensities similar to those in patients with upper gastrointestinal lesions and improved the tumour:normal mucosa

PpIX sensitisation ratio to 5:1. The treated patients showed superficial mucosal necrosis in the areas exposed to laser light.

The first study of ALA-PDT for HGD in BO treated five patients with a median length of 5cm.[Barr et al., 1996] Oral ALA 60mg/kg was administered, followed by 630 nm laser light via a 3cm cylinder diffuser-tipped fibre optic at a power density of 150mW/cm^2 and an energy fluence of 90-150J/cm^2. All had squamous regeneration. Two patients were found to have subsquamous BO (buried glands), though no remaining HGD was identified.

Gossner *et al* treated 32 patients with ALA-PDT using 60 mg/kg ALA given orally and 635nm laser light delivered 4-6 hours after drug dosing through a 2cm cylinder diffuser-tipped fibre optic at a power density of 100mW/cm^2 to a light dose of 150J/cm^2.[Gossner et al., 1998] Ten patients had HGD, and the remainder intramucosal cancer. Patients were maintained on omeprazole for the duration of the study. Dysplasia was eradicated in all patients with HGD, and there was complete remission of the cancers in 17/22 patients (77%), giving an overall success rate of 27/32 (84%). This remission was maintained during follow up of 1-30 months (mean 9.9 months). Squamous regeneration was seen in 68%, though the presence of non-dysplastic buried glands was noted in some patients. A mean of 1.7 treatment sessions were required for the eradication of mucosal tumours. Of note no tumour more than 2mm in depth was included in the study.

In the only double blind, randomized, placebo controlled study reported for BO with low grade dysplasia, 36 patients were randomized to receive oral ALA (30mg/kg) or placebo.[Ackroyd et al., 2000] This was followed 4 hours later by endoscopy and treatment of up to 6cm of BO using green (514nm) light. A response was seen in 16/18 (89%) of patients in the ALA group, with a median area decrease of BO of 30% (range = 0-60%). In the placebo group, a median area decrease of 0% was seen (range 0-10%). Of those that responded in the ALA PDT group all maintained regression to normal squamous epithelium over the entire 24-month follow-up period, and no dysplasia was observed in the treated areas of BO which remained. In the placebo group, persistent

low-grade dysplasia was found in 12/18 (67%) of patients followed for 24 months ($p<0.001$).

Kelty *et al* studied the optimum dosage regime for ALA-PDT. [Kelty et al., 2004a] Twenty-five patients with BO were randomized to receive low dose (30mg/kg) or high-dose (60mg/kg) oral ALA, activated by red light (635nm). All patients showed a macroscopic response, with squamous regeneration. The overall median reduction in the area of Barrett's mucosa was 60%, with no significant difference between groups. Buried glands were identified in six patients (24%), but were not associated with a particular regime. Major side effects were minimal and there were no perforations or strictures. Nausea occurred more frequently (n=5) in patients who received 60mg/kg ALA than in patients in the low dose group (n=3). Other side effects included hypotension, angina, fever, odynophagia and mild elevation of liver function tests.

Our group has shown that the efficacy of ALA-PDT for eradication of HGD in BO is closely related to the light dose used. Mackenzie *et al*. demonstrated that, when using 60 mg/kg ALA with red laser light, a light dose of 1000J/cm was more effective than lower doses.[Mackenzie et al., 2007a] A correlation was observed between light dose delivered and treatment response. In a randomised control trial of 27 patients we have gone on to demonstrate that red laser light (635nm) was more effective than green laser light (512nm) when using ALA 60mg/kg.[Mackenzie et al., 2009] Additionally patients receiving 30mg/kg of ALA relapsed to HGD significantly more frequently than those receiving 60mg/kg. Kaplan–Meier analysis of the 21 patients who were subsequently treated with this optimal regimen demonstrated an eradication rate of 89% for HGD and a cancer free proportion of 96% at 36 months' follow-up.

The first long term results of ALA PDT in patients with HGD were described by Pech.[Pech et al., 2005] This was a six year observational study that evaluated both efficacy and survival rates of 35 patients with a total of 44 ALA-PDT procedures. All patients received 60mg/kg ALA activated by red laser light. Complete remission was achieved in 34 of 35 (97%) of patients with HGD. Only 6% of patients with HGD had

progression to cancer during the median follow up period of 37 months. 6 patients (18%) developed a metachronous lesion, 5 of these underwent successful repeat treatment. The calculated 5 year survival was 97%. A further 31 patients with intra-mucosal cancer were studied with a total of 38 PDT treatments carried out. 29% had recurrence of metachronous lesions during median follow up period of 37 months. Calculated 5 year survival in this group was 80%.

Adverse events

Oesophageal strictures following ALA occur less commonly than with Photofrin, as the drug is mostly taken up in the mucosa.[Mackenzie et al., 2008] Photosensitivity reactions are rare and often mild as patients are sensitive to light for only 36 hours. More common side effects from oral ALA are nausea and vomiting and transient increases of serum alanine transaminase (ALT).[Regula et al., 1995]

There has been one case of acute neuropathy reported after ALA.[Sylantiev et al., 2005] The authors surmised that the patient likely had a silent porphyria prior to treatment. On the basis of available evidence current doses used in PDT are highly unlikely to result in neurological or other systemic toxicological findings.

Two deaths have been reported following ALA PDT in two separate studies.[Forcione et al., 2004;Haringsma et al., 2004] One death was reported as occurring 24 hours post PDT in a patient who was treated in an ambulatory setting. The patient was randomised to receive 13-cis-retinoic acid 14 days prior to treatment with ALA-PDT and died of acute cardiopulmonary failure; autopsy revealed aspiration pneumonitis.[Forcione et al., 2004] The cause of death in the other study was not identified. Other serious adverse reactions reported to date include hypotension and unmasking of angina pectoris although these appear to be self limited and manageable in an in patient setting.[Mackenzie et al., 2007a]

Foscan

Foscan (m-tetrahydroxyphenyl chlorin or mTHPC) is a powerful photosensitiser approved in Europe for the palliative treatment of advanced squamous cell carcinoma of the head and neck. Foscan is administered by intravenous injection after a drug-light interval of 3-4 days at a wavelength of 652nm (Summary of Product Characteristics, biolitec Pharma).

Clinical Studies

Javaid *et al.* in 2002, successfully treated 5 out of 7 patients with HGD or IMC at a median follow up of 1 year.[Javaid et al., 2002] Another study reported successfully treating 12/12 patients with HGD or IMC using green light to activate mTHPC for PDT with a median follow-up of 18 months. Just one patient required further PDT and this was successful.[Etienne et al., 2004]

Our centre has reported a non randomised study of 19 patients treated with Foscan PDT which compared red and green light activation via a diffuser balloon, and a bare tip fibre activated by red light.[Lovat et al., 2005] Seven had HGD and 12 had T1 or T2 cancers, all were unfit for surgery. The red light diffuser group achieved CR-HGD of 70% (4/6 patients with cancer and 3/4 with high-grade dysplasia). 0/3 patients achieved remission in the green light group. When using the bare-tipped fibre, there was one procedure-related death as described below and only 1/5 patients with cancers were successfully treated. Two others were downgraded to high-grade dysplasia.

Adverse Events

There have been two oesophageal perforations reported with mTHPC PDT, from taking multiple biopsy specimens too soon after therapy.[Lovat et al., 2005] Additional contributing factors were one patient received a very high light dose to a single area, and the other patient had received Nd-YAG laser prior to treatment. Skin photosensitivity is shorter than Photofrin, but lasts up to 1 month after treatment. Stricture formation has occurred in 13% (5/38) of patients presented in the 3 studies above. mTHPC is mainly

distributed in the submucosa although drug is also found in the mucosa.[Mlkvy et al., 1998]

In summary, although isolated studies showed promising initial results of Foscan PDT for HGD in BO, long term efficacy and safety data is lacking. The data on the use of Foscan for intramucosal cancers is inferior to newer techniques for these lesions (EMR) and serious adverse events are more common. For these reasons Foscan PDT is rarely used for the treatment of BO.

3.2.2 Thermal therapy

Argon plasma coagulation

Argon Plasma Coagulation (APC) is a noncontact technique in which monopolar energy is delivered to tissue using ionized argon gas, via a probe held a few millimeters from the target surface. There are many studies that report short term success rates for complete reversal of dysplasia and metaplasia between 60-100%, with efficacy apparently dependent on the power used and total energy delivered to the tissue.[Madisch et al., 2005;Attwood et al., 2003;Basu et al., 2002;Pereira-Lima et al., 2000;Schulz et al., 2000;Morris et al., 2001] In a RCT of 64 patients with NDBO comparing ALA PDT vs. APC, APC was associated with a significantly higher CR-IM than ALA PDT (97% vs. 50% respectively).[Kelty et al., 2004b] Limitations of the study were the suboptimal dose of ALA (30mg/kg), no stratification by length of BO and patients with less than 12 month follow up included in analysis.

The long-term efficacy of APC is questionable however, with recurrence rates as high as 66% in one study.[Mork et al., 2007] This may be a consequence of the relatively superficial injury inflicted by APC, as well as the inherent difficulty of applying the energy uniformly over the area of abnormal mucosa. Serious adverse events reported include oesophageal perforations, pneumomediastinum, strictures (4 -9%) and significant gastrointestinal bleeding following therapy at higher powers (60-90W) at 4-9%.[Ragunath et al., 2005;Pereira-Lima et al., 2000] These complication rates, and the introduction of newer ablation techniques have rendered APC largely obsolete for the

eradication of Barrett's oesophagus, although APC could still be used to eliminate small islands of Barrett's metaplasia.[Spechler et al., 2010]

Multipolar electrocoagulation

Multipolar electrocoagulation (MPEC) operates by delivering thermal energy to the oesophageal tissue by passing a current between two or more electrodes mounted on a probe that is advanced through the working channel of the endoscope. Sampliner *et al*. used MPEC to successfully treat 10 patients with BO.[Sampliner et al., 1996] In another study, Kovacs *et al*. reported an 80% reversal of BO in 27 patients.[Kovacs et al., 1999] The main disadvantage of MPEC is the relatively uncontrolled depth of injury which may vary from 1.7mm to 4.8 mm, depending on watt setting, degree of pressure applied to the probe, and duration of application.[Dulai et al., 2005] Therefore, the skill and the experience of the performing physician will determine the effect of the treatment and the occurrence of side effects.

Radiofrequency ablation

Radiofrequency ablation (RFA) using the HALO System (Barrx Medical, Sunnyvale, CA, USA) is a new technique for field ablation in the oesophagus. The HALO System uses ultra short pulse radiofrequency energy that delivers constant power of 40 W and energy density from 10-15 J/cm^2. A uniform ablation depth of 0.5-1 mm is achieved, thereby affecting the mucosa whilst preserving the submucosa. There are two devices, a balloon mounted electrode for field ablation (HALO^{360}, figure 3.10) and a smaller paddle device for focal ablation (HALO^{90}, figure 3.11). All catheters are single-use disposable devices. Clinical trials in U.S. and Europe have suggested that it is safe and effective for treating non-dysplastic IM, LGD and HGD in BO. The HALO Ablation System was most recently reviewed by the FDA in 2006, although the device has been cleared for human use since 2001. These devices also have a CE mark for use in Europe and has recently been approved in the UK by NICE for the treatment of HGD arising in BO. The technical set up is simpler than PDT, with no need for drug administration or hospital admission.

To perform RFA, the endoscopist first sprays the mucosa with a mucolytic agent (1% N-acetyl cysteine) in order to maximise energy delivery to the mucosa. The diameter of the

oesophagus is then determined using a 34 mm sizing balloon, normally not under direct vision. The appropriate sized HALO^{360} ablation catheters (sized 18-34 mm diameter) is then chosen and placed over the target field, which is treated in 3cm segments. Radiofrequency energy is delivered through the electrodes under direct vision to produce heat that vaporises the metaplastic tissue. Once the initial ablation is achieved the mucosa slough is cleaned, and the procedure is repeated (see figure 3.12). Contraindications include oesophageal varices, previous radiotherapy and previous myotomy. If there is evidence of fibrosis in the wall of the oesophagus, an ablation balloon with a diameter smaller than that determined by the measuring balloon is recommended to prevent oesophageal tears. RFA is not recommended if an oesophageal stricture is present as inflation of the treatment balloons (typical diameters of 28 to 31 mm) may cause perforations. Patients return 2–3 months after initial RFA treatment for repeat ablation until there is no visible columnar lined oesophagus.

Figure 3.10 HALO^{360}generator, sizing balloon and treatment balloon

Figure 3.11 HALO[90] focal ablation device

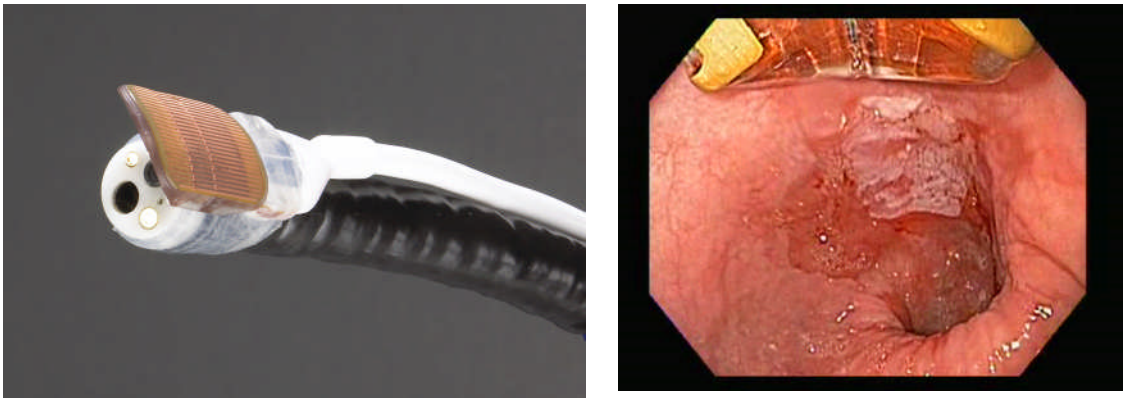

Figure 3.12 Endoscopic view of Barrett's oesophagus before and after RFA with HALO[360] device

From left to right a) circumferential BO with patchy squamous regeneration after failed PDT b)HALO 360 RFA device with balloon inflated, the white cauterised tissue of the first ablation can be seen proximally c) view of tissue after second ablation with tan appearance to ablated mucosa, d) healing with squamous regeneration 3 months post treatment

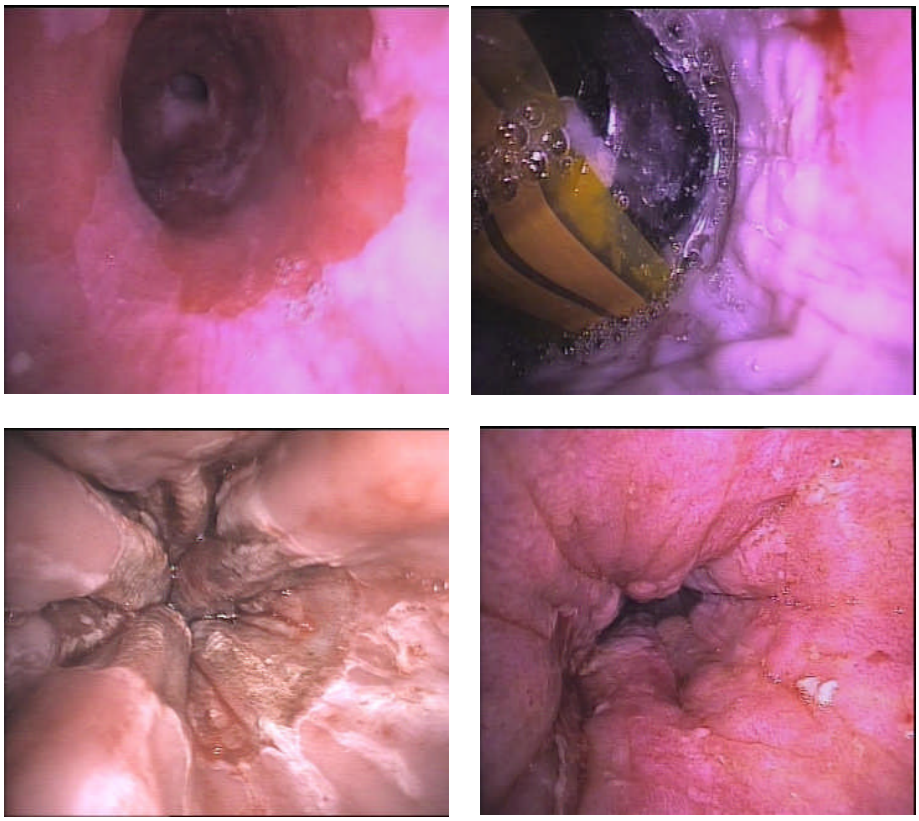

Clinical Studies

An early key study by Dunkin *et al.* determined the optimal ablation parameters for human oesophageal epithelium using the Halo^{360} balloon-based electrode.[Dunkin et al., 2006] Immediately prior to oesophagectomy, the subjects underwent endoscopy and ablation of segments of non-tumour-bearing oesophageal epithelium. Thirteen subjects were randomized to one of three energy density groups: 8, 10, or 12 J/cm^2 and ablative therapy was applied once proximally and twice distally. Following resection, the histological endpoints were complete epithelial ablation, maximum ablation depth and residual ablation thickness. Complete epithelial ablation occurred using two settings (10 J/cm^2 (twice) and 12 J/cm^2 (once and twice)) and the maximum depth of injury was the muscularis mucosae.

A 16 centre US Registry reported initial data on the use of HALO RFA at 12 J/cm^2 for HGD.[Ganz et al., 2008] Of 142 patients enrolled, 92 patients had at least 1 follow-up endoscopy and efficacy data was reported at 12 months following initial ablation. Among those patients, complete reversal of HGD (CR-HGD) was achieved in 90% (83/92) at a median 1-year follow-up; 80% (74/92) had complete reversal of dysplasia (CR-D) and 54% (50/92) had complete reversal of BO with no IM (CR-IM). No serious adverse events were reported and no SSBO was noted. One stricture occurred

In a randomised controlled trial of 127 patients (63 with HGD and 64 with LGD) randomised in a 2:1 study design, treatment with the HALO^{360} and HALO^{90} RFA devices was compared with a sham procedure. [Shaheen et al., 2009a] CR-D was achieved in 81% of those with HGD in the ablation group, as compared with 19% of those in the control group ($p<0.001$). For LGD the CR-D was 91% in the ablation group, as compared with 23% of those in the control group ($p<0.001$). For all patients CR-IM was 77% in the ablation group and 2% of patients in the sham group at 12-month follow-up ($p<0.001$). The rate of progression from HGD to cancer was significantly lower in those patients treated by RFA than those treated by sham procedure at 12-month follow-up (2% [1/42] and 19% [4/21] respectively) ($p = 0.04$). No LGD patients progressed to cancer in either group, consistent with the known low risk, transient nature and high inter-observer variability of this diagnosis. Although the length of follow-up in the RCT was insufficient

to assess the recurrence of Barrett's oesophagus after therapy, more recent data emerging has demonstrated that the 1 year results seem durable at 3 years.[Shaheen et al., 2010]

Other single centre studies from the US and Europe have demonstrated a CR-HGD between 83-96% with an average of 1.4 ablations per patient.[Roorda et al., 2007;Gondrie et al., 2008] A multi centre European trial has demonstrated preservation of the functional integrity of the oesophagus as measured by oesophageal physiology studies in 10 patients, and 100% eradication of dysplasia was also observed.[Bergman et al., 2006] The same group went on to study the properties of the neo-squamous mucosa following ablation. 22 patients were evaluated pre and post RFA for p53 and Ki67 immunohistochemical staining on biopsies, and FISH analysis for genetic abnormalities at chromosomes 1, 9 and 17 on cytology specimens.[Pouw et al., 2009] The authors found p53 or abnormal FISH probe distribution in all patients at baseline, which was not evident in the neosquamous mucosa at follow up.

There were several limitations to methodology of this study however. TP53 IHC is not as reliable a marker as PCR as it is method dependent. Ki67 is a common marker of proliferation known to be increased in cancer cell populations, but does not inform on presence of residual genetic abnormalities. Evaluation with FISH can be limited by the probes used (only 3 chromosomes evaluated) and sampling error of the brush cytology technique, which may not sample buried glands. Although no buried glands was reported in these samples, and 100% of the squamous epithelium was visualised, only 37% of biopsy samples had evidence of a lamina propria, so one cannot be certain that buried glands were not evident in the unapparent underlying mucosa. A better method may have been assessment of LOH, DNA ploidy or methylation of the biopsy samples.

The utility of HALO RFA for the treatment of non-dysplastic BO has been reported in a multicentre study involving eight US sites (ablation of intestinal metaplasia or AIM trial).[Sharma et al., 2007;Fleischer et al., 2008] There were two phases of the trial, AIM-I evaluated the dose-response and safety of ablation using 6, 8, 10, 12 J/cm^2 in 32 patients with a Barrett's length of 2-3 cm. The complete response rate for eradication of all

Barrett's mucosa was 0%, 10%, 67% and 55%, respectively, with histological clearance of Barrett's epithelium in 93%, 65%, 100% and 100%, respectively. Ablation at 10 J/cm^2 (two applications per session) was thereby established as the dosing regimen for the subsequent AIM-II phase.

In AIM-II, 70 patients underwent ablation at baseline, followed by an endoscopy with a biopsy at 1, 3, 6, and 12 months.[Fleischer et al., 2008] A second ablation was performed at 4 months for any patient with residual BO at 1 or 3 months. At one year follow up, 69 of 70 patients were available and the CR-IM was 70%. There were no biopsy specimens with signs of buried glands. According to the authors, this trial has been extended indefinitely, with a focal ablation device (HALO^{90}) used to treat any residual or recurrent disease present after 12 months follow up. Five year follow-up data from this study was recently published. [Fleischer et al., 2010]Of 50 patients who achieved CR-IM, 92% remained in remission at 5 years. Four patients relapsed to IM, and CR-IM was re-established in all after a single focal RFA session.

Adverse Events

Perhaps the largest study on safety experience with HALO RFA was of 508 HALO 90 procedures in the USA, with no serious adverse events.[Rothstein et al., 2007] Symptom diaries showed mild and transient symptoms after ablation which generally resolved by day 4. Within the randomised controlled trial adverse events included oesophageal stricture formation (6% per patient), gastrointestinal bleeding (1% per patient) and chest pain requiring hospitalisation (2% per patient).[Shaheen et al., 2009a] The reported oesophageal perforation rate is 0.02% per procedure (10/64,000 procedures, unpublished data from BARRX Medical).

3.2.3 Cryospray ablation

Cryospray ablation is a noncontact method of causing tissue destruction by application of liquid nitrogen or refrigerated gas onto the target mucosa. Initial devices used a probe tip but problems similar to MPEC (adhesion of the probe to the tissue, difficult control of depth of injury, risk of perforation) were incurred. Prototype devices that used spray

delivery of the cryogen through a catheter were subsequently developed in the late 1990s for use in the oesophagus.[Pasricha et al., 1999]

There are 2 different devices for cryotherapy in the GI tract. One device (CryoSpray Ablation, CSA Medical Inc, Baltimore, Md) uses low-pressure liquid nitrogen spray delivered through a 7-Fr catheter passed through the working channel of a standard endoscope (see figure 3.13). A separate orogastric or nasogastric tube placed alongside the endoscope is required to evacuate the expanded cryogenic gas. The other device (Polar Wand; GI Supply, Camp Hill, Pa) uses C02, and was built based on the Joule-Thompson effect, which refers to a drop in temperature of a liquid gas when its pressure drops. The device has undergone pilot testing in pig oesophagus but no studies in BO have been reported. [Raju et al., 2005]

Figure 3.13 Endoscopic view of spray cryotherapy

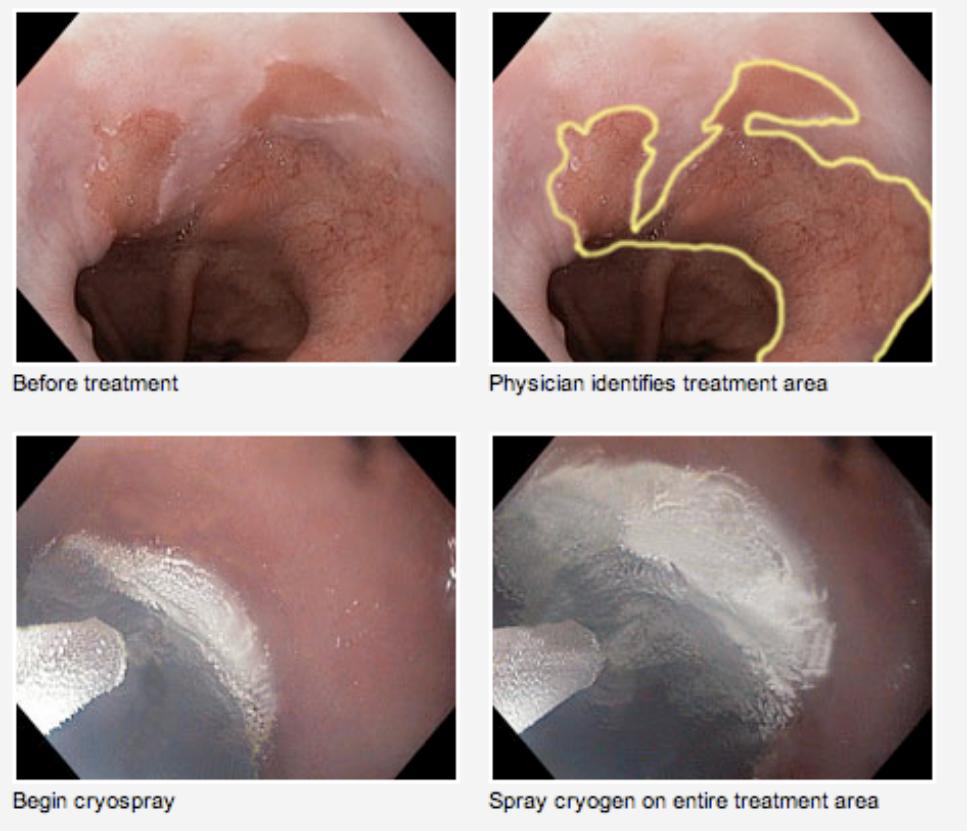

Clinical Studies

There are few studies on the efficacy of liquid nitrogen cryotherapy for ablation of BO. A pilot study of 11 patients with BO, including 5 with LGD and 1 with HGD, showed no dysplasia in any biopsy specimen after treatment with CSA at 1 and 6 months.[Johnston et al., 2005] No significant complications occurred and the treatment was well tolerated. Multi-centre pilot studies published in abstract from, have demonstrated CR-HGD of 89-93%, with a mean number of 4 treatment sessions for both studies.[Dumot et al., 2007;Shaheen et al., 2009b] The procedure seems well tolerated with no perforations or strictures reported. A multicenter registry, akin to the HALO RFA registry, is in development.[Dumot and Greenwald, 2008]

3.3 Endoscopic Resection

3.3.1 Endoscopic Mucosal Resection

Endoscopic Mucosal Resection (EMR) is an endoscopic technique developed for removal of sessile or flat neoplasms confined to the superficial layers (mucosa and submucosa) of the gastrointestinal tract. Several studies have demonstrated that EMR is safe and effective for complete resection of superficial lesions arising in BO.[Pech et al., 2007;Peters et al., 2007;Ell et al., 2000;May et al., 2002] An advantage of EMR, contrary to other ablative techniques, is the removal of a tissue specimen, which can be evaluated for accurate histopathological staging. EMR specimens are much larger than conventional endoscopic biopsies, typically 10-30mm in size. This allows for assessment of the vertical depth of tumour invasion, and the presence of lateral or deep margin involvement by carcinoma which cannot be assessed using standard mucosal biopsies.[Prasad et al., 2007a;Lauwers et al., 2009] This is important as the rationale of accurate staging of T1 OAC for potentially curative endoscopic therapy is the very low rate of lymph node metastases limited to the mucosa (T1a) of 0-0.03% vs. submucosal cancers (T1b) which have an 18-41% lymph node metastases rate. [Nigro et al., 1999;Fernando et al., 2002;Rice et al., 1998] In addition, two recent studies have demonstrated that there is less

interobserver variability among pathologists in the analysis of EMR samples than biopsy specimens for the diagnosis of dysplasia.[Wani et al., 2010;Mino-Kenudson et al., 2007b]

There are several techniques for EMR in the oesophagus which may be broadly classified into techniques with and without suction. Examples of techniques without suction include the “inject and cut” technique and the “strip biopsy” technique, when a specific solution (saline or adrenaline solution) is injected into the submucosa under the lesion prior to snare resection with a blended electrosurgical current.[Tada et al., 1988] Suction or “suck and cut” techniques use a cap that is placed on the end of the endoscope, which is then placed over the region of interest and suction applied to bring the mucosa into the cap. The cap can be either pre loaded with a 0.3 mm monofilament stainless steel wire snare or, perhaps the most practiced method, a modified multiband variceal ligator (Duette multiband mucosectomy (MBM) kit, Cook, Ireland, see figure 3.14).[Inoue et al., 1994;Chaves et al., 1994;Soehendra et al., 2006;Fleischer et al., 1996] This method is described in figure 3.15.

Figure 3.14 Modified multiband variceal ligator

Duette multiband mucosectomy (MBM) kit, Cook, Ireland

Figure 3.15 Image sequence of EMR procedure

Left to right – a) Nodular area at 11 o'clock position b) EMR cap is seen on tip of endoscope as suction is applied to mucosa c) band placed with some minor haemorrhage d) snare inserted into cap e-g) snare is deployed underneath band and electrosurgical current applied h) polypoid lesion is sucked into cap and removed i) crater formed post EMR with mucosa visible

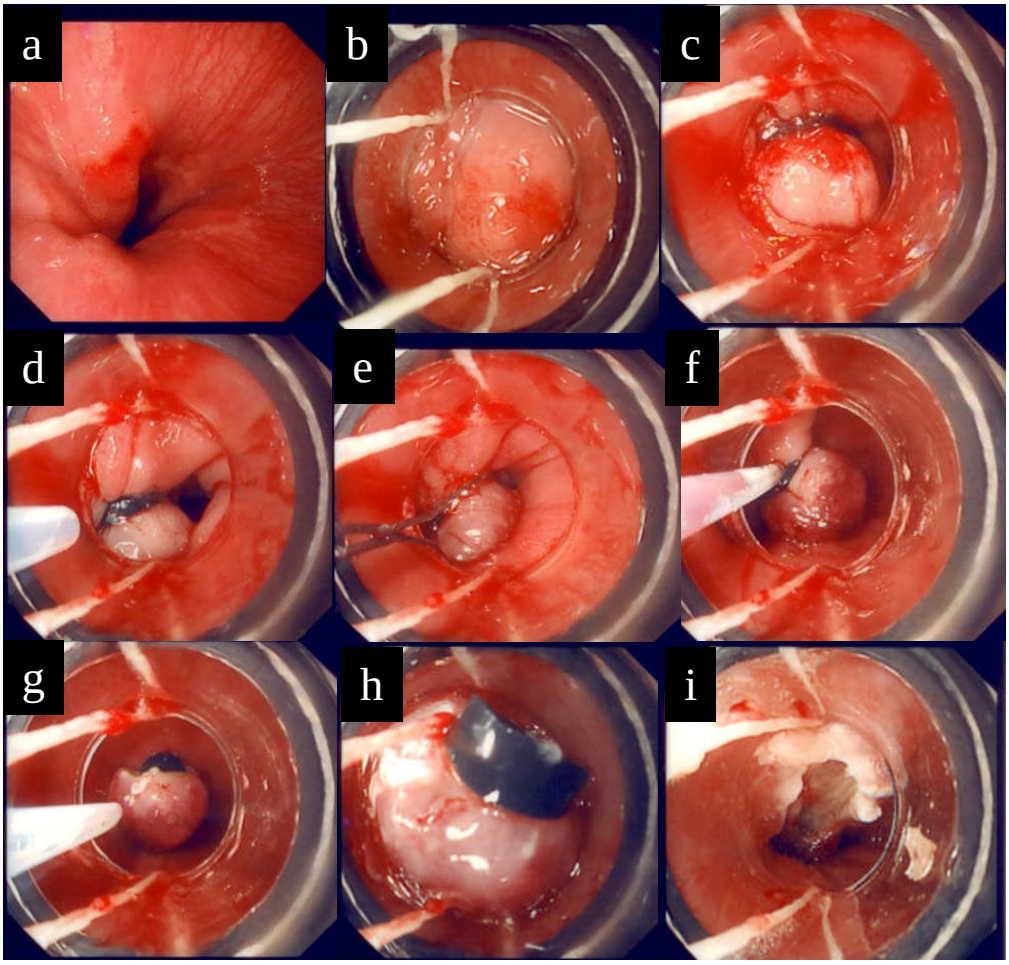

Clinical Studies

The majority of early studies on the use of EMR in BO come from the Wiesbaden group in Germany. Ell *et al*. prospectively evaluated the role of EMR in 61 patients with intramucosal cancer and 3 patients with HGD arising in BO.[Ell et al., 2000] These patients were then separated into two groups according to risk of progression or metachronous lesions defined by four criteria.

1) Lesion diameter
    a. Low risk - <20 mm
    b. High risk - >20 mm
2) Endoscopic staging according to Paris classification
    a. Low risk - Type I (polypoid), Type IIa (Flat and elevated), Type IIb (flat) or Type IIc (depressed) lesions <10mm
    b. High risk - Type III (ulcerated)
3) Histopathology grade
    a. Low risk - well or moderately differentiated adenocarcinoma or HGD
    b. High risk - poorly differentiated adenocarcinoma
4) Depth of invasion
    a. Low risk - limited to the mucosa (T1a)
    b. High risk - involving the submucosa (T1b)

In the low risk group (36 patients) complete remission was achieved by EMR alone in 97% of cases. For high risk group (28 patients) complete remission was achieved in only 59%. Over a mean follow up period of 12 months, recurrent or metachronous carcinomas were found in 14% of cases, and all underwent repeat EMR with clear margins.

In a larger prospective study 100 patients with low-risk lesions (as previously described) were treated with either cap-assisted or ligation-assisted EMR.[Pech et al., 2007] Using this approach a 98% CR-D was achieved and overall calculated 5 year survival was 98%. There are however several criticisms of this paper. The authors present overall 5-year survival of 98%, though cancer free survival would have been a stronger end point, which could not be concluded as only 11 patients reached this follow up. It is generally accepted that complete R0 resection is a key feature of curative treatment for cancer, including early oesophageal cancer. [Kelsen et al., 2007;von Rahden and Stein, 2008] The authors presented their basal R0 resection rate as 100%, though one may expect this given an inclusion criterion was ‘lesions limited to the mucosa (m type) on the basis of staging procedures and proved by histology of the resected specimen’. In fact the resection specimens were predominantly lateral R1, with only one third being complete R0

resections. The R0 rate is even more questionable, considering that the histopathological evaluation of the specimen may be severely confounded when the technique is piecemeal, which was noted in 30% of patients.

The study design further limits meaningful interpretation of the data, as the analysis was not undertaken on an intention to treat basis, but rather as a cohort study design which was highly selected according to pathological staging after EMR. Indeed different treatment was initiated in the follow up phase as some patients received field ablation (with either APC or ALA PDT) post EMR whereas others did not, and separate analysis of these 2 groups was not presented. Finally the author's claims that 'EMR is superior to surgery with regard to morbidity and mortality, and at least equivalent to it with regard to the long-term survival' may be premature from the data presented, as no surgical data was analysed from a similar patient cohort. The same group has subsequently published a study on a larger group of 349 patients treated with EMR +/-PDT for HGD or IMC with mean 5 year follow up. [Pech et al., 2008] This study demonstrated a higher recurrence rate of 21.5%, lower CR-D of 96% and a drop in the 5-year survival rate to 84%.

Prasad *et al.* compared surgical and endoscopic approaches to T1a cancer in a retrospective cohort study of 178 patients.[Prasad et al., 2009] One hundred and thirty two patients underwent endoscopic therapy, 75 EMR alone and 57 EMR + PDT (ENDO group). Forty six patients underwent oesophagectomy (SURG group). The median size of the lesions treated endoscopically was 1 cm (interquartile range [IQR], 0.9–1.6 cm). Fifty-nine percent of EMRs were performed using the Olympus EMR cap, 21% using the Duette multiband device, and the remaining 20% by using the single-banding device followed by snare resection. Remission rate were comparable between the EMR alone and EMR + PDT groups (96 and 91% respectively). Sixteen patients had recurrent lesions from the ENDO group: 14 were treated with repeat EMR, 1 with oesophagectomy and 1 with chemoradiation. Follow-up evaluation was 244 person-years in the SURG group and 465 person-years in the ENDO group. There was no significant difference in cumulative mortality between the two groups, 17% (23 of 132) in the ENDO group and 20% (9 of 46) in the SURG group. The authors concluded that overall survival in patients with

intramucosal cancer treated endoscopically appears to be comparable with that of patients treated surgically.

Adverse events

Complication rates of EMR are very low from published series. When assessing 12 trials published on EMR alone in 805 patients the overall acute minor bleeding (treated with single modality, no drop Hb>2g/dl or need for transfusion) was in the range 0.6% to 6%. Strictures occurred in 4% and increased in frequency when greater than 50% of the oesophageal lumen was resected. Perforations are very rare in the oesophagus (0.12% of all patients) when compared to the stomach (4.9%) [Minami et al., 2006].

Combination of EMR and Field Ablation

Although the short term success rates for complete elimination of all neoplasia are high, ranging from 83-98%, complete eradication of all Barrett's mucosa is rarely achieved. The development of new or recurrent lesions during follow-up is seen in a considerable number of patients (0-39%). Subsequent studies have addressed the question whether a combination of EMR and field ablative therapy is more effective for long term cure than EMR alone. These are summarised in Table 3.4.

The overall CR-HGD ranges from 83-98% with recurrence rates of 0-33%, although the majority of studies have a short mean follow up of 12 months. One study, that evaluated the combination of EMR and ALA PDT in 20 patients with HGD or IMC, reported a significant difference in the success rate that was dependent on the presence of residual HGD after EMR.[Peters et al., 2005] The overall success rate was 15/20 (75%) but when the patients were separated into two groups based on the presence or absence of residual HGD in the remaining BO segment, the rate was 55% for residual HGD vs. 100% for no residual dysplasia. This success rate was calculated at 3 months however, and 4/15 cases subsequently relapsed to HGD/OAC within 1 year of treatment, and were not amenable to rescue EMR. Therefore the overall CR-HGD was 55%. Criticisms of this paper include the study design and the dosing of ALA (40mg/kg) which may be considered sub-optimal treatment.

Table 3.4 Clinical results of patients treated with combination of endoscopic mucosal resection and field ablative therapy

AUTHOR	ABLATION THERAPY STUDIED	NO PTS TREATED	CR-HGD	FOLLOW UP (MO)	NO OF TREATMENT SESSIONS	RECURRENCES
[Pacifico et al., 2003]	EMR + sp-PDT	24	20 (83%)	12 +/- 2	n/a	0
[Buttar et al., 2001a]	EMR + sp-PDT	17	16 (94%)	13	2.5	1 (6%)
[May et al., 2002]	EMR + ALA-PDT	9	8 (89%)	34 +/- 10	3.8 +/- 2.5	3 (33%)
[Peters et al., 2005]	EMR + ALA PDT	20	15(75%)	30 (22-31)	2.4	4 (20%)
[Ganz et al., 2008] (subgroup analysis HALO registry)	EMR + HALO RFA	24	21 (88%)	12 +/- 4	1 +/- 1 RFA, EMR n/a	n/a
[Gupta et al., 2010]	EMR + HALO RFA and/or APC	51	50 (98%)	11.5	4.9	2 (4%)
[Pouw et al., 2010b]	EMR + HALO RFA	23	22 (95%)	22	n/a	2 (9%)

The only prospective cohort study of the combination of HALO RFA and EMR published to date was undertaken in 3 European centres on 23 patients, 16 with IMC and 7 with HGD. [Pouw et al., 2010b] The worst residual histology results, post EMR but pre RFA were HGD (10 patients), LGD (11 patients), and intestinal metaplasia (3 patients). CR-D and CR-IM after field ablation were 95% and 88% respectively. Two patients required rescue EMR, although none have required additional therapy after a median follow up of 22 months. Complications included delayed bleeding (n = 1) and dysphagia (n = 1).

In a recent US multicentre study (published in abstract form) 51 patients, the majority with HGD or IMC (95%), were treated with RFA (23 patients) APC (13) or both (15). The mean time to achieve CR-IM was 17.4 months (range, 2.6–48.1), with length of BO as the only significant predictor. Complications included bleeding (n=6), stricture (n=3) and one perforation. After a mean follow-up of 11.5 months (range, 0–66.1), 1 patient progressed to cancer, 2 had recurrent HGD, and 1 had recurrent IM.[Gupta et al., 2010]

These studies demonstrate the combination of EMR plus field ablation may be more effective than EMR alone, although the recurrence rate of 0-33% is still high and the follow up of these studies is short. Disadvantages of this approach are the number of treatment sessions required to achieve CR-HGD, ranging from 3-5, and need for continued close surveillance during follow up.

Complete Stepwise Endoscopic Resection

A new approach to the endoscopic treatment of BO is the complete removal of the Barrett's segment by EMR, dubbed 'Stepwise Endoscopic resection (SER)' in Europe or 'complete Barrett's eradication (CBE)' in the US. The efficacy and safety of this approach has been demonstrated in two studies. The first was a single centre US study of 49 patients (33 HGD, 16 IMC), 32 of whom were analysed.[Chennat et al., 2009] EMR was undertaken using multiband ligator, cap-assisted, and / or "inject and cut" techniques and the mean number of treatment sessions was 2.1. CR-IM was achieved in 31/32 patients after a mean follow up of 22.9 months. The rate of symptomatic oesophageal stenosis was 37%, and all were successfully managed by endoscopic treatment. No perforations or uncontrollable bleeding occurred. The second was a multi-centre European study which treated 169 patients with high-grade dysplasia or early carcinoma by complete EMR of their Barrett's segment.[Pouw et al., 2010a] After a median of 2 treatment sessions CR-D was achieved in 95%, and CR-IM 89%, and this was maintained after a median follow up of 27 months. The recurrence rate for metachronous disease was 1.8%. Importantly, the most advanced histological findings were always encountered at the initial EMR session, where the most suspicious lesion was removed first. The rate of

symptomatic oesophageal stenosis in this study was 50%, and a third of these were graded as severe as they required more than 5 dilatation sessions. Serious adverse events included perforation in 4/169 patients or 2.4% of study population, and bleeding (4/169). These results are the largest experience to date with circumferential EMR although the retrospective cohort design, enrolment of BO <5cm length and restriction to highly skilled endoscopists at large volume centres limit the generalisability of the study.

It remains to be seen which approach for the ablation of Barrett's mucosa is most effective. A randomised control trial has been undertaken in Europe to compare SER with combination of EMR + HALO RFA, and preliminary results were recently published in abstract form. [Van Vilsteren et al., 2009] Forty-seven patients with HGD or IMC and < 5cm BO were randomized, 25 to SER and 22 to RFA. CR-IM was achieved in 96% and 95% of subjects in each group and the median number of sessions required to reach this end point was similar: 2 in the SER group and 3 in the RFA group. The incidence of stenosis was significantly higher in SER group (86%) vs. RFA group (14%) ($p<0.001$). There was one perforation, from the SER group. Based on there preliminary results, the authors recommended a combined approach of focal EMR for visible lesions followed by RFA for complete eradication of remaining BO, although final results of this study with long term follow up and information on rates of recurrence are awaited.

3.3.2 Endoscopic Submucosal Dissection

Endoscopic Submucosal Dissection (ESD) has been developed and used primarily in Japan for en bloc removal of large (usually more than 1.5 cm), flat GI tract lesions. The procedure is usually done in several steps. First, the margins of the lesion are marked by electrocautery, and submucosal injection is used to lift the lesion. Then, a circumferential incision into the submucosa is performed around the lesion with specialized endoscopic electrocautery knife (e.g. ceramic tip knife, triangle tip knife, flex knife, hook knife, standard needle knife). Finally, the lesion is dissected from underlying deep layers of GI tract wall with the electrocautery knife and removed. This technique requires meticulous endoscopic control and the use of a cap to help with the submucosal dissection.

ESD has been attempted in the context of intramucosal Barrett's cancer to achieve en bloc resection but experience to date is limited.[Seewald et al., 2008] Yoshinaga *et al.* performed ESD in 15 cases of junctional T1 cancers due to Barrett's esophagus (14 short segment and 1 long segment).[Yoshinaga et al., 2008] En bloc dissection of the lesion was achieved in all cases and the size of the resected specimen ranged from 25 mm to 60 mm. The success rate was determined by the depth of invasion – 11 T1a, 4 T1b. Of the T1a cases no recurrences were observed during a mean follow-up of 30 months.

The major proposed advantage of ESD over EMR is the ability to remove a neoplastic lesion *en-bloc*, which provides more precise determination of its vertical and lateral margins and, in gastric cancer, a reduced rate of local recurrences when compared with piecemeal resection. However, ESD is a technically challenging and lengthy procedure that sometimes requires hours to complete and serious complications such as perforation or strictures are common. Furthermore in BO, reflux induced inflammation can cause submucosal fibrosis and increased difficulty. These concerns have limited the use of ESD in BO.

3.4 Subsquamous SIM

A concern following all ablative therapies is the partial treatment of Barrett's epithelium with healing and squamous regeneration over the top of the Barrett's mucosa, which is hidden from the endoscopist's view at follow up, so called subsquamous specialised intestinal metaplasia (SSIM). The presence of SSIM is reported following all ablative therapies, with a frequency 0%-40% after PDT, and 0-60% after APC. There have been several cases reports of adenocarcinoma arising unnoticed underneath normal squamous tissue, at a rate of 0-3.7%. [Gossner et al., 1998;Overholt et al., 1999;Overholt et al., 2003] One case series of 52 patients undergoing Photofrin PDT found the rate to be as high as 35.1%.[Mino-Kenudson et al., 2007a] A more recent study, the largest of SSIM to date, evaluated 33,000 oesophageal biopsies in patients undergoing PDT within a randomised trial. [Bronner et al., 2009] The rate of SSIM was 5.8-30% of patients treated, but a similar frequency was found in the group treated with PPI alone (2.9-33%). In a randomised controlled trial of radiofrequency ablation, the frequency of subsquamous SIM was reduced post therapy, (25 to 5%) and increased in the PPI alone group (25-

40%).[Shaheen et al., 2009a] Other studies have shown that the neoplastic potential of SSIM post PDT, as measured by Ki67 (a proliferative marker) and DNA ploidy, may be lower than that of pre PDT SSIM. [Hornick et al., 2008] The significance of SSIM is yet to be determined.

3.5 Summary

The emergence of endoscopic therapy for the treatment of HGD in BO has been paralleled by studies into the use of PDT and APC. These techniques have been shown to be effective in reversing dysplasia and present a viable alternative to oesophagectomy. More recent techniques for ablation of Barrett's epithelium are RFA and cryospray ablation with liquid nitrogen, which has shown promising results in single centre studies. These techniques are potentially advantageous over PDT, with no need for drug administration, hospital admission or general anaesthetic, meaning patients can have the procedure as a day case. Initial efficacy and safety data are promising, though long term follow up is awaited.

Dysplasia is however an imperfect marker of cancer risk and convincing evidence of long term cancer prevention is lacking. Questions also remain regarding the long term durability of the ablated Barrett's mucosa, and there is much interest in the use of biomarkers as surrogate prognostic biomarkers. Genetic abnormalities, including p16 and proliferation markers have been shown to persist post PDT and predict recurrent dysplasia. Prospective studies on the use of biomarkers to guide further treatment and surveillance intervals are awaited.

In conclusion, endoscopically delivered minimally invasive therapy presents a viable alternative to surgery for patients with HGD in BO. Which therapy is chosen will depend on many factors, including regional availability, institutional expertise, cost, and ultimately patient acceptability.

Chapter 4
Aims of this thesis

Chapter 4 Aims of this thesis

The central aim of this thesis is to develop optical techniques for the risk stratification and treatment of patients with Barrett's oesophagus. Risk stratification will be assessed by evaluation of the optical properties of the nucleus by digital image analysis, and evaluation of the optical properties of the mucosa by ESS. The DNA replication licensing factors will be assessed by immunohistochemistry as potential surrogate biomarkers for nuclear abnormalities. Finally the use of PDT to treat dysplasia will be evaluated.

DNA ploidy by flow cytometry has not been adopted for the routine risk stratification of cancer progression in BO, despite reaching phase 4 biomarker status. DNA ploidy analysis by image cytometry has great potential as an alternative technique which has been shown to have prognostic significance in many cancers, but data in BO is lacking. The first part of this thesis will aim to validate the use of image cytometry to detect DNA ploidy. This will be addressed by optimising the technique and then comparing accuracy with flow cytometry carried out at the University of Washington, which has a strong pedigree of research in this field. We will then test image cytometry as part of a multi centre MRC funded biomarker validation study. This is a case control series of 500 patients with non dysplastic BO from the Northern Ireland Barrett's Oesophagus Registry (NIBR). Image cytometry will also be evaluated for two new potential applications – risk stratification following PDT for HGD in BO and analysis of cytology specimens.

The second part of my thesis will investigate nucleotyping (NT) – a new methodology which uses high resolution digital images to analyse nuclear texture and hence inform on chromatin organisation. Firstly the accuracy of NT will be assessed in the comparison of dysplastic and non-dysplastic BO. If this is achieved, the utility of NT as a prognostic biomarker will then be evaluated on the same nuclear monolayers used in the aforementioned NIBR case-control study. The combination of ICDA and NT as a single platform chromosomal instability biomarker will also be assessed.

In the third section I will investigate DNA replication licensing factors in oesophageal adenocarcinoma. These factors play a key role in regulation of the cell cycle and may act as surrogate markers for DNA ploidy abnormalities. By using laser capture microdissection and image cytometry, I will evaluate the correlation of DNA ploidy abnormalities with immunohistochemical staining of these novel potential biomarkers.

In the fourth section of this thesis I will test Elastic Scattering Spectroscopy (ESS) for the detection of DNA ploidy abnormalities *in vivo*. The work will include a prospective cohort study to compare the effect of different spectrometers on accuracy of DNA ploidy diagnosis. A prospective pilot study of ESS will be conducted, with appraisal of a real time ESS targeted biopsy protocol vs. a four quadrant random biopsy protocol. In addition, the field effect in Barrett's carcinogenesis will be explored.

The final section will focus on the study of minimally invasive endoscopic therapies. Firstly a randomised controlled trial of PDT for HGD in BO, comparing ALA and photofrin, will be completed. Efficacy, safety and quality of life data will be collected and analysed. Finally, in a case series, I will evaluate safety and efficacy of radiofrequency ablation plus endoscopic mucosal resection for the treatment of patients who have failed PDT.

Chapter 5

Validation of image cytometry for the detection of DNA ploidy abnormalities

Chapter 5 Validation of image cytometry for the detection of DNA ploidy abnormalities

5.1 Introduction

The development of neoplasia and malignancy is associated with defects in genes in control of the cell cycle, and ultimately proliferation and death. The cell cycle phases are shown in figure 5.16. Cells designated in the G0 phase are not cycling at all; cells in the G1 phase are either just recovering from division or preparing for the initiation of another cycle; cells are said to be in S-phase when they are in the process of synthesising new DNA; cells in the G2 phase continue to grow in preparation for mitosis; and cells in the M phase are in mitosis, undergoing the chromosome condensation and organisation that occur immediately before cytokinesis resulting in two daughter cell each with equal 2C DNA (2 copies of each chromosome or 46 chromosomes).

Figure 5.16 Schematic of eukaryotic cell cycle

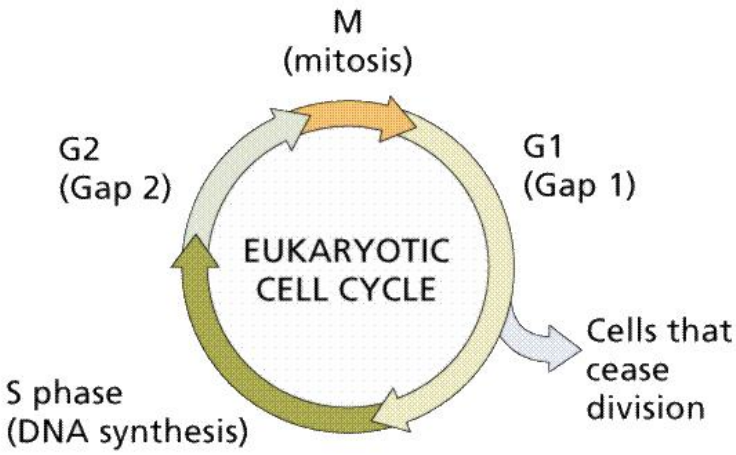

Cell cycle checkpoints are used by the cell to monitor and regulate the progress of the cell cycle, and are designed to ensure that damaged or incomplete DNA is not passed on to daughter cells. Two main checkpoints exist: the G1/S checkpoint and the G2/M checkpoint. The G1/S checkpoint is a rate-limiting step in the cell cycle and is also

known as restriction point. This is mainly controlled by the cyclin D kinase (CDK) inhibitor p16 which inhibits CDK4/6 from binding to cyclin D1. The G2/M checkpoint prevents the cell from entering mitosis (M phase) if the genome is damaged. The cell division control (cdc) 2-cyclin B kinase is pivotal in regulating this transition. TP53 plays an important role in triggering the control mechanisms at both G1/S and G2/M checkpoints.

The majority of eukaryotic cells reside in non-proliferating 'out-of-cycle' states. Initiation of DNA synthesis at specific sites (origin firing) is tightly restricted to permit duplication of the genome once only per cell cycle and transition through the G1/S and G2/M checkpoints is tightly regulated in a normal cell population.[Going et al., 2002] In cancer cell populations several important pathways have been shown to deregulate the cell cycle and promote carcinogenesis by delivering excessive signals to cycle cell check points. These include the Wnt pathway in colorectal cancer and the Ras pathways in pancreatic, colorectal and lung cancer.

In Barrett's oesophagus DNA content abnormalities, large scale genomic instability due to deregulation of the normal cell cycle, may be an important precursor to cancer. Several studies have documented DNA content abnormalities (aneuploidy or tetraploidy) in advancing stages of neoplastic progression in parallel to increased proliferative activity.[Reid et al., 1992;Ottesen et al., 2000;Blant et al., 2001;Rajagopalan et al., 2003;Pretorius et al., 2009;Bondi et al., 2009] A series of landmark studies by Reid's group in Seattle demonstrated the relative risk of progression from BO to OAC was significantly greater for patients who displayed aneuploidy and/or tetraploidy than those patients who demonstrated a diploid cell population.[Reid et al., 2000b;Reid et al., 2001;Rabinovitch et al., 2001] The most commonly used method to quantify DNA content of cells is flow cytometry (FC), which allows quantification of the S phase fraction, G2/tetraploidy fraction and aneuploid cell populations. Cytometry depends on the detection of the substance of interest by a specific dye, and the ability to measure the concentration of that dye. Flow cytometry uses either DAPI (4',6-diamidino-2-phenylindole) or propidium iodide, which are fluorescent stains that bind

stoichiometrically to DNA, i.e. the amount of stain is proportional to the amount of DNA. The tissue is disaggregated to form a nuclear suspension and then stained prior to processing through the flow cytometer. Many different systems exist with inherent problems of inter-laboratory variablilty and maintenance of quality control. In addition FC is expensive to set up, nuclear suspension preparation is labour intensive and more than 10,000 nuclei are needed for accurate histogram interpretation. For these reasons FC has not been adopted for routine clinical use in BO.

An alternative method for quantifying DNA content is image cytometry DNA ploidy analysis (ICDA). With this method (also referred to as Digital Image analysis or laser scanning cytometry) the nuclear suspension is spun onto a glass slide to form a nuclear monolayer. The slide is subsequently treated with Feulgen to stain the DNA or chromosomal material in the specimen. Feulgen only stains aldehydes, and after cytoplasm digestion the only aldehydes remaining are those formed from the hydrolysis of DNA (by HCl). Feulgen staining, like DAPI and propidium iodide, is stoichiometric and therefore provides a quantitative measure of the DNA in the nucleus. Image galleries of the nuclei are captured with a high resolution black and white digital camera under transmitted green light using a 546 nm filter. As ICDA measures the total amount of DNA per nucleus, the complete image of the nucleus is required, and the nucleus should be distinct from its background environment. Cut or overlapping nuclei (so called doublets) should not be assessed. These problems can be overcome by segmentation software that accurately separate nuclei into galleries for analysis. Using a range of pre-defined criteria relating to the physical properties of the nuclei including total area, symmetry, eccentricity, and optical density the image cytometry software selects nuclei. These ‘rules’ for nuclei selection from the slide are kept deliberately broad, resulting in the collection of a number of partial or doublet nuclei whilst minimising the risk that whole nuclei are ‘missed’ on account of being very large or ‘oddly’ shaped. Ideally, a minimum of 300 non overlapping nuclei should be measured.[Russack, 1994]

Flow cytometry and image analysis are both useful tools for examining cellular DNA, and the strengths and weaknesses of each are shown below in Table 5.5.[Russack, 1994]

Potential sources of error in FC are tetraploid and >5c cell populations due to interpretation of these cell populations as probable doublets, whereas ICDA can accurately detect tetraploid and >5c cell populations by direct visualisation. In contrast, lower-resolution histograms generated using digital image analysis make discerning near diploid nuclei less likely. Stated another way, flow cytometry can distinguish moderate-to-large cell populations with small DNA abnormalities, whereas image analysis can distinguish very small populations of cells with major DNA abnormalities.[Russack, 1994] The comparison of the two techniques has been evaluated in many tumours with concordance rates between 82-94%. [Chen et al., 1995;Lee et al., 1991;Bauer et al., 1990;Kaern et al., 1992]

Table 5.5 Comparison of flow and image cytometry

Adapted from Russack et al – Image cytometry current applications and future trends [Russack, 1994]

Flow Cytometry vs. Image Analysis

	Flow cytometry	Image analysis
Specimens	Fresh, frozen, paraffin-embedded	Same
Controls	Normal peripheral blood lymphocytes, preferably gender specific; alternately, nucleated animal erythrocytes	Normal cells in specimen or norma animal cells (e.g., rat hepatocytes
Sample preparation	Disaggregation of tissue to make cell suspension (fresh cells only) or nuclear suspension (fresh, frozen, paraffin-embedded)	Imprints; cytospins; direct smears; monolayers of cell or nuclear suspensions; tissue sections
DNA staining	Fluorescent intercalating dyes (propidium iodide, ethidium bromide, acridine orange) base-pair affinity dye (DAPI, Hoescht dyes)	Feulgen stain or other stoichiometric nuclear stain
Quantitation of DNA staining	Fluorescence intensity	Optical density
Quantitation of proliferative activity	Computerized statistical calculation of S-phase fraction using same data input as for DNA ploidy evaluation	Simultaneous or parallel staining of specimen with Ki-67; computerized calculation of % nuclei stained or % nuclear area stained
Advantages	Rapid analysis of large cell populations; high-resolution histograms; good for detecting near diploid populations	Only small numbers of cells required; direct morphologic correlation; good for detecting small aneuploid populations; good for detecting tetraploid populations
Disadvantages	Requires large numbers of cells or nuclei; indirect morphologic correlation	Moderately labor intensive; statistical evaluation more difficult

Our centre has previously compared FC vs. ICDA in BO, using 10 samples snap frozen in liquid nitrogen at endoscopy from the University of Washington (UW) in Seattle. The nuclei were then liberated using a standardised methodology [Rabinovitch et al., 2001] and prior to staining for flow cytometry the sample was split into two portions. These were then assessed blindly at UW and UCL. Five cases were diploid and five aneuploid/tetraploid, and consensus for agreement was achieved in all cases. The proportions of abnormal nuclei and mode of peaks in the abnormal samples were also similar.

The methodology used for the processing of tissue specimens for image cytometry utilised at UCL differs from UW, as thick sections (40-50 μm) are cut from formalin fixed paraffin embedded (FFPE) samples. This is a more practical way of obtaining tissue, as most hospitals use FFPE tissue for routine histopathology whereas the availability of liquid nitrogen to snap freeze samples during an endoscopy list is limited. An additional benefit is the ability to analyse archival material, valuable when planning longitudinal studies on disease progression. To use ICDA with paraffin embedded blocks, and show that this is a robust method for detecting DNA content in BO, it is necessary to test its accuracy *versus* an independent centre with expertise in FC, at the University of Washington in Seattle.

5.2 Aims of this chapter

The aims of this chapter are to evaluate the storage, transport, processing and use of different types of staining, for evaluation of DNA content abnormalities by ICDA. These initial experiments will optimise our technique for the transportation of samples to UW for a comparative study on FFPE samples. The utility of ICDA as a prognostic biomarker will then be evaluated in a multicentre nested case control study of disease progression and a single centre case control study of relapse following PDT. Finally an experiment to evaluate ICDA from cytology brushing samples as a potential screening tool was planned.

5.3 Materials and Methods

The method of processing samples for image cytometry analysis from paraffin embedded tissue was adapted from the European Society of Analytical Cellular Pathology (ESACP) guidelines [Bocking et al., 1995] and the methodology published by Hedley *et al.* [Hedley et al., 1983].

5.3.1 Monolayer preparation

This methodology can be divided into two steps; the liberation of nuclei from paraffin embedded tissue and the Feulgen staining process. The methodology is summarised in Appendix A.

5.3.2 Measurement of DNA ploidy

The Fairfield DNA Ploidy system (Fairfield Imaging, Kent, UK) is an automated image cytometric analyser that consists of a Zeiss Axioplan microscope (Zeiss, Jena, Germany), a 546-nm green filter, and a black-and-white, high-resolution digital camera (model C4742-95, Hamamatsu Photonics, Japan). Optical density and nuclear area were measured and integrated optical density of each nucleus was calculated. Background optical density was corrected for each nucleus. Segmentation software (a range of pre-defined criteria relating to the physical properties of the nuclei) automatically selects whole nuclei. At least 1000 nuclei were scanned automatically and sorted into 4 separate galleries for each cell type: nuclei of interest for measurement, lymphocytes, plasma cells and fibroblasts. The lymphocytes were used as reference cells to determine the position of the diploid peak (2c). All galleries were then edited manually to discard any cut or overlapping nuclei. The integrated optical density of each nucleus of interest was calculated and a histogram of DNA content produced. Ploidy-related parameters such as DNA index (DI) and percentages of cells exceeding 5c (5c ER) and 9c (9c ER) were also noted.

5.3.3 Histogram interpretation

Histograms were analysed according to European Society for Analytical Cellular Pathology (ESACP) guidelines [Bocking et al., 1995] as follows -

i. A specimen was defined as diploid when there was only one peak (which was 2c, or DI 0.9-1.1) during the G0 or G1 phase, or when there was a second 4c peak (DI 1.9-2.1) representing less than 6% of the total, and when the number of nuclei with a DNA content of more than 5c did not exceed 1% of the total.

ii. A specimen was defined as DNA tetraploid when there was a population of 4c nuclei (DI 1.9-2.1) more than 6% of the total, representing stage G2 of the cell cycle.

iii. A specimen was defined as aneuploid when there was a population of nuclei with abnormal DNA content, separated from the diploid peak to the right (DI > 1.1), and representing more than 2.5% of the total or when the number of nuclei with a DNA content of more than 5c or 9c exceeded 1% of the total. Aneuploid cases were further divided into near diploid aneuploid (1.11-1.29) and aneuploid (1.30-1.89).[Lindahl et al., 1994]

iv. A specimen was defined as hypodiploid when there was a population of nuclei with abnormal DNA content, separated from the diploid peak to the left (DI < 0.9), and representing more than 2.5% of the total.

All specimens were given unique coded identifiers and the histograms were reported blindly by two independent observers.

5.3.4 Quality Control - Coefficient of Variance

The quality of a DNA histogram is estimated from the width of the 2C peak of DNA from cells in G0 of the cycle. Coefficient of variance (CV) of the 2C peak is defined as the standard deviation of the peak divided by the mean for a uniform population of particles, and was calculated automatically by Fairfield Imaging software. The accuracy of DNA content measurement is greater when the CV of the 2C peak is smaller, and this gives a better estimation of the percentage of cells in the different compartments of the cell cycle.

5.4 Optimisation of nuclear monolayer preparation

5.4.1 Experiment on storage of nuclear suspension at different temperatures

Introduction

To ensure accurate comparative analysis of FC and ICDA, a nuclear suspension from sample collected at UCL would need to be equally separated, prior to processing at UCL and transportation for processing in UW, Seattle. We do not know, however, whether samples may deteriorate over time, what storage media is optimum and what temperature the samples should be stored at. The aim of the following experiments was to determine if samples taken from paraffin embedded blocks can be stored following digestion of nuclei, without any deterioration in the sample or affect on results.

Methods

Thirty paraffin embedded blocks of biopsy samples were analysed from a group of patients with known OAC. Two 40μm sections were cut and nuclei liberated by digestion over 2 hours using Proteinase XXIV (concentration 5mg/ml, Sigma- Aldrich, Dorset, UK). All samples were then split, and half of the supernatant (750μl) was stained using Feulgen stain (Schiff's reagent, Raymond A Lamb, Sussex, UK) and processed as described in Appendix A. The remaining 750μl suspensions of the 30 samples were assigned at random in a 1:1 ratio to storage over 2 weeks, either in a dark fridge at + 4°C or in a freezer at -20°C. Following storage these samples were taken out and re washed with PBS, prior to cytospinning and staining. Analysis was undertaken comparing the histograms prepared for baseline samples with the matched stored samples. A minimum threshold of 300 nuclei was set for histogram interpretation.

Results

None of the monolayers prepared from samples stored at 4°C yielded sufficient nuclei on scanning, precluding further assessment. Four monolayers from the 15 frozen samples were successfully scanned and analysed (see Table 5.6). There was a significant difference in the mean CV between the two methods, see Figure 5.17.

Figure 5.17 Box and whisker plot of successful cases pre and post freezing

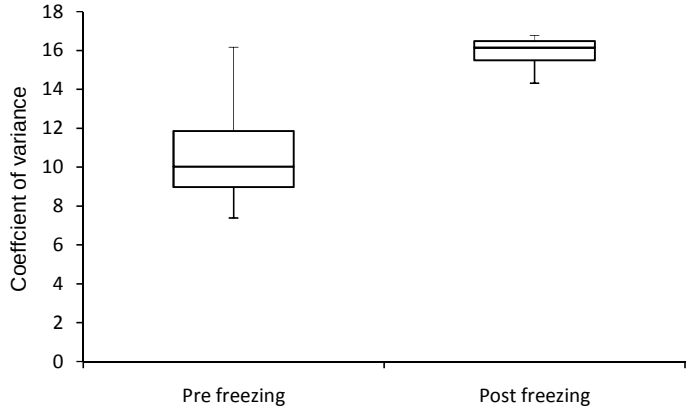

Table 5.6 Number of biopsies visible and nuclei collected per block processed

The individual slide numbers, corresponding number of nuclei cleaned and used for analysis, and coefficient of variance are shown.

Block number	Date first processed		CV	After 2 weeks		CV
1	17/09/2008	1624	8.38	23/10/2008	435	16.77
2	17/09/2008	1587	8.07	25/11/2008	<300	
3	17/09/2008	1148	10.02	25/11/2008	<300	
4	18/09/2008	1741	16.76	25/11/2008	<300	
5	18/09/2008	1701	17.73	25/11/2008	<300	
6	18/09/2008	1411	11.95	25/11/2008	<300	
7	19/09/2008	1514	13.48	25/11/2008	<300	
8	19/09/2008	1758	11.29	18/11/2008	<300	
9	19/09/2008	1780	9.57	18/11/2008	<300	
10	19/09/2008	1696	10.45	25/11/2008	512	16.4
11	19/09/2008	1793	11.76	18/11/2008	<300	
12	22/09/2008	1355	7.38	25/11/2008	1463	15.9
13	22/09/2008	1688	9.59	18/11/2008	<300	
14	22/09/2008	1761	9.78	25/11/2008	401	14.31
15	19/09/2008	1663	8.30	25/11/2008	<300	

Conclusion

These data suggest that neither method was successful enough to warrant use for further studies. This may preclude transportation of nuclear suspensions from FFPE tissue to Seattle.

5.4.2 Experiment on storage of nuclear suspension in formalin and ethanol at room temperature

Methods

12 endoscopic mucosal resection (EMR) specimens were used for this experiment. After nuclear suspension preparation the remaining sample was split into two eppendorf tubes (750ul each). Then 750µl of either 10% formalin or 70% ethanol was added making a total volume of 1500µl. These nuclear suspensions were then stored at room temperature for 7 days. Following storage the samples were spun down into pellets and resuspended in PBS to a total volume of 1500µl. 100µl was then spun onto slides to form a nuclear monolayer. For this experiment the minimum nuclei was set at 50.

Results

The results from this experiment are shown below in Table 5.7. The majority of specimens (11/12) were suitable for analysis, with one uninterpretable by all methods. More samples were interpretable with formalin (73%) than ethanol (36%), whilst 3/12 were not interpretable by either method. After 2 weeks in formalin the result was changed from diploid to aneuploid in 2 preps and tetraploid to aneuploid in a third prep. Only 2 preps yielded more than 300 nuclei. Qualitative analysis demonstrated the nuclei look smaller and more intensely stained after 2 weeks in ethanol.

Conclusion

Storage of the nuclear suspension in ethanol is associated with a high rate of uninterpretable monolayers, making this an unsuitable medium for transportation. Although formalin fixation post nuclear suspension preparation performs better then ethanol, neither is accurate compared to standard fresh nuclear prep as evidenced by increase in CV and reduced numbers of interpretable nuclei.

Table 5.7 Comparison of storage in formalin and ethanol

ID	Nuclei in Go peak at baseline	Baseline result	Formalin Nuclei	Formalin CV	Result	DI	Ethanol Nuclei	Ethanol CV	Result	DI
1	327	Aneuploid	6		n/a		66		n/a	
2	522	Tetraploid	122	3.64	Aneuploid	1.71	22		n/a	
3	<300 (238)	Diploid	0		n/a		2		n/a	
4	531	Diploid	198	1.97	Aneuploid	1.27	3		n/a	
5	308	Diploid	200	2.49	Diploid		53	3.72	Diploid	
6	<300 (150)	Diploid	115	5.85	Diploid		0		n/a	
7	Did not scan		0		n/a		0		n/a	
8	2367	Aneuploid	524	10.05	Aneuploid	1.66	368	11.71	Aneuploid	1.83
9	278	Suspicious	377	1.88	Aneuploid	1.24	184	2.55	Aneuploid	1.17
10	516	Diploid	295	4.35	Diploid		0		n/a	
11	<300 (75)	Diploid	58	3.29	Diploid		66	3.29	Diploid	
12	800	Diploid	53	2.36	Diploid		160	2.80	Diploid	

5.4.3 The influence of tissue volume on the accuracy of DNA ploidy

Introduction

In order to utilise archival material for biomarker studies it may be necessary to take several sections of the biopsy tissue for different projects. Biopsy volume is however variable per block, from between 5 biopsies to a single biopsy specimen measuring 0.1 cm^3. The use of 2-3 40 μm sections (as described above) may pose a problem if the biopsy is of small volume, as this may use all available material. It is therefore important to optimise our technique, aiming to utilise as little tissue as possible whilst maintaining accurate histogram interpretation. The aim of this experiment was to determine whether a single 40 μm section from a block with multiple embedded biopsies is sufficient for ICDA.

Methods

Twenty three tissue blocks from patients with Barrett's oesophagus were identified. The number of biopsies per block were 5 (2 patients), 4 (8 patients), 3 (5 patients), 2 (4 patients) and 1 (3 patients). A single 40 μm section was cut using a Leica microtome and nuclear monolayers were prepared as described previously.

Results

All 23 monolayers were scanned using the Fairfield Imaging DNA Ploidy version 1.5.2 software with parameters set as up to 1000 fields to scan and 1500 nuclei to grab. Successful slides were defined as those on which at least 300 nuclei were collected. A failure rate of 8/23 or 35% was calculated as 8 out of the 23 slides scanned yielded less than 300 nuclei each. Eleven slides yielded more than 1000 nuclei each, however none of them reached the ideal target of 1500 nuclei. The maximum number of nuclei collected was 1497 from a block that contained 5 biopsies, and the minimum was 448 from a block that contained 2 biopsies.

Table 5.8 presents the failure rates calculated after grouping the blocks based on the number of biopsies present in each paraffin block. When there were 5 biopsies available, the failure rate was observed to be 0%. Conversely, this rate was 100% when there was only one biopsy in the block. The failure rate appeared to have an inverse relationship with the number of biopsies available, i.e. the failure rate decreased with an increasing number of biopsies. This trend is illustrated in Figure 5.18.

Table 5.8 Failure rates using number of biopsies available as the independent variable

Number of biopsies on block	Number of blocks *	Mean nuclei collected if successful
1	3 (3)	0
2	5 (2)	869
3	5 (1)	1242
4	8 (2)	1229
5	2 (0)	1399

**number of blocks failed in brackets*

Figure 5.18 Failure rates using number of biopsies available as the independent variable

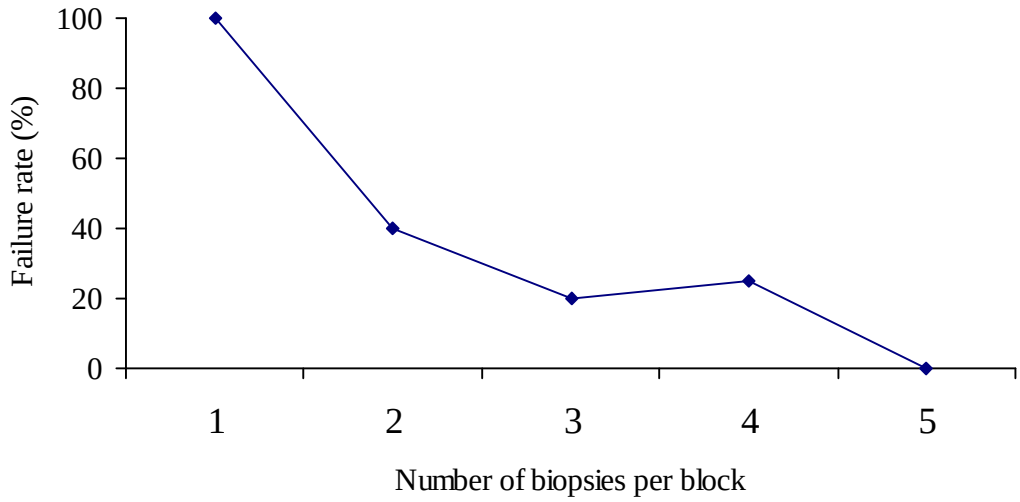

Conclusion

The volume of tissue is related to the failure rate of ICDA. A minimum of 2 biopsies are required if taking a single 40μm section.

5.4.4 Discussion

The experiments carried out thus far demonstrate the problems with storage of nuclear suspension preps, at different temperatures and in different storage media. No transportation method for nuclear suspension was feasible. Hence, to produce accurate results when comparing FC vs. ICDA, it was decided to transport the FFPE tissue sections to the UW laboratory and carry out nuclear suspension preparation, and subsequent monolayer preparation, in Seattle.

These experiments also demonstrate tissue volume influences DNA ploidy outcome, with high failure rates when less than 2 biopsies were used. It was decided, on this basis, to take larger EMR or oesophagectomy samples to UW, to increase the likelihood of success in the experiment.

5.5 Comparison of Flow Cytometry and Image Cytometry for detection of DNA ploidy abnormalities

This work is the first half of the paper ' Image cytometry accurately detects DNA ploidy abnormalities and predicts late relapse to high-grade dysplasia and adenocarcinoma in Barrett's oesophagus following photodynamic therapy' and was published in the British Journal of Cancer in 2010, with JM Dunn as first author. All nuclear suspension preparation and image cytometry gallery analysis was carried out by me. All Flow cytometry analysis and interpretation was carried out by Dr P Rabinovitch, UW, Seattle.

5.5.1 Introduction

ICDA is a comparable technique to FC for the detection of DNA ploidy abnormalities. ICDA is advantageous as set up cost is low, only a small number of nuclei are required, it is more sensitive for the analysis of tetraploid cell populations [Russack, 1994] and it is routinely performed on FFPE samples which allows analysis of archival material, valuable when planning longitudinal studies on disease progression. The aim of this study is to evaluate the accuracy of ICDA vs. FC.

5.5.2 Methods

35 patients with dysplasia or OAC, who underwent oesophagectomy or EMR between 2005 and 2008, were randomly selected from the UCL Barrett's oesophagus database. FFPE blocks were retrieved and 48 blocks were chosen for transportation to UW, 16 EMR specimens and 32 blocks from oesophagectomy specimens. EMR blocks had a minimum of 3 pieces of tissue per blocks and were either LGD, HGD, carcinoma in situ or intramucosal cancer. Of the oesophagectomy specimens, 25 had invasive adenocarcinoma. A further 7 blocks of cancer free margins (6 squamous oesophagus, 1 Barrett's oesophagus) were used as controls.

Histology

A 5 μm section was cut and stained in Haematoxylin and Eosin (H&E), before evaluation by 2 of 3 specialist GI pathologists at UCL. All 48 samples had consensus agreement.

ICDA

A single 40 μm section was cut on the Leica RM2155 microtome and transported at room temperature to Seattle. The protocol for ICDA was the same as that described in Appendix A. After filtration the nuclear suspension was re-suspended in 1.5mls of PBS and then split, with 400 μl for ICDA and 1100 μl for FC. A nuclear monolayer was then prepared using 100 μl of nuclear suspension and stained with Feulgen-Schiff reagent using standardized methodology.[Bocking et al., 1995] The remaining 300 μl of nuclear suspension was placed in 1.2 mls of 10% formalin and stored.

Flow cytometry

Standard FC was performed according to a conventional protocol and the manufacturer's instruction. Briefly, following splitting of the nuclear suspension the 1100 μl of supernatant was triturated with a 26 gauge needle, re-suspended in an isotonic pH 7.4 buffered solution with 0.1% nonidet P-40 detergent, 10μg/ml diamidino-2-phenylindole (DAPI) and 1% RNAse, and filtered through a 40μm steel mesh. The analysis was performed on a Cytopeia InFlux cytometer using UV excitation. 50,000 cells were analysed, if available, and in all cases acceptable histograms contained at least 10,000 cells and a CV below 6.0%. DNA content and cell cycle were analyzed as previously described, using the software program MultiCycle (Phoenix Flow Systems, San Diego, California, US).[Rabinovitch, 1994]

5.5.3 Results

Flow cytometry at UW was unable to yield a result on 3 of the 48 samples. ICDA also failed to yield a result on these and one other sample. Of the 44 remaining samples, 41 (93%) were classified identically between the 2 centres. Raw data is presented in Appendix B. Representative histograms of a diploid case (figure 5.19), and aneuploid case (figure 5.20) and a case displaying both aneuploid and tetraploid populations (figure 5.21) are shown below.

Figure 5.19 Comparison of Flow and Image cytometry – diploid (case 12)

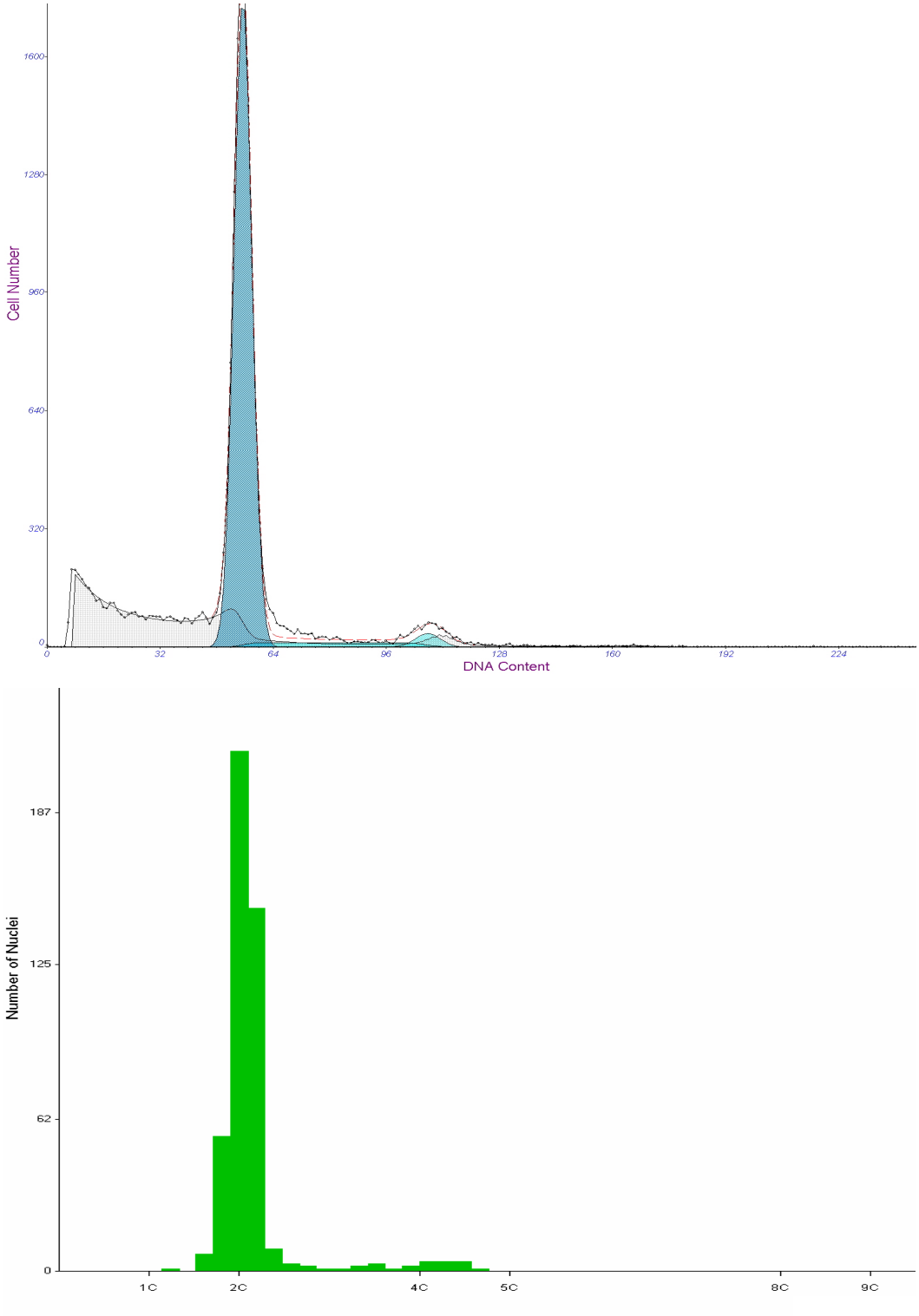

Figure 5.20 Comparison of Flow and Image cytometry – aneuploid (case 36)

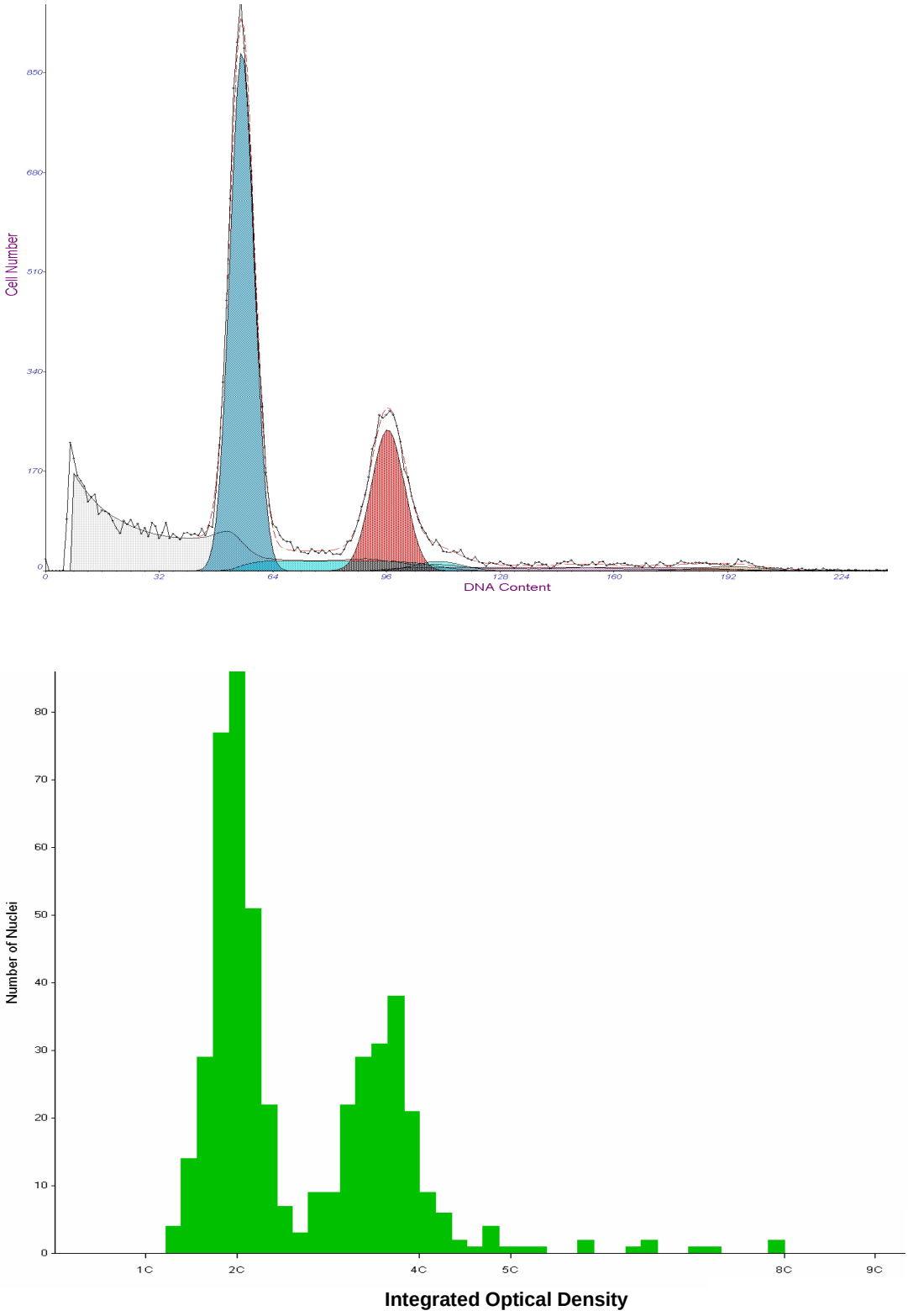

Figure 5.21 Comparison of Flow and Image cytometry – aneuploid and tetraploid (case 8)

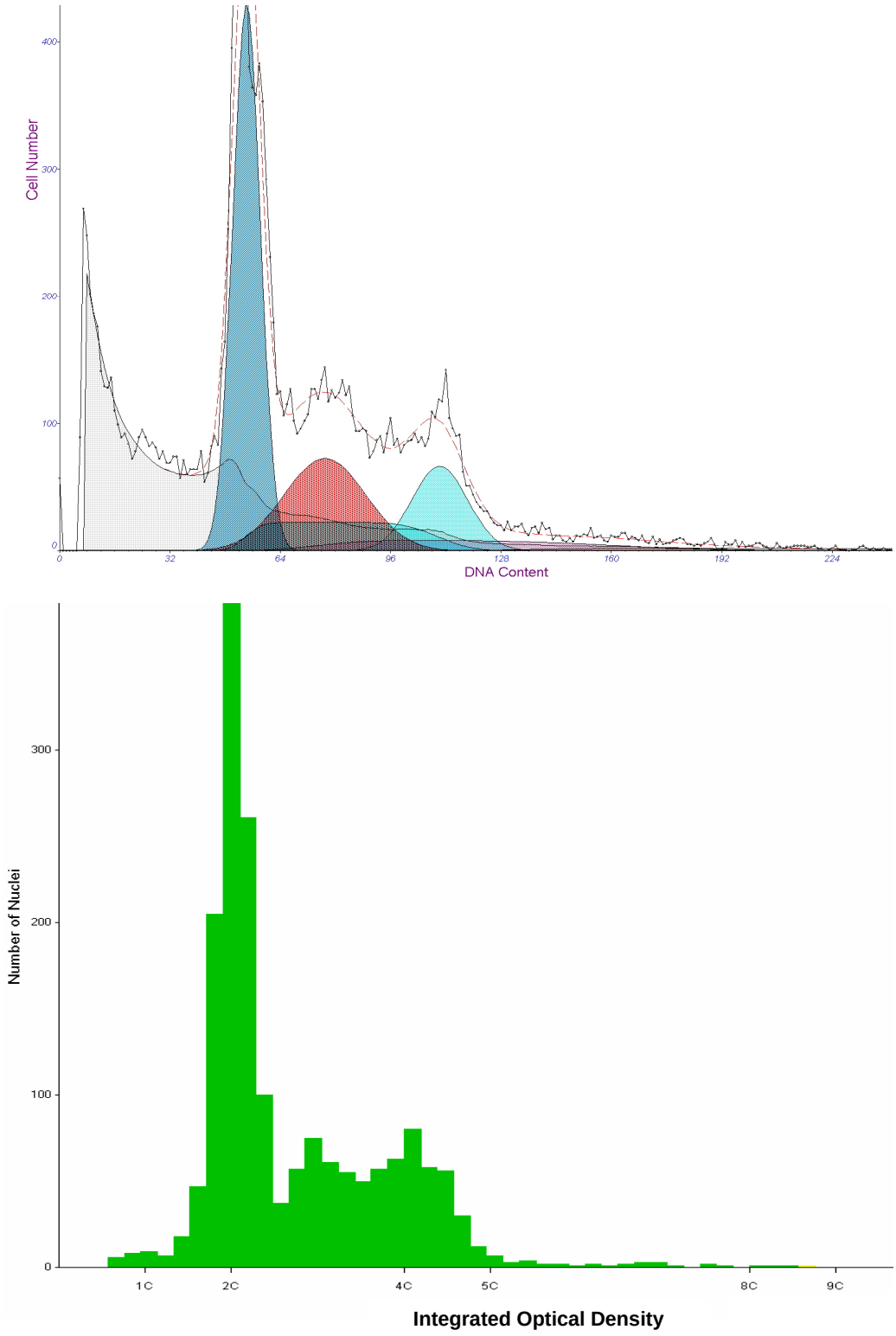

Of the 3 cases that were discordant, 2 were reported as aneuploid by UW but were diploid by UCL (see figures 5.22 & 5.23). The near diploid peak that is commented on in figure 5.22 is not found in image cytometry galleries, though this may merely reflect a wider coefficient of variance from UW interpreted as near diploid aneuploid, with a tighter peak at UCL. An alternative explanation is the rule file took these nuclei out, but there was no evidence that the peak had been automatically removed by the software on review of the galleries.

The second case (figure 5.23) has similar histograms, but we felt the small peak seen at DI 1.5 was not of sufficient magnitude to be called aneuploid by our criteria. The 3rd discordant specimen was classified as tetraploid by UCL but diploid by UW (Figure 5.24). There were low nuclei numbers for both centres in this sample, though when analysing the UW graph there is some noise at DI = 2 which has been gated out. We have kept this in after inspection of the image gallery, which demonstrates abnormal nuclei within this peak. This case demonstrates an advantage of ICDA over FC, the ability to make a diagnosis of DNA ploidy abnormalities in the tetraploid region despite very low nuclei number.

Figure 5.22 Disconcordant histogram 1 (case 28)

Note that both analysis methods show evidence of two separate G2 peaks

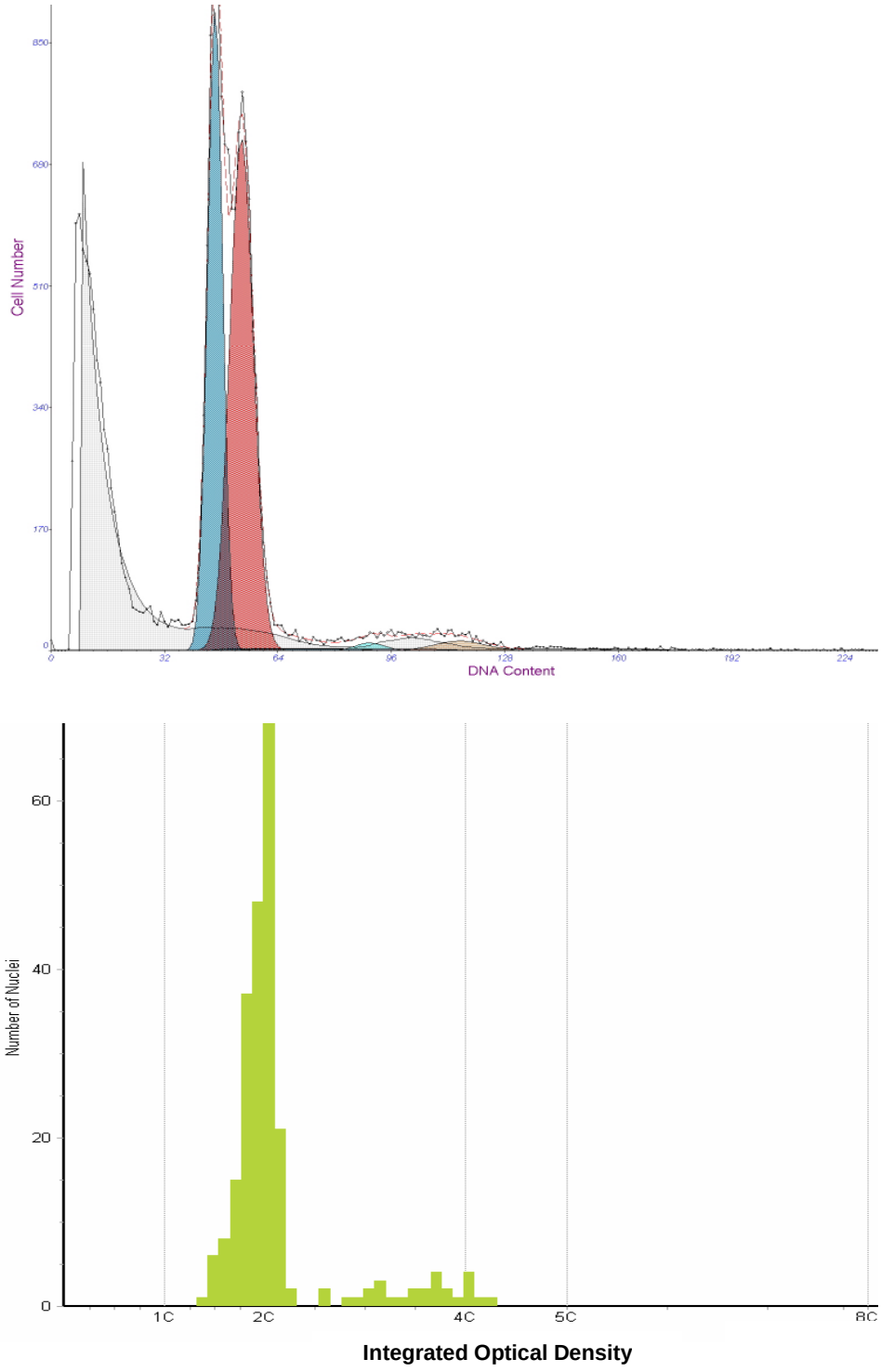

Figure 5.23 Disconcordant histogram 2 (case 22)

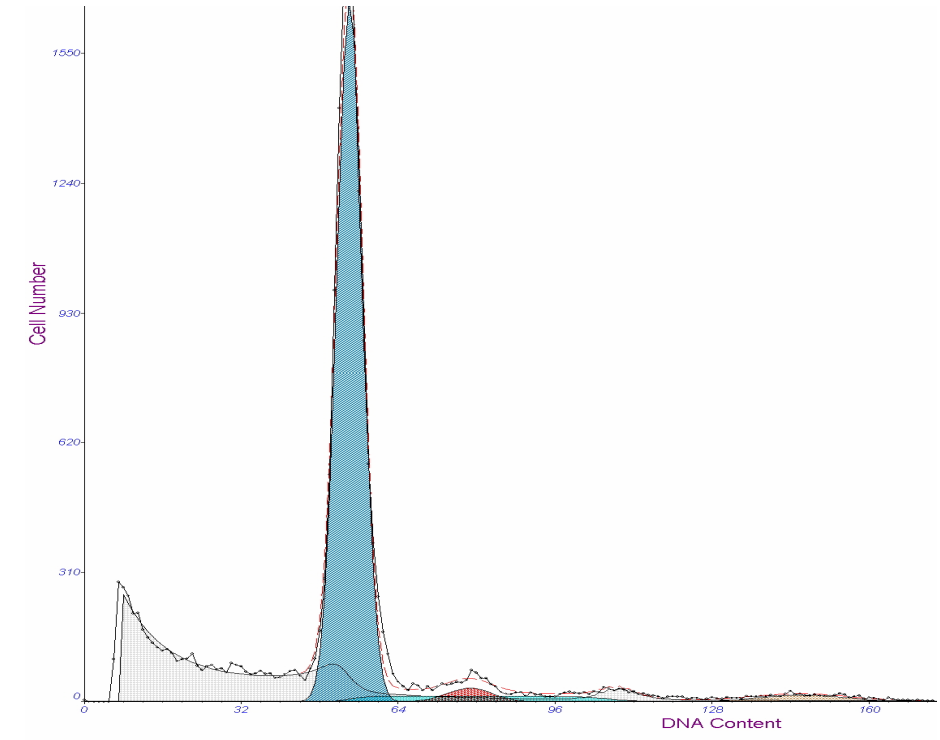

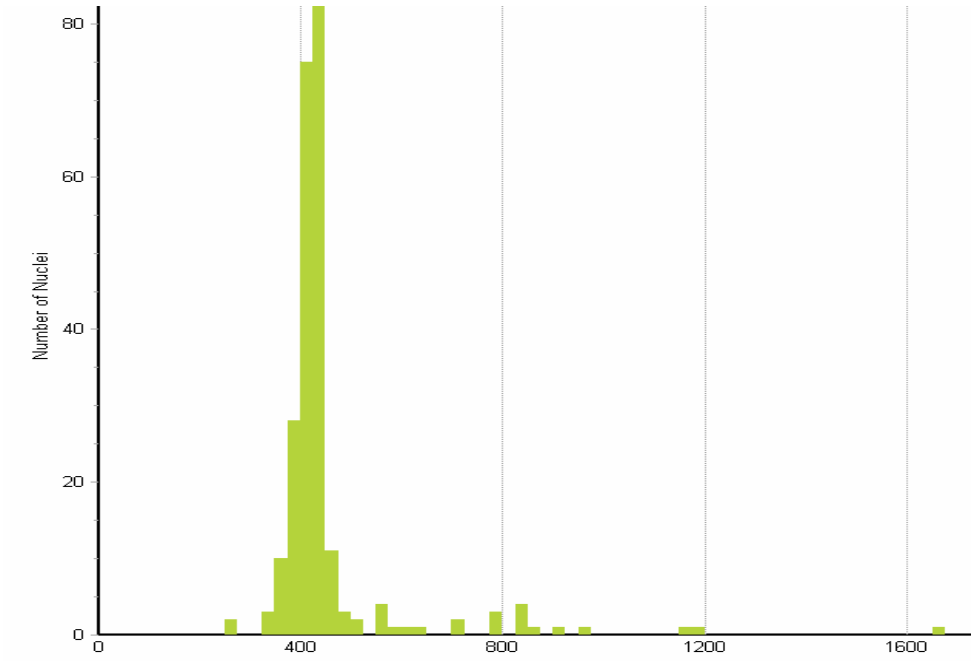

Figure 5.24 Disconcordant histogram 3 (case 10)

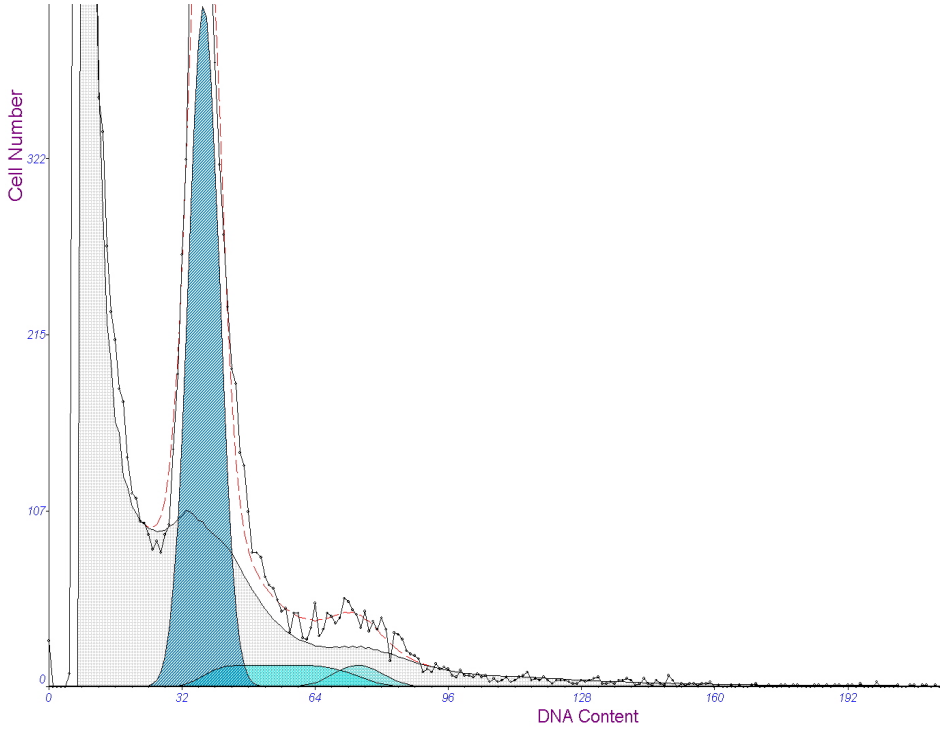

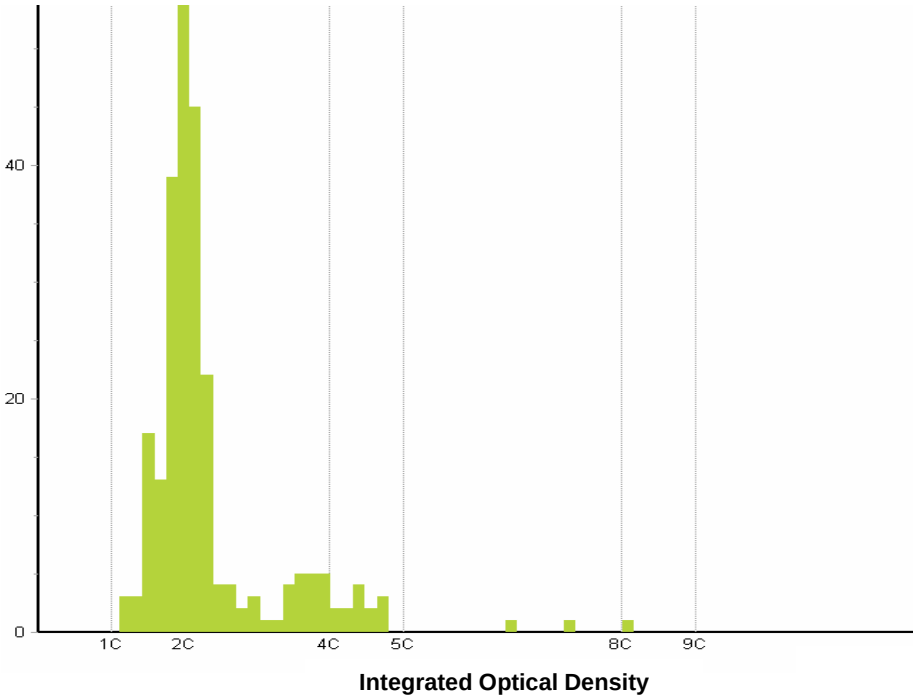

5.5.4 Discussion

These data demonstrate ICDA is highly accurate for the diagnosis of DNA ploidy abnormalities when compared to FC, the current gold standard. These findings are strengthened by the blinded study design, and comparison with a reference laboratory with a wealth of experience in FC and Barrett's oesophagus. This experiment demonstrates the potential advantages of each technique. Image cytometric DNA analysis accurately quantifies DNA tetraploidy, by permitting direct visualisation and selection of cell populations that are in the 4c region. The importance of DNA tetraploidy in BO has been previously documented by the Seattle group, with a tetraploid fraction above 6% associated with an elevated risk of progression to cancer.[Rabinovitch et al., 2001] Moreover, it is unusual to find an elevated S phase fraction in combination with a DNA tetraploid fraction above 6%, consistent with the group's published findings that elevated S phase fractions are not statistically associated with risk of progression to cancer in BO, whereas DNA tetraploid fractions are.

In contrast to ICDA, flow cytometry analysed significantly larger cell samples and provided histograms with better resolution, so aneuploid peaks in the near-diploid range were more readily detected. The importance of near diploid aneuploidy is unclear. Previous flow cytometry data from UW showed 9% of patients with DI 1.1-1.35 progressed to cancer, compared with 44% who had DI > 1.35. [Rabinovitch et al., 2001] Importantly, in that study, no patient with a near diploid DNA content progressed to cancer within 5 years of their baseline endoscopy.

The comparison of the two techniques has been evaluated in many tumours with concordance rates of 70-94% in breast cancer [Chen et al., 1995;Lee et al., 1991;Baldetorp et al., 1992] and 81-100% in gynaecological tumours.[Kaern et al., 1992;Esposito and Fuchs, 1994] In Barrett's oesophagus the published data comparing the two techniques is limited to a single study by Goyal *et al.* on 27 patients, 10 normal controls and 17 with Barrett's adenocarcinoma.[Huang et al., 2008] Image cytometry was carried out on thin sections of FFPE tissue and areas of interest marked before scanning using Automated Cellular Imaging System (ACIS). This method is potentially

advantageous as mixed squamo-glandular epithelium, which may variably dilute the glandular epithelium of interest, is not included. The authors concluded that ICDA detected aneuploidy in all adenocarcinoma samples while FC missed the diagnosis of aneuploidy in 29%. There were however limitations to this study. ICDA and FC were carried out in the same laboratory with no independent review of histograms, and there was no validation of FC technique. The two techniques were carried out on different cut samples (7μm image cytometry, 2 x 50μm FC) thereby making it difficult to draw a direct comparison. Finally no patients were reported as DNA tetraploidy, an important independent marker of disease progression. This may be explained by the study design, as only cancers were analysed for DNA ploidy, and DNA tetraploidy can appear early in the cascade of genetic change. This may also be explained by introduction of a cutting error of the larger tetraploid nuclei when using 7μm sections, leading to underestimation of tetraploid fraction.

In conclusion DNA ploidy measured by ICDA is accurate when compared to flow cytometry on thick sections, with advantages of cost effectiveness, potential for automation and routine analysis of paraffin embedded tissue. It is important to note that both ICDA and flow cytometry examine predominantly whole nuclei, and it is less likely that these findings would be replicated by analysis of cut nuclei from thin sections.

5.6 DNA ploidy measured by ICDA as a prognostic biomarker in BO

This collaborative project was funded by the MRC and Dr Fitzgerald is Principal Investigator (Addenbrooke's Hospital, Cambridge). Co-investigators include Prof. Murray, Drs Johnston, McManus, Mulholland and Arthur (Northern Ireland), Prof. Novelli, Dahmane Oukrif and Dr Lovat (UCL) and Drs Bird-Lieberman and Lao-Sirieix (Cambridge). The work presented in this chapter is on the DNA ploidy aspect of the study and forms part of the planned paper that will be submitted with myself as first author. As the patient data was blinded to all investigators in order to reduce bias, all of the statistical analysis on DNA ploidy results was carried out centrally by Dr Mulholland.

5.6.1 Introduction

The previous study demonstrated that ICDA results correlate with flow cytometry. By inference we would expect to see increased risk of cancer in non dysplastic BO with aneuploidy when measured by ICDA, thereby reproducing the DNA ploidy results from the Seattle group ten years ago. In order to test this hypothesis we set out to evaluate ICDA in a multicentre phase 3 biomarker study. This study, referred to as the Barrett's Oesophagus Study (REC Number - 07/NIR02/109), assessed a panel of biomarkers using tissue from patients in the Northern Ireland Barrett's Oesophagus Register (NIBR). The NIBR includes 9,332 adults diagnosed with columnar-lined oesophagus within Northern Ireland (population 1.7 million) between 1993 and 2005, and is the only population based register of Barrett's oesophagus that exists worldwide.

The register was constructed by examining pathology reports from all oesophageal biopsies taken in NI during this period, with subsequent clinical case note review. BO was defined as an endoscopically visible Barrett's segment with histologically proven SIM. Individual patients were identified within the dataset and were followed up for death and oesophageal malignancy (until December 2005) by matching with mortuary files at the NI Registrar General's Office and NI Cancer Registry database of incident cancers. Patients undergoing treatment for HGD were identified through the case note review. The patient samples are extremely well characterised clinically [Murray et al.,

2003] and the potential for using this cohort for the assessment of biomarkers has been demonstrated using P53 immunohistochemical staining.[Murray et al., 2006] In the current proposed study predictive biomarkers to be investigated, other than DNA ploidy (ICDA), are methylation (PCR), cyclin A and TP53 expression (immunohistochemistry), lectins (HPA, PNA, UEA-1) (fluorescence histochemistry), and ErbB2 status (FISH, q-RT-PCR, immunohistochemistry).

5.6.2 Study design

Cases were characterised as patients with BO who had progressed to OAC or HGD, and controls were characterised as patients who had not progressed to these states. Three controls were chosen for each case, and matched for age (within 5 years), sex and year of diagnosis. The initial diagnostic and follow-up biopsies of the cases (progressors) and controls (non progressors) were obtained from four NHS pathology laboratories in the province in which they were stored. HGD outcomes were classified as 2 separate clinical diagnoses within 12 months or 3 separate diagnoses of HGD regardless of time period. All were available for histological confirmation by Professor Novelli (MN) and Dr McManus (DM).

Power calculation

In order to detect an odds ratio for biomarker positivity of 2.5, using a two tailed test with significance level of $p<0.05$ and a power of 80%, the proposed study required 100 cases and 300 controls. 108 cases of progression to OAC or HGD and 324 controls were found to be eligible for inclusion in the study.

Histopathology review

Verification of the BO phenotype (presence of SIM and grade of dysplasia) was performed independently by 2 specialist upper GI pathologists (MN and DM). Any classification discrepancies were reviewed and agreed at a consensus meeting.

Statistical analysis

The biomarker results were entered into a conditional logistic model (after transformation if indicated) in order to compare the prevalence of biomarker positivity between cases

and controls, allowing for the matched design of the study. The effect of potential confounders (specimen storage, demographic or clinical variables) was addressed by including these as additional explanatory variables in the statistical models. The conditional logistic model enabled a scoring system to be derived combining information from several biomarkers, and clinical factors, reflecting the risk of OAC.

5.6.3 Methods

ICDA

This was undertaken as described in Appendix A. Preparation of monolayers was undertaken by Jason Dunn, Dahmane Oukrif (Clinical Scientist) and Yishyene Chew (laboratory technician). The digestion time was set at 2 hours and hydrolysis time at 45 mins. The number of nuclei collected was set at 1000. All galleries were cleaned and histograms produced by JD. All histograms were subsequently reviewed by JD and MN, who were blinded to patient case details and histological diagnosis. In cases of disagreement on DNA ploidy diagnosis an independent third adjudicator was called upon (Professor HE Danielsen, Oslo).

Using these parameters 118 samples failed, either because there were too few nuclei to scan or that the nuclei on the monolayer were not stained sufficiently, producing scans with blurred nuclei or wide coefficient of variance. This represented 33% of all monolayers and precluded meaningful data interpretation of the case control study, as the power calculation was not valid. When these results were reported back centrally for review, it was found that the majority of failures originated from the Altnagelvin Hospital (88% of samples from this hospital failed, compared to 12% of samples from the other 4 centres combined). On qualitative analysis of the nuclear monolayers it appeared that these samples had been over digested, as we saw no nuclei at all and very little nuclear debris. In an attempt to adapt our protocol to this hospital, it was decided to undertake a series of experiments to evaluate digestion time and proteolysis

a) Optimisation of nuclear monolayer preparation on samples from the Altnagelvin Hospital

Experiment on variance of digestion time

Introduction

Proteinase XXIV is isolated from *Bacillus licheniformis,* a serine proteinase not specific for a given peptide bond but demonstrating preference for hydrolyzing at the carboxyl side of large uncharged amino acid residues (tyrosine, asparagine and glutamine). Proteolytic digestion of formaldehyde-fixed tissue is necessary to break cross-linked peptide bonds and optimal proteinase digestion is highly dependent on both the duration of fixation in formaldehyde, and the type of tissue being digested. [Battifora and Kopinski, 1986;Fleming et al., 1992] As the type of tissue was the same it is possible that the duration of fixation was different (i.e shorter) at the Altnagelvin Hospital, leading to weaker cross-linked bonds and over-digestion when using our standard digestion time. To test this hypothesis an experiment was designed to determine the optimum conditions for digestion over various times using the Altnagelvin Hospital blocks.

Methods

10 blocks from Altnagelvin Hospital were chosen at random for analysis. Blocks were reviewed by Professor Arthur and all had three small paraffin embedded biopsy samples, each measuring 0.1x 0.1 x 0.1 cm. Three 40 μm sections were cut from each block and randomly assigned to eppendorf tubes marked A, B and C. The samples were then processed for DNA ploidy as previously described, with 200 μl of 0.05g/ml of Proteinase XXIV used for digestion of the cytoplasm. Digestion times were 60 minutes for A, 45 minutes for B, and 30 minutes for C. In order to vary digestion time accurately it was necessary to start the preps, and hence immersion in the water bath, at different time points as follows –

Prep A – Start at zero
Prep B – Start after 15 mins
Prep C – Start after 30 mins

An alternative method would have been to start all simultaneously and then quench the digestion process with glycine. As we were unsure as to the volume required or time taken to stop digestion process, the former method was decided upon. Once all nuclear suspensions were removed from the water bath, 1300 μl of chilled PBS was added and standard methodology for monolayer preparation was followed thereafter. In order to accurately assess the slides quantitatively, the image grabber software was set to 1000 nuclei and the time taken to achieve this was recorded. A slide that took more than 1000 frames was considered a failure for the purposes of this study, but image analysis was undertaken on the amount of nuclei captured up to that point to assess the coefficient of variance.

Results

Of the 10 samples analysed 4 were successful (Table 5.9). There was no significant effect on the CV of these 4 samples by varying the digestion time. The level of section examined also did not influence the result. There were very low numbers for case 594 and therefore the DNA ploidy results presented were inaccurate, with three different results. Of the 6 preps that failed at 30 minutes, all failed at 45 and 60 minutes. In all six there were only a few nuclei on each monolayer, and all looked over digested.

Table 5.9 Experiment varying digestion time

Case	Section level	Digestion time (mins)	Result	Scan time	Nuclei G0 peak	CV	DI	DI peak
594	3	60	Diploid	>120	29	4.72	1.01	
	2	45	Aneuploid	>120	18	2.93	1.00	1.14
	1	30	Tetraploid (11%)	>120	52	3.83	1.00	1.94
624	3	60	Failed	>120				
	1	45	Diploid	>120	38	7.51	0.99	
	2	30	Diploid	>120	110	7.02	0.96	
668	1	60	Diploid	>120	279	9.18	0.98	
	2	45	Diploid	>120	52	6.04	1.01	
	3	30	Diploid	>120	330	7.47	1.04	
694	3	60	Diploid	>120	67	4.24	1.00	
	2	45	Diploid	>120	386	3.99	1.02	
	1	30	Diploid	>120	247	3.78	0.98	

Conclusion

There was no improvement in monolayer preparation on reduction of digestion time with Proteinase XXIV. With only ¼ of the digestion time the samples remained overdigested. This may suggest that the majority of digestion takes place within the first 30 minutes using proteinase XXIV. Possible methods of decreasing the rate would be to decrease the temperature of the water bath or to reduce the concentration of the Proteinase. Both these experiments would be of value if more tissue was available but unfortunately this was not the case. An alternative method was to use an already established alternative technique for proteolytic digestion such as pepsin. We therefore decided to test both these methods in a comparative study of pepsin and proteinase.

Comparison of different proteolytic agents

Introduction

Pepsin is a well validated alternative to Proteinase XXIV that is used by the Rabinovitch lab in Seattle for Flow cytometry from FFPE tissue. A concentration of 1% pepsin pH 1.5 at 37°C for 60 minutes is their standard protocol. The aim of this experiment was to compare pepsin with different concentrations of proteinase on the preparation of nuclear monolayers.

Methods

10 sections were withdrawn from the UCLH BO study archive. These were all patients enrolled in PDT studies, and represent a mixture of non dysplastic BO and HGD. Three 40μm sections were cut from each block and randomly assigned to three different ependorf tubes marked A,B,C. Standard methodology was followed up to the digestion step, then the samples were allocated as follows

A Pepsin (Digestall 3, Invitrogen, California, US) at 37C for 1 hour
B Proteinase XXIV at concentration 0.025 mg/ml at 37C for 1 hour
C Proteinase XXIV at concentration 0.05 mg/ml at 37C for 1 hour

Standardised methodology was followed thereafter to produce Feulgen stained nuclear monolayers. These were all scanned for 1000 nuclei as previously described.

Results

Of the 10 samples, 7 yielded a result by all 3 methods. Raw data is presented in Appendix C. Proteinase failed to yield a result at either concentration on samples 4, 5 and 10. Comparison of CV of the G0 peaks is shown in figure 5.25. There was a trend for lower CV with pepsin than proteinase across all samples. There was discordance on case 2, which was called diploid using pepsin but suspicious using proteinase at both concentrations. The CV was very high for both these samples (10.1 and 8.1 respectively), and it is likely the pepsin result is more accurate. Samples that were concordant for

aneuploidy (6, 7 and 9) had similar DI of the aneuploid peaks, although the CV was significantly lower with pepsin.

Figure 5.25 Effect on CV of G0 peak with different proteolysis agents

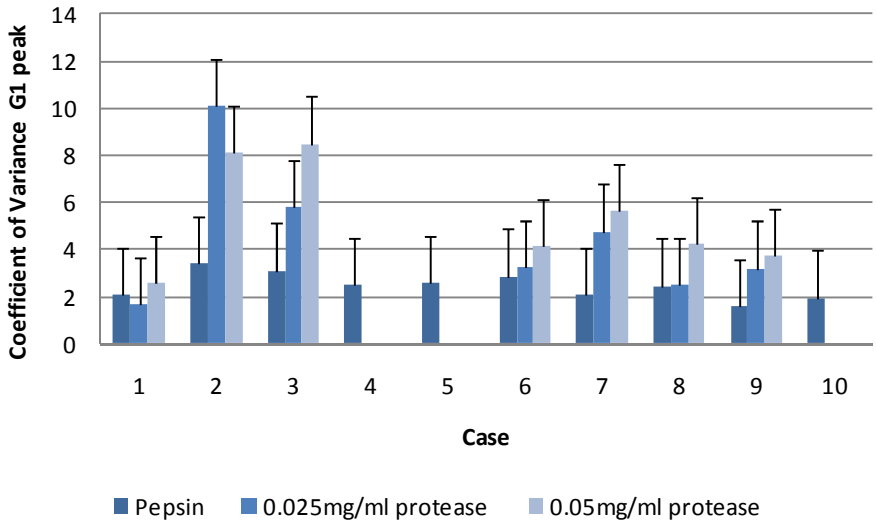

Conclusion

This experiment demonstrates there is no difference in the DNA ploidy result when comparing proteinase at different concentrations and pepsin. There was a difference in the failure rate, which was 40% with Proteinase vs. 0% using pepsin. These failures all came from tissue blocks of small volume. The comparison of Proteinase XXIV, pepsin and trypsin for flow cytometry from FFPE samples has been studied previously. Tagawa *et al* demonstrated that trypisn (Schutte method) gave somewhat better results than proteinase and pepsin (Hedley method), in both gastric and colon cancer, with lower CV and greater pick up rate of aneuploid peaks.[Tagawa et al., 1993] Both these methods used Propidium iodide however, and may not be generalisable to staining with Feulgen.

Our results demonstrate that pepsin may be a better proteolytic when only a weak impact on the release of single cells from paraffin-embedded blocks is required, such as digestion of smaller tissue or tissue with weaker fixation bonds. The results were presented to the NIBR study group and it was agreed that the 119 cases that failed would be re-analysed using pepsin.

5.6.4 Results

Index samples from 414 individuals were evaluated for ICDA between May 2009 and August 2010, a total of 94 cases and 320 matched controls. The 94 cases consisted of 56 definite OAC, 13 gastric cardia cancers and 25 HGD. After review by two expert pathologists (DM and MN), five cases (2 OAC, 1 gastric cardia cancer and 2 HGD cases) were found to have evidence of HGD or OAC at their initial BO diagnosis and were therefore excluded from analysis, leaving 89 cases and 291 matched controls.

Characteristics of cases and matched controls

Patient characteristics are shown in Table 5.10. Gender, age and year of BO diagnosis were all matching criteria in the study design. Cases and controls did not differ by matching criteria, nor laboratory of origin or length of BO segment, although this was unknown for approximately half of participants. Notably, the only case that originated from short-segment BO was a HGD outcome. Significantly more cases were diagnosed as having indefinite or low grade dysplasia at their first BO diagnosis compared with controls. The mean (±SD) follow-up time for cases and controls (i.e. time from BO diagnosis to outcome diagnosis) was 4.06 ± 2.95 years (range 0.5-12.1 years) and 7.42 ± 2.91 years (range 1.1-12.9 years) respectively.

Table 5.10 Characteristics of cases and matched controls

Characteristic	**Cases** ***n= 89 (%)***	**Controls** ***n= 291 (%)***	**p-value**
Gender			
Male	67 (75.3)	218 (74.9)	0.94
Female	22 (24.7)	73 (25.1)	
Age at BO diagnosis (mean ± SD)	63.8 ± 11.9	63.8 ± 11.3	0.99
Length BO segment			
Long	43 (48.3)	141 (48.45)	
Short	1 (1.1)	9 (3.1)	0.59
Unknown	45 (50.6)	141 (48.45)	
Lab/Hospital of origin			
Altnagelvin	21 (23.6)	46 (15.8)	
Antrim	19 (21.3)	79 (27.1)	
Belfast City	11 (12.3)	52 (17.9)	0.27
Craigavon	7 (7.9)	16 (5.5)	
Royal Victoria	31 (34.8)	98 (33.7)	
Vienna score of index BO*			
1	71 (79.8)	284 (97.6)	<0.001
2-3	18 (20.2)	7 (2.4)	

DNA ploidy analysis

Of the 380 patients samples, 339 (89%) were successfully analysed by ICDA. This represents a total of 82 cases and 257 matched controls. The results for ICDA are shown in Table 5.11 and 5.12. For statistical reasons categories were combined so that 'probable' diploid, aneuploid and tetraploid were assumed to be definite. There was a significant difference in the number of patients with either aneuploidy, tetraploidy or hypodiploid in the progressors group compared to the non-progressor group.

Table 5.11 Comparison of DNA ploidy results for all samples – categories collapsed

DNA ploidy status	**Cases** ***n=82 (%)***	**Controls** ***n=257 (%)***	**p-value**
Diploid	46 (56.1)	216 (84.1)	
DNA ploidy abnormality	36 (43.9)	41 (15.9)	<0.001

Table 5.12 Comparison of DNA ploidy results for all samples

DNA ploidy analysis	**Cases** ***n=82 (%)***	**Controls** ***n=257 (%)***	**p-value**
Diploid	46 (56.1)	216 (84.0)	
Aneuploid	20 (24.4)	21 (8.2)	<0.001
Tetraploid	7 (8.5)	10 (3.9)	
Aneuploid&Tetraploid	4 (4.9)	0 (0.0)	
Hypodiploid	4 (4.9)	2 (0.8)	
Suspicious	1 (1.2)	8 (3.1)	

Unadjusted and multi-variate regression analysis

Results from unadjusted regression are shown in Tables 5.13 and 5.14. There was a significantly increased risk for progression to OAC and HGD when DNA ploidy abnormalities were present (OR = 4.04; 95% CI = 2.33-7.03). This remained significant when gastric cancers (that were presumed OAC) and HGD were removed from analysis. The risk was higher with aneuploidy (OR = 4.40; 95% CI = 2.15-8.98) than tetraploidy (OR=3.09; 95% CI =1.10-8.68). Hypodiploid yielded the highest odds ratio but the 95% confidence interval was very wide due to small numbers.

Table 5.13 Unadjusted risk estimates for ICDA (separated by ICDA result)

	All cancers & HGD		
DNA ploidy	**Cases** ***n=82***	**Controls** ***n=257***	**OR (95% CI)**
Diploid	46	216	1.00
Aneuploid	20	21	4.40 (2.15-8.98)
Tetraploid	7	10	3.09 (1.10-8.68)
Aneuploid&Tetraploid	4	0	-
Hypodiploid	4	2	12.10 (1.29-114.5)
Suspicious	1	8	0.58 (0.07-4.80)

Table 5.14 Unadjusted risk estimates for ICDA (categories combined)

	All cancers & HGD			**All cancers**			**Confirmed OAC**		
DNA ploidy	**Cases** ***n=82***	**Controls** ***n=257***	**OR (95% CI)**	**Cases** ***n=67***	**Controls** ***n=210***	**OR (95% CI)**	**Cases** ***n=58***	**Controls** ***n=181***	**OR (95% CI)**
Diploid	46	216	1.00	39	176	1.00	33	151	1.00
Abnormal	36	41	4.04 (2.33-7.03)	28	34	3.65 (1.99-6.71)	25	30	3.81 (1.97-7.36)
p for trend			<0.001			<0.001			<0.001

Multivariate adjusted risk estimates were then calculated using age, gender, year of BO diagnosis, origin of specimens, % biopsy fragments showing intestinal metaplasia, degree of dysplasia, and the batch number that the sample was sent in. These results are summarised in Tables 5.15 and 5.16. DNA ploidy abnormalities remained a significant predictor of risk for HGD and cancer (OR = 2.98; 95% CI = 1.55-5.71). The risk was higher with tetraploidy (OR = 3.23; 95% CI = 0.93-11.3) than aneuploidy (OR=2.39; 95% CI =1.01-5.67).

Table 5.15 Multivariate adjusted risk estimates for ICDA (separated by ICDA result)

	All cancers & HGD		
DNA ploidy	**Cases** ***n=82***	**Controls** ***n=257***	**OR (95% CI)**
Diploid	46	216	1.00
Aneuploid	20	21	2.39 (1.01-5.67)
Tetraploid	7	10	3.23 (0.93-11.3)
Aneuploid&Tetraploid	4	0	-
Hypodiploid	4	2	14.36 (1.36-151.3)
Suspicious	1	8	0.18 (0.01-2.60)

Table 5.16 Multivariate adjusted risk estimates for ICDA (categories combined)

	All cancers & HGD			**All cancers**			**Confirmed OAC**		
DNA ploidy	**Cases** ***n=82***	**Controls** ***n=257***	**OR (95% CI)**	**Cases** ***n=67***	**Controls** ***n=210***	**OR (95% CI)**	**Cases** ***n=58***	**Controls** ***n=181***	**OR (95% CI)**
Diploid	46	216	1.00	39	176	1.00	33	151	1.00
Abnormal	36	41	2.98 (1.55-5.71)	28	34	2.91 (1.40-6.04)	25	30	3.22 (1.43-7.22)
p for trend			0.001			0.004			0.005

Effect of age, sex and length of BO

The effect of the length of Barrett's segment, age and sex were then assessed on unadjusted and multivariate analysis. These results are summarised in tables 5.17-5.19. There was an increased risk of progression to OAC/HGD in patients with long segment BO and DNA ploidy abnormalities that was independent of the length of the Barrett's segment on multivariate analysis (OR = 5.25; 95% CI = 1.18-23.32). There was an increased risk of progression to OAC/HGD in patients who were over the age of 60 years and had DNA ploidy abnormalities (OR = 4.23; 95% CI = 1.85-9.66), which was not significant in patients under the age of 60 with DNA ploidy abnormalities (OR = 1.23; 95% CI = 0.34-4.46). There was a moderate increased risk of progression to OAC/HGD in male patients who had DNA ploidy abnormalities (OR = 2.35; 95% CI = 1.06-5.22), which was not seen in female patients with DNA ploidy abnormalities (OR = 1.77; 95% CI = 0.45-6.94).

Table 5.17 Risk estimates for DNA ploidy for those with BO segment length recorded as long

	All cancers & HGD			
DNA ploidy	**Cases** ***n=36***	**Controls** ***n=63***	**Unadjusted OR (95% CI)**	**Adjusted OR (95% CI)**
Diploid	17	54	1.00	1.00
Abnormal	19	9	7.50 (2.48-22.68)	5.25 (1.18-23.32)
p for trend			<0.001	0.03

Table 5.18 Risk estimates for DNA ploidy by age at BO diagnosis

	All cancers & HGD			
	Cases ***n=27***	**Controls** ***n=88***	**Unadjusted OR (95% CI)**	**Adjusted OR (95% CI)**
<60 years old				
Diploid	16	74	1.00	1.00
Abnormal	11	14	3.45 (1.37-8.70)	1.23 (0.34-4.46)
p for trend			0.009	0.75
	Cases *n=55*	Controls *n=166*	Unadjusted OR (95% CI)	Adjusted OR (95% CI)
≥60 years old				
Diploid	30	139	1.00	1.00
Abnormal	25	27	4.66 (2.30-9.46)	4.23 (1.85-9.66)
p for trend			<0.001	0.001

Table 5.19 Risk estimates for DNA ploidy by gender

	All cancers & HGD			
	Cases ***n=63***	**Controls** ***n=199***	**Unadjusted OR (95% CI)**	**Adjusted OR (95% CI)**
Males				
Diploid	37	169	1.00	1.00
Abnormal	26	30	3.93 (2.07-7.46)	2.35 (1.06-5.22)
p for trend			<0.001	0.04
	Cases *n=20*	Controls *n=61*	Unadjusted OR (95% CI)	Adjusted OR (95% CI)
Females				
Diploid	10	50	1.00	1.00
Abnormal	10	11	4.39 (1.47-13.08)	1.77 (0.45-6.94)
p for trend			0.008	0.41

Risk of progression with dysplasia alone

The effect of dysplasia on risk was then assessed, and is summarized in table 5.20. Low grade or indefinite for dysplasia conferred a significant increased risk of progression to OAC/HGD (OR = 11.33; 95% CI = 3.97-32.36). Eight patients had HGD/OAC on the index samples when reviewed by 2 pathologists, and these were subsequently removed from the study. These patients had a markedly significant risk of progression although the confidence interval was wide (OR=23.10: 95% CI = 3.69-144.6).

Table 5.20 Risk estimates for dysplasia scoring

	All cancers & HGD			
Vienna	**Cases** ***n=89***	**Controls** ***n=291***	**Unadjusted OR (95% CI)**	**Adjusted OR (95% CI)**
1 (IM)	71	284	1.00	1.00
2-3 (indef/lgd)	18	7	11.60 (4.26-31.60)	11.33 (3.97-32.36)
p for trend			<0.001	<0.001

Combination of DNA ploidy and dysplasia

The combination of DNA ploidy abnormalities and dysplasia was then used in a risk panel, and the results are described in Table 5.21. The presence of DNA ploidy abnormalities and IND or LGD conferred a high risk of progression to OAC/HGD (OR = 23.98; 95% CI = 6.84-84.10). A similar increased risk was observed in patients who were diploid with IND/LGD or in patients with DNA ploidy abnormalities in non-dysplastic BO (OR = 2.60 and 2.44 respectively).

Table 5.21 Risk estimates for combination of ICDA+dysplasia scoring

	All cancers & HGD			
	Cases ***n=82***	**Controls** ***n=257***	**Unadjusted OR (95% CI)**	**Adjusted OR (95% CI)**
Diploid & No dysplasia	42	211	1.00	1.00
DNA ploidy abnormality & no dysplasia	20	38	2.34 (1.17-4.66)	2.44 (1.29-4.62)
Diploid & IND or LGD	4	5	5.51 (0.85-35.71)	2.60 (0.61-11.05)
DNA ploidy abnormality & IND or LGD	16	3	24.21 (6.53-89.83)	23.98 (6.84-84.10)

5.6.5 Discussion

The results of this multicentre blinded nested case control study show that DNA ploidy abnormalities measured by ICDA are significant independent risk factors for the development of OAC and HGD in BO. This risk remained significant following multivariate analysis by age, gender, year of BO diagnosis, origin of specimens, % biopsy fragments showing intestinal metaplasia, degree of dysplasia, and the batch number that the sample was sent in. This work was further strengthened by the study design, using a well described cohort with long term follow up. All analysis was undertaken blinded to the outcome and consensus was reached on interpretation of all histograms by two investigators (JD and MN). The success rate of 89% was achieved by varying the parameters of the monolayer preparation, although this problem was unique to one hospital, and it is unlikely that a change in the preparation will be necessary for future work.

Further analysis demonstrated age over 60 years, male gender and long segment BO signified an increase risk for progression to cancer when DNA ploidy abnormalities were present. Low grade or indefinite for dysplasia were significant predictors for progression to OAC/HGD (OR = 11.33; 95% CI = 3.97-32.36), but this risk was further increased if DNA ploidy abnormalities were present (OR = 23.98; 95% CI = 6.84-84.10). Importantly, LGD and DNA ploidy abnormalities conferred the same risk of progression to OAC/HD as the presence of HGD.

Half of the cases that progressed to cancer were in the diploid non dysplastic group. In other words, although the presence of DNA ploidy abnormalities confers a greater risk of progression to OAC/HGD in this study, the absence of these abnormalities did not confer a benefit. This may be explained by sampling error, both at endoscopy and when cutting sections from FFPE tissue blocks. There may also be a temporal effect if the biopsies at baseline were taken too early before the onset of cancer. We are hoping to evaluate the interim biopsies of these patients to evaluate if aneuploidy developed at a later date. Another explanation is that 10% of patients with OAC will not display chromosomal instability, and this may explain the slightly higher OR in patients with confirmed OAC

than when gastric cancers which were presumed OAC were included. We will therefore analyse the outcome biopsies of the cases, to determine the percentage of patients who had aneuploid/tetraploid cancers.

Caution must therefore be exercised in reduction of surveillance intervals on the basis of ICDA alone. Other markers of chromosomal instability, such as 9p and 17pLOH have been shown to increase relative risk of OAC, and a combination of markers is likely to have more value in prognostication than any individual marker. It is hoped that the other biomarkers investigated in this study may provide more information on this group of diploid high risk patients, and the results are awaited.

Nevertheless ICDA alone is a valuable positive predictive biomarker, as its presence confers an increased risk of cancer progression which, in the presence of IND or LGD, is equivalent to HGD. The combination of dysplasia scoring and DNA ploidy status may therefore provide a useful algorithm for risk stratification –

i. No dysplasia and diploid
    a. Risk unknown. Continue current surveillance interval.
ii. DNA ploidy abnormality and no dysplasia, or LGD/IND and diploid
    a. Moderate risk. Increase surveillance interval to annual.
iii. DNA ploidy + LGD/IND
    a. High risk. Consider minimally invasive therapy.

This may provide financial savings as the LGD group, which currently equates to a six monthly surveillance interval according to BSG guidelines, may be more accurately stratified by ICDA into a moderate risk group and higher risk group. This strategy would need to be evaluated in a phase IV biomarker study before uptake into routine clinical practice. In summary this study has demonstrated that ICDA is a clinically applicable and useful tool for risk stratification in BO. We confirm the findings of the work undertaken by the Reid group 10 years previously, that aneuploidy and tetraploidy are important independent markers of cancer progression in Barrett's oesophagus.

5.7 DNA ploidy measured by ICDA as a prognostic biomarker in non-dysplastic BO post PDT

This work is the second part of the paper – 'Image cytometry accurately detects DNA ploidy abnormalities and predicts late relapse to high-grade dysplasia and adenocarcinoma in Barrett's oesophagus following photodynamic therapy' published in the British Journal of Cancer in 2010, with JM Dunn as first author.

5.7.1 Introduction

Although complete ablation of a Barrett's segment is the ideal response to treatment, complete reversal of HGD (CR-HGD) at 1 year is currently used as a marker of treatment success post ablative therapy.[Overholt et al., 2007;Shaheen et al., 2009a] Nevertheless, in one series late relapse beyond 2 years occurred in up to 23% of patients.[Overholt et al., 2007] It is therefore necessary to perform regular surveillance endoscopy and biopsy, which is both unpleasant for patients and expensive. This has generated interest in the potential utility of biomarkers to predict success of treatment. The aim of this study is to determine whether residual DNA ploidy abnormalities after successful treatment with PDT predict late relapse to HGD or cancer.

5.7.2 Methods

The criteria for inclusion were:

a) Confirmed HGD prior to treatment

At least two endoscopies prior to PDT (with large-capacity four-quadrant biopsies every 2cm of BO) demonstrating HGD. Histology was confirmed by two experienced independent specialist GI pathologists. Endoscopic mucosal resection (EMR) was undertaken of any raised areas and only patients with residual HGD after EMR were given PDT. DNA ploidy was analysed on all 4 biopsies from each 2cm level of BO. All patients had DNA ploidy analysis on HGD biopsies at one or multiple levels from their enrolment endoscopy.

b) Successful treatment with no dysplasia at follow up

All patients were treated with 5 aminolaevulinic acid (ALA) PDT as previously described.[Mackenzie et al., 2007a;Mackenzie et al., 2009] Ethical approval was granted for the study (EudraCT No: MF 8000 21074).

Following PDT patients underwent endoscopy with four-quadrant biopsies every 2cm from the treated oesophagus at 6 weeks, 4 and 12 months after PDT and at 18, 24, 36, 48 and 60 months. At each follow up endoscopy after PDT care was taken to ensure that the whole of the treated area was sampled, to ensure no buried glands were missed in areas that had healed with squamous regeneration. Assessment of DNA ploidy post PDT was carried out on all specimens with glandular epithelium, or mixed squamo-glandular epithelium. Biopsies with squamous epithelium alone were not analysed.

All patients treated with PDT who were free of residual disease at 12 months were included in this prospective study. To be considered disease free patients must have had at least three endoscopies over at least 12 months post PDT. Relapse was defined as presence of HGD or cancer during follow up.

Statistical Methods

All analysis was performed using either SPSS® for Windows statistical package (SPSS Inc., Version 14.0, Chicago, Il, U.S.A) or Stata for Windows (StataCorp LP, Version 10.1, USA) The two tailed p value of <0.05 was considered significant. Hazard ratios for late relapse (HGD or cancer beyond 1 year) were estimated using the Cox proportional hazards model and their significance was assessed using the log-rank test (for categorical factors: sex, the presence of DNA ploidy abnormalities before 4 and 12 months after treatment) or the Wald test (for continuous variables: age, and length of BO pre PDT).

5.7.3 Results

A cohort of 30 patients who were treated with ALA PDT for HGD arising in BO, and who remained clear of dysplasia for at least 12 months after treatment, were studied for factors predictive of future relapse. In particular DNA ploidy was assessed by ICDA on all biopsies taken prior to treatment, and at 4 and 12 months post treatment. There were 13 cases of late relapse (7 cancer, 6 HGD) and 17 patients who remained free of relapse for a mean of 44 months (including 12 months).

There were 1177 months of follow-up (from treatment) in the 30 patients (mean 39 months/patient, IQR 12-64 months) corresponding to just over 68 years beyond one year

post treatment. The annual rate of recurrence (including cancer beyond one year) was 19%. Median relapse free interval was 3.6 years. Patient characteristics and results of survival analysis are shown in Table 5.22. None of age, sex, or length of Barrett's pre PDT had a significant effect on late relapse.

Table 5.22: Patient characteristics and survival analysis

	Mean	IQR	HR	95%CI	p-value
Male	83%		0.47	0.12 to 1.78	0.25
Age (years)	69	60 - 77	1.01	0.96 to 1.07	0.62
Barrett's Length prior to PDT (cm)	5.7	4 - 7	1.07	0.88 to 1.30	0.51
Aneuploidy pre PDT	83%		0.75	0.20 to 2.79	0.66
Aneuploidy 4 mo post PDT	33%		4.1	1.3 to 13.0	0.009
Aneuploidy 12 mo post PDT (n=29)	34%		3.6	1.05 to 12.3	0.029
Aneuploidy 4 and/or 12 mo post PDT	47%		8.2	1.8 to 37.8	0.0012

A total of 469 samples were processed for DNA ploidy from these 30 patients. A summary of the raw data is presented in Appendix D. Representative histograms are shown in figures 5.26 and 5.27. Prior to treatment all but 5 of the 30 patients were aneuploid and there was no significant difference in relapse rates with aneuploidy. At 4 months after treatment, 10 patients were aneuploid. Patients who were aneuploid at 4 months were significantly more likely to have late relapse (Hazard ratio (HR) = 4.1, p=0.009). At 12 months DNA ploidy was assessed in 29 patients: 10 were aneuploid and 2 had DNA tetraploidy, both also had aneuploidy. Aneuploidy at 12 months was a significant predictor of subsequent relapse (HR= 3.6, p=0.03).

We then compared all 14 patients with DNA ploidy abnormalities at 4 or 12 months with those that were diploid. This variable was extremely predictive of recurrence beyond 12 months (HR=8.2; 95% CI = 1.8-37.8; log-rank p=0.001). It is noticeable that the survival curves begin to diverge earlier for DNA ploidy at 4 months compared to DNA ploidy at

12 months (Figure 5.28). We therefore also analysed DNA ploidy as a time dependent covariate, taking DNA ploidy at 4 months as the covariate value for recurrence between 12 and 20 months and DNA ploidy at 12 months (if available) to predict recurrence beyond 20 months post treatment.. This time dependent covariate gave a hazard ratio of 6.3 (95% CI = 1.7-23.4, log rank p=0.0015). None of the other variables recorded had a significant effect on recurrence beyond 12 months.

Figure 5.26 Histograms from a patient who relapsed to cancer at 24 months

Aneuploid histogram prior to PDT with DI 1.7 (left) and persistent aneuploidy4 months post PDT with DI 1.7 (right)

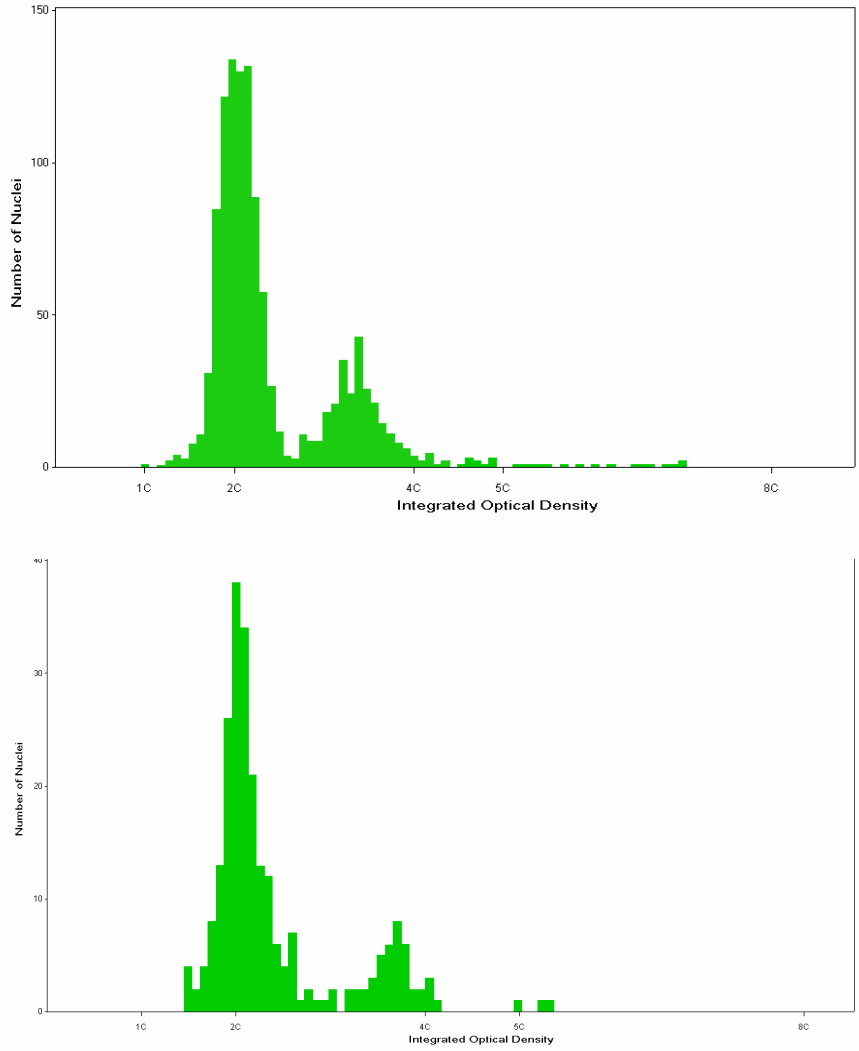

Figure 5.27 Histograms from a patient who remains disease free at 42 months

Aneuploid histogram prior to PDT with DI 1.8 (left) and diploid 4 months post PDT (right)

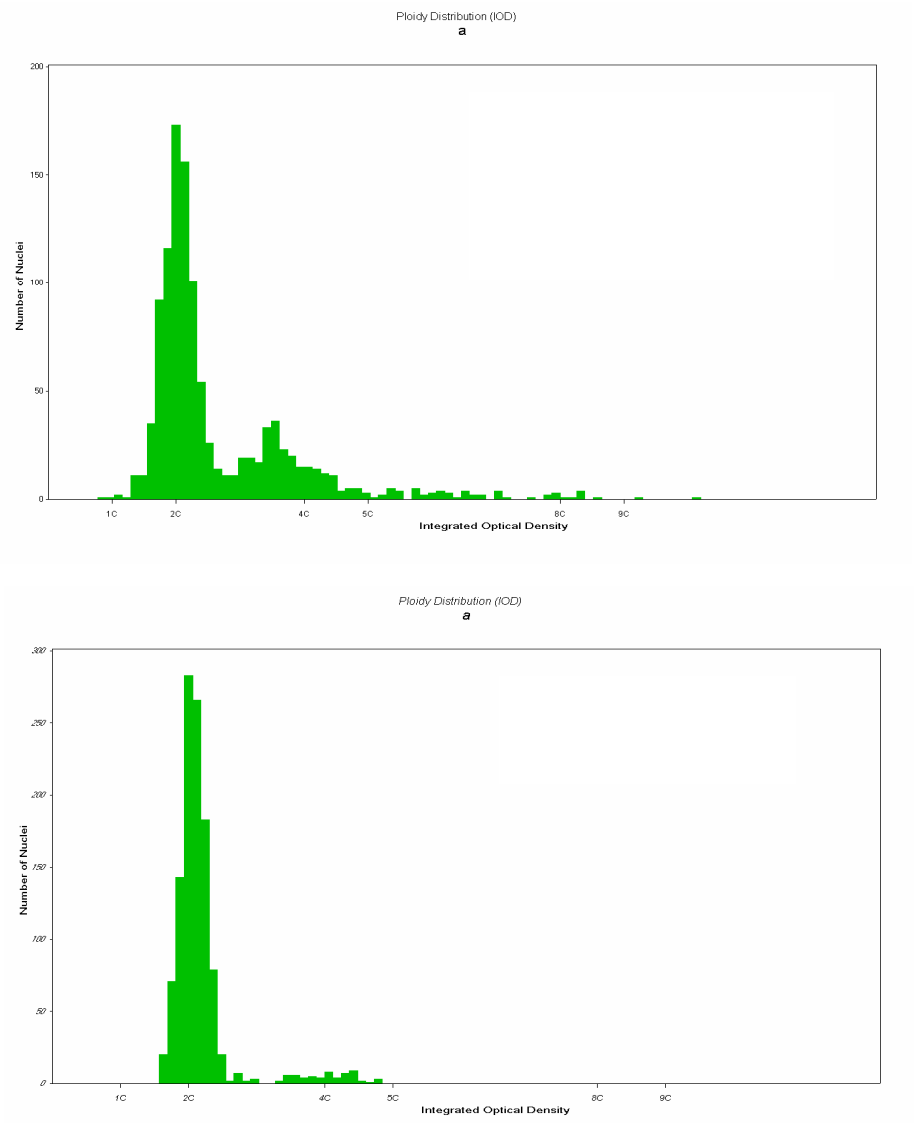

Figure 5.28 Kaplan Meier disease free survival estimates according to DNA ploidy status

Blue = Diploid, Red = aneuploid or tetraploid

a) DNA ploidy status at 4 months post PDT

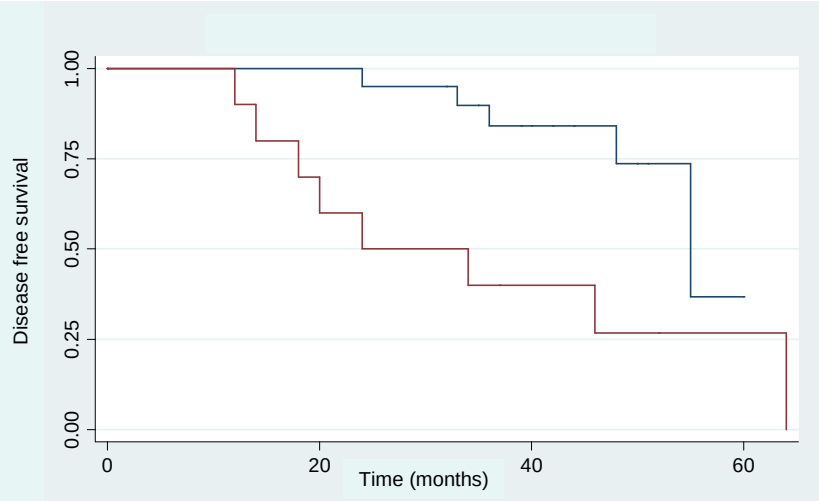

Follow up (months)	12	24	36	48
Number of patients at risk	30	26	20	10

b) DNA ploidy status at 1 year

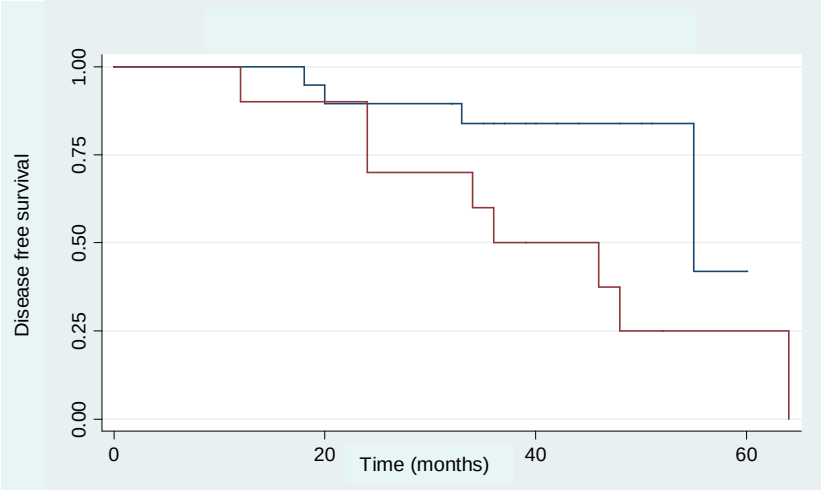

Follow up (months)	12	24	36	48
Number of patients at risk	30	26	20	10

c) DNA ploidy status at both time points post ALA PDT

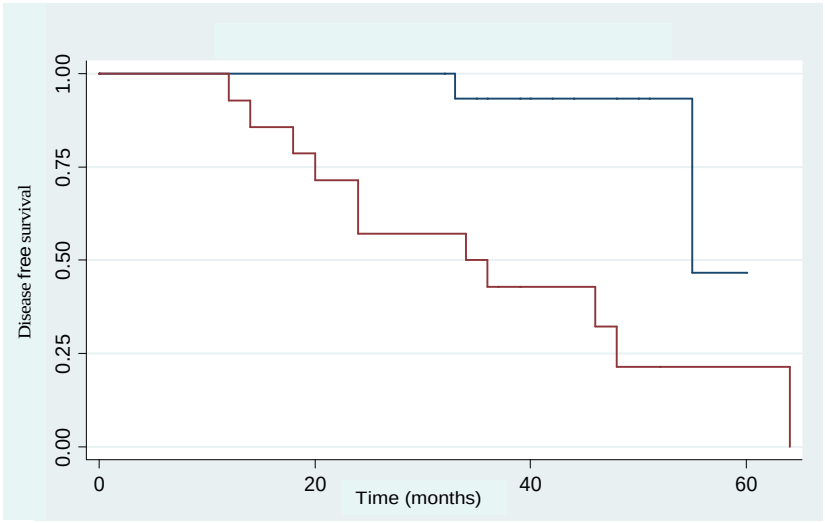

Follow up (months)	12	24	36	48
Number of patients at risk	30	26	20	10

5.7.4 Discussion

We have demonstrated the value of DNA ploidy measured by ICDA as a biomarker to predict late relapse to HGD and cancer in BO, following successful treatment of dysplasia by photodynamic therapy. DNA ploidy abnormalities after treatment conferred a hazard ratio of 8.2 (95% CI = 1.8-37.8) for developing recurrent HGD or cancer. Rabinovitch *et al.* previously demonstrated aneuploidy arising in non-dysplastic BO, as measured by flow cytometry, conferred a relative risk for progression to cancer of 4.4 (95% CI = 1.4–14). [Rabinovitch et al., 2001] These earlier data are consistent with the findings of our study.

The importance of residual genetic abnormalities in Barrett's epithelium following PDT has previously been postulated. Foultier *et al.* assessed the influence of DNA ploidy abnormalities on outcomes in patients with early gastrointestinal cancer (oesophageal, gastric, colorectal) treated by haematoporphyrin derivative PDT. [Foultier et al., 1994] Aneuploidy (measured by FC) at 4 month follow up was associated with a poor response, with only 5 of 15 patients with aneuploidy achieving complete remission, compared with 12 of 17 patients without aneuploidy. Prasad *et al.* reported on the correlation of

histology with biomarker status after photofrin PDT, where overall fluorescence in situ hybridization (FISH) positivity for a panel of biomarkers (including loss of p16 and p53) was seen in 60% of non responders to sp-PDT vs. 19% of responders. [Prasad et al., 2008] No individual biomarker however, was shown to predict success or failure of therapy.

DNA ploidy changes before and after PDT suggest that ALA acts directly on cancer cells in addition to vascular effects leading to oxygen deprivation and apoptosis.[Foultier et al., 1994] 13/30 patients did not achieve reversal of DNA ploidy abnormalities despite normal histology, which suggests dysplastic cell populations in BO do not act in the same way to treatment. One postulated theory on the histogenesis of BO is that heterogeneity arises from multiple independent clones, in contrast to the selective sweep to fixation model of clonal expansion previously described.[Leedham et al., 2008] This may explain why sub populations of cells may occur that are resistant to therapy and continue to display genetic abnormalities.

The occurrence of diploid cell populations in HGD tissue was noted in 5 patients prior to treatment. 3/5 patients have relapsed, with 2/3 cases showing no DNA ploidy abnormalities in the first year after PDT. Further analysis of DNA ploidy was undertaken on all biopsies taken from these patients after 1 year, and both showed DNA ploidy abnormalities before developing cancer. In the first, aneuploidy was found at 2 years post PDT, 6 months before cancer was diagnosed. In the second, DNA tetraploidy was found 18 months post PDT. Cancer developed 3 years later. This may be explained by sampling error, as small aneuploid populations may be missed by ICDA. Another argument would be ALA PDT induced mutation and up regulation of an aneuploid clone not previously quantified. This has been shown in studies on glioblastoma cell lines where ALA can lead to up regulation of putative cancer stem cells that are resistant to therapy.[Morgan and Petrucci, 2009]

There are some limitations to this study. Despite significant differences between groups, the sample size is small. Kaplan-Meier plots and survival analysis methods allow for whatever follow up time is available for each person, thereby maximising our sample size

and allowing statistically significant conclusions to be drawn. The significance of endoscopic sampling error is difficult to quantify. It is possible that small foci of dysplasia may be missed at follow up endoscopy using current standard four-quadrant surveillance. However after 3 clear endoscopies we estimate this miss rate to be small.

DNA ploidy measured by ICDA is accurate when compared to flow cytometry, with advantages of cost effectiveness, potential for automation and routine analysis of paraffin embedded tissue. It is important to note that both ICDA and flow cytometry examine predominately whole nuclei, and it is less likely that these findings would be replicated by analysis of cut nuclei from thin sections. Furthermore DNA ploidy abnormalities by ICDA predict risk of relapse following ablative therapy, and may be clinically useful as a biomarker by allowing an individualised approach to patient follow up. If stratifying risk according to DNA ploidy status following ablative therapy then patients with residual aneuploidy would require intensive surveillance, whereas diploid patients may return to 3 yearly surveillance and be reassured of a very low cancer risk. The reduction in the frequency of follow up endoscopies for the majority of patients would also provide financial savings for healthcare services. The study is limited by its retrospective design and a larger prospective study using reversal of DNA ploidy abnormalities as an end-point for treatment success would be valuable.

5.8 Prospective study of ICDA on cytology specimens

5.8.1 Introduction

The use of DNA ploidy as a prognostic biomarker both before and after development of dysplasia makes this a useful tool in decision making process in BO. The processing of biopsy specimens for is however labour intensive and expensive. It is also limited by the time it takes to process a sample. It can take up to 2 weeks to process a biopsy after a section has been cut for pathologist and the biopsy is embedded in paraffin. As ICDA uses the same FFPE tissue then the same problem of time lag between tissue retrieval and diagnosis exist. In addition there is the unknown quantification of sampling error, when analysing multiple random four quadrant biopsies. Finally the tissue required from a

block varies according to the volume of tissue and therefore is dependent on the endoscopist's biopsy technique.

An ideal sampling technique for DNA ploidy would therefore be simple to undertake, quick to process and sample a large field of the Barrett's segment. Brush cytology is a commonly used technique in endoscopy and its use has been demonstrated in diagnosis of oesophageal candidiasis [Scott and Jenkins, 1982], BO [Wang et al., 1992], squamous cell cancer [Wang et al., 2005] and Cholangiocarcinoma [Boberg et al., 2006]. In patients with Barrett's oesophagus cytology has been shown to have a sensitivity of 80% for the diagnosis of HGD, but only 20% for LGD.[Saad et al., 2003] More recently studies have been published on the detection of genetic abnormalities using a sponge in the oesophagus [Lao-Sirieix et al., 2009] and using brush cytology to detect DNA ploidy abnormalities from the bile duct [Sears et al., 1998] and lobular ducts in breast cancer [Sauter et al., 2004]. There have been no experiments undertaken to assess the feasibility of using cytology to detect DNA ploidy in Barrett's oesophagus. The aim of this prospective study was to assess diagnostic accuracy of brush cytology samples for the detection of DNA ploidy abnormalities, and compare with FFPE biopsy samples taken simultaneously.

5.8.2 Methods

This was a prospective single centre cohort study of patients undergoing Barrett's surveillance at UCLH. Ethical approval was obtained (REC number 08/H0808/8) and all patients signed informed consent prior to the procedure. The cytology brushing was performed under direct endoscopic vision using a disposable brush (Boston Scientific, Watertown, Massachusetts, US). Cytology samples were taken from each quadrant using the same brush with care taken to avoid trauma and blood contaminating the sample. The whole length of the Barrett's segment was sampled starting at the most proximal extent of the gastric folds and ending at the top of the tongues. The tip of the brush was then cut with wire cutters, placed into 2ml eppendorf tubes and stored in 10% formaldehyde solution. Samples were kept at 4°C until processing. Processing was carried out as previously described, using Pepsin rather than proteinase. An oesophageal biopsy series

was then taken every 2cm from the posterior wall throughout the entire length of the Barrett's segment. These samples were analysed for ICDA as has been described previously.

5.8.3 Results

Paired brush cytology & biopsy specimens were obtained from 73 patients undergoing BO. The median age was 66 years (range 34-85 years), 71% were male and the median length of BO segment was 6cm (range 1-12cm). Eleven have failed – 4 cytology samples and 7 FFPE samples. The distribution of histology grade among the 62 patients with matched cytology and FFPE samples is summarised in figure 5.29.

Figure 5.29 Distribution of matched FFPE samples according to histology grade

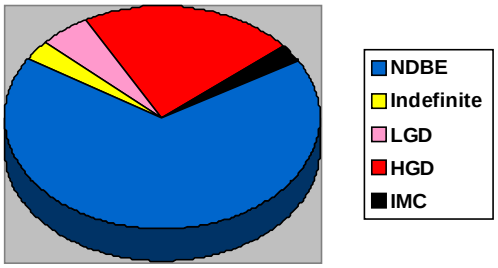

When assessing DNA ploidy the percentage with aneuploidy was 25% in the NDBO group when assessed on FFPE samples vs. 5% using cytology brushings (see Table 5.23). There was no significant difference between the two methods for the rate of DNA ploidy abnormalities detection in the dysplastic BO group.

Table 5.23 Percentage of DNA ploidy abnormalities diagnosed on cytology and FFPE specimens vs. histology

	SIM n = 44	Indefinite n=2	LGD n=4	HGD n= 10	Cancer n=2
DNA ploidy on brush cytology	5%	0%	25%	70%	50%
DNA ploidy on biopsy	25%	50%	50%	80%	0%

Table 5.24 Comparison of each method

	DNA ploidy +ve on cytology	**DNA ploidy -ve on cytology**
DNA ploidy +ve on biopsy	8	14
DNA ploidy -ve on biopsy	3	37

Using ICDA from FFPE tissue as a gold standard, cytology diagnosed DNA ploidy abnormalities with a sensitivity of 36% and specificity of 93% (see Table 5.24). When ICDA from cytology specimens was evaluated in the cohort of patients with dysplastic BO, sensitivity increased to 73% with specificity of 86%. 17/65 had a mismatch in the diagnosis by the 2 methods. 82% of these patients were called diploid on cytology but were aneuploid on FFPE, compared to 18% called aneuploid on cytology but diploid on biopsies.

5.8.3 Discussion

Detection of DNA ploidy abnormalities from cytology specimens is not as sensitive as analysis of biopsies, although this simple test does have a high specificity. The cytology brushings performed badly in the NDBO group, which makes up the vast majority of patients undergoing BO surveillance. The vey low sensitivity of cytology for DNA ploidy abnormalities would seem to make it unsuitable as a primary screening tool. The percentage of patients with DNA ploidy abnormalities, as measured by FFPE, does however seem high in this group. Furthermore this cohort may not be representative of a general hospital surveillance programme, as these patients were referred with known BO to tertiary centre care.

ICDA cytology performed better in patients with dysplasia, although this is probably explained by confounder bias, as DNA ploidy abnormalities increase in prevalence with the degree of dysplasia. ICDA on cytology samples did detect a further 3 patients with DNA ploidy abnormalities who had not been detected from analysis of biopsies. This simple test may therefore be useful as an additional test to detect high risk patients, or when biopsies cannot be performed at endoscopy due to a stricture or concerns re

bleeding and trauma. Accuracy is not high enough to warrant using ICDA by cytology instead of endoscopic surveillance with four quadrant biopsy at present. Future work that may improve accuracy is the use of a sponge capsule that can pick up a larger number of nuclei, and sample a larger surface area.[Sirieix et al., 2003;Lao-Sirieix et al., 2009] Assessing the utility of ICDA with a panel of other cytological biomarkers may improve diagnostic yield and a prospective study using the sponge capsule would be valuable.

5.9 Summary

The experiments presented in this chapter demonstrate that ICDA is an accurate method for the assessment of DNA ploidy abnormalities arising in BO. The comparison with flow cytometry is strengthened by our collaboration with a reference laboratory that pioneered the work on FC in BO 10 years ago. Aneuploidy and tetraploidy by ICDA are also predictors of future cancer risk in NDBO, when blindly evaluated in a large case control study. DNA ploidy abnormalities alone conferred a significantly increased odds ratio for progression to HGD/OAC, which was further increased when IND or LGD was present.

Work presented in this chapter also shows that aneuploidy /tetraploidy are of prognostic significance after ablative therapy. DNA ploidy abnormalities measured by ICDA at 4 months and 1 year predicted cancer progression following histologically successful treatment with ALA PDT. This has potential for clinical application to guide surveillance intervals and potentially offer re-treatment. Finally the utility of brush cytology was evaluated as a potential screening tool for aneuploidy, although the results did not compare favourably with random biopsy sampling, and FFPE tissue evaluation should remain the current standard for ICDA.

Chapter 6

Nucleotyping

Chapter 6 Nucleotyping

6.1 Introduction

There is much interest in the utility of molecular biomarkers in BO, both to predict which patients may develop cancer (and therefore offer therapy) and to aid prognostication by guiding surveillance intervals following therapy. Genomic instability seems to be a fundamental property of neoplastic progression that develops before the onset of cancer, and a large body of evidence now suggests that most oesophageal adenocarcinomas arise in association with a process of gain or loss of whole chromosomes or large portions of chromosomes.[Reid et al., 2010] In the previous chapter the utility of DNA ploidy abnormalities measured by ICDA as a prognostic biomarker was demonstrated – both in patients treated with PDT and ablation naïve patients. There are some flaws to this approach; ICDA, although accurate when compared to FC, may not be able to quantify small aneuploid populations in the near diploid region; DNA ploidy abnormalities are probably rare early events in progression to cancer, with LOH at 9p and 17p occurring more frequently at an earlier stage; ICDA can only be assessed on nuclear monolayers from thick sections; a combination of CIN markers has been shown to be more effective in predicting cancer risk than DNA ploidy alone. [Galipeau et al., 2007]

Nuclear textural analysis is a methodology that describes the chromatin distribution pattern of nuclei, by interrogation of nuclear DNA structure and organisation both quantitatively and qualitatively. As chromosomal instability correlates with large scale re-arrangement of nuclear chromatin, nuclear texture analysis has potential as a novel measure of chromosomal instability. Nuclear textural analysis can be performed on the same high resolution digital images of stained nuclei used for ICDA, [Yogesan et al., 1996] and has also been described on light microscopes images taken from thin (5 micron) H&E stained sections of the oesophagus, colon and prostate.[Weyn et al., 2000] Nuclear textural features have been shown to aid prognostication in several cancers including prostate, breast, head and neck and gynaecological tumours.[Yogesan et al., 1996;Tengs et al., 2008] Although work has been carried out on thin sections for many

tumour types, in general classification has not been shown to add prognostic information.[Bozzo et al., 1998;Bibbo et al., 1987;Scarpelli et al., 1999] The utility of nuclear textural analysis for the assessment of BO and risk of progression to OAC has not been evaluated.

6.2 Chromatin structure and organisation

The DNA of eukaryotic cells is tightly bound to small basic proteins (histones), to form protein/DNA complexes which are called chromatin. Chromatin packages DNA into a smaller volume to fit in the cell, strengthens the DNA to allow mitosis and meiosis, and serves as a mechanism to control expression and DNA replication. Although histones are the major proteins of chromatin, a wide variety of non-histone chromosomal proteins such as transcription factors and scaffold proteins also exist.

There are many levels of chromatin organisation, as demonstrated in figure 6.30. At the first level are nucleosomes, the basic structural unit of chromatin. DNA wraps around histone proteins forming these nucleosomes in a so called "beads on a string" structure. The packaging of DNA into nucleosomes forms chromatin fibres of approximately 10 nm in diameter. At the second level the nucleosomes form a helical 30 nm chromatin fibre, referred to as the solenoid. At the next level the solenoid forms the DNA loops, which are approximately 250nm in diameter.

Figure 6.30 DNA organisation and chromatin structure

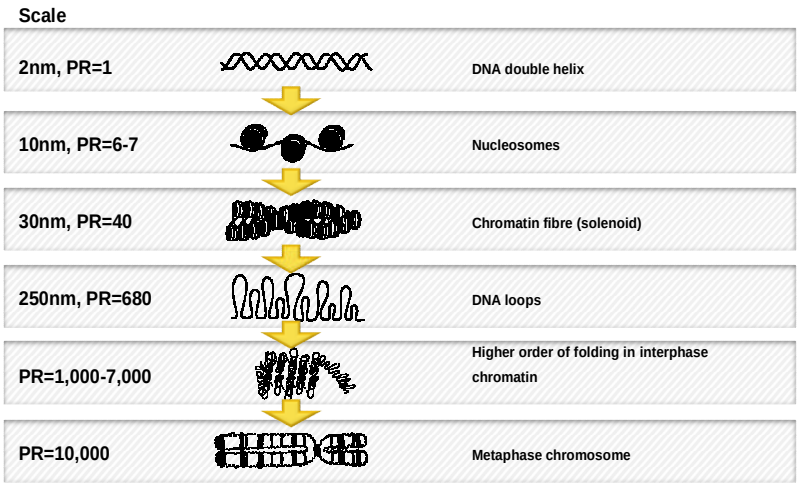

During interphase (G1-S-G2) the chromatin organisation within the nucleus reflects the transcriptional/translational activity of the cell. The interphase chromatin is divided into two types, heterochromatin (condensed form) and euchromatin (extended form) (see figure 6.31). Heterochromatin is non-transcriptionally active. Euchromatin is transcriptionally active as the DNA forms a dispersed open structure, allowing for recognition and activity on DNA by the transcriptional machinery. Finally during mitosis chromatin becomes highly condensed to form compact metaphase chromosomes that are distributed to daughter nuclei.

Figure 6.31 Transmission electron micrograph (TEM) of an interphase mouse liver cell nucleus

The intensely stained dark pixels represent heterochromatin (and the nucleolus) and the lighter pixels represent euchromatin (courtesy of H.E Danielsen)

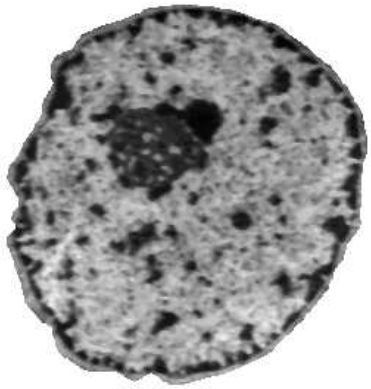

6.3 History of nuclear textural analysis

Although studies describing nuclear texture analysis were first published in the 1970s, it is only the last decade that has seen a surge in interest in the methodology as a potential prognostic biomarker. This is probably due to advances in computer processing power over that time and better understanding of the statistical caveats involved in interpretation.

6.3.1 Early studies

The basic approaches to modern statistical textural analysis were first described by Pressman, who applied a Markovian approach to analyze the nuclear texture of cervical carcinoma.[Pressman, 1976] In 1984 Jagoe *et al.* used shape and texture analysis to distinguish between liver cell nuclei from normal hepatocytes and from hepatoma

cells.[Jagoe et al., 1984] Kriete *et al.* applied texture analysis to transmission electron microscopy (TEM) images of cell nuclei from thyroid gland tumours.[Kriete et al., 1987] Danielsen *et al.* also observed a stepwise development of changes in the chromatin in liver carcinogenesis on high resolution image analysis on TEM images from mouse liver. [Danielsen, 1991] These initial methodological studies undertaken on TEM images of cancer cells led to the identification of several textural features. These features were then adapted for a new methodology, using images from nuclear monolayers rather than TEM. These were then evaluated in clinical studies.

6.3.2 Clinical Studies

In a retrospective study a group of 20 patients with advanced metastatic prostate cancer were separated equally into two groups on the basis of disease progression and survival following treatment by orchidectomy.[Jorgensen et al., 1996] Group A was considered therapy resistant with disease progression and death over a 2 year follow up. Group B were considered therapy sensitive with survival and no signs of disease progression after 3 years follow up. Nuclear texture analysis was able to correctly classify subjects into each group (correct classification rate or CCR) 90% of the time, using only 3 textural features. Validation of the textural feature set on an independent data set has also been presented.[Jorgensen et al., 1996] In a study of bladder cancer cell lines nuclear chromatin texture analysis of 40 features was performed to explore if nuclear phenotype was related to radiation sensitivity.[Rajab et al., 2006] A classification function, defined using these features, correctly classified 82% of all cells into their radiosensitive or radioresistant groups based on their pretreatment chromatin phenotype.

Dreyer *et al.* showed that fractal texture features (chromatin measurements) can be used to assess malignancy in tissue sections as an alternative to DNA ploidy.[Dreyer et al., 2001] Guillaud and colleagues showed that subvisual changes in chromatin texture could be detected by quantitative histopathology in cytologically normal as well as abnormal samples.[Guillaud et al., 2004] The same group then went on to test this is in a follow up study on grades of cervical intraepithelial neoplasia, but no significant correlation was found.[Guillaud et al., 2005] The authors undertook a sub-analysis on 5 patients and

suggested that changes in chromatin organisation occur due to co-infection with human papilloma virus. As 55 texture features were used, one could argue this result is almost certainly due to overfitting of the data. This is a criticism that may be applicable to the majority of texture analysis studies, as the sheer quantity of textural features that may be obtained makes statistical bias an inherent problem. To address this there are statistical caveats that have been introduced and a summary of these is described below.

6.4 Basic terms and principles in digital imaging and textural analysis

In digital pathology of thin sections (4-6micron) the two-dimensional (2D) physical image is divided into small regions called pixels (picture elements). The most common sampling scheme is a rectangular sampling grid, so the image is divided into horizontal lines of adjacent pixels. Each pixel has an integer location or address (row number and column number) and a quantified integer pixel value representing the integrated intensity of light over the area of the pixel. The measured intensity of light may be proportional to the amount of light transmitted through a specimen or the intensity of fluorescence in the sample.

When analysing black and white images of nuclear monolayers stained with Feulgen, the measured intensity of light is proportional to the DNA content at each pixel and is referred to as the grey level. Visual textures are patterns of repetitive basic elements called texels. Each texel contains several pixels, each of which can be defined by its grey level (see figure 6.32). Analysis of the patterns of repetition of the grey level in texels therefore correlates with the organisation and structure of chromatin.

Figure 6.32 Example of a nucleus stained with Feulgen and captured by digital imaging

The schematic on the left demonstrates a texel comprising 9 pixels in a 3x3 square. The numbers in each square correspond to the grey level of each individual pixel.

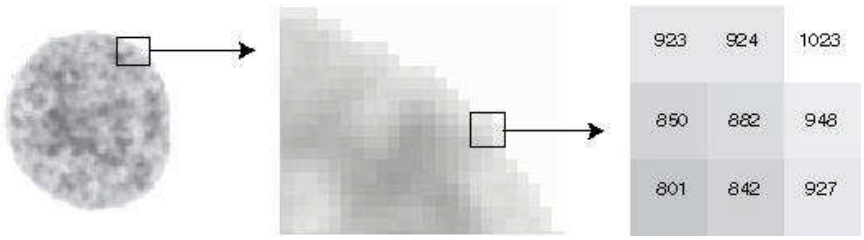

This information can be quantified using statistical analysis, ranging from simple *first order statistics* which are based on information about single pixels, through *second order statistics* which measure the differential between groups of 2 or more pixels (i.e. gradients) to more complex *higher order statistics* which describe qualities of distributions based on information from a number of pixels (i.e. patterns).

6.4.1 First order Statistics

First-order statistics measure the likelihood of observing a grey value at a randomly chosen location in the image. First-order statistics can be computed from the histogram of pixel intensities in the image. These depend only on individual pixel values and not on the interaction or co-occurrence of neighbouring pixel values. The analysis of integrated optical density (IOD), which relatively measures DNA content after DNA staining, is an example of first order statistics. IOD is calculated by a summation of the nuclear optical density (OD) of each pixel, which in turn is directly proportional to the pixel grey level value. Therefore, for nuclei with approximately the same DNA content, the mean grey level decreases with an increasing nuclear area. For nuclei with approximately the same nuclear area, the mean grey level increases with an increasing nuclear DNA content.

6.4.2 Second order Statistics

The relationship between image grey level values in pixel pairs or sequences of pixels of a given widow size are stored in matrices. *Second-order statistics* are defined as the likelihood of observing a pair of gray values occurring at the endpoints of a dipole (or needle) of random length placed in the image at a random location and orientation. These properties may be defined as the gray level co-occurrence matrix (GLCM).

Grey Level Co-occurrence Matrix

The co-occurrence based approach to the analysis of visual textures has been widely used for nuclear texture analysis since the method was first introduced by Haralick in the 1970s.[Haralick, 1979] The GLCM approximates the joint probability distribution of two pixels. A relative large number of static (non-adaptive) textural features can then be extracted from these matrices. Static feature extraction is usually performed by computing a number of pre-defined (ad hoc) weighted sums of matrix elements, which

are either based on the value of each matrix element or on the position of the element within the matrix. The usual procedure is then to perform a feature selection, in order to obtain a subset of features to be used in a classifier. For example, from Haralick's work 14 textural features were calculated. The number of features used is largely user dependent, so by using a larger number of features a greater discriminatory power might be achieved but this is paralleled by a reduction in statistical accuracy. This is a problem if using a large number of features when the available data set is limited, as there is an increased risk of overfitting the data. This has led to strategies to limit the number of features used whilst maintaining discrimination.

Adaptive textural features

Using an adaptive features approach, extra weight is given to matrix elements that discriminate well between the two classes. This is advantageous as only a few consistently valuable features are used, therefore reducing the number of dimensions of the dataset and the subsequent probability of overfitting. This relatively new method has been previously shown to outperform the static features approach when applied to the most difficult set of 45 Brodatz texture pairs [Albregtsen et al., 2000] and in a mouse liver nuclei.[Nielsen et al., 2004]

Despite these advances in statistical analysis, a deficiency of 2^{nd} order statistics is that the features measured are global averages across entire images rather than direct measurements within the scale of a texel. The GLCM method does not directly measure the distance between pixels and hence the subsequent geometric position of the texel in the nucleus is unknown. This information is important as chromatin content, and therefore texture, may change between the peripheral and central parts of cell nuclei.

6.4.3 Higher order Statistics

Grey Level Entropy Matrix

Higher order statistics refer to the interrogation of 3 or more pixels grouped in texels, which has been previously defined as the Grey level entropy matrix (GLEM).[Yogesan et al., 1996] Entropy is a measure of uniformity, so homogeneous structures will give low

entropy values whereas inhomogeneous structures will give high entropy values. The matrix element $P(i, j \mid w)$ contains the estimated probability of a first order grey level entropy value j within a window of size $w \times w$ centered around a pixel with grey level value i. [Yogesan et al., 1996]

The logarithmic entropy is defined as

$$j = -\sum_{i=1}^{G} P(i) \log \{P(i)\}, \quad P(i) > 0,$$

where $P(i)$ is the normalized frequency of occurrence of grey level i within the window of size $w \times w$, and G is the number of grey level quantization levels in the image. For example, in the studies that are described below the number of grey levels in the image were reduced by re-quantization from 1024 to 64 prior to the computation of the matrices, and the matrices were computed with a window size of 9×9 pixels.

Static textural features

Previously nine features have been defined based on the GLEM, which have been shown to be of prognostic value in prostate cancer.[Yogesan et al., 1996] These nine features are weighted sums of the normalized GLEM element values, based on relatively simple weight functions. As this is a large number of features we can use the adaptive features approach, described above, to reduce this to the most useful textural feature set.

Adaptive textural features

Using the adaptive features approach only two adaptive features from the Grey Level Entropy matrices are extracted.[Yogesan et al., 1996] For each patient the nuclear images are grouped into area intervals according to the number of pixels in the image (A_0 = < 1000 pixels, A_1 = 1000-1999 pixels, A_2 = 2000-2999 pixels, …, A_{10} = > 10000 pixels).[Nielsen and Danielsen, 2006] Within each of these area groups (A_a), the average entropy matrix $P(i, j \mid w, A_a, \omega_c)$ and the variance entropy matrix $\sigma^2(i, j \mid w, A_a, \omega_c)$ is computed. We then calculate average matrices $\overline{P}(i, j \mid w, A_a, \omega_c)$ and

$\overline{\sigma^2}(i, j \mid w, A_a, \omega_c)$ over all the learning set cases in each class ω_c. Based on these matrices, we compute a class difference matrix and a squared Mahalanobis class distance matrix, i.e., the squared difference between the two class element values, divided by the average of the two class variances for that particular GLEM element.[Nielsen and Danielsen, 2006] Using these class difference and distance matrices, two adaptive features are extracted from each nucleus. A mean feature value is then calculated for each patient from all nuclei defined by the area intervals A_a, where α= 1-5.

For the purposes of our clinical studies the GLEM adaptive features method was used for nuclear texture analysis. This method, described by Professor Danielsen's group at the University of Oslo, is distinct from previous methods of nuclear texture analysis and is referred to as nucleotyping.

6.5 Aims of this chapter

The aim of this chapter is to explore the use of nucleotyping in the assessment of patients at risk of developing cancer in BO, and compare to ICDA.

In order to validate this method in BO the following experiments were designed

1. Assessment of nucleotyping methodology on nuclear monolayers from 40 micron sections
    a. To compare results with histology
    b. Assess if NT is correlated with DNA ploidy
2. Assess nucleotyping as a predictor of future cancer risk in BO on 40 micron nuclear monolayers

6.6 Comparison of nucleotyping and ICDA for the assessment of dysplasia arising in BO using nuclear monolayers

6.6.1 Materials and Methods

Patient selection

A total of 120 patients from the UCLH Barrett's oesophagus cohort were included in the study. These were separated into two groups according to histology. The first group (group 0) had SIM on four quadrant biopsy at baseline surveillance endoscopy, which was confirmed by 2 specialist GI pathologists. To confirm that these patients were true non-dysplastic with low risk of progression all had at least one follow up surveillance endoscopy two years later, which also showed SIM only. The median follow up was 51 months (IQR 25-120). The second group (group 1) had HGD confirmed by 2 specialist GI pathologists. Analysis was undertaken on representative biopsies displaying SIM or HGD from one level of BO per patient. Two 40μm sections were cut from FFPE tissue and then nuclear monolayers were prepared and stained with Feulgen as previously described. [Pretorius et al., 2009]

Digital Image Analysis

ICDA was carried out as previously described in chapter 5.3. All the slides were studied using Nucleotyping Analysis System (Room 4, Kent, UK). This is an automated image cytometric analyser that consists of a microscope (Axioplan 2, Zeiss, Jena, Germany), a 546-nm green filter, and a black-and-white, high-resolution digital camera (AxioCam MRm, Zeiss, Jena, Germany). The pixel resolution obtained with this lens is 254 nm per pixel on the cell specimen. After shading correction the cell nuclei were selected randomly, but in a systematic meandering way, and then were positioned in digital image galleries. Each gallery comprised 512x512 pixels with 8 bits per pixel and an average of 2,000 pixels per nucleus. 5000 nuclei were automatically captured and at least 300 were measured in each case. The Nucleotpying (GLEM + adaptive features) method was used for nuclear texture analysis.

6.6.2 Statistical Methods

Experimental design

Designing a classifier and properly evaluating its performance requires a training set and test set containing sufficient number of cases.[Schulerud et al., 1998;Nielsen et al., 2008] The training set is used to design the classifier, while the test set is used for evaluating its performance. In the training set, the cases' outcome is known and actively used to design the classifier. We used a prospective sampling method and patients from each group were randomly assigned to either the training set or the independent test set in 1:1 ratio.

Designing and applying the classifier

The classifier was designed based on the training set. Two adaptive nuclear texture features and their difference were calculated for each case. Each of the 3 resulting features were evaluated on the training set using linear discriminant analysis in SPSS® for Windows statistical package (SPSS Inc., Version 14.0, Chicago, Il, U.S.A). The feature with highest correct classification rate (CCR) was selected. This single feature was then applied to the test set where the outcome was not known.

6.6.3 Results

Patient characteristics and results of DNA ploidy analysis are shown in table 6.25. Gender and race did not differ significantly among groups. There was a significant difference in mean age between group A (55 years (range 28-81)) and group B (70 years (range 47-84)). Barrett's segment length ranged from 1 to 15 cm and was significantly lower in patients in the non-dysplastic group. There was a significant difference in the presence of DNA ploidy, with no patients displaying DNA content abnormalities in the non-dysplastic group vs. 65% in the dysplastic group.

Table 6.25 Clinical characteristics of patients

		Group 0 (non-dysplastic)	**Group 1 (dysplastic)**	**T-test**
Number patients analysed		54	58	
Age (years)	Mean (+/- SD)	54.7 +/- 11.4	69.6 +/- 9.2	$p < 0.001$
Gender	Male/Female	42/12	49/9	$p = 0.42$
Barrett's Length (cm)	Mean (+/- SD)	4.8 +/- 2	7.0 +/- 3.8	$p < 0.001$
DNA ploidy abnormality	%	0	65	$p < 0.001$

Adaptive features

Of the 120 cases, 112 were suitable for analysis with >300 nuclei. This amounted to n=55 in the training set (26 Non dysplastic BO, 29 dysplastic) and n=57 in the reserved blinded validation set (28 Non dysplastic BO, 29 dysplastic). The two adaptive features that gave the highest CCR on the training set were High entropy emphasis and Entropy Homogeneity. These features gave a correct classification rate of 83% (see figure 6.33). We then applied these adaptive features to the reserved blinded validation set which gave a CCR of 78% (see figure 6.34). When all 112 patients were evaluated the sensitivity and specificity for dysplasia by nucleotyping was 71% and 93% respectively. This compared to a sensitivity of 70% and specificity of 100% for DNA ploidy abnormalities. When analysis was undertaken combining both markers in a panel, the overall sensitivity was 76%, specificity 93%, and CCR=84%

Figure 6.33 Graph demonstrating nucleotyping model discriminant analysis on the training set

Group 0 – Non dysplastic BO, Group 1 – dysplastic BO

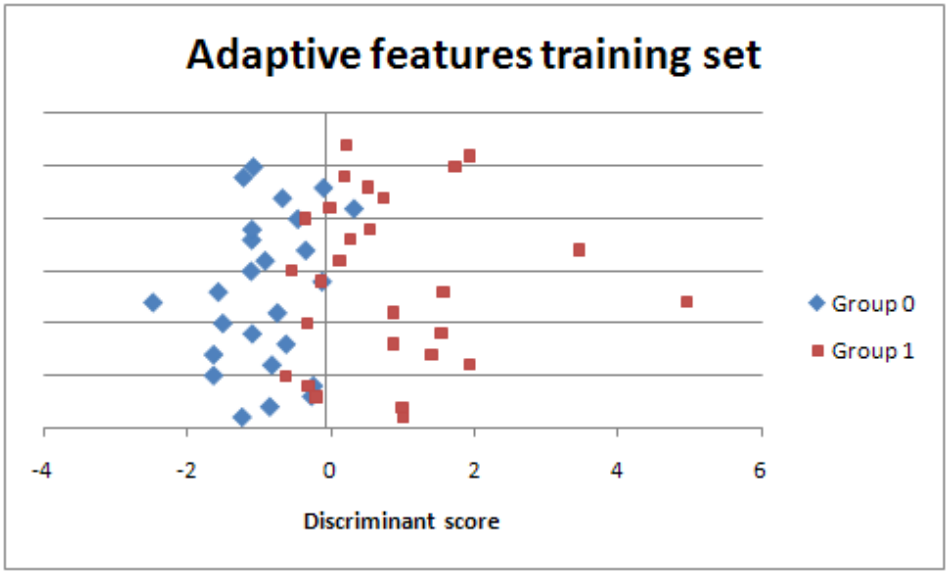

Figure 6.34 Graph demonstrating nucleotyping model discriminant analysis on the validation set

Group 0 – Non dysplastic BO, Group 1 – dysplastic BO

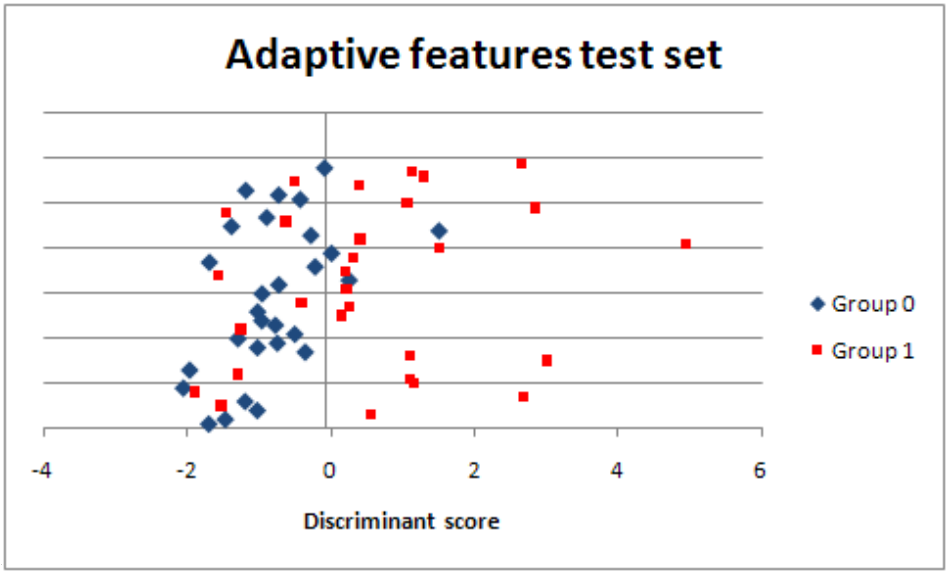

As noted above, nucleotyping classified some of the non dysplastic in the dysplastic category and some of the dysplastic in the non-dysplastic category. We set out to investigate these patients further and evaluate whether the apparently false classification had any clinical or histological relevance. Thirteen patients in the dysplastic group were classified incorrectly. This might be due to sampling error, as these outliers had longer segments BO compared to rest of group (median for HGD misclassified = 9cm {IQR = 3-14cm}, median for rest HGD = 7cm {IQR = 1-15cm}). Four cases from the non-dysplastic BO group were misclassified as dysplastic by nucleotyping. Two patients were indefinite for dysplasia on biopsies 2 years later and a third patient had aneuploidy but no dysplasia on biopsies 3 years later. The 4th patient had no dysplasia or DNA ploidy abnormality after 3 years follow up. It therefore remains to be seen whether these patients had sub-microscopic changes that could not be assessed by histopathology.

6.6.4 Discussion

These results show that nucleotyping can accurately classify patients according to their histological grade. Our method uses digital image analysis on the same nuclei used to assess DNA ploidy, which is advantageous as this can be translated into a single platform measure of chromosomal instability, with potential for automation and high throughput. Furthermore this combination of features was independently tested on a blinded validation set, therefore reducing errors of bias or overfitting of data that are inherent to other statistical models.

When we combined DNA ploidy and nucleotyping into a chromosomal instability panel, we found our correct classification rate (CCR) was better than either test in isolation. Nucleotyping yields extra information over DNA content, as changes in chromatin condensation may occur in apparently diploid cells. This is illustrated by the four cases from the non-dysplastic BO group that were misclassified as abnormal by nucleotyping, three of which have subsequently progressed to aneuploidy or indefinite for dysplasia. If nucleotyping is picking up sub-microscopic changes that occur before DNA ploidy or dysplasia, then the length of follow up in this experiment may be too short and underestimate the CCR of nucleotyping.

Despite the improved CCR when a combination panel was used, there remained some dysplastic patients who were misclassified as normal. This may be explained by error of whole biopsy sampling, as small foci of dysplasia may be cut out in the process of nuclear monolayer preparation. A way to overcome this would be to use multiple samples from each patient or laser capture microdissection of the dysplastic areas.

The statistical analysis used to generate each model was complex, using higher order statistics. When analysing several feature combinations from multiple data points, care must be taken not to introduce errors in statistical analysis by overfitting of data. This can occur when a feature set or parameter values may accurately describe the samples in the training set rather than general properties of the group. Using the separate training and testing sets approach is therefore a necessity, as if the selection procedure in the training phase results in overfitting, this will be demonstrated in the test set. Encouragingly, when using adaptive features (and hence strongly reducing the probability of overfitting) the CCR was similar both in the training and test sets, indicating that our classifier model was not subject to statistical bias by overfitting. In addition we used the Grey Level Entropy Matrix adaptive features method for the first time in an *in vivo* study. This method was previously shown to outperform the classical static features in a study on the most difficult set of Brodatz texture pairs.[Nielsen et al., 2004] This unified statistical approach may allow for generalisable interpretation of data in future nuclear textural analysis studies.

One major limitation of our study is the use of dysplasia to separate the two groups, rather than development of OAC, as this hardwires the inaccuracy of HGD diagnosis into our algorithm. In addition there may be confounding bias from age and length of BO, both significantly increased in the dysplastic group. As this was a discovery study testing several textural features on small group of patients it was felt that two histologically distinct groups were necessary for algorithm generation. To further test this algorithm a follow up experiment was undertaken to assess the galleries of nuclei from the NIBR study.

6.7 Case control study of nucleotyping as a prognostic biomarker in non dysplastic BO

This work was undertaken on biopsies from the NIBR study, a collaborative project previously described in Chapter 5.6.

6.7.1 Aims

The aim of this study is to evaluate nucleotyping as a prognostic biomarker in non dysplastic BO and compare with DNA ploidy as measured by image cytometry.

6.7.2 Methods

The nuclear monolayer galleries presented in Chapter 5.6 were used for this study. The previously described algorithm, derived using the GLEM + adaptive features method, was tested on these galleries.

6.7.3 Results

Nucleotyping analysis

The results for NT are presented in Table 6.26 and 6.27. Of the 89 cases, 9 cases failed, leaving 80 cases and 242 matched controls. Samples were classified into a good prognostic group (0) or a poor prognostic group (1) according to the previously generated algorithm. There was no significant difference in the number of patients classified as poor prognosis by nucleotyping in the progressor group and the non-progressor group.

Table 6.26 Comparison of NT results for all samples

Characteristic	Cases *n= 80 (%)*	Controls *n= 242 (%)*	p-value
Predicted group			
0	44 (55.0)	130 (53.7)	0.84
1	36 (45.0)	112 (46.3)	

Unadjusted and multi-variate regression analysis

Results of regression analysis are shown in Tables 6.4. Classification according to nucleotyping was not associated with increased risk for progression to OAC and HGD by either unadjusted or multivariate adjusted analysis.

Table 6.27 Unadjusted and multivariate adjusted risk estimates for NT

	All cancers & HGD			
Predicted NT group	Cases *n=80*	Controls *n=242*	Unadjusted OR (95% CI)	Adjusted OR (95% CI)
0	44	130	1.00	1.00
1	36	112	0.99 (0.57-1.72)	0.96 (0.46-2.01)
p for trend			0.97	0.91

Combination of Nucleotyping and DNA ploidy

The combination of Nucleotyping and DNA ploidy abnormalities was then used in a risk panel, and the results are described in Table 6.28. There was an increased risk of progression to OAC/HGD when both NT/ICDA were positive (OR = 3.36; 95% CI = 1.06-10.68). There was no significant increased risk of progression when there was disconcordance between the two tests on multivariate adjusted analysis.

A three test biomarker panel was then assessed, comprising dysplasia scoring, NT and ICDA, and results are summarised in Table 6.29. The combination of LGD or IND, NT poor prognostic group and DNA ploidy abnormalities was associated with a significantly increased risk of progression to OAC/HGD on univariate analysis, but this did not reach statistical significance on multivariate analysis. This may be due to the very small sample size of 11 cases and 2 controls.

Table 6.28 Risk estimates for combination of ICDA + NT

	All cancers & HGD			
	Cases *n=79*	Controls *n=239*	Unadjusted OR (95% CI)	Adjusted OR (95% CI)
Diploid & NT score 0	26	102	1.00	1.00
Ploidy abnormal & NT score 0	17	25	2.63 (1.23-5.60)	1.83 (0.76-4.42)
Diploid & NT score 1	17	97	0.74 (0.36-1.51)	0.84 (0.35-2.00)
Ploidy abnormal & NT score 1	19	15	5.07 (2.13-12.07)	3.36 (1.06-10.68)

Table 6.29 Risk estimates for combination of ICDA + dysplasia + NT

	All cancers & HGD			
	Cases *n=79*	Controls *n=239*	Unadjusted OR (95% CI)	Adjusted OR (95% CI)
Diploid & NT score 0 & no dysplasia	24	98	1.00	1.00
All intermediate combinations	44	139	1.45 (0.80-2.61)	1.30 (0.64-2.63)
Ploidy abnormal & NT score 1 & IND/LGD	11	2	23.52 (4.88-113.40)	4.83 (0.40-58.99)

6.7.4 Discussion

When NT was added to ICDA the risk of progression was significantly increased when both were abnormal (OR= 3.36; 95% CI = 1.06-10.68), which was higher than ploidy alone (OR = 2.98; 95% CI = 1.55-5.71). Also 67% of cases that went on to develop cancer were picked up when a combination of the two tests were used, compared to only 46% when DNA ploidy abnormalities were used. Put another way, an extra 17/79 patients were found using NT that subsequently developed cancer.

Despite this, the misclassification rate was higher than would have been predicted from our pilot study, with a high false positive rate. It is difficult to explain this result, given the CCR from the previous study. One may argue that there has been an error in processing the specimens, perhaps due to failure of correct sampling of the abnormal cell populations. Alternatively the training set of 55, with only 26 non dysplastic BO, may have been too small to extrapolate to this larger population based study. It would also be useful to evaluate the clinical criteria that were used in the multivariate analysis to ascertain if there was any biological significance to the cases that were misclassified,

such as active inflammation on biopsies or poorly controlled reflux as evidenced by high dose PPI therapy. As the study is blinded until the final biomarkers are evaluated, this work was not possible for this thesis.

6.8 Summary

The methodology described in this chapter demonstrates that nucleotyping adaptive features can be used to analyse galleries of nuclei from biopsies of Barrett's oesophagus that have been assessed by ICDA. The textural features used to differentiate normal from dysplastic tissue were similar to those used in studies of other early cancers. Furthermore when we combined ICDA and NT an 84% correct classification rate for dysplastic BO was achieved.

The results from the NIBR study were somewhat disappointing as nucleotyping failed to predict cancer progression when used as a test in isolation. When the combination of ICDA and NT was used as combination panel an increased sensitivity for progressors to OAC was noted, but this was attenuated by a reduction in specificity. Using a panel of dysplasia scoring and NT/ICDA there was a trend towards significance which was seen on univariate analysis but lost on multivariate analysis. This may be explained by sample size and needs further evaluation.

These data demonstrate that combination of ICDA/nucleotyping is a promising single platform test for assessing chromosomal instability, which may aid pathologists in the diagnosis of dysplasia. This test has potential as a novel biomarker for cancer progression, although further studies are necessary to improve the algorithm accuracy, as the misclassification rate was high when used on patients from the NIBR study. To improve the algorithm it would be advantageous to retrain on a half of this group when the outcome is known and then test on the blinded reserved test set. This work may only be undertaken when the study is unblinded, which is outside the timeframe of this thesis.

Chapter 7

Investigation of DNA Replication Licensing Factors as potential surrogate markers for DNA ploidy abnormalities

Chapter 7 Investigation of DNA Replication Licensing Factors as potential surrogate markers for DNA ploidy abnormalities

7.1 Introduction

In the previous chapters the value of digital image analysis of nuclei for the evaluation of chromosomal instability in BO has been demonstrated, using both ICDA and nucelotyping. DNA ploidy and nuclear texture abnormalities are associated with increased risk of progression to cancer in patients with non-dysplastic BO, thus lending themselves as potential biomarkers for large populations enrolled in surveillance programmes.

There are problems with the implementation of such a strategy on a large scale. A combined ICDA/Nucleotyping system is currently expensive, at around £150,000, due to costs of optical hardware and computers with large processing power. The preparation of a monolayer is relatively labour intensive and a skilled laboratory technician plus equipment are required on site. Although several steps in the process have the potential for automation it is unlikely that the whole process will be completely automated. As was demonstrated by the Altnagelvin Hospital, not all samples are the same and there may be a need for adaptation of the protocol. In addition the cleaning of galleries requires human input, which consequently requires training of a technician.

For these reasons adoption of ICDA/NT outside of research centres and into district general hospital pathology departments is unlikely. Therefore a central hub of research centres with laboratories already suited to this type of work would need to be set up, and then regional pathology departments would send their samples to those centres. This may result in a huge number of samples and work for a very small reward, as the majority of patients with NDBO would be diploid.

A simple test is therefore needed, that allows screening of the patient for DNA ploidy. Once screened as high risk for DNA ploidy this could be confirmed by formal ICDA/NT

analysis. As this is a screening tool, the test would need to be highly sensitive for aneuploidy, to maximise the negative predictive value of the test. To be suitable for widespread clinical use this candidate surrogate biomarker would need to be quantified from samples that are easy to obtain (serum, tissue biopsy) and the assay method simple, accurate, highly reproducible and cheap using standard laboratory equipment.

7.1.1 Protein biomarkers

Protein biomarkers are in general the easiest to assess, as protein expression in a fixed or frozen tissue section can be quantified using immunohistochemistry (IHC). IHC localizes specific antigens (e.g. proteins) in tissue or cells using antibodies, enzyme conjugates and substrate-chromogens. The antigen-antibody reaction can be evidenced with an optical microscope. The antibodies used are either polyclonal or monoclonal (usually from mouse or rabbit) in origin. Visualising an antibody-antigen interaction can be accomplished in a number of ways. In the most common instance, an antibody is conjugated to an enzyme, such as peroxidase, that can catalyse a colour-producing reaction (immunoperoxidase staining).

The majority of pathology departments will have experience with IHC staining techniques, which are often semi-automated, with protein quantification using standard laboratory microscopes. In many types of cancer these stains have been adapted to be used by pathologists to examine tissue biopsies where cancer is suspected. For example e-cadherin to differentiate between ductal and lobular carcinoma in situ of the breast [Moll et al., 1993], C-kit receptor for gastrointestinal stromal tumours [Andersson et al., 2002] and alpha fetoprotein for hepatocellular carcinoma [Brumm et al., 1989].

More recently IHC stains have been used to assess the prognosis of tumours by the quantification of proto-oncogenes. One example is ErbB2/HER-2, which modulates the expression and function of cell cycle regulators and is important for cell differentiation, adhesion and motility.[Kaptain et al., 2001] HER-2 gene amplification and protein over-expression exists in about 20% of breast cancers and is linked to a poor prognosis.[Slamon et al., 1987] This has led to its routine use as a prognostic and

predictive marker in breast cancer.[Ellis et al., 2004] Moreover the finding of HER-2 positivity allows for a targeted treatment strategy. Trastuzumab (herceptin) is a monoclonal antibody that specifically targets HER-2 protein and has been shown to enhance survival rates in both primary and metastatic HER-2 positive breast cancer patients.[Smith et al., 2007;Slamon et al., 2001]

HER-2 has also been implicated in gastric cancer, and it has been consistently associated with disease progression and poor outcome. HER-2 overexpression by IHC has been shown to occur at a similar rate to breast cancer, around 20% of resected tumours.[Tanner et al., 2005;Hofmann et al., 2008] The efficacy of herceptin in gastric cancer was then evaluated in a phase III RCT, the ToGA trial, the results of which showed that trastuzumab added to chemotherapy significantly prolonged survival — from a median of 11.8 months with chemotherapy alone to a median of 16 months.[Bang et al., 2010] This has led to the recent approval of Herceptin for the treatment of HER-2 positive gastric cancer in Europe by the European Commission. This demonstrates the potential for an IHC stain to have widespread clinical use. Despite much interest for the role of the HER-2 pathway in BO, convincing evidence that this may be utilized as marker of progression to OAC is lacking.

7.2 DNA replication licensing factors

The DNA replication licensing machinery ensures precise duplication of the genome and contributes to regulation of the cell cycle and genomic stability. As aneuploidy represents dysregulation of the normal cell cycle and failure of precise DNA replication, then cell cycle proteins that are involved in these pathways may increase our understanding of the underlying mechanisms of aneuploidy. Analysis of the DNA replication licensing pathway and measurement of the replication licensing factors (RLFs) may therefore be exploited as potential biomarkers for future cancer risk and prognosis. The phase specific distribution of the RLFS is shown in figure 7.35.

Figure 7.35 Phase-specific distribution of cell-cycle biomarkers in proliferating cells and out-of-cycle states

Reproduced with kind permission from G.H.Williams.[Rodriguez-Acebes et al., 2010]

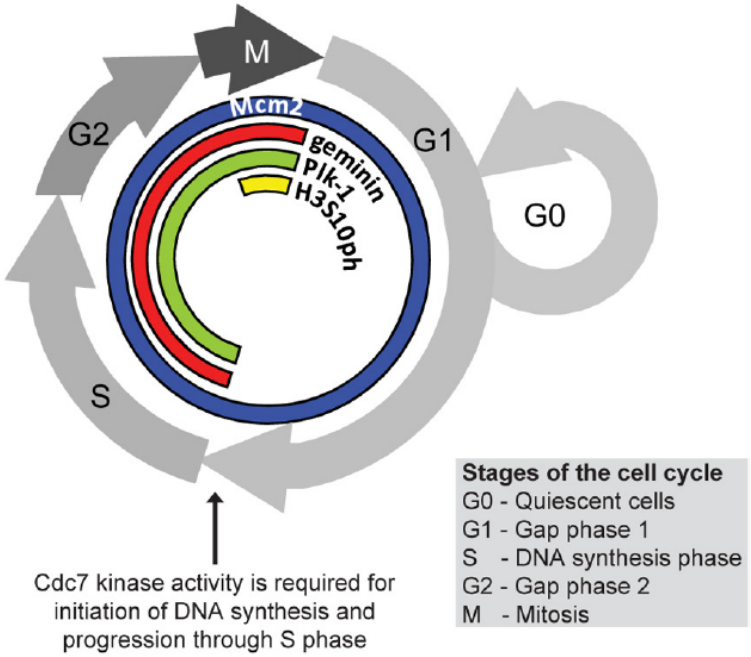

7.2.1 G1 phase

Pre-Replicative complexes and minichromosome maintenance proteins

The pre-replicative complexes are made up of several co-ordinating RLFs which include the origin recognition complex (ORC), Cdc6, Cdt1 and minichromosome maintenance (Mcm) proteins.[Bell and Dutta, 2002] During G1 phase, the ORC constitutively binds to the origins of replication and functions as a substrate for Cdc6 and Cdt1. The binding of Cdt1 induces the recruitment of the hexameric Mcm complex (comprised of Mcm 2–7) to chromatin, forming the pre-RC at replication origins. These have the ability to unwind DNA and thereby establish competence for DNA replication in S phase.[Mendez and Stillman, 2000;Blow and Hodgson, 2002;Dimitrova et al., 2002]

Mcm proteins are ubiquitously expressed in cells throughout the cell cycle, and are degraded when mammalian cells exit cell cycle into quiescent, differentiated, and senescent states.[Sirieix et al., 2003] They are therefore markers of G1-S-G2-M phases

and are referred to as proliferation makers. Abnormalities of mcm proteins predate the development of dysplasia [Sirieix et al., 2003] and appear to be a common early event in tumourogenesis that has led to much interest in their potential utility as biomarkers in cancer.

Another proliferative marker that has been studied more extensively is Ki67. Ki67 is an epitope of a nuclear protein recognized by the MIB-1 monoclonal antibody. The protein is frequently expressed throughout the cell cycle of proliferating cells, and it has not been detected in non-proliferating cells.[Gerdes et al., 1984] During the G1-S-G2 phases Ki67 is located primarily in nucleolar and peri-nucleolar regions, and it appears to be associated with condensed chromatin.[Kreitz et al., 2000] The function of the Ki67 protein is still unknown, however, it appears to be required for cells to progress through the cell cycle.[Schluter et al., 1993]

7.2.2 G1-S phase

Initiation/elongation of the replication fork and cyclin dependent kinases

DNA replication in eukaryotic cells is dependent on the phosphorylation of the pre-replicative complex (pre-RC) at the origin of replication. Two complexes of proteins mediate this event, the cyclin dependent kinase (CDK) complex, and the Cell division cycle (Cdc) 7 kinase- activator of S phase kinase (ASK) complex. [Lei and Tye, 2001]

Human Cdc7 kinase is a highly conserved serine/threonine kinase that consists of 574 amino acids with a molecular weight of 55 kDa. Activity oscillates throughout the cell cycle but its main action is to promote origin firing and entry into S phase by phosphorylating the minichromosome maintenance complex.[Kulkarni et al., 2009] Inactivation of Cdc7 in mouse embryonic stem cells leads to growth arrest with rapid cessation of DNA synthesis, suggesting requirement of Cdc7 functions for ongoing DNA synthesis.[Kim et al., 2003] Furthermore a cascade of checkpoint response is triggered which leads to activation of p53 and subsequent apoptosis.

7.2.3 S-G2 phase

License removal and geminin

Replication initiation is tightly coupled to removal of the license, to prevent re-initiation of DNA replication within a single cycle. This is achieved by the repression of origin licensing by geminin, which has high expression in the S-phase, and acts by competitively binding to Cdt1, thereby blocking Mcm2–7 re-loading onto chromatin.[Tada et al., 2001;Wohlschlegel et al., 2000;McGarry and Kirschner, 1998] This step is critical as origins must fire once, and only once, in each cell cycle to ensure genomic stability.

Geminin is a nuclear protein made up of approximately 200 amino acids, with a molecular weight of 24 kDa.[McGarry and Kirschner, 1998] Geminin is absent during G_1 phase and accumulates through S, G_2 phase and M phases of the cell cycle. Geminin levels drop during the M phase, when it is degraded at the metaphase/anaphase transition. It has been shown (in cancer cell lines) that inhibition of geminin results in re-replication of portions of the genome, resulting in the emergence of cells with giant aneuploid nuclei.[Zhu and Depamphilis, 2009] Inactivation of geminin also causes centrosome over duplication, which, together with abrogated G_2-M checkpoint mechanisms, results in multiple mitotic defects that may also promote chromosome mis-segregation and aneuploidy.[Tachibana et al., 2005]

7.2.4 G2-M phase

Mitosis and PLK-1

Polo-like kinase 1 (PLK-1) is a key regulator of all stages of mitosis, particularly the exit from mitosis.[Eckerdt and Strebhardt, 2006] Polo-like kinases are involved in centrosome maturation and formation of the mitotic spindle, regulation of chromosome segregation, cytokinesis (division into two daughter cells) and a stable subsequent G1 phase. Most of these functions have been linked to the activation of anaphase-promoting complex/cyclosome (APC/C). When mitosis is normally completed APC/C facilitates the degradation of geminin at the metaphase/anaphase transition, and the de-phosphorylation

and subsequent activation of replication factors. This permits the initiation of a new round of DNA replication. If there is abnormal centrosome amplification this may lead to multipolar spindles and can result in unequal segregation of chromosomes and subsequent aneuploidy and tumorigenesis.

Evidence for the role of PLK-1 in mitosis comes from northern blot analyses which demonstrate PLK-l mRNA levels are highest in tissues with a sizeable proportion of proliferating cells.[Clay et al., 1993;Lake and Jelinek, 1993;Golsteyn et al., 1994] In cultured cells, both PLK-l mRNA [Lake and Jelinek, 1993] and protein levels [Golsteyn et al., 1994] were low during G1 phase, but increased during S phase and reached maximal levels during G2 and M phases.

Another potential marker of mitosis is the measurement of phosphorylation of histone H3 at Ser-10 (H3S10ph), which has been implicated in chromosome condensation and entry into mitosis. H3S10ph is available as an IHC antibody stain and has been shown to correlate with the mitotic indices of human endometrium more closely than Ki67.[Brenner et al., 2003]

7.2.5 Clinical studies

Several studies have evaluated the role of RLFs in cancer progression. Mcm2 has been shown to be of value as a prognostic marker in meningiomas, [Hunt et al., 2002] breast cancer [Gonzalez et al., 2003] and renal tumours [Rodins et al., 2002]. In Barrett's oesophagus Going *et al.* first demonstrated that Mcm2 and Mcm5 surface positivity correlated with the severity of dysplasia.[Going et al., 2002] Sirieix et al, using the same immunostaining kit for mcm2 antibodies, demonstrated that aberrant surface expression increases along the metaplasia-dysplasia-carcinoma sequence. [Sirieix et al., 2003] In that study mcm2 was also shown to be more sensitive than Ki67 for detection of dysplasia. Other previous studies have shown that as the severity of dysplasia increases, the amount of proliferation present in the epithelium detected by IHC staining for proliferating cell nuclear antigen (PCNA), Ki67 or Mcm2 also increases.[Hong et al., 1995;Gray et al., 1992] The location of proliferating cells appears to differ as dysplasia progresses with

increased staining at the surface and upper portions of the crypts rather than being confined to the crypt bases.[Going et al., 2002]

Geminin has been shown to be upregulated and have prognostic value in renal [Dudderidge et al., 2005], breast [Loddo et al., 2009], ovarian [Kulkarni et al., 2007] and penile cancer [Kayes et al., 2009]. Recent data from Williams' group has studied the use of a two stage staining technique for both mcm2 and geminin.[Loddo et al., 2009] One hundred and eighty two patients with breast cancer were subdivided into different 'cell-cycle' phenotypes; Type I (out of cycle) mcm2 < 30% and geminin –ve; Type II (in cycle G1 delayed/arrested) mcm >30% but geminin –ve; Type III (actively cycling) mcm2 and geminin positive. There was a significant difference between 5 year survival when comparing type I and II (89 and 87%) vs. type III (56%). The authors concluded there biomarker algorithm provides novel insights into the cell cycle state of dynamic tumour cell populations in vivo.

Cdc7 kinase has been shown to correlate with tumour grade of ovarian cancer as well as aneuploidy [Kulkarni et al., 2007]. PLK-1 has been evaluated in 49 patients with oesophageal squamous cell carcinomas, with a significant difference in 3-year survival rates between those with low PLK-1 mRNA expression (54.9%) versus high expression (24.8%).[Tokumitsu et al., 1999] Conversely, in the same study, 55 gastric carcinomas (73%) of 75 patients were revealed to over express PLK-1 mRNA, but the expression status showed no correlation with prognosis.

7.3 Aims of this chapter

The aim of the following experiment is to evaluate replication licensing factors in the presence and absence of DNA ploidy abnormalities, in an attempt to establish a surrogate marker for DNA ploidy that can be utilized as a high throughput immunohistochemical screening tool for the assessment of cancer risk in BO.

7.4 Materials and Methods

Oesophagectomy specimens from 10 patients with adenocarcinoma were evaluated. All patients had endoscopic evidence of Barrett's columnar lined oesophagus, which was confirmed by the presence of SIM. A total of 29 blocks were chosen from these patients representing; the site of the tumour; sites adjacent to the tumour displaying BO; sites of squamous oesophagus. The aim of evaluating these blocks was to capture different stages of dysplasia within each patient/specimen.

The samples were then cut serially as follows
5 μm section for H&E
40 μm section for laser capture microdissection + ICDA/NT
5 μm sections for mcm2, geminin, Ki67, cdc7 kinase, PLK 1, H3S10ph
5 μm section for H&E

All 5 μm sections were laid into a water bath and attached to electrostatically charged slides (Superfrost Plus slides (Visions Biosystems, Newcastle Upon Tyne, UK). The 40 μm sections were mounted onto UV excited P.A.L.M. membrane slides (Positioning and Ablation with Laser Microbeams (P.A.L.M.) Microlaser Technologies, Germany).

7.4.1 Haematoxylin and Eosin

Each section was deparrafinised in xylene and then rehydrated through stepwise reducing concentrations of ethanol (100%, 95%) to water. The slide was then stained with Mayer's haematoxylin for 15 minutes and rinsed in running tap water for 20 minutes. The slide was then counterstained with Eosin (2 minutes). Finally the slide was dehydrated in 95% and 100% ethanol before clearing in xylene and mounting.

Areas of intestinal metaplasia, gastric mucosa, dysplasia or cancer were marked on images from the index H&E section and correlated with the subsequent cut slides. These findings were confirmed by repeat analysis of the final H&E slide to confirm the morphology had not changed.

7.4.2 Immunostaining

Antibodies

A rabbit polyclonal antibody against human geminin was generated as previously described.[Wharton et al., 2004] Ki67 monoclonal antibody (MAb) (clone MIB-1) was obtained from DAKO (Glostrup, Denmark). Mcm2 MAb (clone 46) was obtained from BD Transduction Laboratories (Lexington, KY, USA). Cdc7 MAb was obtained from MBL International (Woburn, MA, USA). PLK-1 MAb (clone 35-206) and Histone H3 phosphorylated on Serine 10 (H3S10ph) polyclonal antibody were obtained from Upstate (Lake Placid, NY, USA).

IHC methods

The 5 micron sections were dewaxed in xylene and rehydrated through graded ethanol to water. The tissue sections were pressure-cooked in 0.1 M citrate buffer at pH 6.0 for 2 minutes and immunostained using the Bondt Polymer Refine Detection kit and Bondt-Max automated system (Vision Biosystems). Primary antibodies were applied at the following dilutions: Ki67 (1:300), Mcm2 (1:2000), geminin (1:600), cdc7 (1:100), PLK-1 (1:1000), H3S10ph (1:300).

Protein expression profile analysis

Protein expression analysis was performed by determining the labeling index (LI) of the markers in each tumour as previously described.[Dudderidge et al., 2005;Shetty et al., 2005;Kulkarni et al., 2007] All slides were scanned into a digital pathology mutlislide scanner (Nanozoomer, Hamamatsu, Japan). These slides were then evaluated at low-power magnification (x100) to identify areas within the regions of interest that had the highest intensity of staining. From these selected areas, 3–5 fields at x400 magnification were evaluated for quantitative analysis, which was performed with the observer unaware of clinicopathological variables.

Both positive and negative cells within the field were counted and any stromal or inflammatory cells were excluded. Cells with any degree of nuclear staining were scored positive. A minimum total of 500 cells from four areas were counted for each region of

interest. The LI was calculated using the following formula: LI = number of positive cells/total number of cells x100 as described.[Kulkarni et al., 2007]

7.4.3 Laser Capture microdissection

The basic principle of laser capture microdissection (LCM) is the capture of groups or individual cells onto a thermoplastic membrane from histological sections of stained tissue.[Emmert-Buck et al., 1996] In conjunction with appropriate staining, this allows accurate assessment of tissue morphology and enables very precise definition of the region of interest. For this study the 29 sections underwent methylene green staining as previously described. [Leedham et al., 2008]

For this experiment the P.A.L.M UV Laser Microdissection system (P.A.L.M. Microlaser Technologies, Germany) was used. The P.A.L.M system consists of an inverted microscope that is connected to a PC for additional laser control and image archiving, a UV laser diode (355 nm), a laser control unit, a joy stick controlled microscope stage with a vacuum chuck for slide immobilization, a CCD camera, and a colour monitor. The P.A.L.M system utilizes a de-focused laser pulse to both cut out the region of interest, and "catapult" tissue into the adhesive cap of an ependorf tube. The laser has an extremely high energy density at a small focal point (< 1 μm) so there is no heat transfer to the adjacent material, hence the term "cold ablation." Also, the UV laser does not affect DNA, RNA, or proteins in the surrounding areas as the 355 nm wavelength of the laser falls short of the absorption spectra for these molecules.

Set up of system

Firstly the laser needs to be calibrated so that the point on the screen correlates with the laser. This was done by drawing a series of L shapes to accurately pinpoint the x and y axes(figure 7.36a). Secondly the UV focus was adjusted. A series of connected lines were drawn as shown in figure 7.36b with the power at 50%. Then the focus was adjusted so that a very fine line was scored into the P.A.L.M membrane slide allowing for accurate laser capture. Increasing the focus past this optimum level will result in the line disappearing, reducing the focus will create a wide ragged line and imprecise capture. Finally the power was set on representative tissue and adjusted until a clean burn was

seen throughout the whole of a circle of tissue (see figure 7.36c). The typical ranges were power 90-95%, UV focus 61-63%, and cut speed of 10-15.

Forty micron sections were used, which are quite thick for LCM (routine use is 6-20 microns) but minimised cutting error that can potentially lead to underestimation of DNA tetraploidy. Using the same 40 micron section thickness also allowed comparison with previous ploidy results.

Figure 7.36 Setting up the P.A.L.M laser capture microdissection system

(from left-to right) – a) Calibrating the x and y axes, b)setting the UV focus, c) adjusting the power

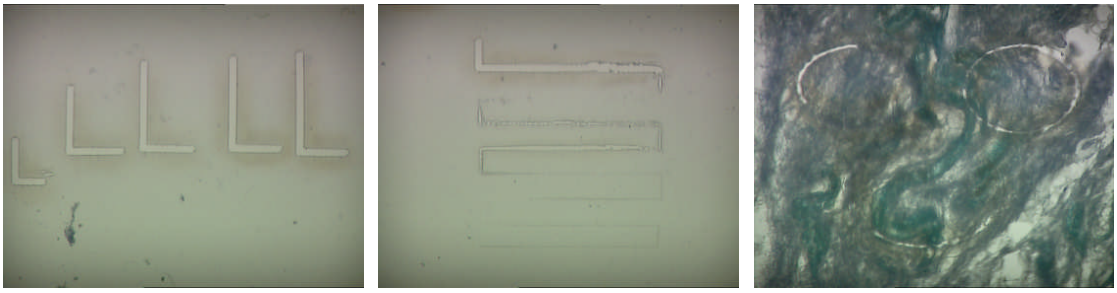

Tissue capture

Sixty one areas were identified and marked by Professor Novelli on the H&E slides. These areas were correlated with the LCM methylene green stained slides and marked with a pen. These areas were then cut out from the laser capture slides and catapulted into the adhesive caps of eppendorf tubes before immersion in UV pre-treated PBS.

7.4.4 ICDA

As the size of the sections was very small in comparison to our previous work on whole biopsy, it was decided to reduce both the concentration of proteinase XXIV and time of digestion, to 0.025 mg/ml for 1 hour at 37ºC. The samples were then processed to form Feulgen stained nuclear monolayers as described in Appendix A. ICDA was carried out on the nuclear monolayers as previously described in Chapter 5.2, but the number of nuclei collected was reduced to 300.

7.5 Results

7.5.1 DNA ploidy from laser capture sections

Of the 61 areas from 29 blocks that were laser captured, 7/61 failed analysis by ICDA. The median number of areas studied per patient was 6 (range = 2-10). Of the 54 areas that were successful, 24 were non HGD and 30 were HGD/Cancer. The histology results and corresponding percentage of sites with DNA ploidy abnormalities are presented in Table 7.30. There is a noticeable trend of increasing DNA index with increasing histological grade (see figure 7.37). The aneuploidy rate in areas of HGD/IMC is 50%, which is somewhat lower than 65% previously noted by the Seattle group [Reid et al., 2000b] and from our nucleotyping experiments (see Chapter 6). Raw data is shown in Appendix E. Figures 7.38 – 7.42 show areas from methylene green stained LCM slides and corresponding DNA histograms.

Table 7.30 Histological classification and DNA ploidy

Histological classification	Gastric	IM	LGD	HGD	IMC	Cancer
Number of areas	1	12	11	11	5	14
% areas aneuploidy	0	0	9	55	40	93

Figure 7.37 Graph demonstrating DNA index vs. histological grade of all 54 areas

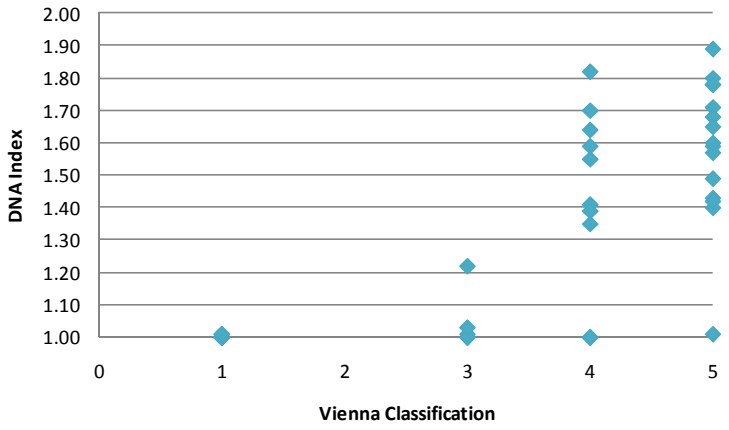

Figure 7.38 Block 29 – Specialised intestinal metaplasia

Images taken before (left) and after (right) laser capture microdissection with corresponding diploid histogram

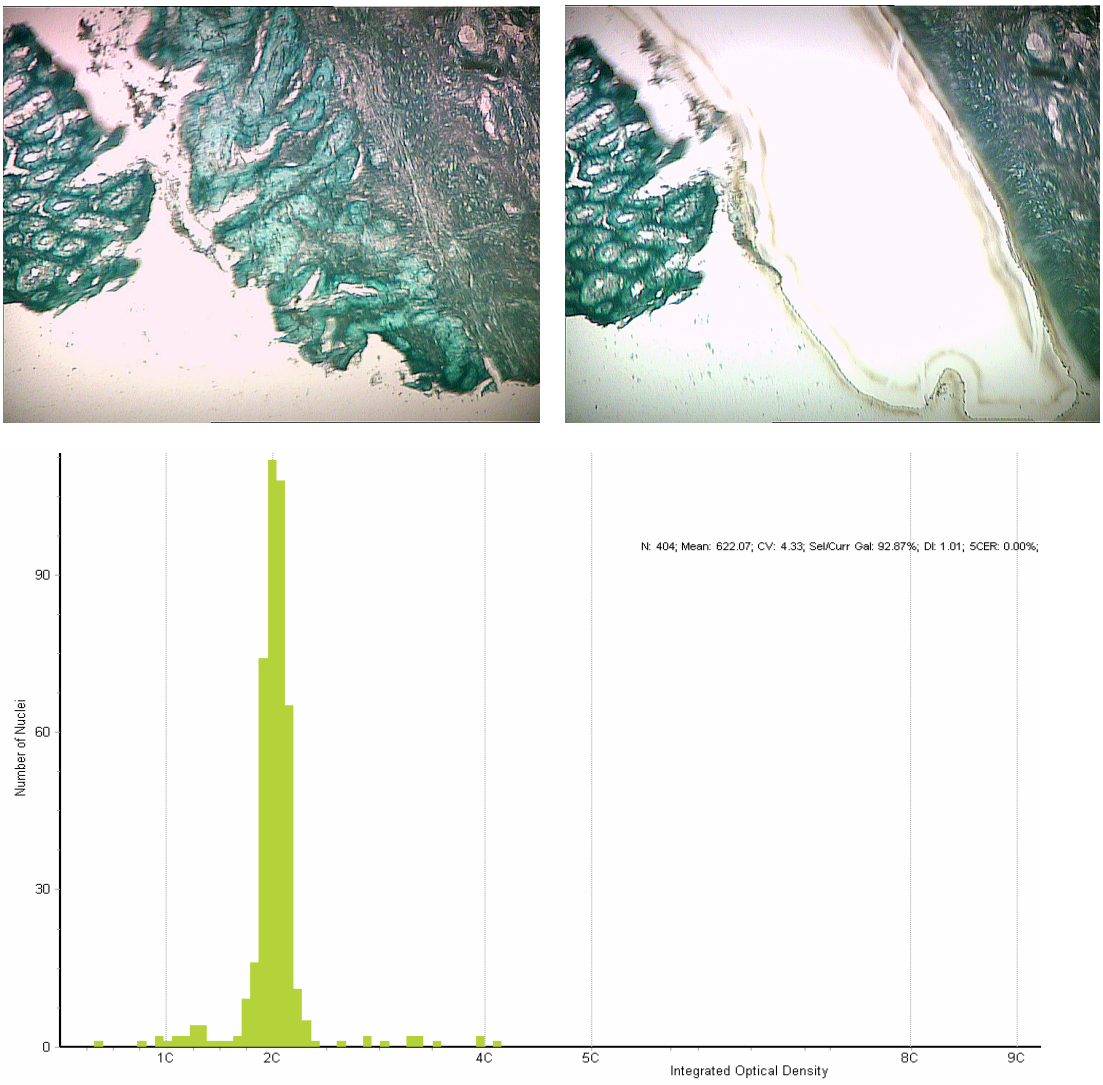

Figure 7.39 Block 8 Area 2 (cancer) and Block 9 area 2 (cancer)

Adenocarcinoma of the oesophagus from the same patient at two different levels. Both histograms demonstrate aneuploid cell populations but with different DI

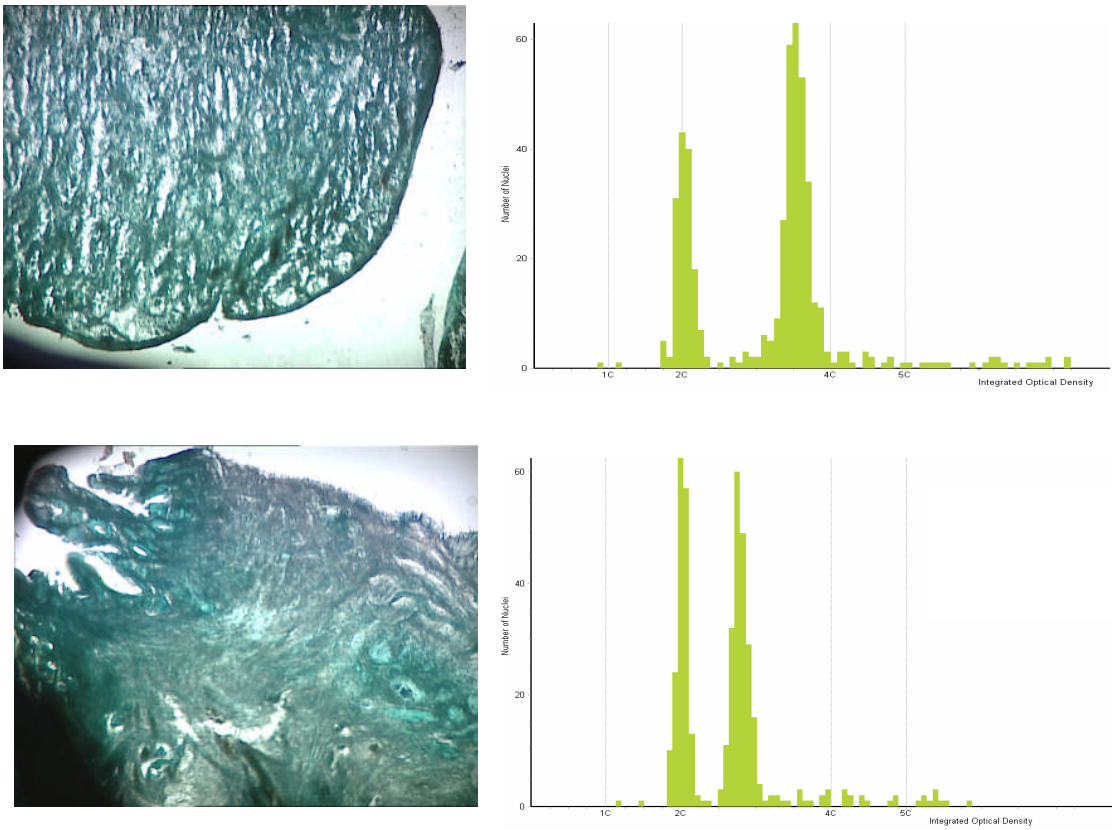

Figure 7.40 Block 17 Area 1 (high grade dysplasia) pre and post cut

The deep stromal layers have been microdissected first, with a corresponding diploid histogram

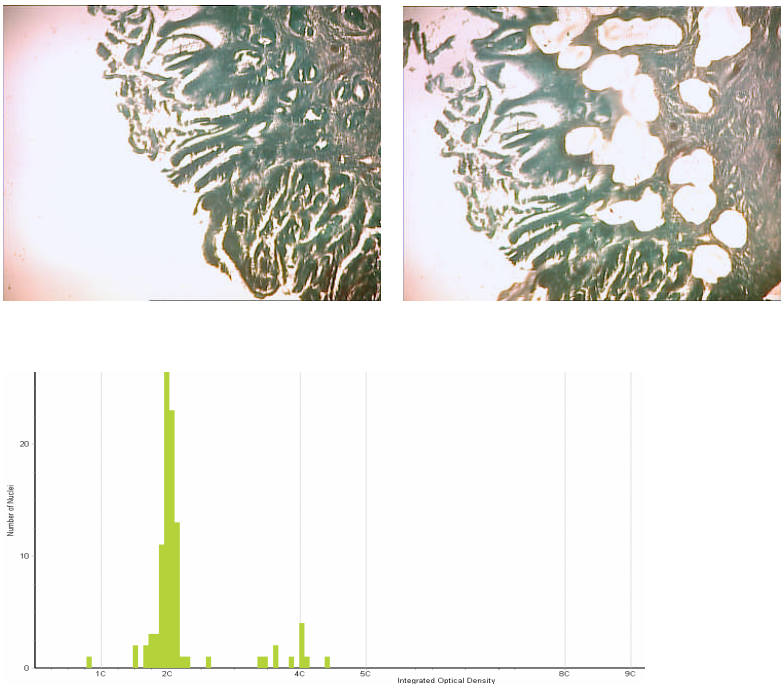

Figure 7.41 Block 17 Area 1 (high grade dysplasia) post cut

The superficial epithelial layer was then dissected with a corresponding aneuploid histogram

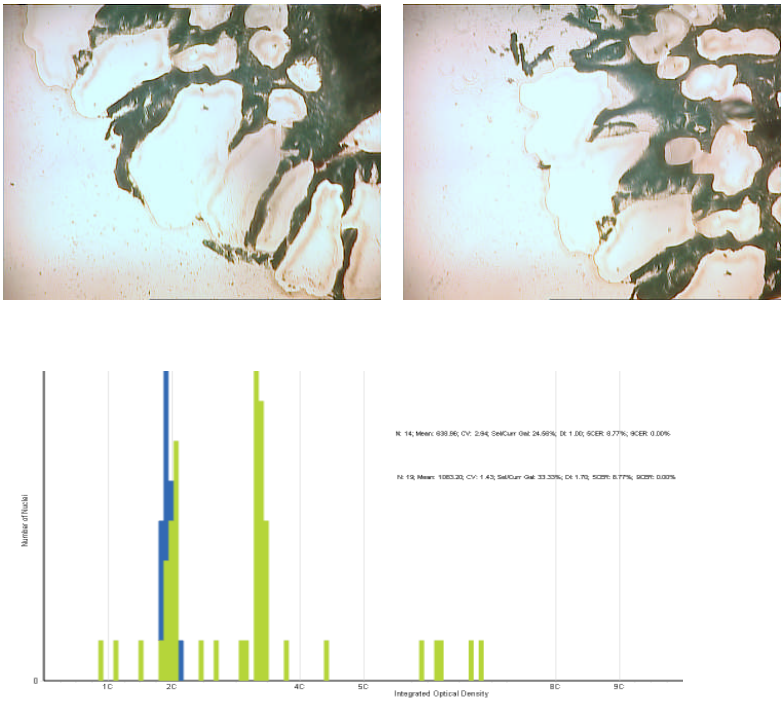

Figure 7.42 Block 22 Collage pre cut and post cut

These slides are a collage demonstrating the accurate co-registration of tissue morphology with corresponding H&E section

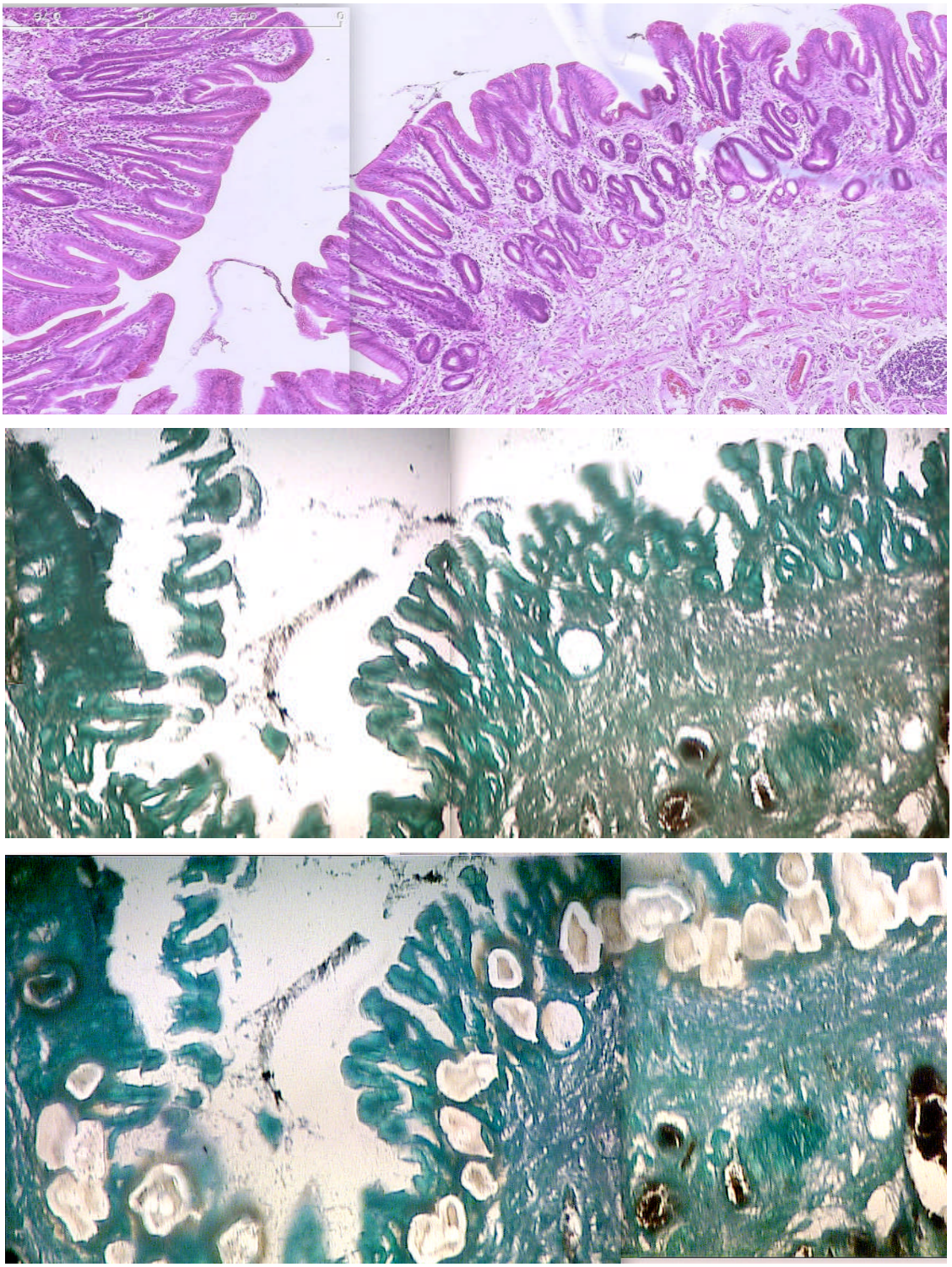

7.5.2 Replication Licensing Factors

Five of six RLFs produced staining in BO tissue that was suitable for analysis. Phospho-H3 did not sufficiently stain the epithelium or stroma in any of the 54 cases so no further analysis was undertaken, although there was evidence of a few mitotic bodies that stained positive indicating that stain had worked. Analysis on the remaining RLFs was undertaken on matched areas where possible. Epithelial cells were counted with care taken to avoid counting stromal cells. This analysis was undertaken by me with some help from a student (Eitan Lovat), which was subsequently recounted to check for accuracy. A representative slide of negative staining is shown in Figure 7.43. This was a diploid case with histology demonstrating SIM. The mcm2 stain was weakly positive, and the remaining stains negative. An area of epithelium that demonstrated both HGD and aneuploidy is shown in Figure 7.44. This stained strongly positive (brown) for 5/6 markers, with only H3S10ph not staining. The geminin stain is rather weak compared to the PLK-1 stain. It is apparent that the epithelial cells stain positive whereas the stromal cells did not stain at all (blue).

Figure 7.43 Block 14 Area 1 x200

Left to right - Upper level - H&E, Ki67, mcm2; Lower level - cdc 7, geminin, PLK1

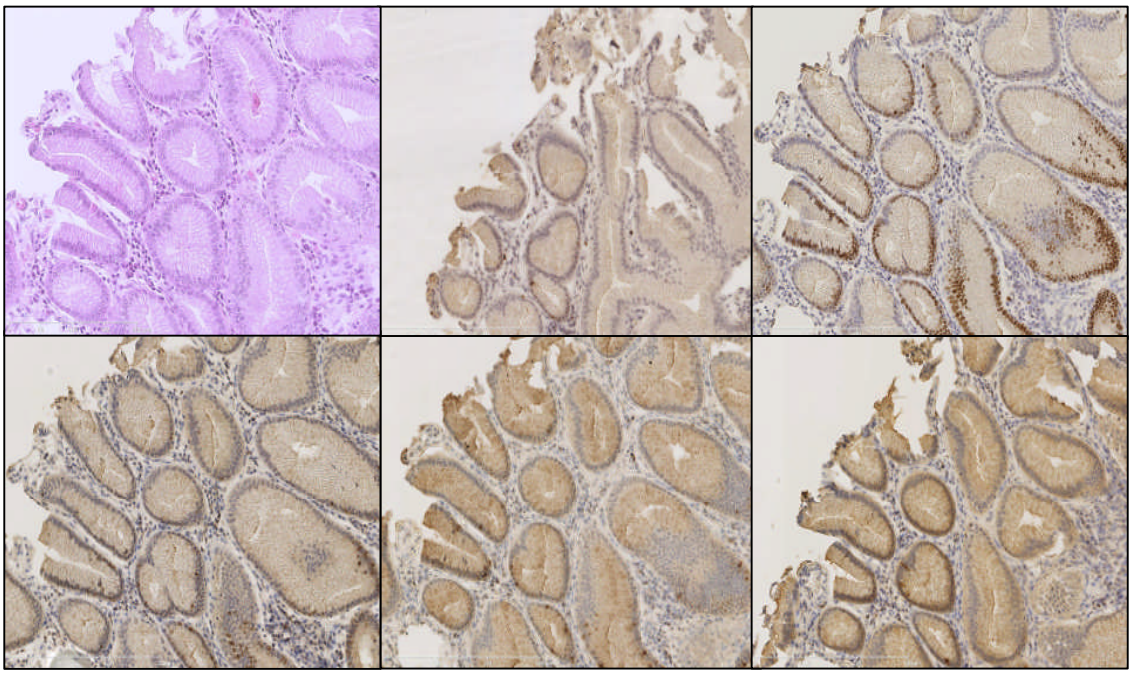

Figure 7.44 Block 23 Area 1 x 400

Left to right - Upper level - Ki67, mcm2, cdc 7; Lower level - geminin, PLK-1, H3S10ph

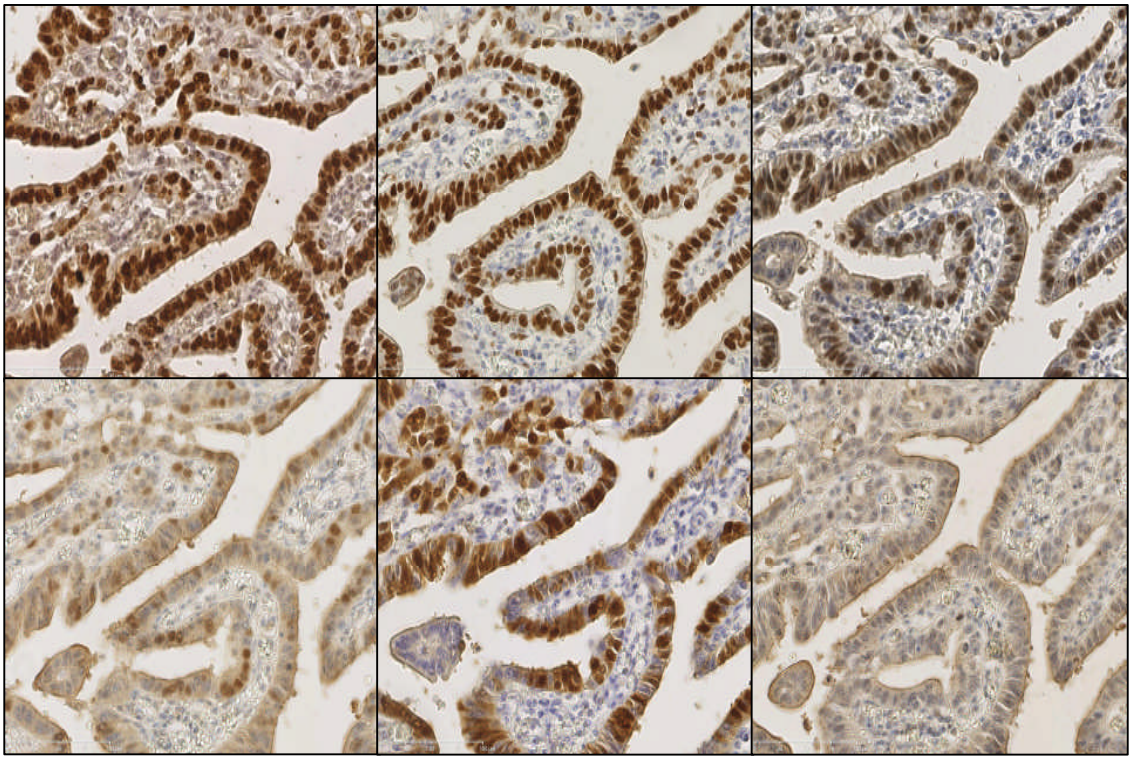

Relationship between RLF and histology

The relationships between each RLF and histological grade, split into non dysplastic BO/LGD and HGD/Cancer, are demonstrated in Table 7.31. When analyzing the median LI there was a significant difference between non dysplastic BO/LGD and HGD/Cancer for geminin, cdc7 and PLK-1. There was no significant difference between the two groups for KI67 or mcm2. An estimation of the rate of cell cycle progression at different parts of the cell cycle was also assessed, by calculating the ratio of the RLFs and Ki67. The ratios of geminin/Ki67, PLK-1/Ki67, and to a lesser extent cdc7/Ki67, were significantly associated with dysplasia, indicative of an accelerated rate of cell cycle progression after G1 in high grade dysplasia and cancer. Conversely the mcm2/Ki67 ratio unchanged. These results are consistent with previous work on these cell cycle markers in other tumor types. [Kulkarni et al., 2007;Dudderidge et al., 2005]

Table 7.31 Relationship between replication licensing factors and histology

RLF Labelling index	Non HGD BO (n=24)	HGD/Cancer (n=30)	P value *
Ki67 (%)	64 (42-80) ‡	80 (74-91)	0.002
Mcm 2 (%)	73 (47-87)	85 (76-90)	0.022
geminin (%)	17 (6-22)	35 (24-43)	<0.001
Cdc 7 (%)	26 (20-42)	46 (33-57)	<0.001
PLK-1 (%)	8 (4-11)	34 (18-39)	<0.001
Mcm2/Ki67	1.02 (0.94-1.13)	1.01 (0.95-1.10)	0.632
Geminin/Ki67	0.21 (0.16-0.31)	0.45 (0.30-0.52)	<0.001
Cdc7/Ki67	0.43 (0.31-0.66)	0.62 (0.41-0.74)	0.088
PLK-1/Ki67	0.12 (0.09-0.19)	0.42 (0.24-0.53)	<0.001

* Mann-Whitney test, $p < 0.001$ is significant

‡ Median (interquartile range)

The IHC stains were then compared with the tissue histology for each section (see figure 7.45). Ki67 and mcm2 were upregulated in all grades of dysplasia with no clear differentiation between grades. Noticeably the vast majority of cancers and HGD were Ki67/mcm2 positive. There was little difference in the level of staining between these two markers of proliferation. When S-G2-M RLFs were analysed, cdc7 kinase, geminin and PLK-1 all showed a trend towards higher LI with worsening Vienna classification (see figure 7.46).

Figure 7.45 Relationship between RLFs and histology

The mean LI values with 95% confidence intervals are plotted vs. Vienna Classification

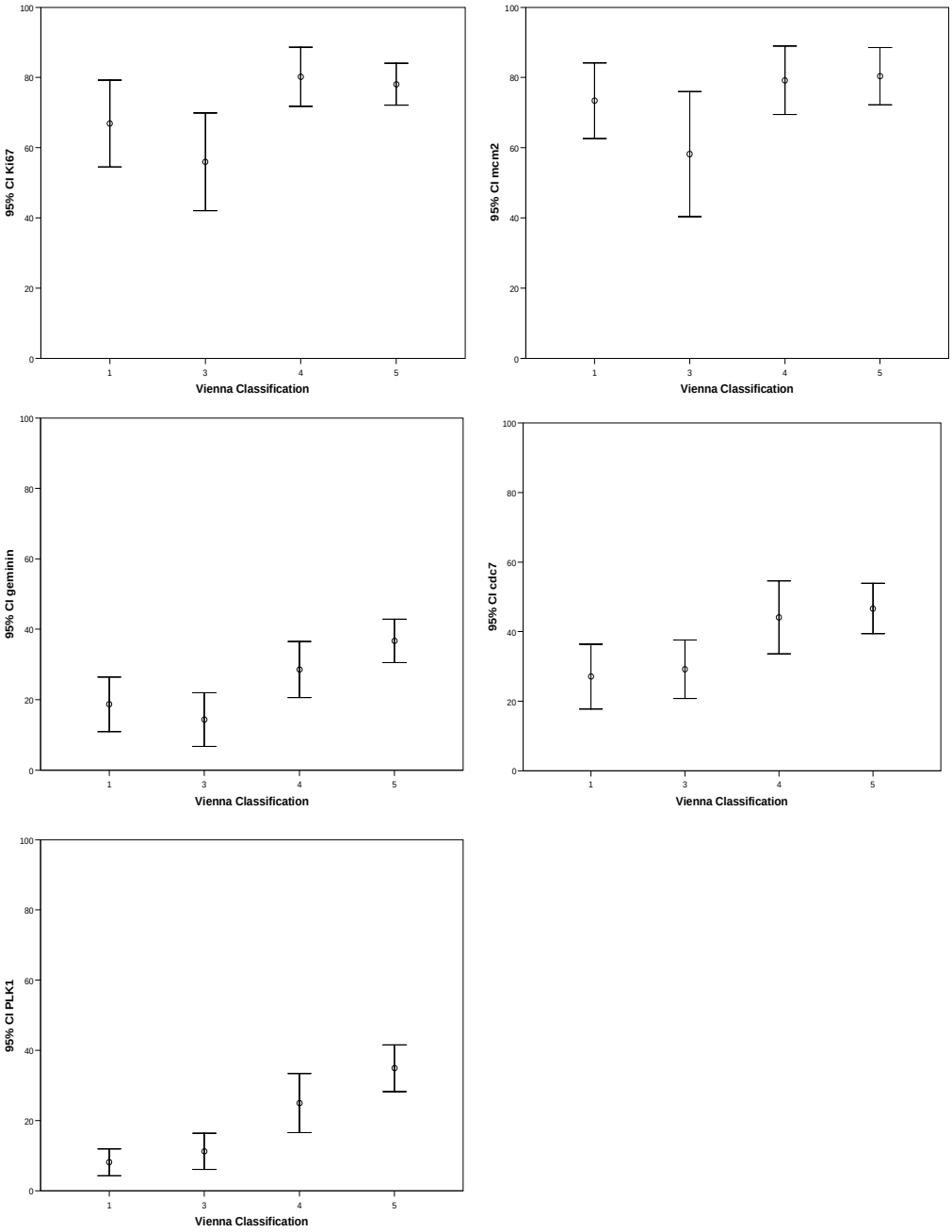

An arbitrary cut off for positivity of 30% was used for the cdc7, geminin and PLK-1 based on a previous study on thyroid tumours which categorised cases into four groups: (-), 0–5%; (+), 6–29%; (++), 30–59%; and (+++), more than 60%.[Ito et al., 2004] Scores were the plotted against frequency of dysplasia. A high PLK-1 expression (IHC score = 2) is not seen in NDBO or LGD. Negative expression of PLK-1 (IHC score=0) tends to decrease from NDBO to LGD to HGD to OAC. Intermediate PLK expression (IHC score = 1) shows a trend by increasing through NDBO/LGD to HGD, but does not occur in OAC. The abrupt change in staining pattern from NDBO to HGD is demonstrated in figure 7.47.

Figure 7.46 Scoring RLFs vs. degree of dysplasia

Cdc 7, geminin and PLK-1 cut off scores 0 = <15%, 1 = 15-29%, 2 = > 30%

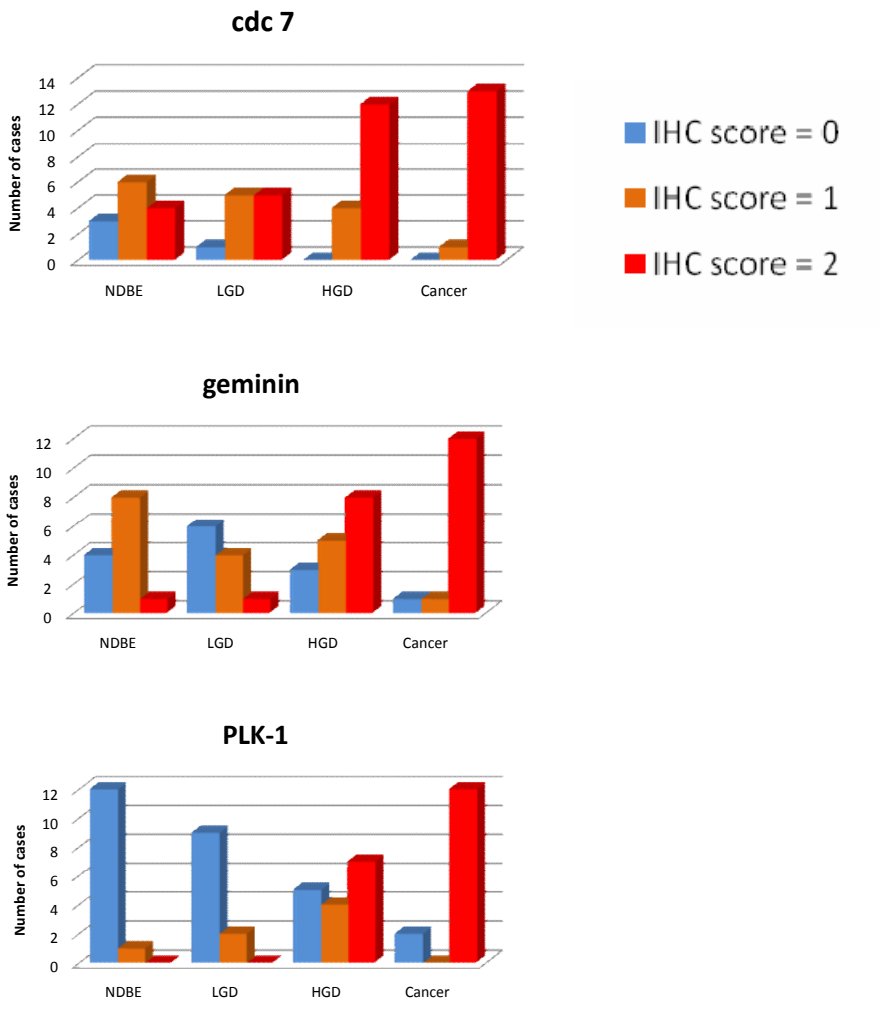

Figure 7.47 Block 14 Change in morphology from NDBO to HGD

This picture demonstrates the abrupt change in PLK-1 staining seen from NDBO (left) to HGD (right)

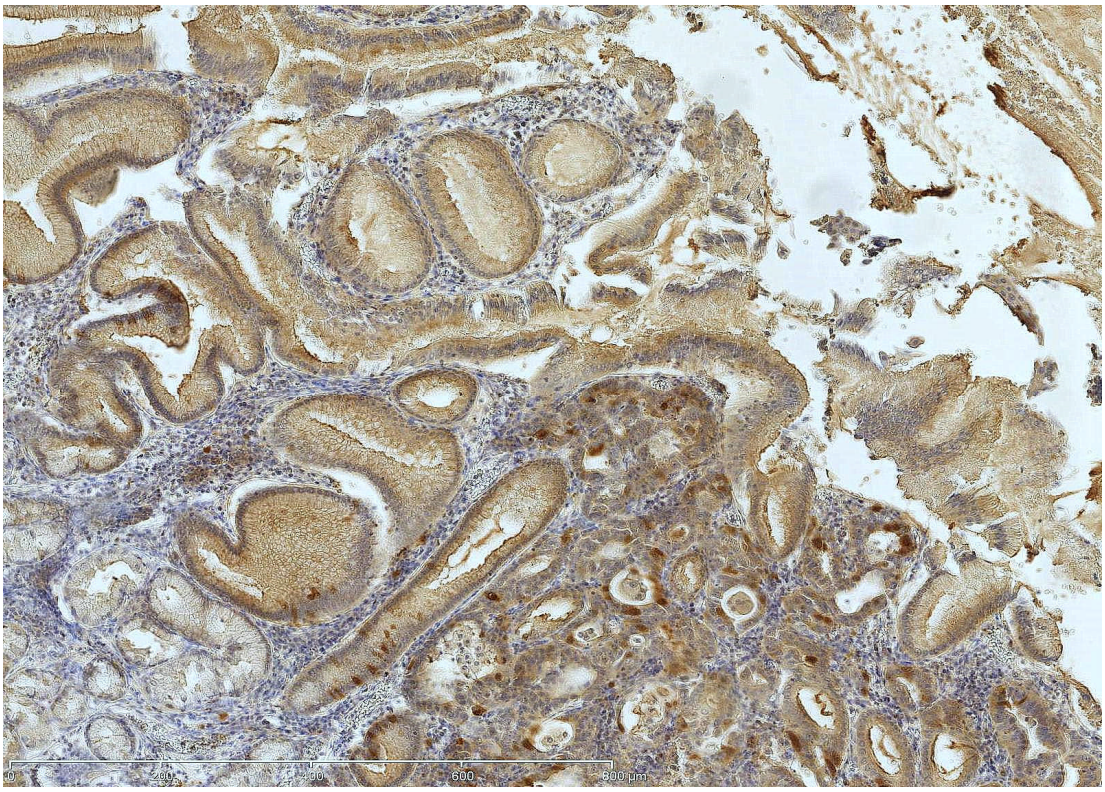

Relationship between RLF and DNA ploidy status

The correlation of DNA index and the RLF markers was evaluated. The LI versus DNA index is plotted for the proliferative markers (figure 7.48) and S-G2-M markers (figure 7.49). Using linear regression analysis the Pearson coefficient was calculated for each replication licensing factor (see table 7.32). PLK-1 had the highest degree of correlation with DNA ploidy status with a $r^2 = 0.776$ ($p<0.01$), whereas geminin and cdc7 performed less well. There was no significant correlation with Ki67 or mcm2 and DNA ploidy status. When PLK-1 was tested using a cut off score of 30%, the sensitivity and specificity for the detection of aneuploidy was 86% and 100% respectively. Figure 7.50 demonstrates correlation with DNA ploidy that was independent of histology.

Figure 7.48 Proliferative markers vs. DNA index

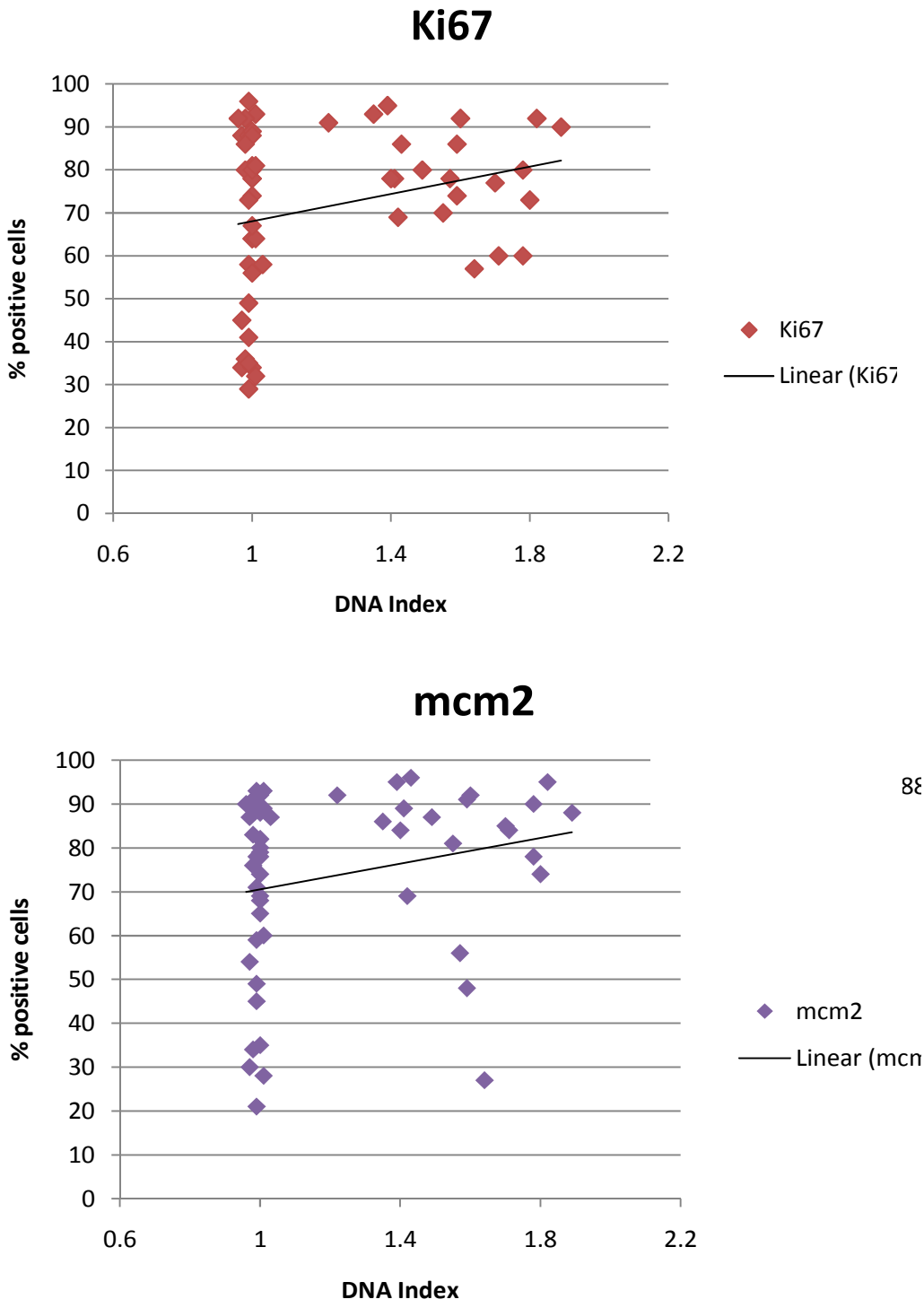

Figure 7.49 S-G2-M markers vs. DNA index

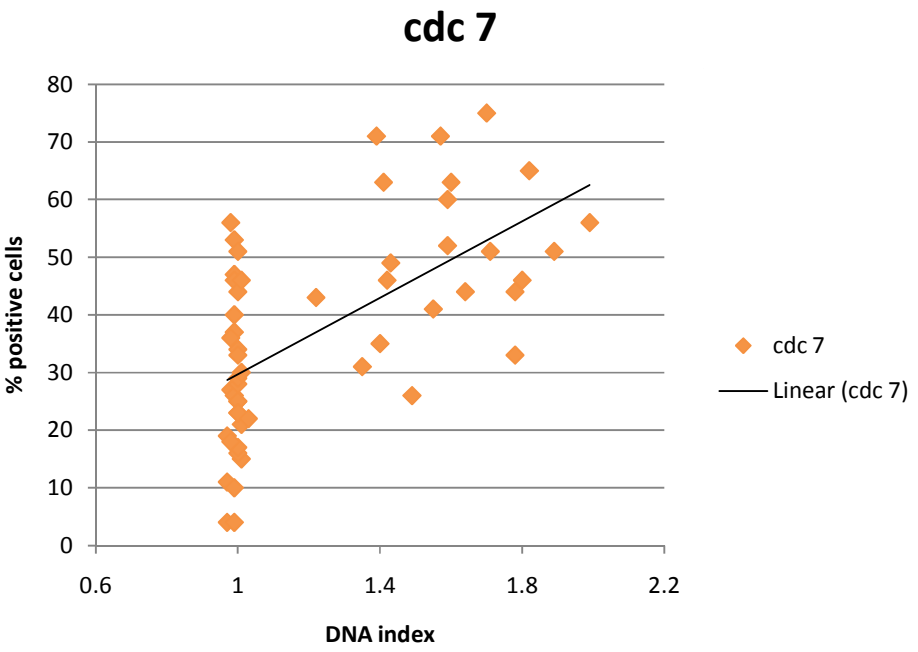

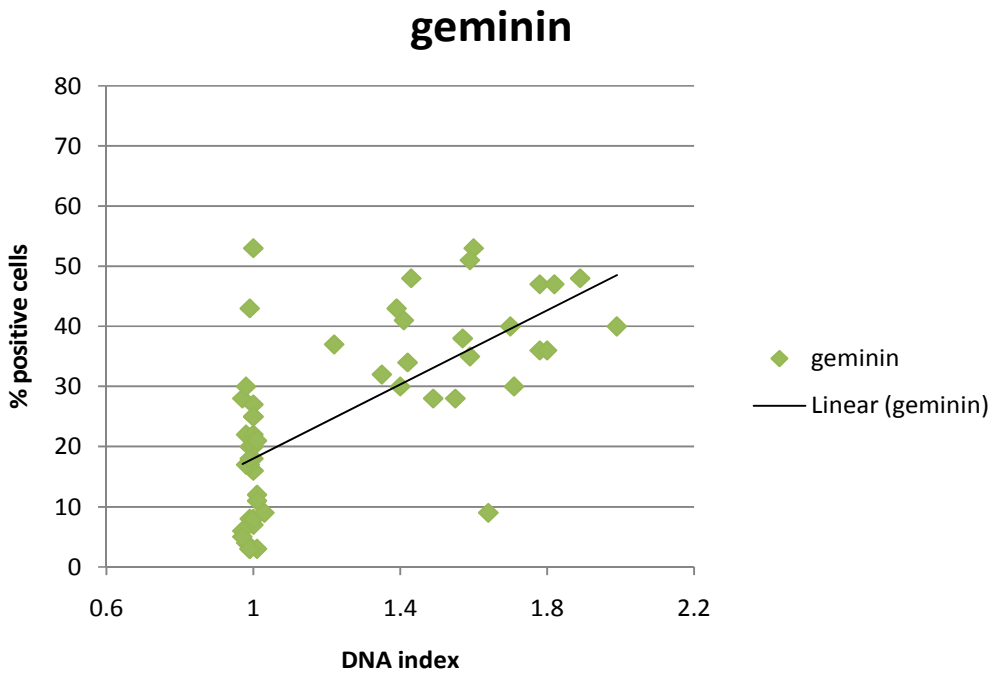

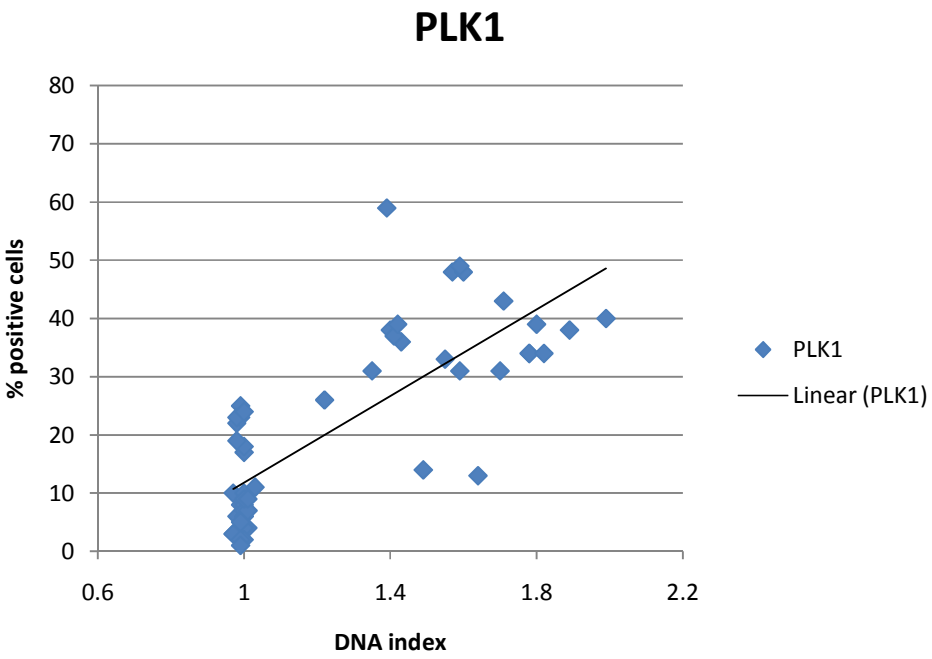

Table 7.32 Correlation of RLFs and DNA index using Pearson's product-moment coefficient

	Pearson coefficient	**Significance (two tailed)**
PLK-1	0.776	p<0.01
geminin	0.665	p<0.01
Cdc 7	0.612	p<0.01
Ki67	0.310	p = 0.02
mcm 2	0.257	p = 0.06

Figure 7.50 Block 12 PLK-1 staining of invasive cancer

Three areas of cancer on one tissue block. Areas A and B are invasive adenocarcinoma (both aneuploid and positive stain) and area C is intramucosal cancer (diploid, and negative stain).

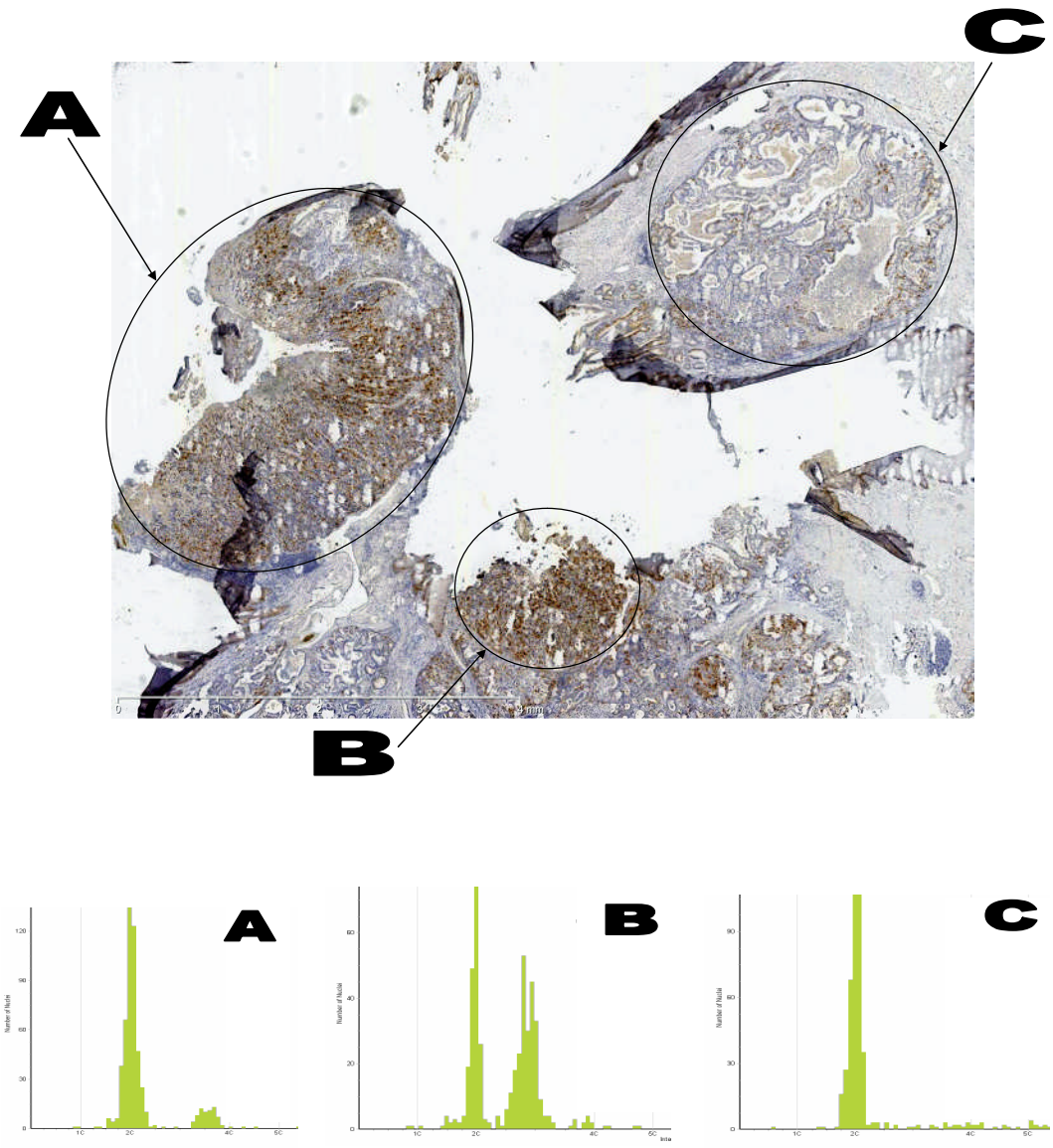

7.6 Discussion

This study was undertaken to evaluate the replication licensing factors as potential surrogate markers for DNA ploidy, to further understand the histogenesis of aneuploidy and explore their utility as potential biomarkers in BO. The RLFs hold a great deal of potential as biomarkers as they can be assessed using IHC. This technique is widely available in hospital histopathology laboratories and is amenable to high throughput screening, using automated immunostaining platforms and quantitative image analysis.

The results of this experiment show that three replication licensing factors, geminin, cdc7 and PLK-1, correlated with aneuploidy status from laser capture microdissected tissue. These RLFs represent the S-G2-M phases of the cell cycle and play a key role in DNA synthesis, centrosome maturation and formation of the mitotic spindle, regulation of chromosome segregation and prevention of reduplication. The increased expression of these markers correlated with increased severity of the aneuploid cell populations, which was quantified by increased DNA index. These data support the hypothesis that aneuploidy is a consequence of cell cycle dysregulation, and that the RLFs are intricately linked to the development of genomic instability.

Of the three markers studied PLK-1 had the highest correlation with DNA ploidy, with a Pearson coefficient of 0.78. To our knowledge this is the first time PLK-1 has been shown to be upregulated in Barrett's dysplasia and adenocarcinoma. When a 30% cut off value was used for positivity, the sensitivity and specificity for the detection of aneuploidy was 89% and 100% respectively. Furthermore there was a significant correlation with severity of dysplasia.

Functionally, PLK-1 falls into the group of targets including Aurora kinases, which are specifically activated during mitosis and highly expressed in human cancer tissues. PLK-1 is overexpressed in a broad range of human tumors, and this is associated with poor prognosis in several types of cancer.[Takai et al., 2001;Knecht et al., 1999] Oncogenic properties of polo like kinases are believed to be due to their role in driving cell cycle progression. Supporting evidence comes from the overexpression studies of PLK-4 in

embryonic fibroblasts which had increased centrosomal amplification, multipolar spindle formation and aneuploidy compared with wild-type cells.[Ko et al., 2005] Furthermore the incidence of spontaneous liver and lung cancers was 15 times high in elderly *Plk4*$^{+/-}$ mice than in *Plk4*$^{+/+}$ littermates. Other studies have demonstrated that PLK-1 interacts with p53 and suppresses its transcriptional as well as pro-apoptotic activity [Degenhardt et al., 2010;Ando et al., 2004]. In our study the proliferation markers Ki67 and mcm2 were upregulated in all grades of dysplasia, and in non dysplastic BO adjacent to cancer. There was no significant difference in staining of these proliferative markers between the two groups. Furthermore neither proliferative marker correlated with DNA ploidy, although Ki67 expression was elevated in all sites with aneuploidy. These findings are in agreement with a recent cohort study by the Reid group, which demonstrated high Ki67-positive proliferative fractions were not associated with future development of cancer.[Chao et al., 2008] In that study there was also no correlation with p16 or p53 mutations, although aneuploidy was not evaluated.

The highly significant association found between the S-G2-M phase RLFs and tumour DNA ploidy status has been shown previously in ovarian cancer.[Kulkarni et al., 2007] A correlation was noted for both geminin and aurora kinases, but PLK-1 was not evaluated. In addition the DNA ploidy analysis was undertaken on whole tissue in that study, which may introduce error as different cell populations can be seen on a single section, and smaller diploid areas may be missed. A good example of this is case 12 (see figure 7.50) where 2 areas of invasive cancer were aneuploid and a third area of intramucosal cancer was diploid, which was also negative for PLK-1, cdc7 kinase and geminin. A further disadvantage of using whole sections of tissue is the inclusion of stromal cells, that may variably dilute the sample with a 2C cell population. Although image cytometry minimises this risk by allowing removal of the stromal cells visually, some may still remain.

By using laser capture microdissection to remove areas of interest the accurate co-registration of aneuploid cell populations with histological staining and RLF expression was achieved. This is a meticulous time consuming technique but was necessary to

unequivocally show that there was a relationship between these markers and DNA ploidy abnormalities. Laser capture also abrogates the risk of stromal cell analysis at the expense of analysing much smaller cell population. By using ICDA accurate histogram interpretation was still achieved with very small number of nuclei. It is unlikely that this experiment could be repeated using flow cytometry, as much larger numbers of nuclei are required for accurate diagnosis. Now that a correlation with geminin, cdc7 and PLK-1 and aneuploidy status has been demonstrated, we may go forward and assess these markers on whole biopsy samples from BO, without the need for further laser capture. This work would be necessary to confirm that RLF markers can be utilised in surveillance biopsy samples and were suitable for high throughput.

The utility of PLK-1 may have wider application than as a prognostic biomarker. Its association with tumorigenesis indicates that PLK-1 is an attractive kinase target for cancer drug development.[Strebhardt and Ullrich, 2006] In contrast to Aurora kinases, little progress has been reported toward potent and selective PLK-1 inhibitors with drug-like properties suited to clinical development. One report on BI 2536, a PLK-1 inhibitor from a novel chemical series with attractive drug-like features, demonstrated highly effective in cancer xenograft models in mice with acceptable tolerability.[Steegmaier et al., 2007] A second report on the discovery and application of a novel potent small-molecule inhibitor of mammalian PLK-1, ZK-Thiazolidinone (TAL).[Santamaria et al., 2007] These drugs may warrant evaluation in Barrett's adenocarcinoma, which often displays an aneuploid phenotype. If this correlates with PLK-1 status, as we have demonstrated, then there is potential to tailor chemotherapy on the basis of cell cycle phenotype.

In summary, this work demonstrates that PLK-1, geminin and cdc7 kinase are upregulated in HGD and adenocarcinoma arising from Barrett's oesophagus and expression is significantly correlated with aneuploidy. These simple immuno-histochemical stains have potential as biomarkers to evaluate future cancer risk and represent novel potential target for therapeutic agents in Barrett's oesophagus, which warrants further study.

Chapter 8
Evaluation of Elastic Scattering Spectroscopy for the detection of DNA ploidy abnormalities

Chapter 8 Evaluation of Elastic Scattering Spectroscopy for the detection of DNA ploidy abnormalities

8.1 Introduction

8.1.1 Theory of Elastic scattering spectroscopy (ESS)

Elastic scattering spectroscopy (ESS) is based on the study of elastically scattered photons (that do not undergo a change in energy) in turbid and absorptive medium. Rayleigh scattering describes the elastic scattering of light by spheres which are much smaller than the wavelength of light, and its interpretation is strongly dependent upon the size of the particle and the wavelengths. The Rayleigh scattering model breaks down when the particle size becomes larger than around 10% of the wavelength of the incident radiation. In the case of particles with dimensions greater than this a more complex analytical solution called Mie's scattering model, or Mie theory, can be used to find the intensity of the scattered radiation.

A simple example of these models is in atmospheric scattering. The blue colour of the sky results from Raleigh scattering, as the size of the gas particles in the atmosphere is much smaller than the wavelength of light. As sunlight passes through the atmosphere, the shorter wavelength (blue/violet) component is Rayleigh scattered more strongly by atmospheric gases than the longer wavelength (e.g. red/yellow) component. The sky light arriving directly to the viewer’s eye from the sun therefore appears to be slightly yellow while the light scattered through rest of the sky appears blue. During sunrises and sunsets, the Rayleigh scattering effect is much more noticeable because the volume of air through which sunlight must pass is significantly greater than when the sun is high in the sky. The remaining unscattered light received by the observer is mostly of a longer wavelength, and therefore appears to be red. In contrast, the water droplets which make up clouds are of a comparable size to the wavelengths in visible light, and the scattering is described by Mie's model rather than that of Rayleigh. Here, the wavelength dependence is much weaker, and the clouds therefore appear to be white or grey.

8.1.2 Scattering and absorption properties of biological tissues

When light interacts with biological tissue, elastic scattering is inevitable (see figure 8.51). Any spatial variation in refractive index leads to light scattering.[Boustany et al., 2010] There is little known, however, about the spatial distribution of cellular molecules and therefore Mie theory has been used to approximate size distributions of tissue scatterers based on angular or spectral scattering patterns. The equations require three parameters to describe the optical properties of any given medium: absorption coefficient, scattering coefficient and scattering phase function. The absorption coefficient (μ_a) describes the probability that a photon of incident light will be absorbed; scattering coefficient (μ_s) describes the probability that a photon will be scattered (will change the direction of propagation); scattering phase function ($p(\theta)$) describes the character of scattering as a probability of changing of the photon propagation direction (p) by angle (θ). This can be mostly forward scatter, backward scatter or neutral (anisotropic scattering). The measured ESS spectrum is therefore related to the wavelength-dependence and angular-probability of scattering efficiency of tissue micro-components, which in turn generates spectral signatures which can be correlated with biological phenomena.

Figure 8.51 Light scattering interactions with tissue

a) The optical geometry for delivery and collection fibers for a typical "optical biopsy" measurement. The fiber probe is placed in gentle contact with the tissue surface; b) cartoon depicting the scattering of photons by denser organelles and nucleus in the cell.

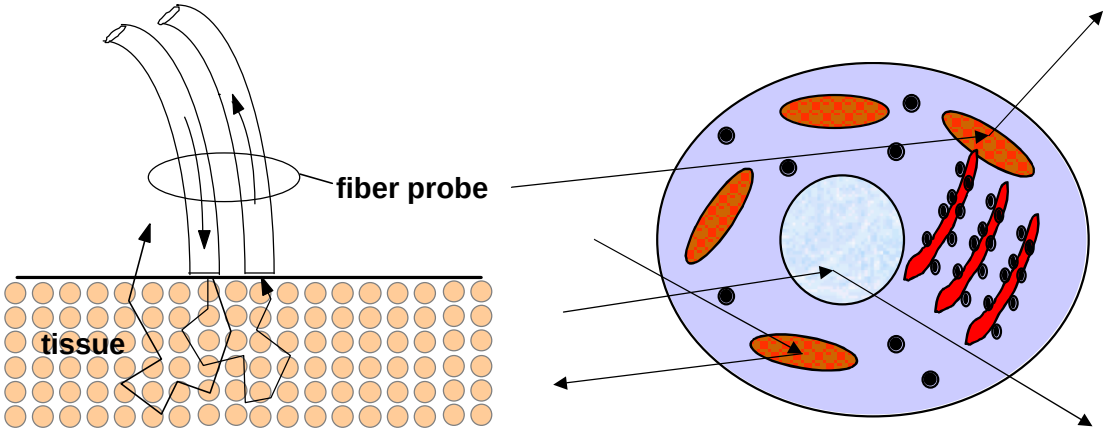

In vivo ESS application is also sensitive to the absorptive properties of biological tissues due to chromophores, which are illustrated in figure 8.52. The ultraviolet/blue part of visible spectrum (200-450 nm) is absorbed by haemoglobin, DNA and proteins. The intense peak of absorption at 350-450 nm is called the Soret band and describes the absorption of vividly-pigmented haem-containing moieties, such as various cytochromes. For example, the cytochromes P450, a diverse class of monooxygenase enzymes, were given their name because they exhibit a Soret peak at 450 nm in their reduced form when saturated with carbon monoxide (CO difference spectrum assay). Other weaker absorbers in this region include DNA, amino-acids, proteins (tryptophan, tyrosine, phenylalanine), and melanin.

The visible part of the spectrum between 450-700nm is dominated by absorption from oxyhaemoglobin (500-630 nm) and deoxyhaemoglobin (540nm). These absorption features are called Q-bands. The near infra-red range from 700-1100nm is said to be the "therapeutic window" as it has the lowest absorption by tissue. The major absorbers are still haemoglobin and deoxyhaemoglobin, although much weaker than at lower wavelengths. Water has a peak at 976 nm which although weak is equivalent to haemoglobin, and this rapidly increases in intensity beyond 1100nm, which limits further ESS measurement.

Figure 8.52 Compilation of absorption spectra of principal chromophores in tissue

(adapted from Hale, Van den Berg, Zijlistra, Wagnieres and Sarna [Hale and Querry, 1973;VandenBerg and Spekreijse, 1997;Zijlistra W et al., 2000;Wagnieres et al., 1998;Sarna et al., 1984])

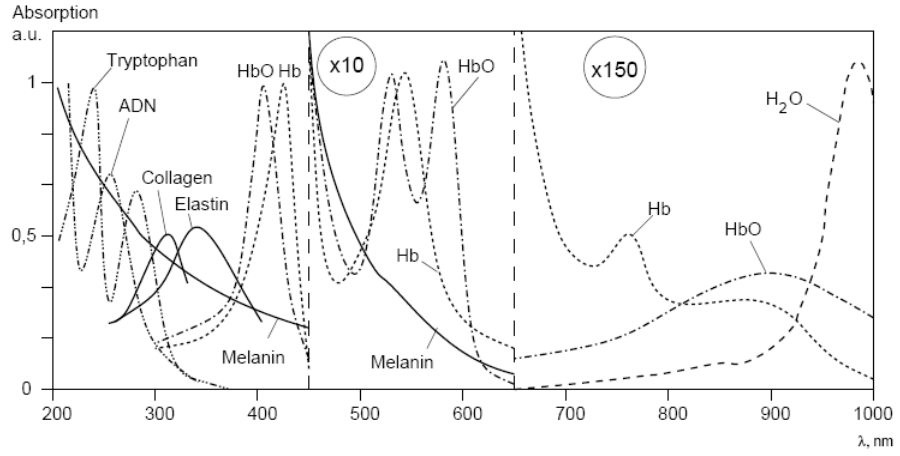

8.1.3 Biological phenomena potentially studied by ESS

Light-scattering spectra from tissues *in vivo* consist of a Rayleigh component due to scattering by small organelles, a large background from submucosal tissue and a relatively small backscattered component due to epithelial cell nuclei. The cellular changes that occur in dysplasia and cancer contribute to a change in the dimension and concentration of scatterers, which in turn can be measured by a change in the shape and amplitude of the backscattered spectrum. These changes include enlargement and hyperchromacity of the cell nucleus [Georgakoudi and Van Dam, 2003;Muller et al., 2003], changes in tissue structure (disorganisation/crowding) and increased concentration of metabolic organelles [Mourant et al., 1998].

The physical correlation of ESS with aneuploidy has been addressed in a study of cancer cell lines. [Mourant et al., 2000] By measuring DNA content by flow cytometry, the DNA index (DI) was calculated for 2 different cell lines, and plotted against high angle scatter (between 110° and 140°). Cell suspensions with higher DI (analogous to aneuploidy) scattered more light than cell suspensions with smaller DI (analogous to diploid). Other characteristics of aneuploid cell populations that may be measured by ESS include distension of the rough endoplasmic reticulum and increased accumulation of cytoplasmic glycogen aggregates in the Golgi apparatus and secretory granules, both shown to occur by Electron microscopy.[Levine et al., 1989] Chromatin content and organisation are also important predictors of cancer progression, as was demonstrated in Chapter 6 using nuclear texture analysis to differentiate dysplastic from non-dysplastic tissue. Since scattering is induced by gradients of the optical index of refraction, ESS spectral signatures will also be altered if the refractive index of nuclei or organelles changes due to an increase in the amount of chromatin or granularity of the chromatin. Biological phenomena that affect the ratio between absorption spectra of haemoglobin and oxyhaemoglobin include tissue oxygenation [Solonenko et al., 2002] and changes in vascularisation [Fridolin and Lindberg, 2000].

8.1.4 Utility of ESS in Barrett's Oesophagus surveillance – studies to date

Our group has previously shown that ESS can detect HGD in patients with a sensitivity of 92% and specificity of 60% [Lovat et al., 2006]. Preliminary data also suggest that ESS can detect aneuploidy in vivo [Mackenzie et al., 2007b], with a sensitivity of 90%, specificity 62% and area under the Receiver Operating Characteristics (ROC) curve (AUC) = 0.79. These studies used complex pattern recognition techniques such as multivariate discriminant analysis, leave one out block validation and error reduction orthogonal subtraction (EROS)[Zhu et al., 2009], to generate algorithms that correctly classify spectra as premalignant or benign tissues. This work is limited by its use of retrospective data for analysis. In addition, if the ESS work is to be generalisable, and potentially mass produced, then there is a need for multiple different boxes that have the same characteristics. All work so far was carried out on two single integrated units, but with different spectrometers and coupled with different laptops. They are referred to as Old box and New box throughout this chapter. The old box has a spectrometer with range 320-920nm, and the new box has spectrometer with range 189-869nm.

8.2 Aims of this chapter

In order to demonstrate that ESS results were generalisable between different boxes a series of experiments was designed to quantify box to box variability in the diagnosis of high grade dysplasia and aneuploidy. Subsequently a prospective cohort study was undertaken to compare boxes with two different spectrometers and allowed for study of the field effect in Barrett's dysplasia. Finally a study was undertaken to assess the utility of targeted real time ESS versus random four quadrant biopsy.

8.3 Materials and Methods

8.3.1 Components of the ESS system

A schematic of the ESS system is shown below. The ESS system consists of an arc lamp, spectrometer, power supply (which are housed together in a single integrated unit) and a laptop computer to control these components and record the spectra (see figure 8.53). Figure 8.54 is a photograph of the unit with its lid removed. The main components that are visible are the Ocean Optics S2000 spectrometer, PerkinElmer LS1130/FX1100

xenon flash lamp and bulb, and a TERN i386-Engine analogue to digital convertor (ADC) with digital I/O. Also visible are two non-electronic components, a lens and filter holder that couples the flash lamp to the fibre and the pot that contains a white material ('Spectralon') that is used to calibrate the system.

Figure 8.53 Schematic of ESS system

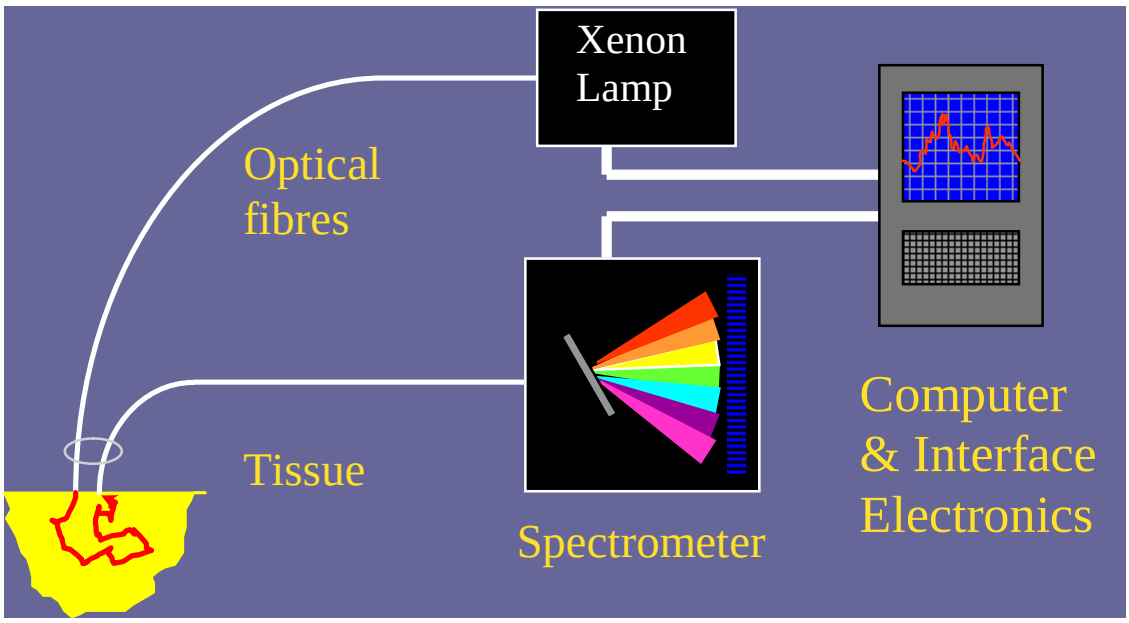

Figure 8.54 Photograph of New box

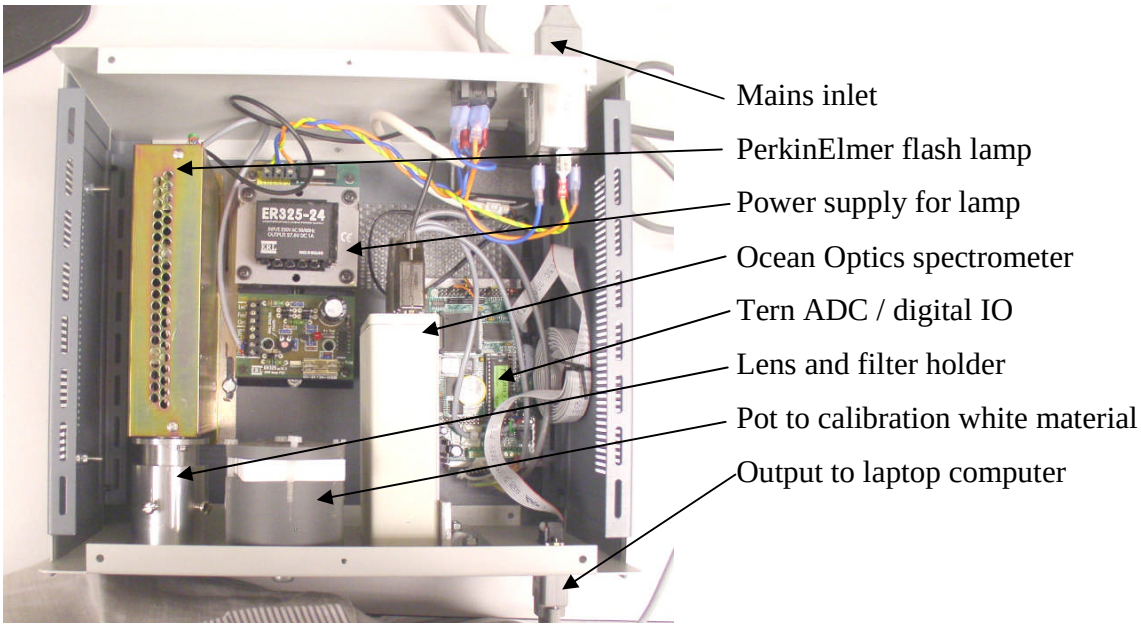

8.3.2 Acquisition of Elastic Scattering Spectra

In order to take optical measurements a flexible fibre-optic probe (see figure 8.55) is passed down a Pentax endoscope. The probe consists of a collection fibre (200 μm diameter), with a fixed centre-centre separation distance of 350 μm from an illumination fibre (400 μm diameter). The fibre assembly is housed in a plastic sheath (outer diameter 2.0 mm) which can pass into the oesophagus via the biopsy channel of a standard endoscope. The fibre is cold-sterilised with the endoscope. The Pentax endoscope is necessary as illumination is with a continuous white light source and a colour chip creates the colour image. Other endoscopes currently available have a black and white CCD and the colour image is achieved by illuminating with revolving RGB filters. These can introduce background light artefacts.

Figure 8.55 Optical fibre and schematic of geometry

It consists of two fibres side by side inside a stainless steel ferrule with the end polished flat

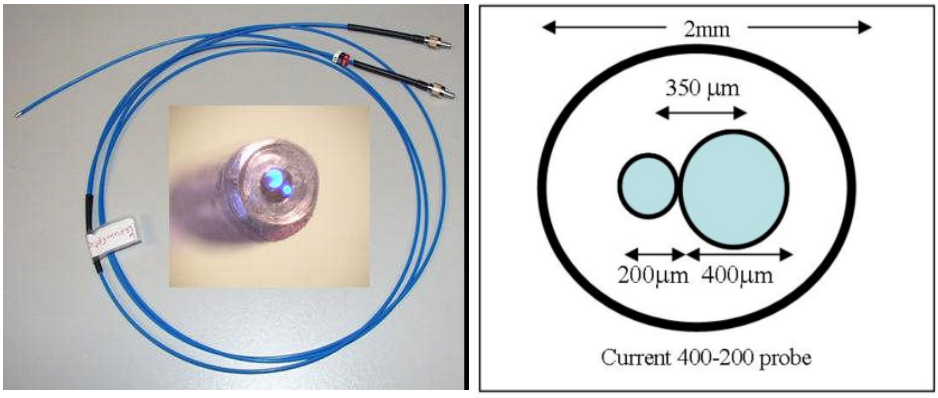

Short pulses of normal white light (λ=320-1000nm) from the xenon arc lamp (PerkinElmer Inc., Fremont, California, US) are directed through the flexible optical fibre touching the tissue to be interrogated. Ultraviolet B and C (100–315 nm) light is filtered out to avoid risk to patients. The light is shone through the underlying tissue for a fraction of a second; the lamp typically flashes 5 – 10 pulses of about 200ns duration at 3 ms intervals. The energy per pulse is about 4.5 x 10^{-7} Joules. Typically ten pulses are used to

collect a spectrum, four spectra are collected at each site and 30 sites are measured within an oesophagus, so the total output energy per session is approximately 0.54 mJ.

The back-scattered light is collected through the 200 μm fibre and propagates it to the spectrometer (S2000 Ocean Optics, Dunedin, Florida, US). The spectrometer outputs the spectrum to the computer for recording and further analysis. Collection and recording of a single spectrum takes approximately 200ms. The A/D on the Tern card sends a series of numbers to the laptop corresponding to the intensities at different wavelengths, the exact wavelengths vary from one spectrometer to the next and before opening the program on the laptop the user has to specify which unit is being used.

8.3.3 Calibration

To ensure quality control of spectral acquisition, three types of reference spectra are recorded from the flat surface of a tissue-simulating phantom prior to tissue interrogation. Tissue stimulating phantoms are polymer constructs with well defined scattering and absorption properties, allowing the system to account for spectral variations in the light source, spectrometer, fibre transmission and fibre coupling.

The first reference is recorded from Spectralon^{TM} (Labsphere. Inc). This is spectrally flat and therefore a measure of reflectance. The second and third references are measured using a scatter only phantom (white phantom) and one which includes a pigment to account for differences in absorption (pink phantom). Immediately before any spectral measurement is made the system automatically records the ambient light within the oesophagus arising from the endoscope light source. In this manner the site-specific exogenous light at the moment of measurement is controlled for.

8.3.4 Statistical considerations

Pre processing of spectra

The raw ESS spectra were visually examined for any obvious outliers caused by acquisition errors, poor contact of the optical probe with the tissue, or other artefacts, and cleaned before analysis. Standard pre-processing was carried out on the spectra to

improve signal quality. Each spectrum is made up of 1000 (new box) or 1801 (old box) intensity points spanning the wavelength range 320 nm to 920 nm. Spectra were smoothed using a linear filter down to 637 by choosing the alternate points to speed subsequent manipulation (Savitsy-Golay method, quadratic model, span 7 below 620 nm and span 20 above 620 nm, where noise was greater). A small portion of the signal noise arises from the hardware. Figure 8.56 shows a graph of the noise at each wavelength as a percentage of the signal.

Figure 8.56 Signal to noise ratio throughout the spectral range for 30 spectralon measurements

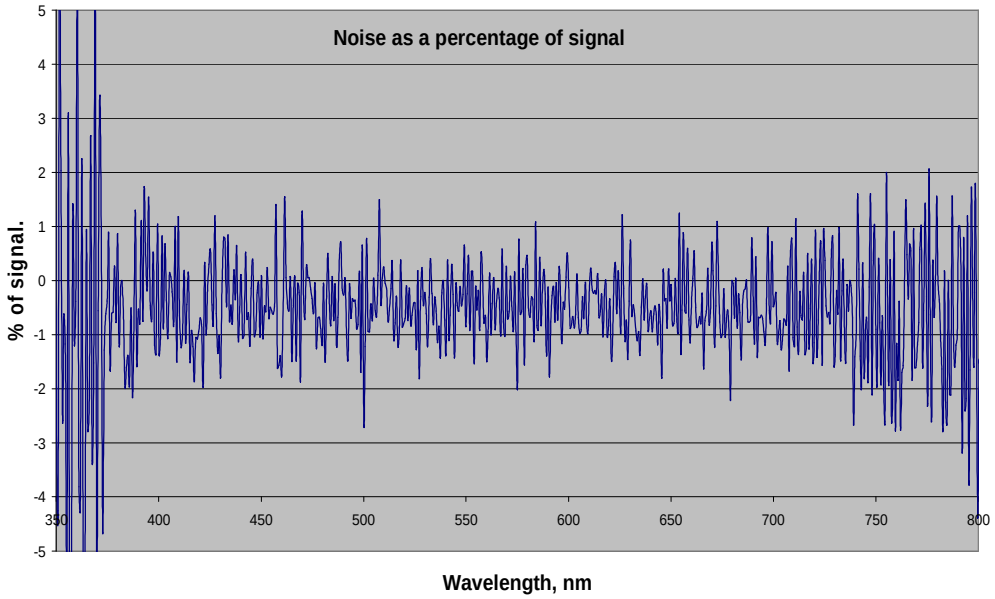

This was calculated by collecting two spectra from the same material, subtracting one from the other, then dividing the result by the strength of the signal at each wavelength and finally converting to percent. Between 320-370 nm and between 890-920 nm, the signal-to-noise ratio of the spectra drops off. This is due to a lower light output from the Xenon arc lamp and reduced sensitivity of the spectrometer at these wavelengths. The 400-900 nm window has the largest signal to noise ratio proportional to other wavelengths, with a root mean square value of 0.84%. Hence only the window between 370 nm and 890 nm was used in the analysis. Using the standard normal variate method,

[20] the spectra were then normalized by setting the mean intensity of each spectrum to zero and the variance to one, allowing for more accurate shape comparison.

Pre processing by error reduction by orthogonal subtraction (EROS)

Of far more significance is movement artefact caused by the endoscopist's hand moving or by patient's breathing, heart beat and swallowing. A new spectral pre-treatment method, error reduction by orthogonal subtraction (EROS), described in detail elsewhere [Zhu et al., 2009] , was then applied to the spectra. EROS uses the replicated measurements of what is nominally the same site to model the structure of the measurement variability. This structured variability is then removed from the spectra by subtracting the first few principle components (within a site) from each spectrum. EROS has been shown to be an effective pre-treatment for Barrett's *in vivo* ESS data by identifying measurement variability between replicated spectra and ameliorating this effect.[Zhu et al., 2009]

Post –processing LDA + PCA

The number of points in a spectrum (order of 10^3) is much larger than the number of spectra in the training set (order of 10^2). Using all points in the spectrum to train the model would result in over fitting of the model. Consequently the data was compressed to between 15 and 30 values using principle component analysis, which has been previously demonstrated on ESS spectra from breast cancer sentinel nodes with virtually no loss of information.[Austwick et al., 2010] Linear discriminant analysis was then applied to these principal components to maximize the discrimination between the two groups.

8.4 Comparison of two boxes for detection of DNA ploidy

8.4.1 Introduction

Since the first experiments that were published by the NMLC on ESS there have been changes in the design of the system, specifically the TERN card and spectrometer. This was undertaken to facilitate use of laptops with updated windows operating systems, as the software for a prospective study was written in Java and the 'Old box' could only be used with Windows 95 which was not compatible. A series of matched optical biopsy

sites had been taken using the ‘new box’ and Dr Mackenzie had previously analysed these data with comparable results for the detection of HGD.[Mackenzie, 2008] This was not a direct comparison however and DNA ploidy had not been assessed. The aim of this experiment was to evaluate the ‘new box’ for detection of DNA ploidy.

8.4.2 Methods

In order to validate the new box we sought to examine a similar number of patients and biopsies. To allow comparison with the ‘old box’, the historical dataset was re-analysed using the same LDA and 20 principal components.

8.4.3 Results

A total of 65 sites form 36 patients were analysed from the ‘new box’ dataset (figure 8.57). The sensitivity for aneuploidy was 59%, specificity 61% and AUC = 0.66. A total of 105 sites from 44 patients were analysed from the ‘old box’ dataset, and the results (figure 8.57). The sensitivity for aneuploidy was 78%, specificity 77% and AUC = 0.84.

Figure 8.57 ROC curve of linear discriminant analysis comparing aneuploidy vs. diploid using ‘new box’ (left) and ‘old box’ (right)

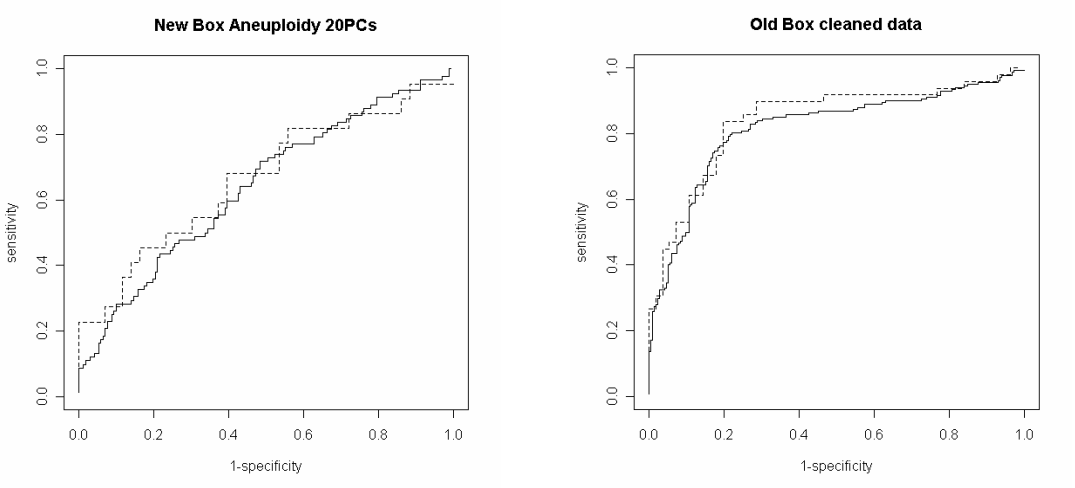

8.4.4 Discussion

Using ‘new box’ we were unable to reproduce the results for DNA ploidy that had previously been described when using the ‘old box’. These units contain different spectrometers, and the ‘old box’ is slightly more sensitive in the near infra-red range. In addition 1801 data points are collected per spectra by the ‘old box’, versus 1000 for the ‘new box’. The data set for the ‘new box’ is smaller and contains less aneuploid biopsy sites, which may influence the results, although a smaller dataset should yield a better AUC as it is more prone to over fitting of data. A smaller dataset may be more prone to errors caused by outliers, which could occur if there was sampling error due to position of the probe or incorrect co-registration of biopsies. These problems are however generalisable to all *in vivo* ESS experiments.

The discrimination between squamous tissue vs. columnar tissue is high for both boxes around 0.97 AUC (data not shown). The loadings of LDA should therefore tell us subtle differences between the 2 boxes. The loadings for each box for squamous vs. columnar and HGD vs. NDBO are shown in Figures 8.58 and 8.59. If we look at the combined spectra for both boxes we can see a separation of the curves at two points, at 450nm and 650-800nm, i.e. the mean intensity of the spectra is significantly different at these wavelengths. The LDA loading, in green, shows how the intensity of each wavelength contributes to the classification, and varies as the differences between the classes changes. The LDA loadings for HGD vs. NDBO (figure 8.59) have been pre-treated with an EROS in order to remove measurement variability form the original spectra. After this pre-treatment the old box LDA loadings are very smooth, whereas new box LDA loadings are quite noisy. It is therefore likely that the old box data is more meaningful and interpretable. In order to investigate this further we elected to test both boxes using tissue-simulating phantoms.

Figure 8.58 Loadings of LDA comparing squamous and columnar tissue using 20 principle components for each box

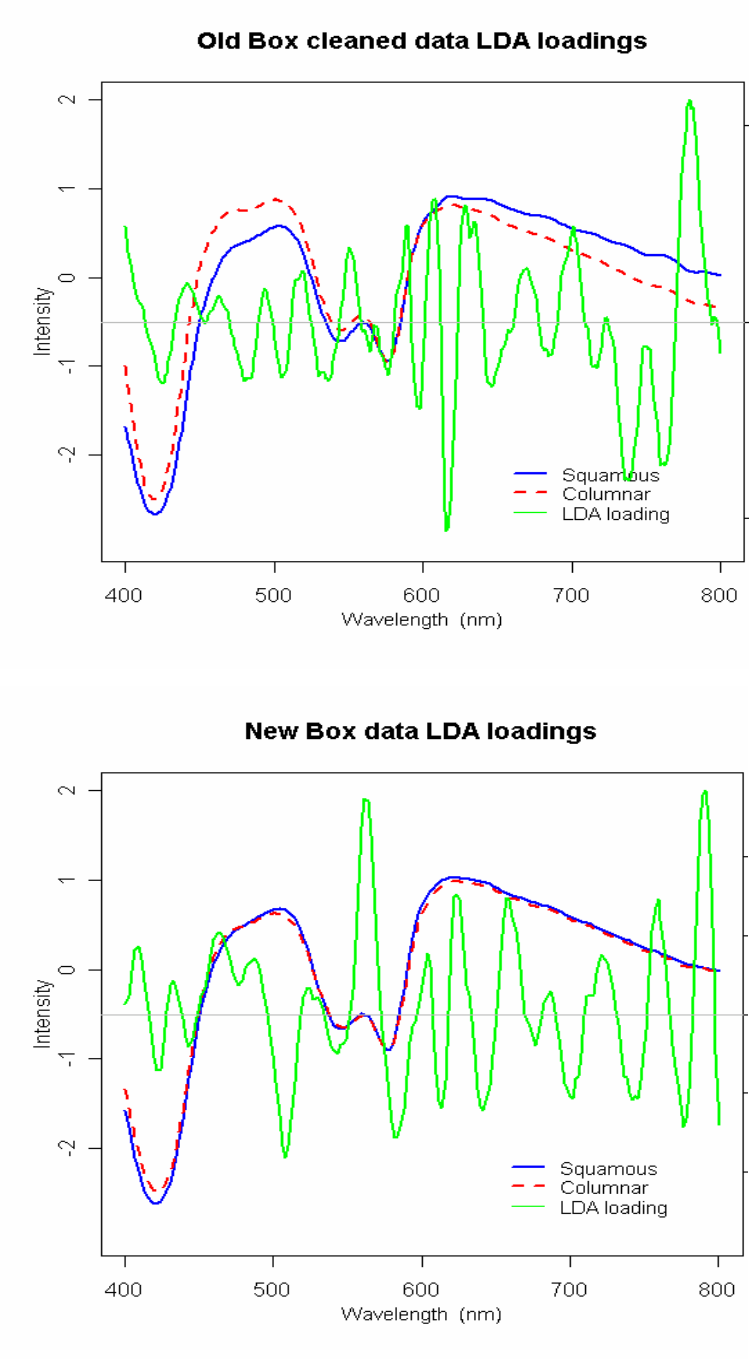

Figure 8.59 LDA loadings for each box when comparing HGD vs. non HGD tissue

20 principle components were used in the analysis

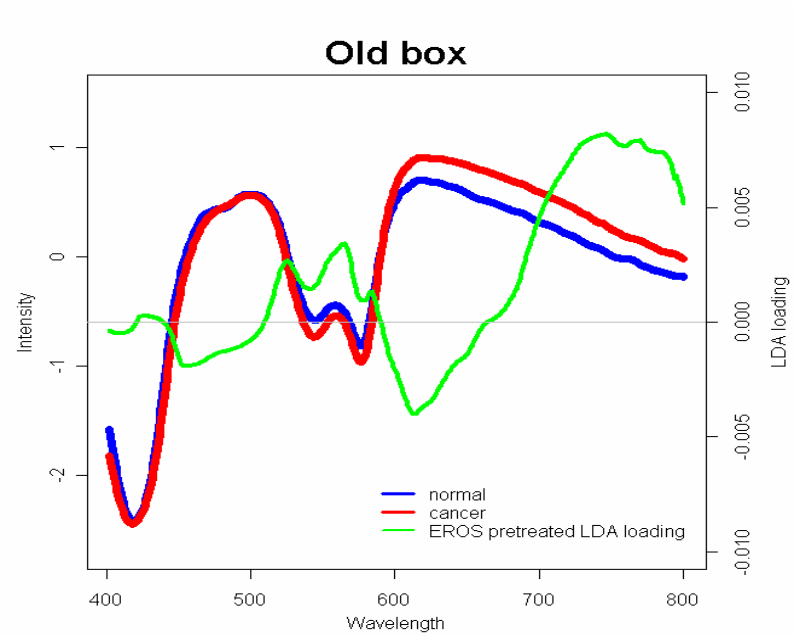

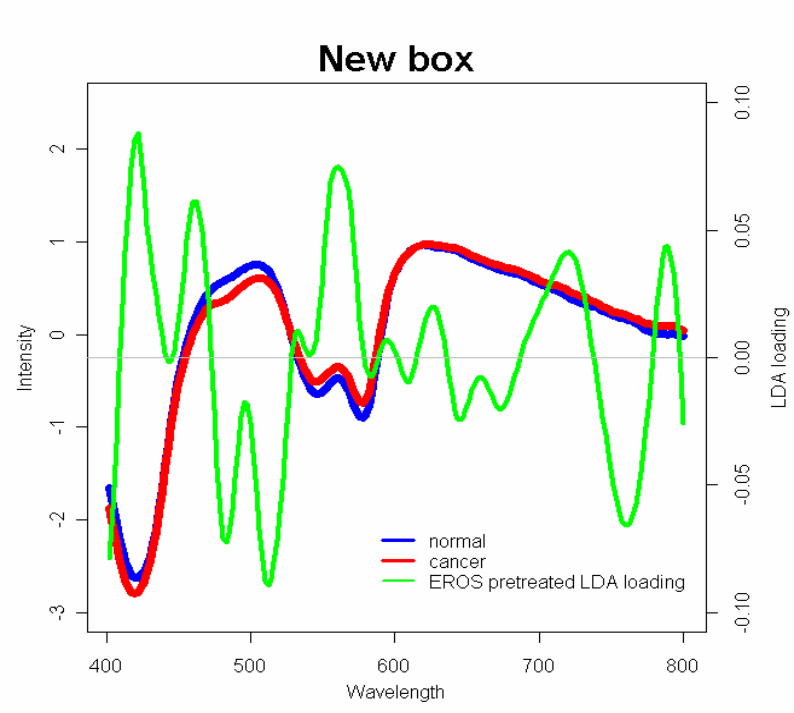

8.5 Investigation of inter-box variability using a tissue-simulating phantom

8.5.1 Introduction

We then designed an experiment to determine how similar the new and old boxes are by using both to collect data from a tissue-simulating phantom. After discussion with Professor Fearn (Professor of Applied Statistics, Department of Statistical Science, UCL) we applied standard algorithms to produce canonical scores. A canonical score is a statistical tool for investigating the relationship between two sets of variables. The purpose of the canonical score is to make separation between the classes as large as possible. We used tissue phantoms for this experiment to reduce signal noise, as noisier spectra (such as from the oesophagus) would have an effect on the variance of the canonical scores. Hence this experiment should be able to detect subtle differences between the two spectrometers.

8.5.2 Methods

The phantom was freshly mixed shortly before the experiment, using the following recipe: 47 ml PBS, 2.5 ml 20% Intralipid, 1.25 ml whole, human blood and a grain of heparin to prevent the blood from clotting. The 'old box' and 'new box' were both calibrated with Spectralon ^{TM} using the calibration pot built into the 'old box'. Twenty or more calibration spectra were collected for each unit. Similar, CeramOptec fibres were used for each system. The fibres were rotated between calibrations to simulate the differences that might occur in practice. The tips of the fibres were then placed in the stirred phantom and a further twenty or more spectra were collected on each box. The calibration spectra were collected first to avoid contaminating the calibration pot with blood from the phantom.

8.5.3 Results

Old Box

Figure 8.60 shows 20 reference spectra taken with the Old Box. The spectra are all presented ratioed to the last spectra taken. Figure 8.61 shows 21 spectra, each ratioed to a particular reference spectrum, i.e. 21 separate reference spectra are used.

Figure 8.60 Spectra taken from calibration pot using Old box

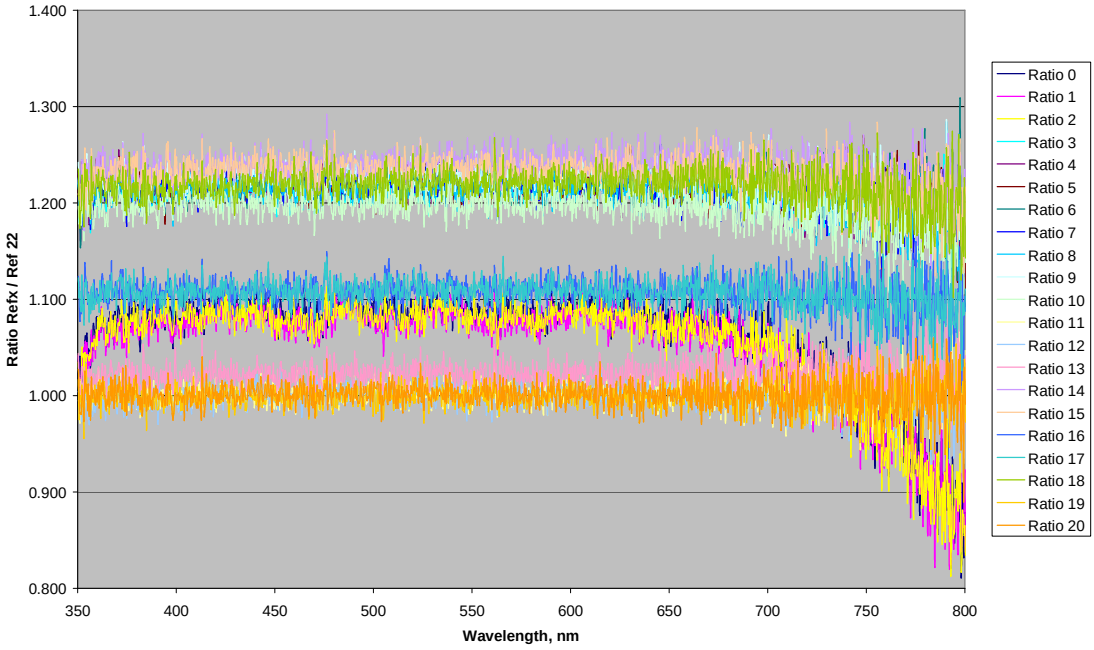

Figure 8.61 Spectra taken from tissue-simulating phantom using Old box

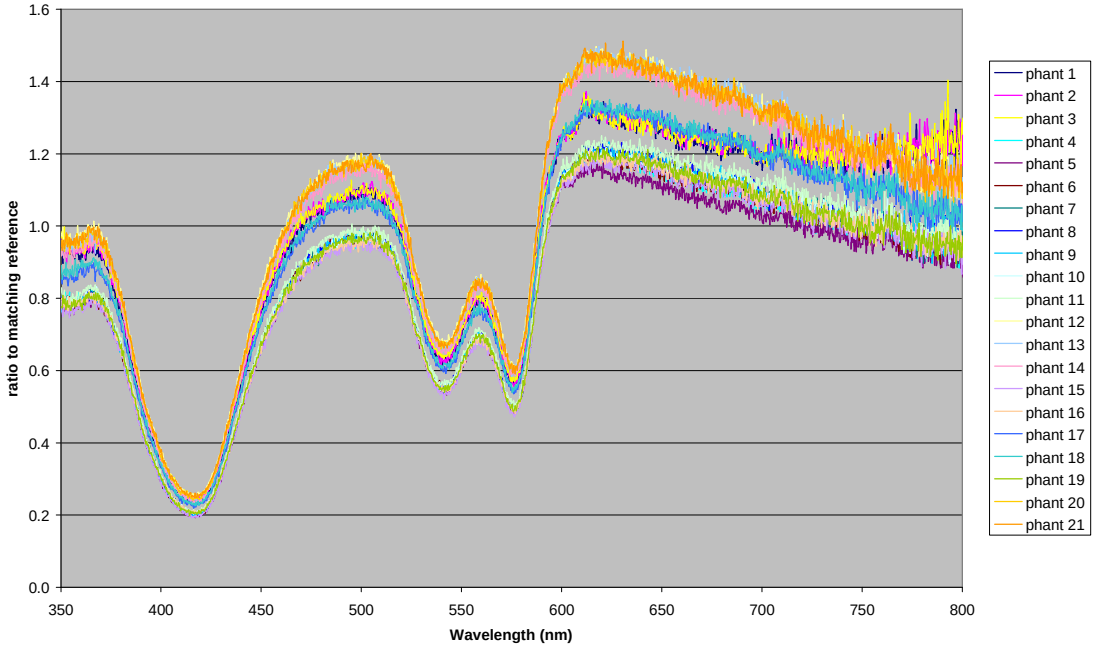

It is striking that, above about 650 nm, the first three reference spectra are very different from the others and not linearly related to them. This was not deliberate and there is no obvious reason for it. As the first three reference spectra differed from the others, so the slope of the first three spectra taken from the tissue simulating phantom is notably different at wavelengths beyond about 650 nm. It is likely that these data are anomalies and as such were subsequently removed from further canonical score analysis.

New Box

Figure 8.62 shows all the reference spectra taken with New Box using the calibration pot incorporated into the Old Box, i.e. the same reference as was used in Figure 8.60. The spectra are all presented ratioed to the first spectra taken. Figure 8.63 shows the 21 spectra taken from the tissue stimulating phantom with new box.

Figure 8.62 Spectra taken from calibration pot using New box

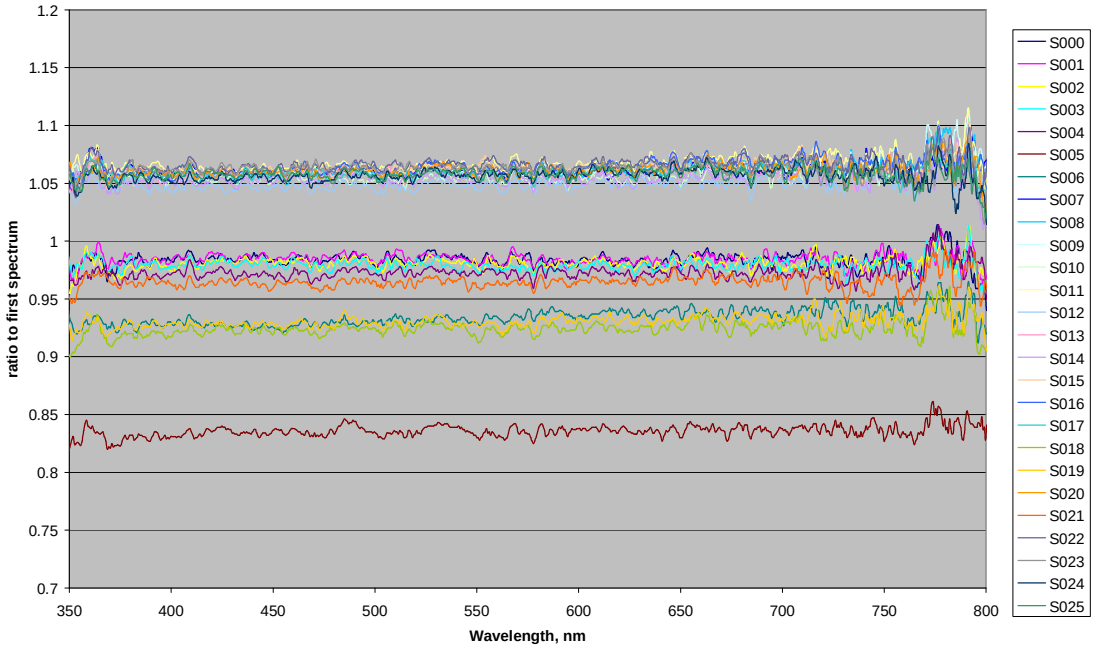

Figure 8.63 Spectra taken from tissue-simulating phantom using New box

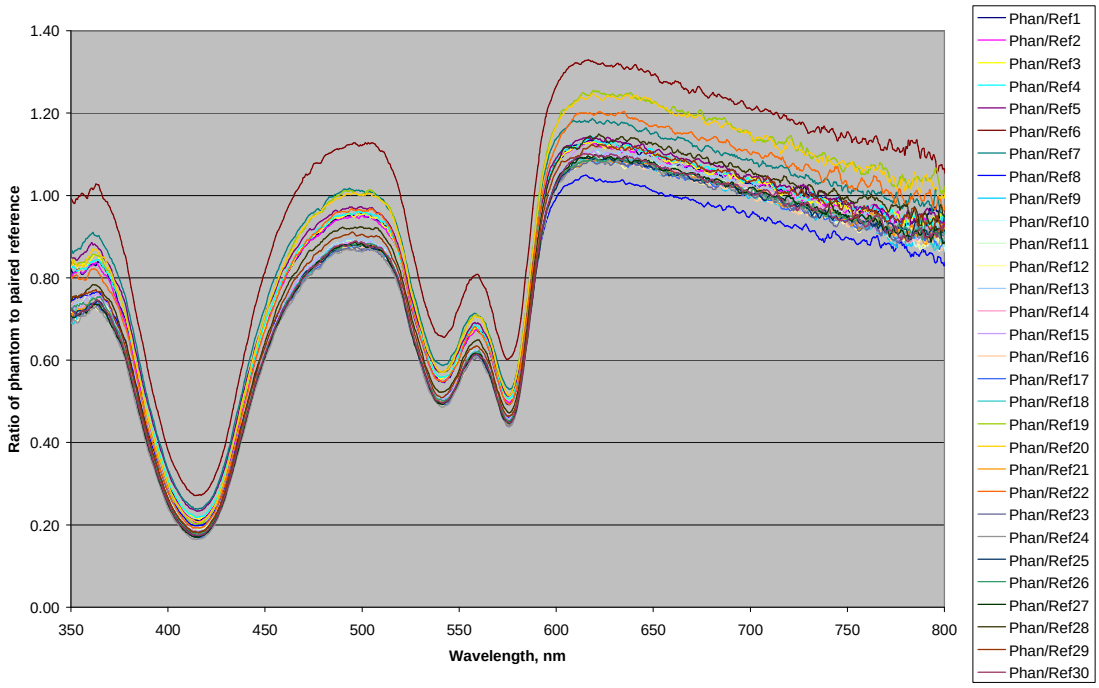

By analysis of the graphs we can see that the signal and noise are different between the two boxes. To test whether this difference was significant a canonical score was calculated for each of the phantom spectra (see figure 8.64). When unmatched data were analysed there was a small difference in the canonical scores between the two boxes, though this was not apparent when matched data was used.

Figure 8.64 Canonical scores generated from phantom spectra

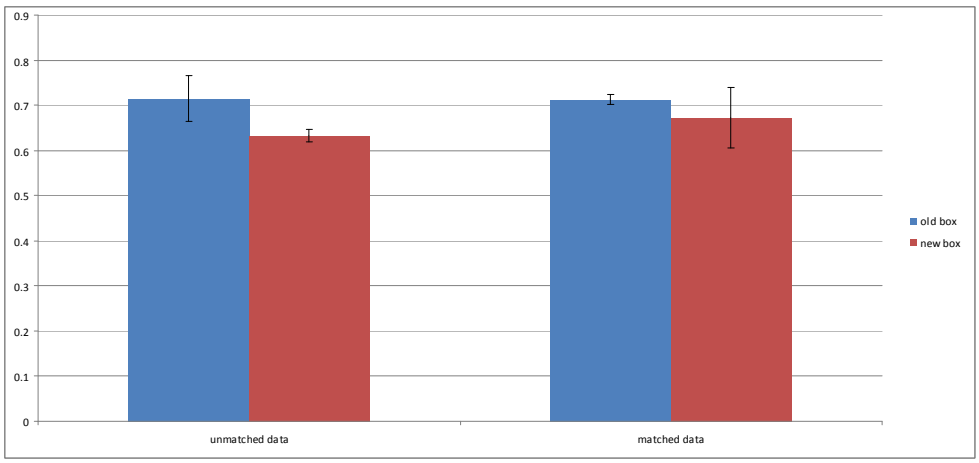

8.5.4 Discussion

These experiments demonstrate that there may be a difference between the two boxes, both by measurement of LDA loadings from *in vivo* patient data and signal to noise ratio from tissue stimulating phantom data. The difference seems to be apparent in the 600-800nm wavelength range, i.e. the red and near infra-red part of the spectrum. In the interval 315-1000 nm optical properties of tissue are highly different: in the UV and visible part of the spectra biological tissues are mostly absorbent, in the red and near infra-red part they have relatively low absorbency, but have strong scattering ability. It is therefore possible that the near infrared part of the spectrum yields more useful information for the detection of molecular abnormalities *in vivo*. A prospective study was designed to test this hypothesis

8.6 Comparison of different types of spectrometer in accuracy of diagnosis of dysplasia and DNA ploidy

8.6.1 Introduction

If we accept that the more informative spectral properties of the tissue are at the near infrared end of spectrum, then the strong haemoglobin absorption in the UV-visible part of spectra may be considered non-useful signal, and should be either eliminated from analysis or its intensity significantly reduced. It is possible to do this either by cropping the data and analysing part of the spectra which is described mostly by scattering, or using a spectrometer that has enhanced intensity at the near-infrared part ranged at 650-1000nm (see figure 8.65). If we hypothesise that a red enhanced spectrometer, more sensitive in the range 450nm-1000nm, would detect more scattering data then this may improve detection rates of molecular abnormalities. A new single integrated unit was constructed with a spectrometer using grating H4 which has a wavelength of 530-1100nm.

The aim of this *in vivo* prospective study was to assess the influence of the spectral range of the spectrometer on accuracy of diagnosis of dysplasia and DNA ploidy abnormalities.

Figure 8.65 Comparison of different spectrometers and wavelength ranges

H3 corresponds to Old box, H4 denoted as red box

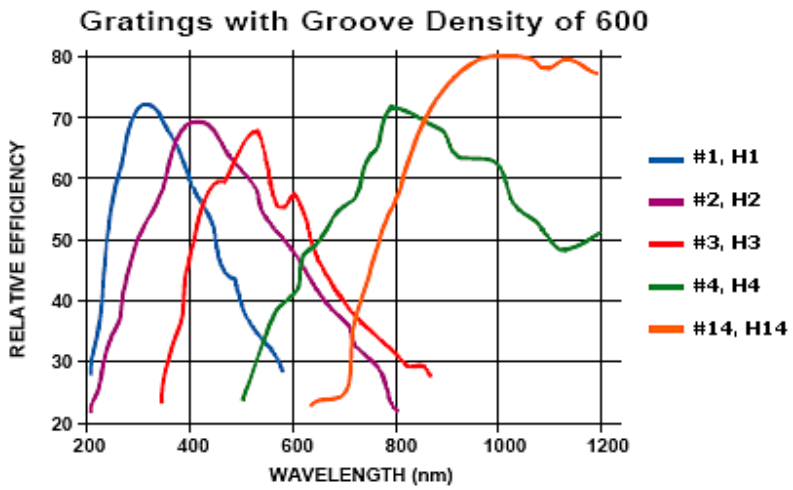

8.6.2 Methods

After identification of the Barrett's segment endoscopically, a series of in vivo optical biopsies were taken from the posterior wall every 2cm. Spectral data were collected sequentially, with a different fibre used for each spectrometer (named old box and red box). Each site was careful matched visually and the order of spectral collection was varied from one box to the other, in an attempt to reduce acquisition bias. Care was taken to ensure that blood in the field was kept to a minimum. A single biopsy matching the site of spectral acquisition from both boxes was then taken, and histopathology reviewed. DNA ploidy was assessed by ICDA on these biopsies as previously described (chapter 5). A diagnostic algorithm of best fit was generated by principle component and linear discriminant analysis on the histopathology and DNA ploidy data.

8.6.3 Results

57 patients were enrolled in the study, with 217 sites biopsied. The data was then cleaned by removal of; unusable spectra; sites with mixed squamous and glandular mucosa; sites with indefinite of low grade dysplasia. As the removal of spectra was unequal between the groups this resulted in different numbers of spectra available for analysis from each

box. The analysis below was therefore undertaken in two ways, unpaired data and paired smaller datasets.

Squamous vs columnar (unpaired data)

Analysis was undertaken on 169 matched sites from 54 patients in the red spectrometer patient cohort. This gave 148 squamous spectra from a total of 665 spectra used in the analysis. ESS using a red enhanced spectrometer was able to distinguish squamous and columnar tissue with AUC= 0.89, sensitivity 91% and specificity 71% (see figure 8.66). Using the old box 193 matched sites from 57 patients were suitable for analysis giving a total of 764 spectra (166 squamous). ESS using the old box was able to distinguish squamous and columnar tissue with AUC= 0.84, sensitivity 91% and specificity 58%.

Figure 8.66 ROC curve squamous vs columnar using Red box (left) and Old Box (right)

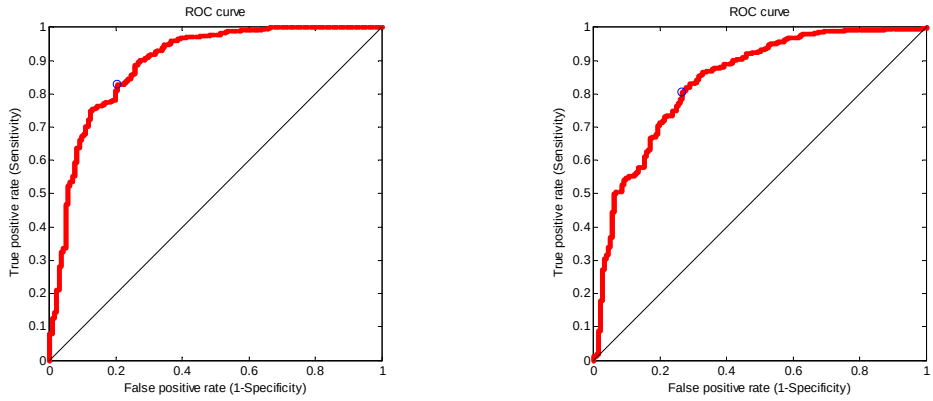

Non-dysplastic BO versus HGD (unpaired data)

Analysis was undertaken on 52 matched sites from 22 patients in the red spectrometer patient cohort. This gave 195 spectra used in the analysis, 94 non-dysplastic BO and 101 HGD. ESS using a red enhanced spectra was able to distinguish squamous and columnar tissue with AUC= 0.85, sensitivity 84% and specificity 83% (see figure 8.67).

Using the old box 39 matched sites from 16 patients were suitable for analysis giving a total of 159 spectra. The AUC= 0.85, sensitivity 86% and specificity 83%.

Figure 8.67 ROC curve HGD vs non-dysplastic using Red box (left) and Old Box (right)

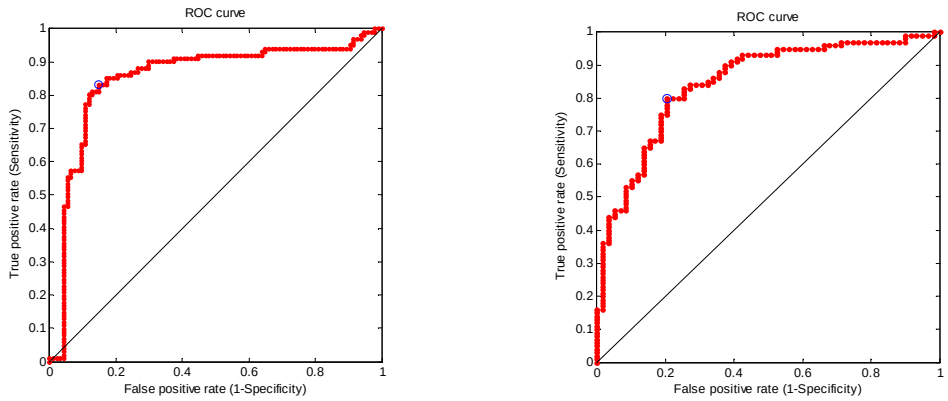

DNA ploidy abnormalities (unpaired data)

Of the 217 sites biopsied DNA ploidy analysis was available from 181 sites, 26 were not reportable and the remainder were mixed squamo-columnar not suitable for ESS analysis. A summary of results according to the Vienna classification of the site (Table 8.33), and the highest Vienna of the patient (Table 8.34) is shown below.

Table 8.33 DNA ploidy status vs histological classification of site

Histological classification	IM	IND	LGD	HGD	Cancer
Number of biopsies	128	6	20	24	1
% aneuploidy	16	83	45	54	100

Table 8.34 DNA ploidy vs maximal degree of dysplasia

Histological classification	IM	IND	LGD	HGD	Cancer
Diploid sites	50	11	17	52	1
Aneuploid sites	9	2	5	28	4
% aneuploidy	15	15	23	35	80

When analysis was undertaken on unpaired data the AUC was again similar between the two boxes, see figure 8.68. For the red box - 125 spectra (59 diploid, 66 aneuploid) were acquired at 36 sites from 17 patients which gave AUC=0.79, sensitivity 90% and specificity 71%. For the old box - 130 spectra (62 diploid, 68 aneuploid) were acquired at 35 sites from 17 patients which gave AUC=0.82, sensitivity 90% and specificity 77%.

Figure 8.68 ROC curve aneuploid vs diploid using Red box (left) and Old Box (right)

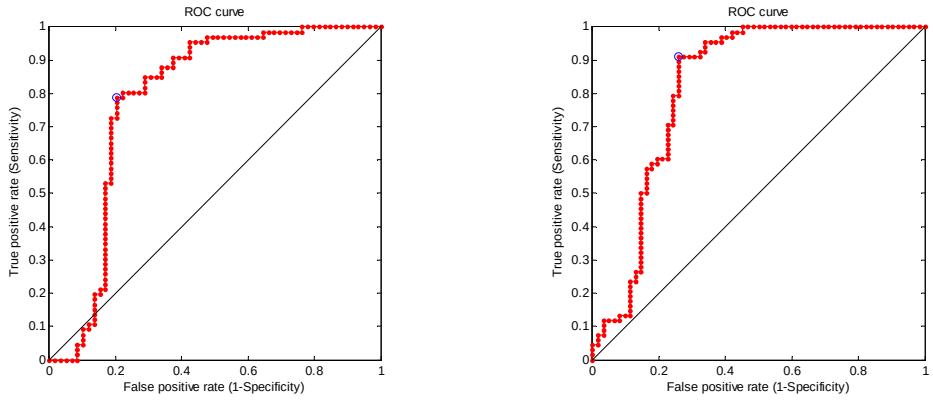

HGD or aneuploid (high risk group) vs non-dysplastic diploid (low risk group)

We then assessed the two boxes for the differentiation of high risk sites (HGD or aneuploidy) and low risk sites (non dysplastic BO and diploid), see figure 8.69. For the red box - 309 spectra (144 low risk, 166 high risk) were acquired at 79 sites from 34 patients which gave AUC=0.77, sensitivity 90% and specificity 80%. For the old box - 289 spectra (93 low risk, 196 high risk) were acquired at 76 sites from 30 patients which gave AUC=0.80, sensitivity 90% and specificity 74%.

Figure 8.69 ROC curve high risk vs low risk using Red box (left) and Old Box (right)

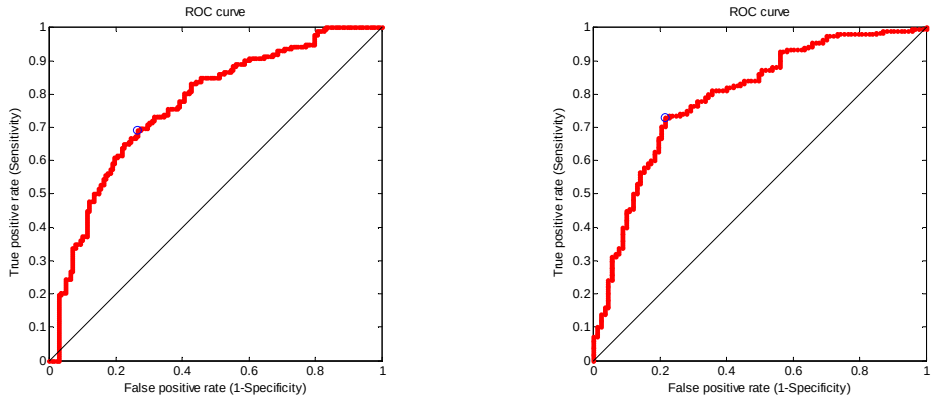

8.6.4 Discussion

These data demonstrate ESS is accurate for the detection of BO and associated HGD and molecular abnormalities *in vivo*, whichever spectrometer is used. Importantly, the red box is compatible with software from newer generation laptop computers, whereas the old box can only be run on a Windows 95 Compaq laptop, which limits its wider application in multicentre studies. The sensitivity of 90% with specificity of 71% for DNA ploidy abnormalities make ESS a useful adjunct to random biopsy, by allowing targeting of abnormal mucosa at high risk, for subsequent ICDA. This strategy could cut the number of biopsies required in Barrett's surveillance programmes, allow quantification of future cancer risk in vivo and possibly target areas of interest for ablative therapy.

There are some limitations to this study. Although the number of sites evaluated were very similar between the two groups the data analysis was unmatched, which does not allow for a true comparison of each box. The reason for this was that some spectra were not acquired correctly, possibly due to probe angle or pressure changes, and this was manifested as spectra that gave spurious results when ratioed. The histology was reviewed by two specialist GI pathologists but, despite this, there may be human error in the histological classification, inaccuracy which is then hardwired into subsequent statistical analysis.

The percentage of DNA ploidy abnormalities in the LGD and NDBO groups is probably higher than one might expect for a general surveillance population, although this may be explained by the high percentage of patients with dysplasia elsewhere, as only 50 sites were diploid with no dysplasia elsewhere. One would expect a surveillance population with NDBO to have a much lower percentage of aneuploid sites. The percentage of diploid HGD sites was however higher than expected, and is consistent with our previous study on RLFs that showed micro-dissected HGD was diploid 46% of the time (see section 7.4). It is possible that these patients had 'out of cycle dysplasia', or alternatively small areas of HGD that were not quantifiable by whole biopsy ICDA. Notably the AUC for HGD was lower than the previously published series, [Lovat et al., 2006] and the subset of diploid patients may partly explain this.

In conclusion these data demonstrate that DNA ploidy and dysplasia can be accurately quantified by ESS *in vivo* using either a red enhanced spectrometer or the standard old box, when analysis is undertaken retrospectively. Our next step was to test these algorithms in a prospective study.

8.7 Barrett's Oesophagus surveillance with Optical biopsy using elastic scattering Spectroscopy to Target high risk lesions (BOOST)

8.7.1 Introduction

For ESS to be useful in clinical practice real time diagnosis at endoscopy is necessary. This may allow for accurate prediction of future cancer risk during surveillance endoscopy, potentially without the need for random biopsy. ESS may also be used to target biopsies to areas of dysplasia, aneuploidy or other molecular abnormalities, with the potential to guide subsequent treatment. In order to test the validity of ESS as an *in vivo* diagnostic tool, a pilot study was designed with the aim of comparing ESS guided biopsy with random four quadrant biopsy for the detection of dysplasia.

8.7.2 Methods

Model Generation: The R engine

It would be optimal to use the entire historical ESS data set to calculate the algorithm as the larger the training set the more accurate the algorithm becomes. Given the potential differences between the spectrometers used to collect data however, it was decided to assess the accuracy of a classification algorithm using a novel, albeit smaller, single unit data set. We therefore analysed the dataset used for the previously published paper (GUT dataset)[Lovat et al., 2006]. Since multiple spectra were taken per site, all spectra from each site were kept together, in either the training set or the testing set, to prevent any bias being introduced through non-independence of data.

Using the algorithm created with linear discriminant analysis, the canonical score for each test spectrum was determined. This allows the spectrum to be assigned into one group or the other. The group into which the spectrum is assigned is determined by the '*cut-off*' canonical score. This score can be adjusted to favour the sensitivity or specificity

or to optimize overall accuracy. The canonical scores calculated for this study, with the corresponding risk of that site having a positive diagnosis of HGD, are shown in Figure 8.70. In order to calculate the positive predictive value for each site an estimation of the relative frequencies of HGD in any given surveillance population was necessary based on the published literature. The frequency of detecting high-grade dysplasia (HGD) at initial (index) diagnosis of BO (i.e. prevalence of HGD within Barrett's) was estimated at approximately 2%, ranging from 1-3% depending upon whether Barrett's is short segment (< 3 cm) or long segment.[Sharma et al., 2006b] In order to interpret these scores *in vivo* a colour was assigned to quantify risk category as shown below in the far right column and figure 8.71.

The new box was used for this study, so only the risk of high grade dysplasia was determined. Ideally the combined risk of DNA ploidy and HGD would have been assessed prospectively, but the old box was not compatible with the laptop with the R engine installed, and the complete red box data set was not available at the time of commencing the study.

Figure 8.70 Positive predictive values dependent on canonical score

Canonical Score	PPV HGD	Colour Assigned on ESS Maps
>3.26	57.6	Dark Red
2.52 -3.25	41.6	Light red
1.30 -2.51	18.5	Pink
-0.25 -1.29	5.0	Light Blue
-1.46 - -0.24	3.6	Dark Blue

Figure 8.71 Colour for each grade of dysplasia assigned by R engine

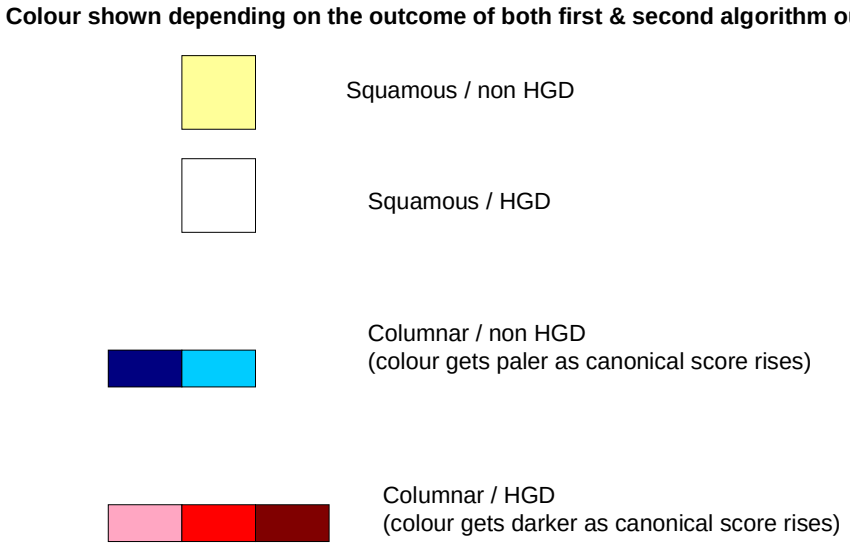

ESS and biopsy protocol

During routine endoscopy the Barrett's segment was mapped using Prague C&M criteria. An optical map of the Barrett's segment was the generated by taking serial optical measurements every 1 cm in four quadrants. Examples of 1cm mapping from Barrett's segments are shown in Figure 8.72. The tip of the optical probe was placed in gentle contact with the tissue and the lamp and spectrometer were triggered via a keyboard or foot-pedal. A median of 4 spectra were taken from each site (mean 3.3).

Areas of high risk (red) were then remapped using ESS and if there was continuing colour map change consistent with dysplasia then a matched targeted large capacity biopsy was taken for histology (see figure 8.73). Care was taken to ensure that the biopsy was taken from the same site as the optical measurement.

Figure 8.72 Screen shot from ESS in vivo programme

This demonstrates columnar epithelium C2M4, with squamous epithelium (yellow) more proximally. The red areas in this scan were biopsied. Histology showed no dysplasia but aneuploidy was demonstrated.

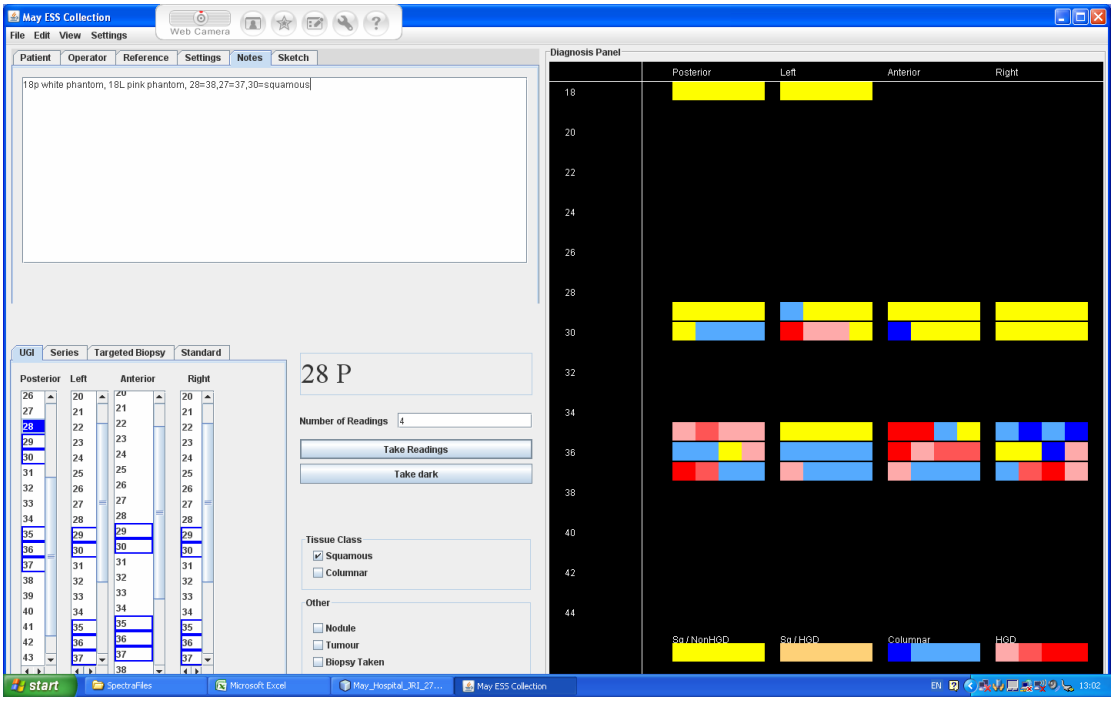

Figure 8.73 ESS in vivo analysis

The area at 33cm from the incisors, posterior wall (33P) is suspicious for HGD but on remapping of the same site no high risk spectra are identified. No dysplasia was identified on random biopsies

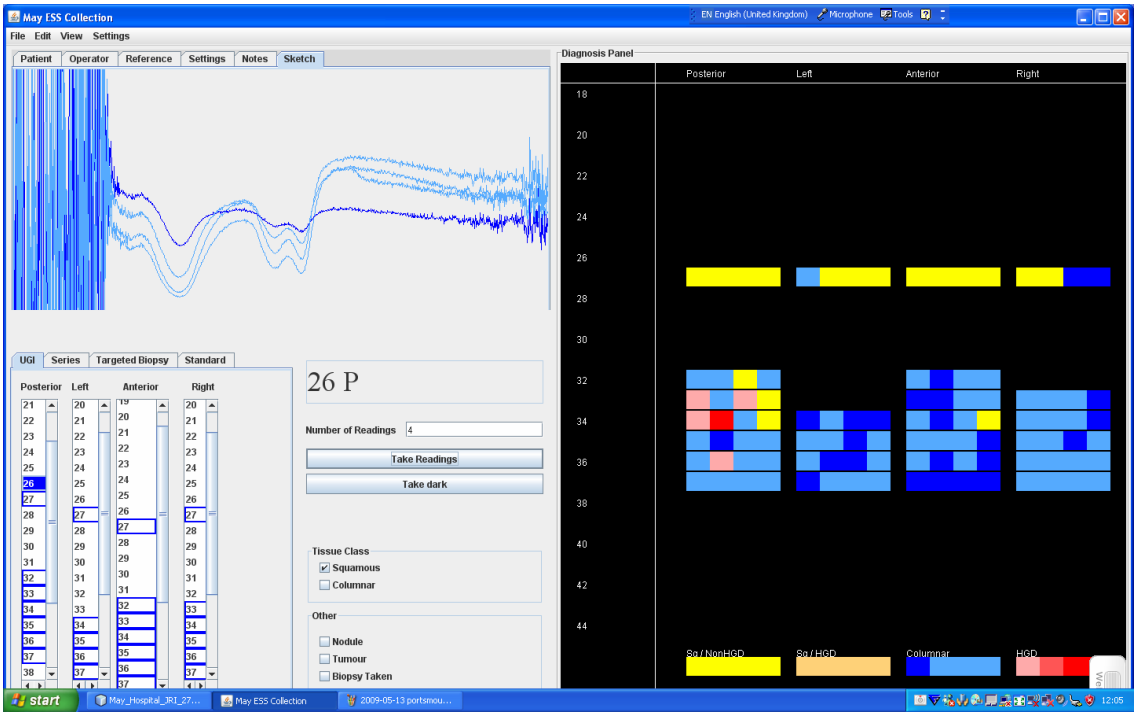

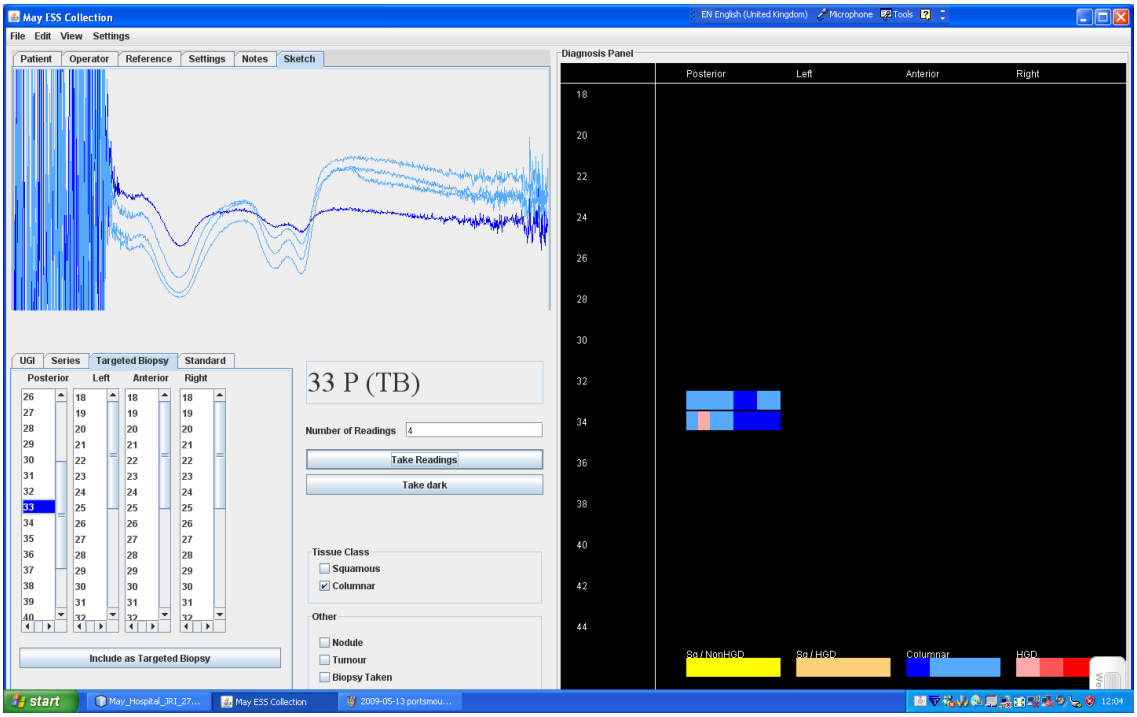

8.7.3 Results

Per patient analysis

26 patients were recruited to this pilot study over a 6 month period and results are summarised in Table 8.35.

Table 8.35 Summary of data from prospective BOOST study

Study ID	Age	Gender	Length of BO	Histology on ESS sites	Histology on random biopsy	Number of ESS biopsy taken	Number of random biopsy	% reduction in biopsy sampling
1	67	M	C1M3	IM	IM	1	8	88
2	76	M	C7M9	IM	IND	5	17	71
3	56	M	C1M2	IM	IM	2	7	71
4	61	M	C1M4	IM	IM	6	12	50
5	52	M	C0M1	IM	IM	3	4	25
6	57	M	C6M6	IM	IM	1	16	94
7	51	F	C4M5	IM	IND	4	13	69
8	66	M	C5M5	IM	IM	3	10	70
9	58	M	C6M7	IM	IM	3	15	80
10	55	M	C4M4	None targeted	IM	0	12	100
11	56	M	C3M4	None targeted	IM	0	12	100
12	62	M	C1M2	None targeted	IM	0	4	100
13	60	F	C1M4	IM	IM	5	8	38
14	65	M	C0M1	None targeted	IM	0	4	100
15	49	M	C1M4	None targeted	IM	0	8	100
16	72	M	C0M2	None targeted	IM	0	4	100
17	61	M	C11M12	IM	IM	2	27	93
18	61	M	C15M15	None targeted	IM	0	37	100
19	63	M	C6M6	None targeted	IM	0	10	100
20	72	M	C2M4	IM	IM	4	6	33
21	69	M	C7M17	None targeted	LGD	0	25	100
22	59	F	C3M4	IND	IND	7	10	33
23	78	M	C6M8	None targeted	LGD	0	15	100
24	60	M	C3M4	None targeted	IM	0	12	100
25	63	M	C1M2	None targeted	IM	0	9	100
26	34	M	C3M4	IM	IM	2	7	71

Twenty five patients were Caucasian and one patient of Asian origin. The median maximal length of BO was 4cm (IQR 1-17cm) and mean age was 61 years (IQR 34-78 years). Of these 26 patients 21 had IM but no dysplasia, 3 were Indefinite for dysplasia and 2 had LGD. One patient (no 21) had submucosal adenocarcinoma in a visible nodule at the GOJ, but EMR was undertaken to this area before ESS measurements were taken.

ESS identified 1 patient with IND which was also noted from random biopsies at the same level. A further 4 patients with histological abnormalities were not identified by ESS. Of the 21 patients with no abnormality on random biopsy, 10/21 had no abnormality on ESS and no targeted biopsies. 11 patients had targeted biopsies from high risk sites, but these sites had no dysplasia on matched biopsies. None of these patients had dysplasia elsewhere. This equated to a 65% mean reduction of biopsies taken per patient in this group.

Per site analysis

A total of 48 targeted biopsies were taken from positive sites on ESS. 47 were non-dysplastic BO displaying IM, and one site displayed changes indefinite for dysplasia. An additional 305 random four quadrant biopsies were taken. 6/305 were abnormal – 4 indefinite for dysplasia and 2 low grade dysplasia. Using a two tailed Fisher's exact test there was no significant difference in the diagnostic yield of random biopsy versus ESS. (p=1) The mean number of biopsies for ESS was 1.9 vs. 12.2 for random biopsy sampling and the mean reduction in biopsies taken per patient was 81%.

Post hoc DNA ploidy analysis

The algorithm used for this model did not include DNA ploidy and therefore a prospective analysis was not undertaken. Retrospective review of DNA ploidy analysis was available on 48 biopsy sites from 15 patients. Of these sites 10 were aneuploid, 1 tetraploid and 37 were diploid. A total of 212 spectra were analysed.

On a per site analysis AUC = 0.92, sensitivity was 91% and specificity 71% with 15 principal components (see figure 8.74).

Figure 8.74 ROC curve of DNA ploidy abnormalities *in vivo*

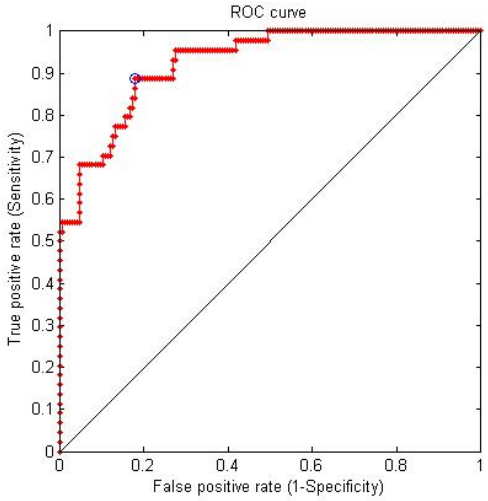

8.7.4 Discussion

This is the first prospective *in vivo* study of ESS to detect high risk sites in Barrett's oesophagus. We have demonstrated that taking real time in vivo ESS measurements is achievable, with a significant reduction in the number of biopsies taken versus random four quadrant biopsy sampling. The study was however limited as there were no areas of HGD that were interrogated by ESS, and therefore the sensitivity or PPV for HGD could not be assessed.

One patient had IMC in a nodule that was not targeted and LGD in flat BO 1 cm above this. The LGD was not picked up by ESS measurements. This led to cessation of the pilot study to further analyse our data and assess why this was missed. LGD was not considered abnormal in the algorithm generation due to the inherent difficulties of consensus histological diagnosis and variability of cancer risk. We evaluated DNA ploidy on biopsies taken at this level, and found these to be diploid. On a previous endoscopy he was found to be tetraploid at a site of SIM, 2cm proximal to the level of LGD. It remains to be seen if the Barrett's segment proximal to the GOJ tumour develops dysplasia. From

the NIBR study we would estimate that these sites (LGD/diploid and IM/tetraploid) have similar risk of progression, but these results were not available at the start of this study.

Although we did not set out to prospectively quantify DNA ploidy, as our algorithm did not work in a similar sized subset of patient (see section 8.4), 25% of patients with targeted biopsies had aneuploidy. In a post hoc analysis, DNA ploidy abnormalities could be differentiated from diploid areas with a sensitivity of 91% and specificity of 71%. So although none of these sites harboured dysplasia, our algorithm could accurately differentiate DNA ploidy in these spectrally abnormal sites. A combined algorithm of DNA ploidy and all grades of dysplasia should therefore increase the negative predictive value of the test whilst maintaining a high yield. A future study to test the red box algorithm (which had not been generated at the commencement of this study) to test the performance of these 2 parameters in an extension to this pilot would be valuable.

8.8 Investigation of field carcinogenesis by ESS

8.8.1 Introduction

Field carcinogenesis, the phenomenon that the proposition that the genetic/environmental milieu that results in neoplasia in one region should be detectable throughout the mucosa. [Kopelovich et al., 1999] As was previously described the Backman group have pioneered research into this field by using LEBS and 4D-ELF to quantify colon and pancreatic cancer prevalence from histologically normal sites away from the abnormal mucosa.[Roy et al., 2009] These sites are not spectroscopically normal by their criteria, although a clear explanation of the physical correlation with the tissue is yet to be presented. Aneuploidy occurs in 75% of colorectal cancers and has a propensity for tumours arising in the left side of the colon. [Lanza et al., 1998] ESS can detect DNA ploidy abnormalities *in vivo*, as we have demonstrated, and it is possible that these histologically normal sites harbour genomic instability that is acting as a bias in the spectroscopic interpretation of the mucosa. In order to test the field effect in BO an experiment was designed to assess the spectral signature of tissue that is normal by both ICDA and histopathology.

8.8.2 Methods

This was a retrospective case control study and data was pooled from the prospective red box study for analysis. This was felt to be the most accurate for strict co-registration of sites, had a large enough pool of normal controls and allowed use of the red enhanced spectrometer. Cases were defined as a patient with an area of non-dysplastic BO that was diploid by ICDA, with either HGD or aneuploidy at one or more biopsy sites throughout the remaining Barrett's segment. Controls were patients with an area of non-dysplastic diploid BO, without any evidence of dysplasia or DNA ploidy abnormalities elsewhere.

8.8.3 Results

A total of 16 BO patients were identified, 11 cases (77% male, mean age 67 years {range = 40-83 years}) and 5 controls (75% male, mean age 66 years {range = 37-80 years}). This equated to 44 spectra that were normal with no abnormality elsewhere, and 84 that were normal with dysplasia/aneuploidy elsewhere. LDA + PCA was undertaken with AUC = 0.85 using 15 principle components, sensitivity = 87% and specificity = 71% (see figure 8.75).

Figure 8.75 ROC curve demonstrating a field effect in BO, independent of DNA ploidy

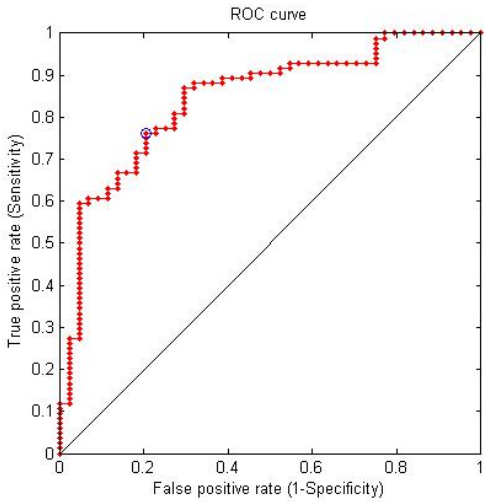

8.8.4 Discussion

These data demonstrate that, in this small group of patients, a field effect can be demonstrated in Barrett's metaplasia by ESS. This is independent of the DNA content of the tissue as each site was diploid on ICDA. This is the first time that ESS has been shown to measure a field effect in Barrett's oesophagus. Work published in abstract form has also demonstrated the potential for field effect measurement by ESS in 11 colon cancer patients [Rodriguez et al., 2010], although DNA ploidy status was not calculated in that study. Emerging work from our centre has also shown ESS can measure a field effect in pancreatic cancer. These studies demonstrate the potential for ESS to be used as an optical biomarker in the GI tract, although further large prospective cohort studies are necessary.

There are however limitations to this study. As this is a jack-knife analysis on a small training dataset it may be subject to overfitting of data, and a larger test set would be required to evaluate whether this is a true effect. Although all biopsy sites were normal they were selected from a database rather than anatomically. A better study may have been to interrogate the mucosa at incremental distances away from the area of abnormality in the Barrett's segment. This is technically difficult to do though, as the distribution of dysplasia is patchy and often not visible endoscopically, and aneuploidy can display a field effect of its own. Taking optical biopsy from squamous mucosa at sites proximal to the Barrett's mucosa may be a solution, as this is easily identifiable by the endoscopist and rarely displays aneuploidy.

The question of the physical correlation of these ESS measurements with the biological properties of the tissue remains. Diploid cell populations may still harbour changes in chromatin structure and organisation that are a measure of chromosomal instability in cancer cell populations, as was demonstrated in chapter 6 by nuclear texture analysis. Another potential early marker of carcinogenesis that may be measured by spectroscopy is methylation, and work from the Backman group in this area is ongoing. It is hoped that these future studies will not only allow an explanation of the physical correlation of

spectroscopic data, but could also contribute to our understanding of the evolution of neoplasia at a cellular level.

8.9 Summary

The work presented here has demonstrated that ESS informs on the genomic instability of Barrett's mucosa, when analysis was undertaken retrospectively. Furthermore in a prospective *in vivo* pilot study, ESS guided biopsy led to a reduction in biopsy requirements and, on post hoc analysis, accurate detection of DNA ploidy. Finally in a retrospective analysis of normal tissue, both by tissue morphology and DNA content, there was a significant difference in ESS spectra when analysing low risk patients (no dysplasia or aneuploidy elsewhere) vs higher-risk patients (aneuploidy or dysplastic elsewhere). This is the first time the field effect has been demonstrated in Barrett's oesophagus.

These findings give an insight to the potential of ESS as a optical biomarker in Barrett's oesophagus, allowing targeting of areas of genomic instability that are at risk of progression and allowing better risk stratification for patients. Furthermore it should be possible to use ESS to assess residual Barrett's mucosa for DNA ploidy abnormalities in normal tissue after ablative therapy, an important marker of relapse that was demonstrated post PDT in Chapter 5.7. The assessment of DNA ploidy by ESS in real time could allow for guided treatment and reversal of these abnormalities by EMR or RFA. Finally the field effect, the theory that future cancer risk may be assessed by an ESS point measurement in the mucosa that is distant from the abnormality, warrants further study. Could an ESS measurement taken from the buccal mucosa inform on risk of dysplasia? A non-invasive tool that could accurately predict risk of neoplastic progression would have a massive impact for population-based screening and could potentially facilitate the ultimate goal - reduction in oesophageal cancer mortality.

Chapter 9
Clinical trials of ablative therapies

Chapter 9 Clinical trials of ablative therapies

9.1 Randomised Controlled Trial of ALA PDT vs. Photofrin PDT

9.1.1 Introduction

PDT is perhaps the best-studied minimally invasive method for mucosal ablation in BO. It is a non-thermal, photochemical reaction which occurs when light activates a photosensitiser in the presence of oxygen.[Bown and Lovat, 2000] Photofrin is the only currently licensed photosensitiser for PDT of HGD in BO, and has been reported to have a success rate of 50-80% at up to 5 years follow up [Overholt et al., 2005;Overholt et al., 1999;Overholt et al., 2007]. Photofrin-PDT is, however, associated with a prolonged light sensitivity of between 1-3 months and an oesophageal stricture rate of around a third [Overholt et al., 1999].

Our group has particularly been studying ALA-PDT for the last 10 years.[Mackenzie et al., 2007a;Mackenzie et al., 2009] This drug does not appear to have the aforementioned complications of Photofrin as its duration of action is shorter and absorption is limited to the mucosa [Loh et al., 1996]. This should lead to low stricture rates and light sensitivity for only 36 hours. ALA-PDT has been shown to have high eradication rates for HGD of 75-89%.[Pech et al., 2005;Mackenzie et al., 2007a] Associated side effects include hypotension, pleural effusions, transient transaminitis and buried Barrett's glands under regenerated squamous epithelium.[Overholt et al., 2007] No comparative studies of these two distinct photosensitisers have been described.

9.1.2 Aims

The original aims of this single-centre RCT were:

i) To establish which drug has a better side effect profile.

ii) To investigate novel measures of efficacy.

Following an interim analysis in 2007 and emerging data from several studies on ALA PDT, a substantial amendment was submitted to the regional ethics committee in January 2008 to include a new study aim

iii) To determine whether PDT using ALA is more efficacious than Photofrin for the complete ablation of high grade dysplasia in Barrett's oesophagus.

9.1.3 Methods

Study design

The primary end points of this study were

- Complete ablation of HGD at 1 year post PDT
- Relapse to HGD after 2 treatments with photofrin or 3 with ALA-PDT
- Development of invasive cancer at any time point
- Development of oesophageal stricture
- Development of cutaneous photosensitivity reactions

Secondary End Points were

- Ability of DNA ploidy to predict success or failure of ALA-PDT
- Comparison of all other side effects of the medications
- Presence of subsquamous intestinal metaplasia
- Assessment of patient Quality of life before, during and after therapy

Inclusion criteria

All patients referred for endoscopic therapy for HGD had a screening endoscopy with EUS prior to enrolment into the study. If there were any visible nodules at enrolment then these were removed by EMR using a MBM kit (Duette, Cook UK). A second endoscopy was then undertaken on all patients 6-8 weeks later to confirm that the remaining Barrett's mucosa was flat and that HGD was present without invasive cancer. If there was evidence of intramucosal cancer or deeper invasion the patient was excluded from the study. Once HGD was confirmed on two occasions by two independent specialist GI pathologists, patients were randomised. The length of the Barrett's section was

determined according to the Prague classification system.[Sharma et al., 2006c] Inclusion and exclusion criteria are shown in Appendix F.

Statistical Considerations

Efficacy

In order to demonstrate a 30% difference in efficacy between the 2 treatment protocols (presuming 80% for ALA and 50% for Photofrin), at a 1-sided significance level of $p<0.05$ and a power of 80%, 33 patients are required in each group allowing for a 10% drop out rate.

Side effect profile

In order to show a 20% difference in development of oesophageal strictures (presuming 1% for ALA and 21% for Photofrin) and cutaneous photosensitivity reactions (5% for ALA and 25% for Photofrin) between the 2 treatment protocols, at a 1-sided significance level of $p<0.05$ and a power of 80%, 33 patients are required in each group allowing for a 10% drop out rate. All analysis was performed using the SPSS® for Windows statistical package (SPSS Inc., Version 14.0, Chicago, Il, U.S.A). The one tailed p value of <0.05 was considered significant.

Randomisation

Patients were stratified according to two criteria – the length of Barrett's segment and the extent of HGD. The first stratification was to long segment (>6cm) or short segment (< or = 6cm) Barrett's oesophagus. The reason for stratifying according to length was due to the size of the treatment balloon, which is 5 or 7cm. Patients who have BO >6cm would therefore require two treatments, increasing the treatment time and risk of strictures due to potential overlap. Patients were then stratified according to the extent of HGD, i.e. single or multiple levels of HGD on 2cm four quadrant biopsy.

Following double stratification, patients were randomised to one of the 2 following treatment schedules:

PDT with oral ALA administration (study arm)

PDT with intravenous photofrin administration (standard treatment control)

PDT Parameters

ALA dosimetry

ALA was kindly supplied by DUSA Pharmaceuticals, New York, USA. Patients were admitted to hospital and given intravenous fluids 8 hours prior to photosensitisation, to minimize the risk of hypotensive episodes as previously described.[Mackenzie et al., 2007a] Patients were prescribed 60mg/kg ALA in 3 divided doses, to be taken 5, 4 and 3 hours prior to treatment. An antiemetic (intravenous ondansetron 4mg) was given 30 minutes before the first dose of ALA was taken orally. Initially all endoscopy was performed under conscious sedation (see figure 9.76) but it was noted that patients were requiring large doses of midazolam and fentanyl for pain, particularly those requiring treatment for two segments which takes 75 minutes. Consequently general anaesthesia was used for patients treated with ALA-PDT after June 2006.

Figure 9.76 Picture of a patient receiving ALA-PDT

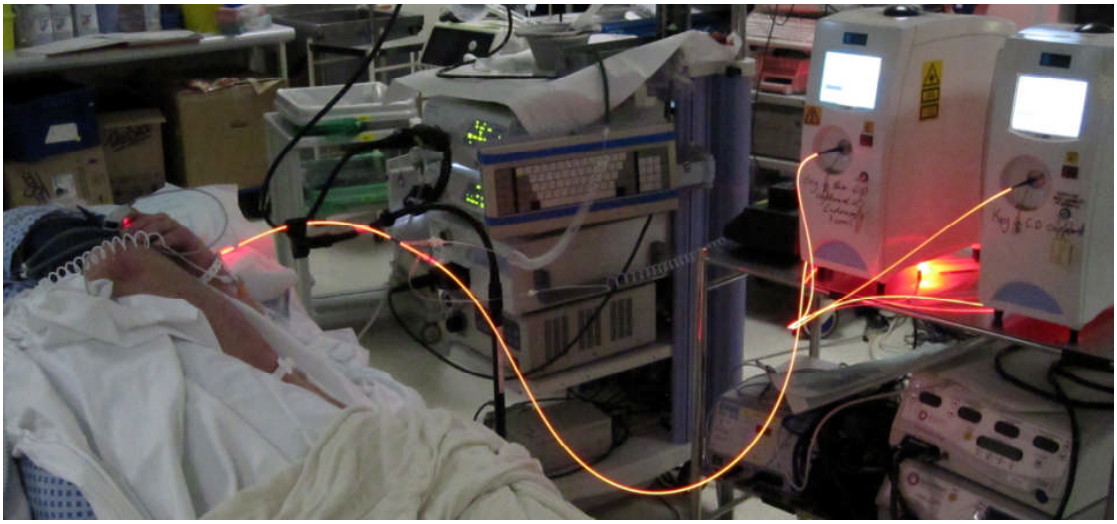

Photofrin dosimetry

Patients were treated according to the summary of product characteristics supplied by Axcan Pharma, and the papers published in this area [Panjehpour and Overholt, 2006;Overholt et al., 2005]. Photofrin was administered 3 days prior to treatment by intravenous injection into a large vein in ante-cubital fossa, at a dose of 2mg/kg. Light precautions were followed immediately after administration and a light meter was

provided with a demonstration of its use. Endoscopy, at 72 hours after drug administration, was performed under conscious sedation with midazolam 2-10mg and fentanyl 50-150μg.

Light Delivery

Following measurement of the proximal and distal margins of the Barrett's segment, a guide wire was placed into the stomach and either an 18mm transparent plastic balloon (for ALA, supplied by DUSA) or a bolster device (for photofrin) was inserted into the oesophagus over the wire to the marked distance (see figure 9.77). The guide wire was removed and a 5 or 7cm cylindrical diffuser fibre (Pioneer Optics, USA) placed in the centre of the balloon or bolster. Up to 7cm of Barrett's could be treated by a single diffuser fibre; longer segments were treated with the delivery device positioned at two levels. The maximum length of BO with HGD that may be treated at one session was 13cm. If two levels were treated the distal segment was treated first, and then the bolster or deflated balloon was pulled back by 5 or 7 cm to treat the second segment. Care was taken to ensure that there was no overlap when using photofrin-PDT given the high risk of stricture formation.

Figure 9.77 Different balloons used for PDT

Left Diffuser fibre with aiming beam lit and inserted into an inflated DUSA balloon (ALA PDT), right Silicone bolster (photofrin PDT) made by Dr C A Mosse at UCL

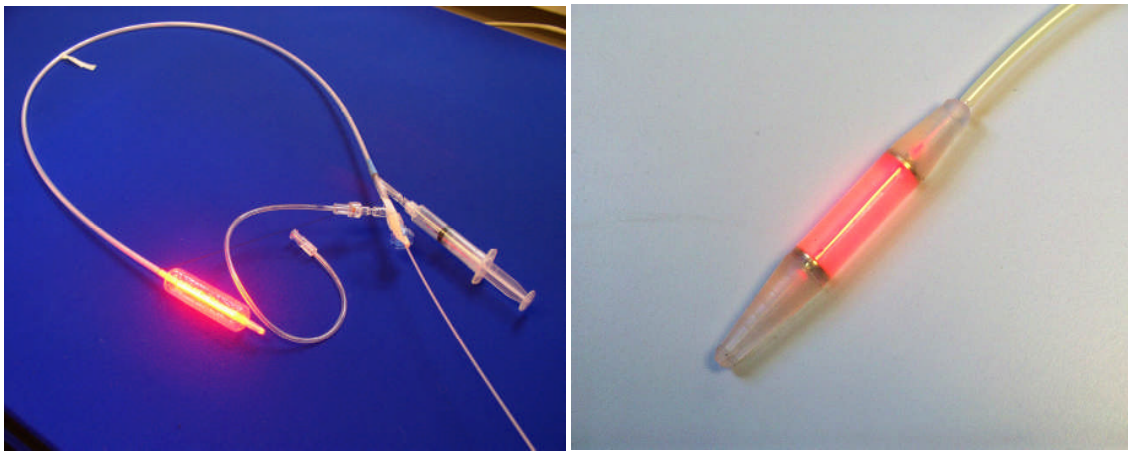

For ALA-PDT, red light (635nm) was delivered by combining the light from three Diomed Diode Lasers (Cambridge, UK) into a single optical fibre with an estimated light dose of 1100J/cm (up to 200J/cm^2 in an 18mm diameter balloon), at a fluence rate of 565mW/cm of diffuser fibre (100mW/cm^2).[Mackenzie et al., 2009] Allowing for 10% light loss this approximated to 1000J/cm. For photofrin-PDT a light dose of 130J/cm at 630nm was used with a fluence rate of 250mW/cm.

Follow up

The follow up protocol after therapy was an endoscopy with four-quadrant biopsies every 2cm from the treated oesophagus at 6 weeks, 4 and 12 months in the first year then at 18, 24, 36, 48 and 60 months thereafter. Adverse event data was collected up to 4 months after treatment. Successful treatment was defined as three endoscopies clear of HGD or Cancer after 1 year (CR-HGD). If a patient had residual or recurrent HGD post treatment then they were retreated. The maximum number of treatments with ALA was 3, with doses more than 8 weeks apart (to allow for taking of biopsies at follow-up endoscopies). A maximum of 2 treatments were allowed with Photofrin due to risk of oesophageal stricture formation (increases from 22% to 50% from 2 to 3 treatments [Overholt et al., 2005]) and doses were at least 3 months apart to minimise risk of cumulative skin photosensitivity. Patients with areas of nodular disease recurrence underwent repeat staging with EMR and, if residual HGD remained, repeat treatment with PDT.

Quality of Life data

There are no validated Quality of Life (QoL) questionnaires for HGD in BO. The major side effects that we expected patients to suffer were those associated with underlying GORD, anxiety and treatment side effects. The selection of validated questionnaires was made after discussion and in collaboration with Dr Jane Blazeby (Bristol University) who designed the European Organization for Research and Treatment of Cancer (EORTC) oesophageal QoL instrument.

The 6 item short-form State-Trait Anxiety was used to assess anxiety associated with surveillance. The short form is comparable to the full inventory, yet has the advantage of being brief. Evidence shows that it is sensitive to fluctuations in anxiety state. EORTC

Oes 18 was used for symptoms specifically related to the oesophagus, and the module is described in detail by the EORTC Quality of Life department (http://groups.eortc.be/qol/documentation_manuals.htm). The Quality of life in reflux and dyspepsia (QOLRAD) questionnaire has 25 items that assess emotional issues, sleep, eating problems, physical and social vitality related to reflux disease. Full reliability and validation data are available and the instrument is sensitive to changes over time. Patients were asked to complete quality of life questionnaires at enrolment and then 3 days, 3 weeks, 6 weeks, 4 and 12 months after treatment. It was important that these questionnaires were self completed to reduce bias.

9.1.4 Study Governance

The study was sponsored by UCL in line with the European Union requirements for good clinical practice (EU-GCP). Ethical approval was received from Berkshire Research Ethics Committee (REC Number 05/Q1602/193) and the study was approved by the Medicine and Healthcare Regulatory Authority (MHRA) as the competent authority for the UK (Eudract Number 2005-005528-15). This study was registered with International Standard Randomised Controlled Trial Number (ISRCTN) Register (ISRCTN 16444200).

9.1.5 Results

Patient Recruitment

Of 128 patients that were screened for eligibility from 2006-2009, 79 patients were recruited to the study and from these 64 underwent randomisation (see figure 9.78). There were no significant differences in age, gender, race, length of BO segment or extent of dysplasia between the two treatment groups (see Table 9.36). The study population for the primary intention-to-treat (ITT) analysis included all 64 patients who underwent randomisation. In this analysis, patients who were lost to follow-up before the 12 month endoscopy were regarded as having had a failure of treatment for the primary outcome. A secondary per-protocol analysis was performed in patients who completed 4 months follow up or failed after 3 treatments with ALA or 2 with Photofrin.

Figure 9.78 Screening, enrolment and randomisation

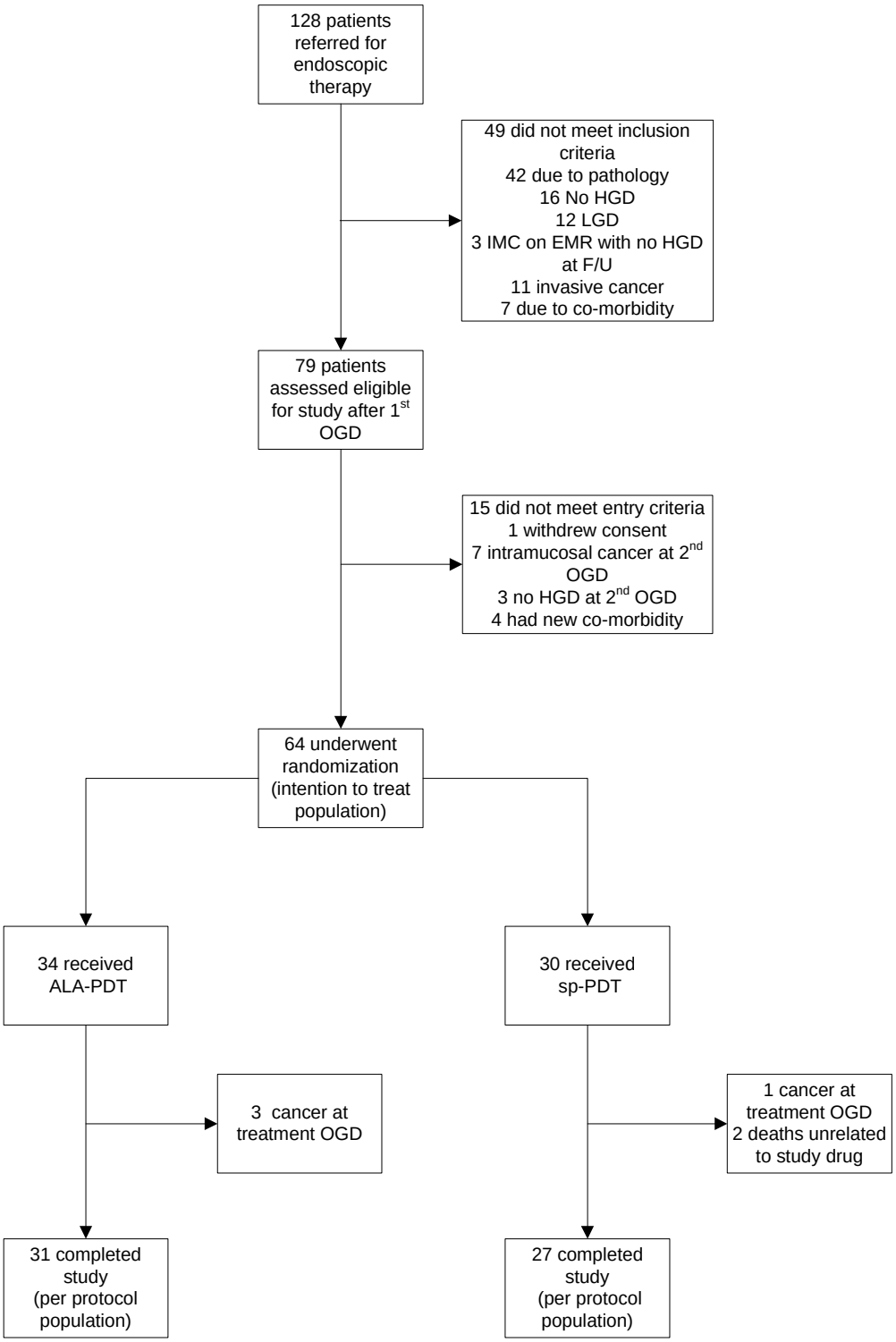

Table 9.36 Patient demographics

Characteristic	ALA PDT *n= 34 (%)*	Photofrin PDT *n= 30 (%)*	p-value
Gender Male Female	 24 (71) 10 (29)	 26 (87) 4 (13)	 P=0.14*
Age (mean ± SD)	 68.3 ± 9.0	 67.5 ± 8.8	 P=0.72**
Race or ethnic group Caucasian Afro-Caribbean	 33 (97) 1 (3)	 30 (100)	 P=1*
Length BO segment Long (>7cm) Short (</=6cm)	 16 (47) 18 (53)	 14 (47) 16 (53)	 P=1*
Length BO short group (mean ± SD)	4.3 ± 1.4	3.7 ± 1.2	P=0.21**
Length BO long group (mean ± SD)	9.6 ± 2.0	9.6 ± 2.3	P=0.92**
Multifocal dysplasia no. (%)	20 (59)	20 (67)	P=0.61*

* Fishers exact test

** student t-test

Efficacy data

Of the 64 patients randomised, 34 were photosensitised with ALA and 30 with Photofrin. Using ITT analysis CR-HGD was 17/34 (50%) in the ALA group and 12/30 (40%) in the Photofrin group (Fishers exact test = ns). A Kaplan Meier of probability of survival without HGD is shown in figure 9.79. Using Log-rank analysis there was no significant difference in disease free survival between the two groups $\chi^2 = 0.29$, p=0.59. Six patients have been withdrawn before their first follow up biopsy, after receiving initial treatment. Four patients (3 ALA, 1 Photofrin) had nodules discovered on the day of treatment and biopsies subsequently confirmed invasive cancer. Two patients have died before the 6 week follow up endoscopy; one secondary to *clostridium difficile* during the hospital admission for treatment; one due to critical aortic stenosis and arrhythmia, which occurred three weeks after treatment and was unrelated to PDT.

Figure 9.79 ITT Kaplan Meier analysis all patients

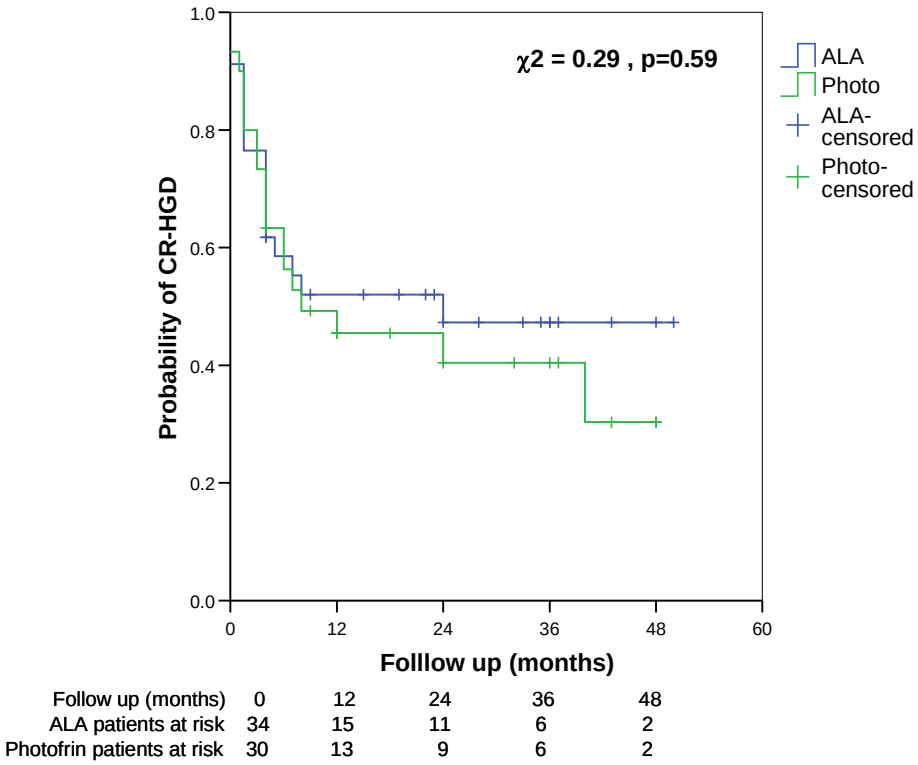

Secondary analysis was undertaken on a per-protocol basis on the remaining 58 patients who reached their 4 month follow up. Remission rates are 20/31 (65%) in the ALA group and 12/27 (44%) in the Photofrin group (Fishers Exact test, p = 0.102). A Kaplan Meier of probability of survival without HGD is shown in figure 9.80. Using Log-rank analysis there was no significant difference in disease free survival between the two groups χ^2 = 1.25, p=0.26. After 4 months follow up 3 patients have since withdrawn from study, all 3 had received ALA and all were clear of HGD at 4/12. One patient withdrew after developing a stricture that required several dilatations (ALA). A second patient committed suicide. A third patient had a stroke and was too frail for further follow up.

Figure 9.80 Per protocol Kaplan Meier analysis

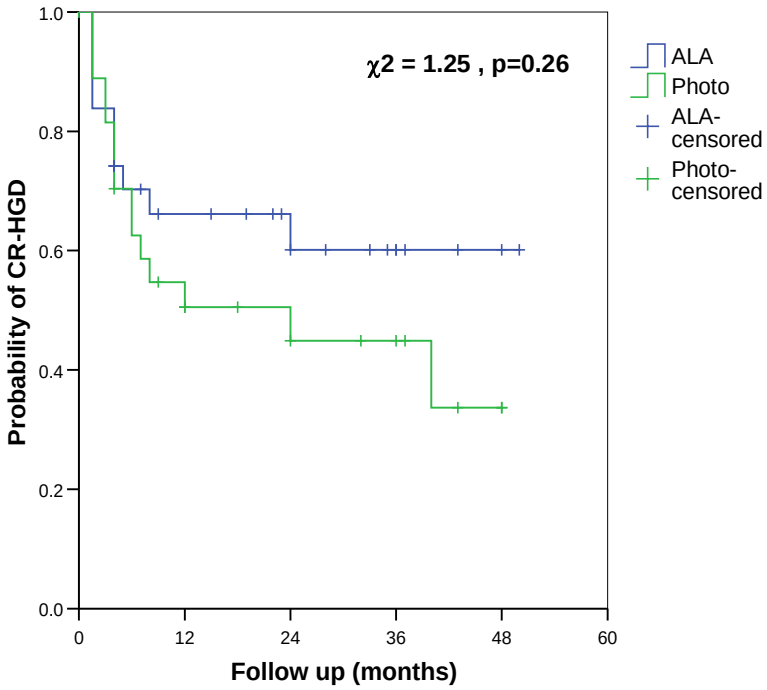

Follow up (months)	0	12	24	36	48
ALA patients at risk	31	15	11	6	2
Photofrin patients at risk	27	13	9	6	2

Progression to cancer

The overall cancer incidence of the 79 patients that were assessed eligible for the study after first endoscopy confirmed HGD was 20% (16/79). The majority of these were prevalent cancers (10/16), defined as occurring within one year of commencing therapy. Of the 25 patients that were treated and failed (per protocol analysis), 6/25 developed cancer, 2/11 in the ALA-PDT group and 4/14 in the Photofrin group (Fishers exact test, p = 0.67) In the ALA group both were T1b, and treated with EMR plus chemoradiotherapy. In the photofrin group three were T1a, two of which were successfully treated with EMR plus RFA and a third was treated by oesophagectomy. The 4th patient succumbed to a T2 tumour with liver metastases 24 months after his initial PDT treatment.

Effect of length of BO segment

30 patients had BO >6cm (14 Photofrin, 16 ALA) and 34 patients had BO ≤ 6cm (18 ALA, 16 Photofrin). Using ITT analysis the CR-HGD in the photofrin group was similar for both treatment lengths, 50% (7/14) for long segment vs. 38% (6/16) for short segment, Fishers exact test = 0.71. Using ITT analysis there was a significant difference in the CR-HGD rates according to length of BO segment within the ALA group - 31% (5/16) in the long segment group vs. 78% (13/18) in the short segment group, Fishers exact test p=0.037. Per protocol Kaplan Meier analysis was undertaken and shown in figures 9.81 and 9.82. Using Log-rank analysis there was a significant difference in CR-HGD between the two groups when stratifying by the length of BO. CR-HGD was significantly more probable when treated with ALA PDT rather than photofrin for BO ≤ 6cm, χ^2 = 4.81, p=0.028. For BO length > 6cm there was no significant difference between the two photosensitisers, χ^2 = 0.30, p=0.59.

Effect of extent of dysplasia

40 patients had multifocal HGD (20 ALA, 20 Photofrin) and 24 patients had unifocal HGD (14 ALA, 10 Photofrin). Using ITT analysis there was no significant difference in the CR-HGD for the photofrin group with multifocal HGD (13/20) vs. unifocal HGD (5/10), Fishers exact test p = 0.34. Using ITT analysis there was no significant difference in the CR-HGD rates according to focality of HGD within the ALA group – 11/20 multifocal vs. 6/14 in the unifocal group, Fishers exact test p=0.36. Per protocol Kaplan Meier analysis was undertaken and shown in figures 9.83 and 9.84. Using Log-rank analysis there was no significant difference in CR- HGD between the two groups when stratifying by the uni- or multifocal HGD. For unifocal HGD χ^2 = 2.10, p=0.15. For mulitfocal χ^2 = 0.26, p=0.61.

Figure 9.81 Analysis according to length of BO segment - > 6cm (per protocol group)

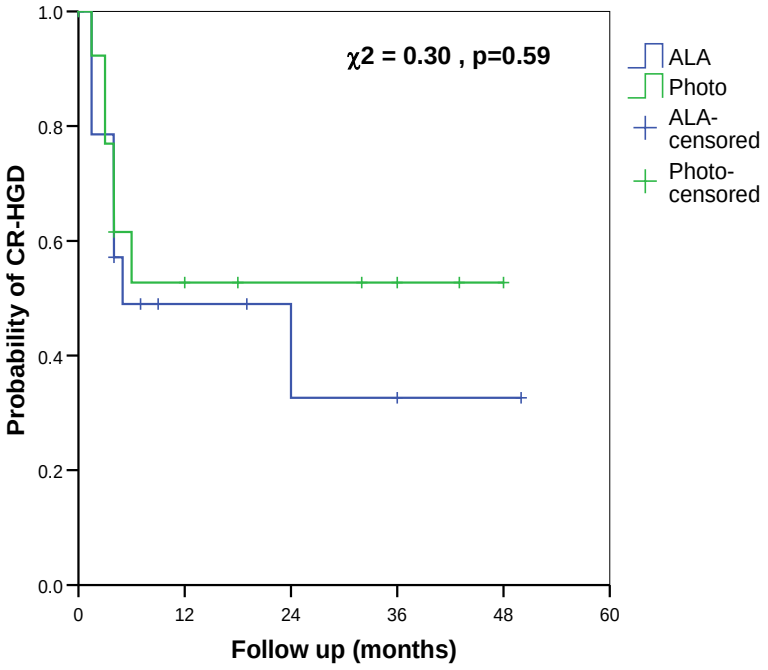

Follow up (months)	0	12	24	36	48
ALA patients at risk	14	4	3	2	1
Photofrin patients at risk	13	6	4	3	1

Figure 9.82 Analysis according to length of BO segment - ≤ 6cm (per protocol group)

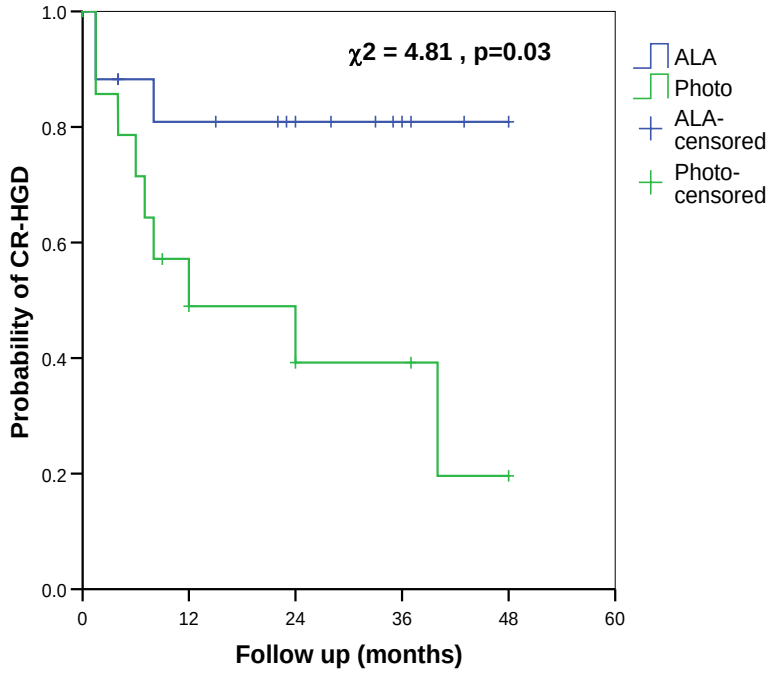

Follow up (months)	0	12	24	36	48
ALA patients at risk	17	11	8	4	1
Photofrin patients at risk	14	7	5	3	1

Figure 9.83 Analysis according to extent of dysplasia – multifocal HGD (per protocol group)

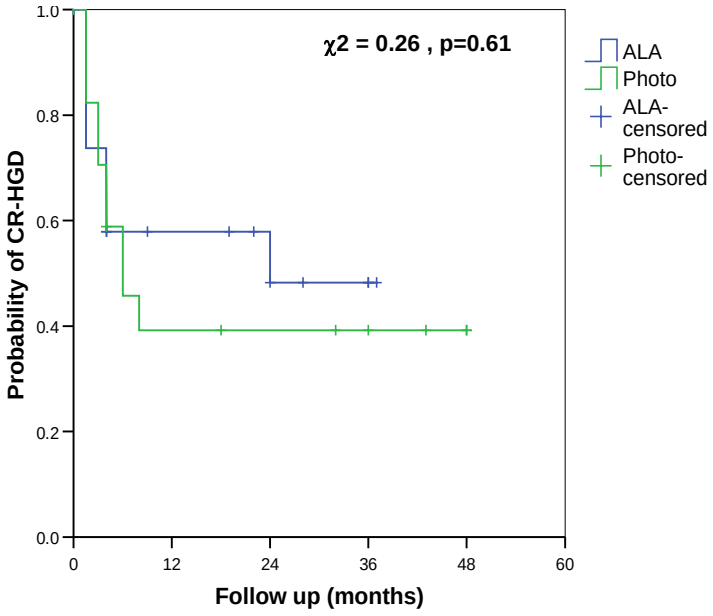

Follow up (months)	0	12	24	36	48
ALA patients at risk	19	8	6	3	1
Photofrin patients at risk	17	6	5	4	2

Figure 9.84 Analysis according to extent of dysplasia – unifocal HGD (per protocol group)

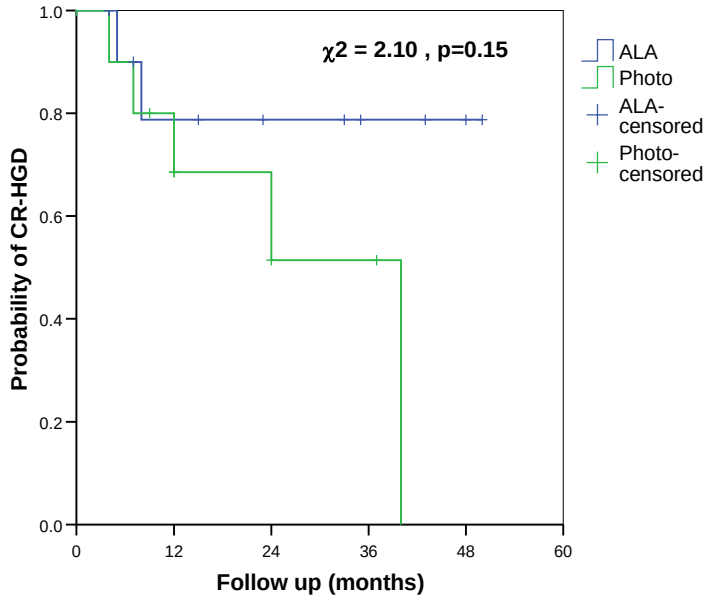

Follow up (months)	0	12	24	36	48
ALA patients at risk	10	7	5	3	2
Photofrin patients at risk	10	7	4	2	0

Effect of successive treatments

Table 9.37 shows the effect of incremental treatments with each drug from the per protocol cohort. It can be seen that if patients do not clear HGD after their first treatment with PDT then subsequent PDT is less likely to result in a cure. If we undertake combined analysis for both photosensitisers and compare a single treatment vs. multiple treatments, 25/27 were successful after one treatment vs. 8/31 for more than 1 treatment, Fishers exact test $p<0.001$.

Table 9.37 Effect of successive treatments (per protocol group)

	ALA-PDT			Photofrin PDT	
	1 treatment	2 treatments	3 treatments	1 treatment	2 treatments
CR-HGD	14	3	3	10	2
Failed	0	2	8	2	13

DNA ploidy post ALA-PDT

We then studied the 28 patients who were treated with ALA-PDT in the per protocol analysis for DNA ploidy abnormalities. 27/28 patients had biopsies available that were processed pre and post treatment and the results are shown in Table 9.38. There was no significant association between CR-HGD and aneuploidy pre PDT, 13/17 vs. 9/10, Fishers Exact test p= 0.621. Following PDT there was a significant difference in the success rate in patients who were aneuploid at 4 months post treatment – 3/17 vs. 9/10, Fishers Exact test p= 0.0008.

Table 9.38 DNA ploidy status pre and post ALA-PDT

	Long segment (n=13)		Short segment (n=14)	
	Success (n=6)	Failed (n=7)	Success (n=11)	Failed (n=3)
Aneuploidy pre PDT	6/6	7/7	7/11	2/3
Aneuploidy post PDT	3/6	7/7	0/11	2/3

Subsquamous IM

Overall 20% of patients (13/64) had evidence of subsquamous IM on biopsies pre PDT. There was no significant difference between the two groups - 27% of ALA patients (9/34) and 13% photofrin patients (4/30), Fishers Exact test p= 0.23. After PDT there was no significant difference in the rate of SSIM between the two groups - 49% of ALA patients (16/33) and 48% photofrin patients (14/29). There was a significant increase in the rate of SSIM post Photofrin PDT compared to pre PDT (paired t-test, t= 3.03, p = 0.005). The increase rate of SSIM post ALA PDT was of borderline significance (t = 3.02, p=0.051). The presence of SSIM post PDT had no significant effect on probability of CR-HGD using Log rank analysis (χ^2 = 0.026, p= 0.872)

Safety data

Safety data is summarised in table 9.39. Of 64 patients treated, strictures developed in 10/30 with Photofrin and 3/34 with ALA (Fishers Exact test, p = 0.027). Skin photosensitivity developed in 13/30 patients treated with Photofrin (one requiring hospital admission) compared with 2/34 with ALA, both of which were transient on the day of treatment (Fishers Exact test p <0.01). Pleural effusions were noted in 6/34 ALA and 3/30 Photofrin (Fishers Exact test, p = 0.48). Three were severe (2 ALA, 1 photofrin) requiring drainage and ITU Admission. Other serious adverse events that occurred were angina, pneumonia, parapharyngeal abscess, GI bleed requiring hospital admission and intractable vomiting.

Table 9.39 Adverse events of ALA and Photofrin PDT

	ALA n=34 (%)	**Photofrin n=30 (%)**	**Fishers exact test**
Photosensitivity	2 (6%)	13 (43%)	p<0.01
Strictures	3 (9%)	10 (33%)	p = 0.027
Pleural Effusions	6 (18%)	3 (7%)	p = 0.48
Transaminitis (ALT x2 ULN)	16 (47%)	0 (0%)	p<0.01
Nausea/vomiting	11 (32%)	8 (27%)	p = 0.76
Chest pain	9 (26%)	9 (30%)	p = 0.79

Quality of life data

Quality of life (QoL) data analysis was accrued for 70% at baseline, 57% at 2 days post treatment, 41% at 3 weeks, 53% at 6 weeks, and 50% at 4 months. There was no significant difference in the percentage completion between the two groups (see table 9.40). A threshold of 50% was set for meaningful data interpretation. Analysis was carried out on questionnaires received at baseline, 2 days, 6 weeks and 4 months following initial treatment with PDT.

Table 9.40 Quality of life data collection

	ALA PDT ***n= 34 (%)***	**Photofrin PDT** ***n= 30 (%)***	**p-value**
Baseline	24/34 (71)	21/30 (72)	1
2 days	18/32 (56)	17/30 (59)	0.81
3 weeks	15/31 (48)	9/27 (33)	0.29
6 weeks	16/30 (53)	14/27 (52)	1
4 months	15/27 (56)	11/25 (44)	0.62

State-Trait Anxiety Inventory (STAI)

Anxiety levels were similar at baseline with no significant difference in scores at 3 weeks, 6 weeks and 4 months (see figure 9.85). There was a significant drop in STAI scores from baseline to 4 months post PDT (both groups).

Figure 9.85 STAI 6 – anxiety scores for ALA and photofrin PDT

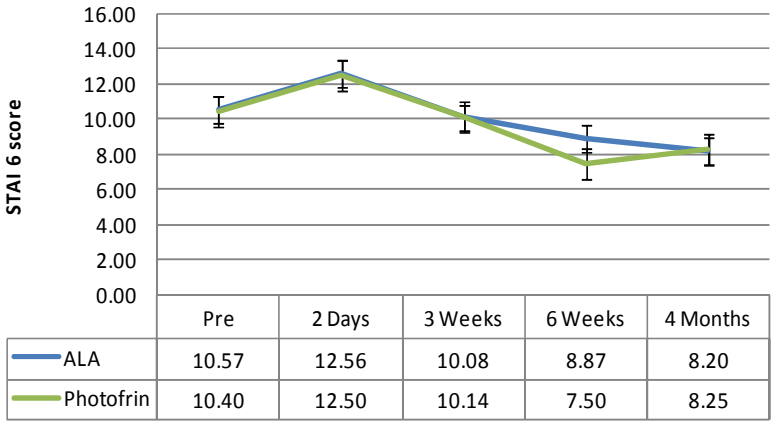

EORTC Oes 18

Chest pain, reflux, dysphagia and problems with eating all scored equally between the two groups at baseline and were significantly increased after PDT with both photosensitisers (see figure 9.86). These levels returned to baseline for reflux and eating by 6 weeks although pain and dysphagia was persistently elevated until 4 months post treatment with Photofrin. Dysphagia score was consistently lower with ALA at all time points after treatment but this difference was not significant.

Figure 9.86 EORTC Oes 18 data at baseline, 2 days, 6 weeks and 4 months post treatment

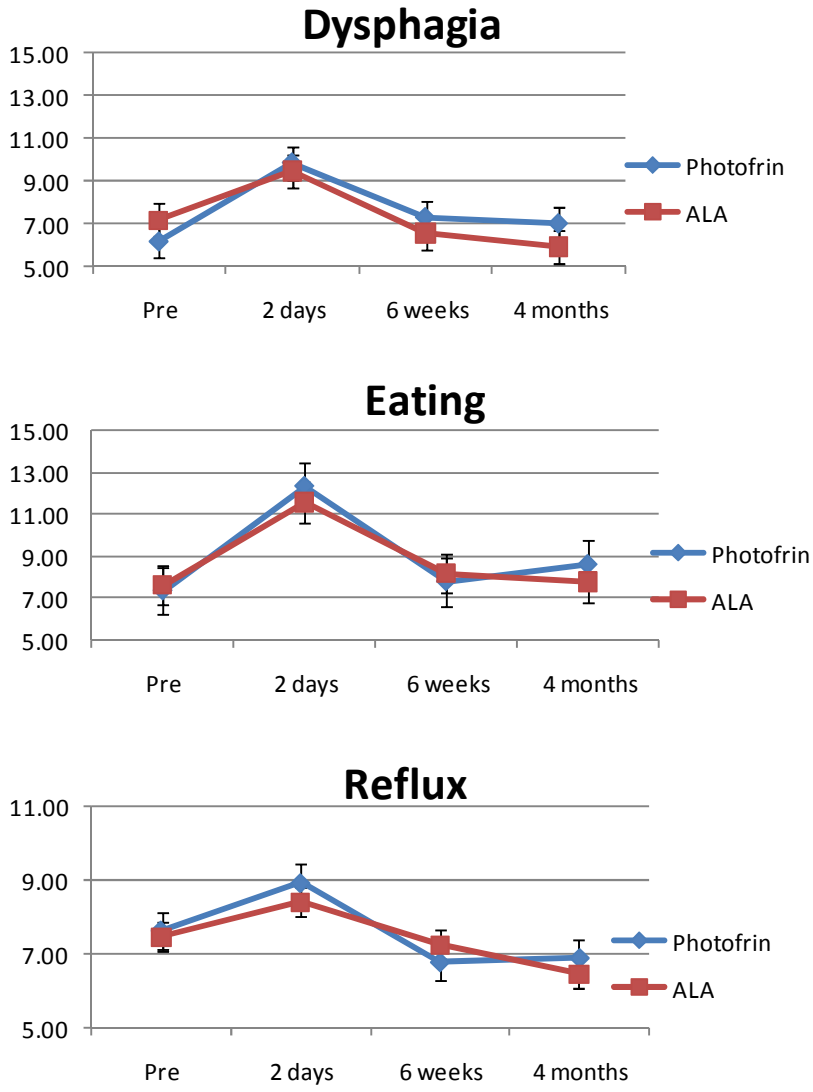

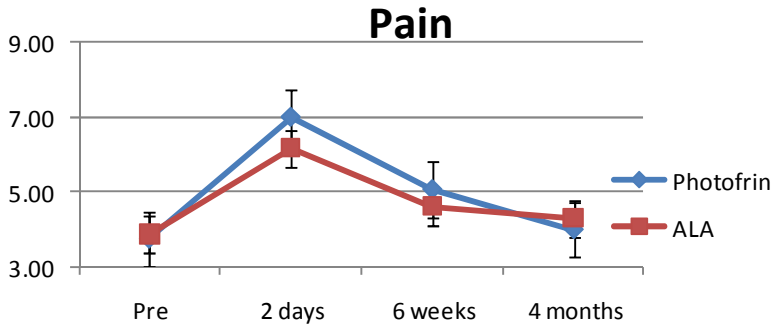

QOLRAD

The emotional distress and sleep disturbance scores were significantly higher before PDT than at 4 months post PDT (see figure 9.87). The emotional distress remained elevated at 6 weeks post ALA-PDT and was significantly higher than photofrin PDT. This may be explained by a fear of the unknown from being in the study arm group, as there is uncertainty whether the novel treatment actually worked. This resolves by 4 months when patients have had results of biopsies from their 6 week endoscopy. The delayed return to normal eating scores is again seen to be slower with photofrin than ALA.

Figure 9.87 QOLRAD data at baseline, 6 weeks and 4 months post treatment

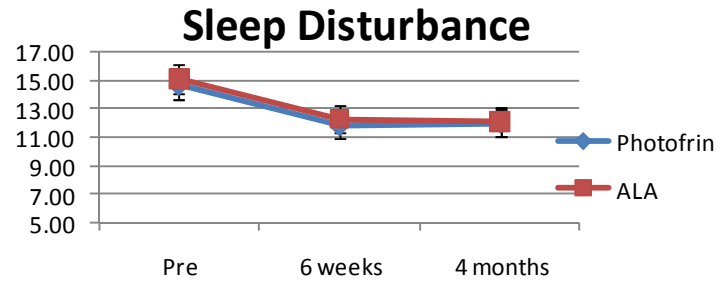

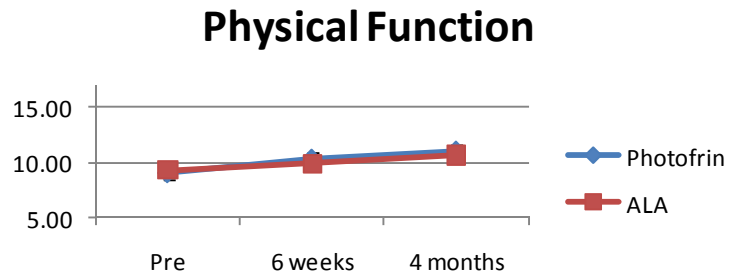

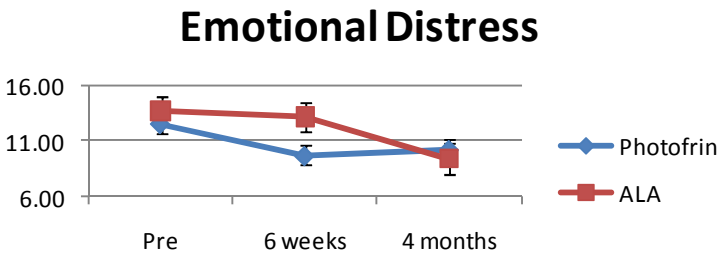

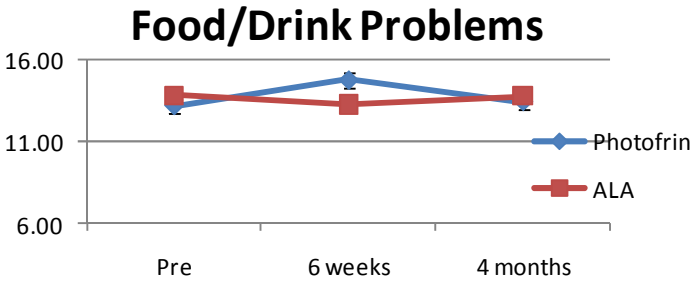

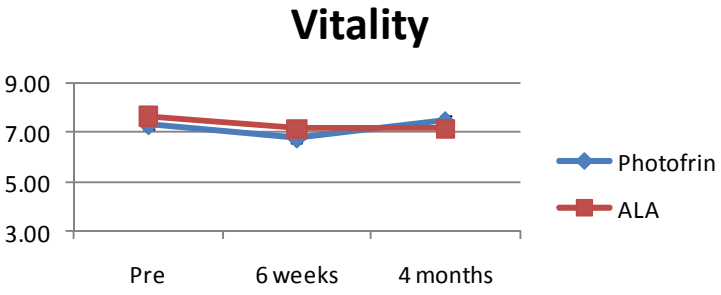

9.1.6 Discussion

The aim of this randomised controlled trial was to compare the efficacy and safety profile of ALA-PDT with photofrin PDT for HGD in BO. There was no statistically significant difference in efficacy between the two drugs when all patients were analysed on an intention to treat basis. When ITT analysis was undertaken on patients with a short segment BO of length ≤6cm there was a significant difference in the CR-HGD of the two drugs, 78% vs. 40%. This is a striking difference particularly as it is only half of the patients that the study was powered for.

The reason for such a significance difference may be due to the pharmacokinetics of ALA, as the therapeutic window is quite narrow and the PpIX levels may have dropped off by the time the 2nd segment is treated. There may also be an ischaemic effect from the balloon, which if compressing the walls at the lower end of the oesophagus for 40 minutes and hence may cause a lack of oxygen to the tissue at the proximal segment. As oxygen is required for the PDT, then this would affect efficacy.

Our data show that ALA has a more acceptable safety profile than photofrin PDT, with statistically significant lower incidence rates of strictures and photosensitivity. The stricture rate is similar to RFA. This can be explained by the absorption of the drug, as ALA-PDT acts at the mucosa whilst not affecting the deeper muscle layers, therefore achieving a depth of injury that is similar to RFA (500-1000 μm). The rate of SSIM at baseline (20%) was similar to the 25% reported in the AIM dysplasia trial [Shaheen et al., 2009a] and other reported series. [Ganz et al., 2008;Sharma et al., 2009b] Following PDT the rate of SSIM was significantly increased (48%). This is higher than the reported rate following HALO RFA of up to 5%.[Shaheen et al., 2009a] The significance of SSIM is unclear however, and in this study, SSIM did not influence the rate of CR-HGD.

Patients reported a significant improvement in their emotional state and reduced anxiety following treatment with both photosensitisers. Eating disturbance is more prolonged following photofrin PDT than ALA PDT. These QOL data were assessed using validated questionnaires, but interpretation was limited by the relatively low response rate of 50%.

From our study we can conclude that photofrin PDT had a poor efficacy that was associated with high rate of strictures, and significant photosensitivity. There was no significant difference in efficacy rates between long and short segments treated with photofrin PDT. In the light of recent evidence on the HALO RFA devices, which have been shown in a RCT to achieve CR-HGD of 81% with a low rate of strictures and buried glands,[Shaheen et al., 2009a] then it would appear that photofrin PDT may not be a useful treatment option for BO in the future.

When the ALA-PDT group with BO ≤ 6cm is evaluated a more favourable comparison with RFA emerges, with ALA PDT achieving a 78% CR-HGD on ITT analysis in a RCT. This is not an unreasonable comparison, as in the HALO RFA RCT all patients had BO of less than 8cm, with the median length 5.3cm. Our findings our strengthened by the rigorous entry criteria to the study, with confirmation of HGD on at least two occasions confirmed by two specialist GI pathologists. That this was a high risk group for progression to cancer is further evidenced by the very high level of DNA ploidy abnormalities at baseline (90%) and prevalence rate of cancer in HGD (13%) which is similar to other studies.[Wang et al., 2009]

Furthermore on achieving CR-HGD the effect of ALA-PDT is durable over a 36 month follow up. This has been previously demonstrated in a smaller cohort study.[Mackenzie et al., 2009] The reason for this may be the effective treatment of DNA ploidy abnormalities, that was demonstrated as a prognostic marker to predict long term success of treatment following ALA-PDT in a previous chapter (section 5.7). In the current study, there was a significant difference in treatment success in patients who eradicated DNA ploidy abnormalities vs. those with residual aneuploid cell populations at 4 months follow up.

ALA is a potentially advantageous treatment for HGD compared to other field ablation modalities, as only one or two treatments may need to be applied. We have demonstrated that although successive treatments with either photosensitiser deliver little improvement in efficacy, of the 14 patients who were successfully treated with BO ≤ 6cm, 11 were successfully treated at first attempt. This compares to RFA or cyrotherapy when an average of 3.5 and 6 treatment sessions respectively are necessary to achieve CR-HGD. [Shaheen et al., 2009a;Shaheen et al., 2009b] Two patients required a 2nd treatment and only one patient needed a 3rd treatment, all for a single focus of residual HGD. These 3 patients, in hindsight, may have been treated more efficiently with rescue EMR.

In conclusion the efficacy of both ALA and photofrin PDT was poor in patients with BO of length > 6cm, and these minimally invasive strategies do not compare favourably to

surgery. HALO RFA may be an option, though it must be stressed that long term randomised controlled data for patients with BO > 8cm is not available. A recent cohort study published in abstract form has demonstrated the combination of HALO RFA plus EMR for patients with very long segment BO (>10cm),[Herrero et al., 2009] but this was associated with lower efficacy rates and higher complication rates than published results on shorter segments of BO from the same group.[Gondrie et al., 2008]

In patients with BO of length ≤ 6cm ALA PDT is a successful treatment strategy, with efficacy rates of 78% on ITT analysis, a low rate of cancer progression (7%) within the first year of treatment and no deaths. One may speculate from our data that a treatment strategy for BO that comprised a single ALA-PDT treatment with subsequent treatment of residual dysplasia, if present, with EMR would successfully treat the majority of patients with HGD in BO ≤ 6cm. This one stop treatment strategy would be inexpensive and beneficial to patients who were unable to attend for multiple endoscopies due to other co-morbidities or travel constraints, as the EMR step could be undertaken at a local hospital. If CR-HGD was not achieved then it may still be possible to offer RFA as a rescue therapy. The efficacy of RFA following PDT has not been previously assessed, so to evaluate this we set out to treat the patients who failed from this study with RFA.

9.2 Radiofrequency ablation for the treatment of High grade dysplasia in Barrett's oesophagus after failed Photodynamic therapy – a case series

The following work was accepted for publication by Endoscopy in January 2011

9.2.1 Introduction

RFA using the HALO System (BÂRRX Medical, Sunnyvale, CA, USA) is a new technique for field ablation in the oesophagus. Clinical trials in U.S. and Europe have suggested that it is safe and effective for treating non-dysplastic IM, LGD and HGD in BO. These devices are approved by the FDA in the USA, have a CE mark for use in Europe, and were recently approved in the UK by NICE for the treatment of HGD arising in BO, following clinical trials demonstrating efficacy and safety from the US and Europe. [Shaheen et al., 2009a;Ganz et al., 2008;Gondrie et al., 2008] We have set up a

HALO RFA registry to prospectively assess efficacy and safety for patients treated in the UK. There are currently 16 participating centres and 150 patients enrolled. To date there are no published studies on the use of the HALO RFA devices in patients who have residual HGD following PDT.

9.2.2 Aims

To prospectively assess efficacy and safety of HALO RFA for patients who have previously failed PDT in a UK registry setting.

9.2.3 Methods

Case series

Fourteen patients who had failed PDT (9 ALA, 5 Photofrin) were treated with RFA between April 2007 and May 2009. Ethical approval was obtained for a UK HALO national registry (Ethics Approval number 08/H0714/27) and all patients signed informed consent. Failure of PDT was defined as presence of HGD confirmed by two independent specialist GI pathologists, following either 2 treatments with Photofrin-PDT or 3 with ALA-PDT using standardised methodology. [Mackenzie et al., 2009]

Study design

EUS and EMR of any visible nodules using a MBM kit (Duette, Cook UK) were performed prior to entry into the study. All patients who underwent EMR had a 6 week follow up endoscopy to confirm residual HGD in flat Barrett's mucosa. All endoscopies were undertaken using high resolution white light endoscopy aided by either narrow band imaging (Olympus) or i-scan enhancement (Pentax). The length of the Barrett's segment was determined according to the Prague classification system.[Sharma et al., 2006c] All biopsies and EMR specimens were reviewed by two specialist GI pathologists and jointly reported according to modified Vienna criteria. [Schlemper et al., 2000a]

RFA system Components

HALO Ablation Systems are CE marked devices manufactured by BÂRRX Medical in the USA and distributed in the UK by Synectics Medical. Field ablation of residual Barrett's tissue post PDT was conducted with the HALO^{360} System at constant power of

40 W and energy density of 12 Jcm^{-2}. Focal ablation of residual BO islands was conducted with the HALO^{90} System, energy density 15 Jcm^{-2}. The careful cleaning of sloughed mucosa between treatments, by using an EMR cap following primary ablation with HALO^{360} or by using the tip of the HALO^{90} device following focal ablation, was undertaken on all patients as previously described. [Gondrie et al., 2008]

Two experienced endoscopists (Dr Laurence Lovat and Dr Matthew Banks) with 2 research fellows (Dr Jason Dunn, Dr Gary Mackenzie) carried out the procedures. Follow up ablations were scheduled at 3 month intervals, according to adapted protocol from BarrX (Figure 9.88). If residual islands were seen that were suitable for HALO^{90}, i.e. less then 2cm and less than 50% circumferential, then HALO^{90} was applied, otherwise treatment was repeated with HALO^{360}. If a patient had an isolated nodule of HGD after all HALO RFA treatments were completed, then rescue EMR was permitted.

Figure 9.88 Adapted study protocol from BarrX Medical

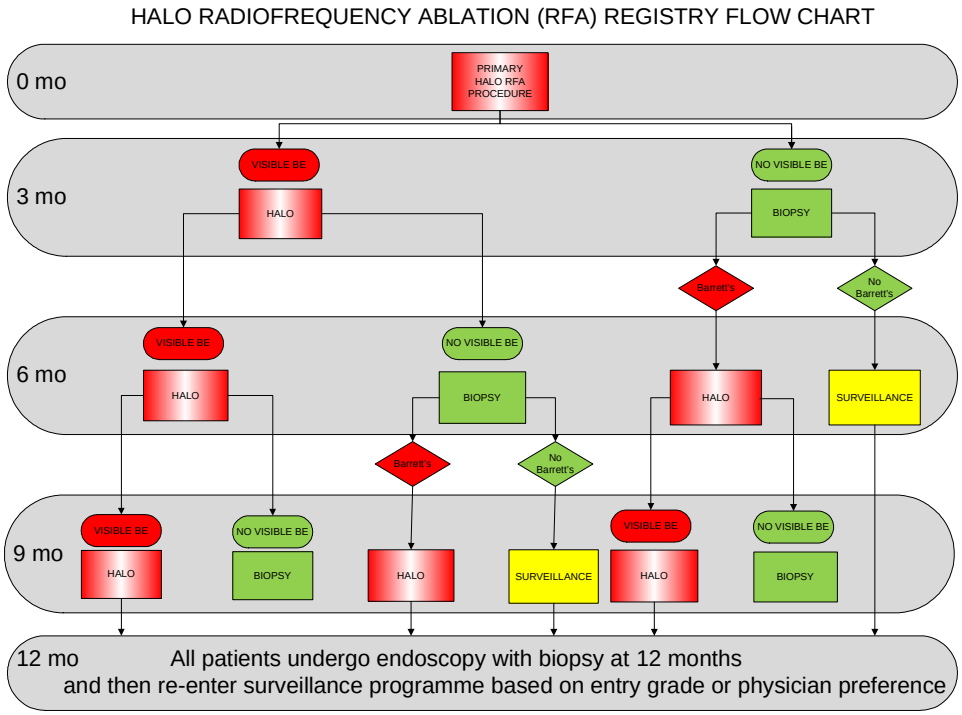

Outcome measures

The primary endpoint of the study was complete histological eradication of dysplasia from all biopsies (Complete reversal of dysplasia (CR-D)). Final outcome was assessed from biopsies taken 3 months after the final treatment with RFA – i.e. after there was no visible BO or after 12 months/4 consecutive ablations (per protocol). A second analysis was undertaken of the histological status at the most recent endoscopy, including any rescue therapy (overall CR-D). Secondary endpoints were eradication of intestinal metaplasia (Complete reversal of Intestinal Metaplasia (CR-IM)), presence of buried glands, adverse event incidence and reversal of DNA ploidy abnormalities. DNA ploidy abnormalities were assessed by image cytometry DNA analysis (ICDA) on biopsies from all patients at baseline and at 3 months follow up. The methodology was as previously described (see chapter 5.2).

9.2.4 Results

Patient characteristics

Mean age was 67 years (range 50-84 years), 87% were male, and all were Caucasian. Prior to RFA the median length of BO was C = 1cm (range 0-5cm), M = 5cm (range 1-10cm). A total of 42 ablations (15 HALO^{360}, 27 HALO^{90}) were carried out, with a median of 1 HALO^{360} (IQR 0-3) and 2 HALO^{90} (IQR 1-3) per patient. Patient demographics and outcomes are presented in Appendix G.

Eradication of dysplasia and IM

CR-D (per protocol) was achieved in 71% of patients after a median of 2 ablations (range 1-3). Three patients required rescue EMR for unifocal nodular HGD (cases 5, 10 & 13). Four patients required additional HALO RFA, two for recurrent flat HGD (4 and 11) and two for LGD (3 and 8). Six of these seven patients were clear of dysplasia and IM in the area of EMR or post RFA at 2 month follow up, and have now completed 1 year follow up with no dysplasia. Overall, with the combination of rescue EMR and RFA, CR-D was achieved in 86% (12/14) and CR-IM was achieved in 43% (6/14) of patients after a median total follow up of 19 months (range 12-38). The median follow up post last RFA

is 12 months (3-24 months). The median reduction in visible BO in the 8 patients who did not achieve CR-IM was 65% (range = 17-94%).

Adverse Events

All patients were treated as day cases under conscious sedation. Two patients were hospitalised; one for a superficial laceration caused by the HALO^{360} device with minor bleeding that resolved spontaneously; one for severe chest pain requiring opiate analgesia one day after 3rd treatment with HALO^{360}. There was one oesophageal stricture post RFA (Case 8) noted at 3 month follow up post first ablation. This was treated by a single session of bougienage dilatation. This patient had undergone laparoscopic fundoplication 12 months previously, and it is likely that both previous PDT and surgery contributed to stricture risk in this case.

Subsquamous IM (SSIM)

SSIM was identified in 0.5% (1/206) of follow up biopsies (1/14 patients). The patient (case 9) was found to have a submucosal adenocarcinoma at 7 months follow up. A biopsy of a residual island of flat BO at the GOJ, taken 5 months post RFA, revealed HGD. On relook endoscopy 2 months later it was decided to perform EMR to accurately stage the area. HGD was present with atypical glands infiltrating around a submucosal arteriole which was consistent with a well to moderately differentiated submucosal OAC. The patient has subsequently had an oesophagectomy and is clear of dysplasia/cancer at 6 months follow up. This patient had buried glands 6 months prior to HALO RFA on four quadrant biopsy of flat BO from the same area where the tumour developed

ICDA

DNA ploidy abnormalities (aneuploidy, tetraploidy or hypodiploid) were observed in 100% of patients on baseline biopsies. At 3 month follow up after final treatment, residual DNA ploidy abnormalities were observed in 100% (2/2) who failed vs. 8% (1/12) who achieved CR-D. Representative histograms are shown in figure 9.89. The association between DNA ploidy and complete response was statistically significantly using Fisher's exact test ($p = 0.03$).

Figure 9.89 Image cytometry DNA ploidy histograms

i) Histograms from case 3 – residual IM but diploid- disease free at 38 months

Aneuploid/Teteraploid histogram prior to RFA DI 1.76 and 1.96

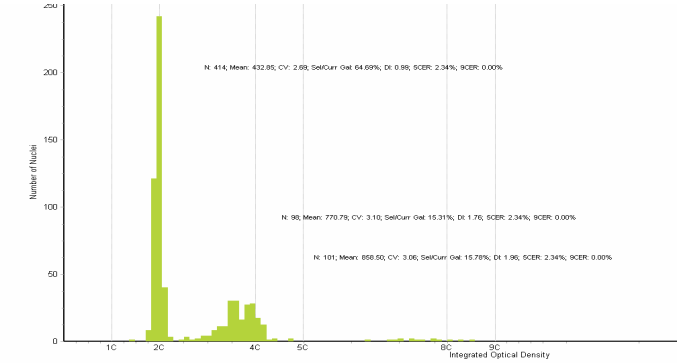

Diploid 3 months post last RFA

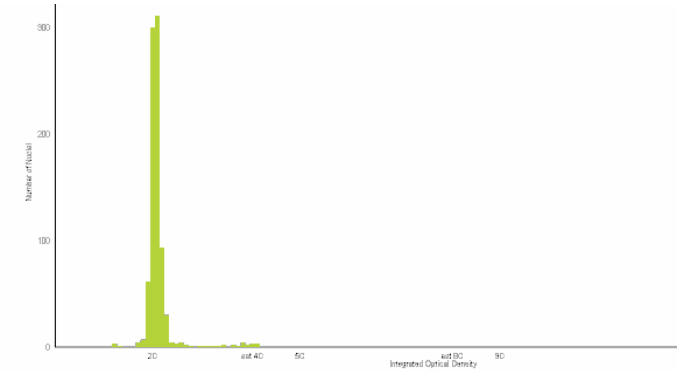

ii) Histograms from case 9 - relapse to cancer at 7 months post last treatment

Aneuploid with DI 1.62 and 5cER 2.39%, 5 months post RFA in glandular mucosa at the GOJ

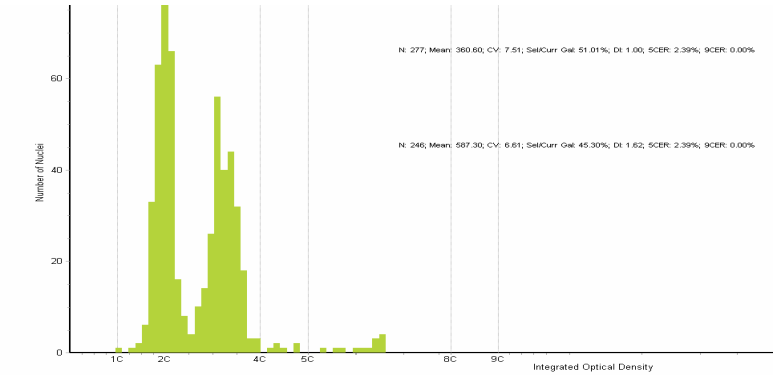

9.2.5 Discussion

This is the first reported series of patients treated with HALO RFA following failure with PDT for HGD in BO. We demonstrate this treatment is effective and safe in this difficult to treat patient group, with an overall CR-D of 86%. The patients described here were all offered oesophagectomy as a treatment option, but either elected to have RFA or were considered to be poor surgical candidates due to comorbidities. Our per protocol CR-D was 71%, which is lower than studies on patients with ablation naïve BO.(5-7) Seven patients required additional therapy after completing the HALO protocol, with recurrences of flat or nodular HGD at the GOJ being most frequent. This recurrence rate seems high but should be viewed within the context of a proven treatment resistant group. In addition endoscopic evaluation of the GOJ is more difficult post PDT, despite the use of HD scopes by experienced endoscopists. This may also explain why our CR-IM is lower than published series, as residual IM mostly occurred just above the GOJ.

Buried glands are a finding commonly associated with BO, both before and after ablative therapy.[Shaheen et al., 2009a;Lantz and Vakil, 2003;Bronner et al., 2009] One advantage of HALO RFA is the very low incidence of buried glands, and the rate in our study (1/206 follow up biopsies) is comparable to other studies. On further review it was found that this patient, who developed submucosal cancer from buried atypical glands, had evidence of buried glands prior to RFA (post PDT). So although the patient had subsequent RFA, this was likely to have been ineffective on the submucosal glands. The importance of buried glands is unclear, as while several studies have shown that these areas may harbour invasive cancer buried below apparently normal squamous epithelium,[Van Laethem et al., 2000;Shand et al., 2001;Overholt et al., 2003;Overholt et al., 2005] others have demonstrated a lower proliferative index than adjacent glandular epithelium.[Hornick et al., 2005] We suggest that buried glands should be viewed with caution post PDT, and resected by EMR before attempting further treatment with RFA.

We demonstrate that all of the patients who failed PDT had DNA ploidy abnormalities prior to RFA, and that these were successfully eliminated in 80% following treatment. In

those patients with residual DNA ploidy, 2/3 have relapsed to HGD or cancer. These data further strengthen the argument made previously, that DNA ploidy abnormalities are useful as a prognostic biomarker following ablative therapy. The utility of other biomarkers including p16 post PDT [Prasad et al., 2008] and proliferative markers post HALO RFA [Pouw et al., 2009] have also been postulated. These studies raise the possibility that residual genetic abnormalities are responsible for late relapse following ablative therapy. Hage *et al.* suggested that because it is difficult to detect these genetic abnormalities the goal of treatment should be complete Barrett's elimination.[Hage et al., 2006] The current goal of therapy with HALO RFA being complete visual elimination of columnar lined oesophagus therefore seems intuitive, and may explain its high cure rates.

This study is limited by its relatively small sample size and, non-randomised design. We also enrolled patients who had failed two different types of PDT, and the criteria for failure were different. Patients were deemed to have failed PDT when treated with Photofrin after 2 treatment session but were allowed 3 sessions with ALA before being considered to have failed, for the reasons outlined above. Finally our median follow up of 18 months is short, though comparable with other studies on RFA. Three year follow up data of RFA for dysplastic BO is emerging, and the promising initial results seem durable. [Shaheen et al., 2010]

In conclusion, these data demonstrate that HALO RFA is an effective and safe treatment option for patients who have received previous endoscopic therapy with PDT and failed. Now that HALO RFA has been approved in the UK for dysplasia arising in BO, it is likely that it will be adopted as the first line endoscopic therapy, and the numbers treated with PDT will dwindle. Nevertheless, as the documented late relapse rate following PDT is 20%, there will be individuals already treated with PDT who will require retreatment, and RFA may be offered in these circumstances.

Chapter 10

Conclusions and future work

Chapter 10 Conclusions and future work

10.1 Conclusions

The aims of this thesis were to

a) Identify a biomarker in BO that predicts future cancer risk
b) Develop the biomarker by validation and testing in a series of clinical studies
c) Assess the utility of advanced optical techniques to better quantify cancer risk
d) Assess ALA-PDT for the treatment of HGD

Chromosomal instability has great potential as a biomarker in BO as it is a common finding in oesophageal adenocarcinoma and increases in prevalence through the metaplasia-dysplasia–carcinoma sequence. [Chaves et al., 2007] DNA ploidy abnormalities are a measure of chromosomal instability, yet despite evaluation in prospective phase 4 biomarker trials, their use has not been adopted routinely [Reid et al., 2000b;Reid et al., 2001;Rabinovitch et al., 2001;Galipeau et al., 2007]. This may be explained by the technical difficulty, inter-laboratory reproducibility and cost of using flow cytometry to analyse DNA content. Image cytometry, an alternative technique that is routinely undertaken on FFPE tissue and has potential for automation, was evaluated and tested.

10.1.1 Aneuploidy measured by image cytometry is a prognostic biomarker in BO

Results from this thesis

ICDA is accurate when compared to flow cytometry on 40 micron thick FFPE sections. The nuclear suspensions could not be transported, so the work had to be carried out on site in Seattle. This work was strengthened by comparison with this reference laboratory and blinding of the results prior to comparative analysis. Then, in a multi centre nested case control study of 420 patients, DNA ploidy abnormalities predicted future cancer risk in patients with non dysplastic BO. The risk of cancer was markedly increased if both LGD and DNA ploidy abnormalities were present, equivalent to HGD. This may allow risk stratification of patients with LGD by DNA ploidy status, into a high risk group

(DNA ploidy abnormality) requiring endotherapy, and a medium risk group (LGD and diploid) requiring close surveillance.

ICDA also allowed risk stratification following histologically successful endoscopic therapy for HGD. In a case control study of 30 patients, the HR of relapse to HGD/OAC was 8.4 in patients with aneuploidy or tetraploidy in residual BO post ALA PDT. DNA ploidy abnormalities were also shown to be significant prognostic factor following ALA PDT in a randomised controlled trial and following HALO RFA for failed PDT. These data present a strong case for routine ICDA as a risk stratification tool in patients with BO both prior to and following therapy. This should only be undertaken on FFPE tissue, as cytology was not sufficiently sensitive for routine use.

10.1.2 Combination of nucleotyping and image cytometry – a single platform CIN marker

Results from this thesis

Nucleotyping is a novel method of measuring chromosomal instability by evaluating nuclear texture analysis. In a case control study, the GLEM method was found to be most accurate for classification of NDBO and HGD with a CCR of 83%. This algorithm was then evaluated on a blinded test set, with a similar CCR. Overall NT gave a CCR= 81%. The combination of NT and DNA ploidy was assessed as a single platform CIN panel and gave a CCR of 84%, higher than either test in isolation.

We then used this algorithm for assessment of future cancer risk in a non-dysplastic population, as part of the NIBR study. In isolation NT was not significantly associated with future cancer risk in this study, using the algorithms generated from smaller discovery study. When combined with DNA ploidy an OR for cancer progression of 6.3 was shown. This is the first time NT has been evaluated in Barrett's oesophagus and the combination of NT/ICDA on nuclear monolayers holds great potential as a single platform CIN biomarker.

Future work

The technological advances of nuclear texture analysis continue at a pace, driven by the surge in computer processing power and the dedicated unit at Oslo University. It is now possible to analyse thin sections for NT by staining on the slide with Feulgen. (See figure 10.90) This could allow for accurate co-registration of tissue morphology with NT abnormalities, a current limitation of our work which is carried out on whole biopsy. A further development is the use of nuclear segmentation software which takes a 100+ slices from a 16 micron nuclear monolayer, to enable 3D reconstruction of the nucleus. (See figure 10.90) This could represent a major advance in our understanding of how chromatin is arranged and its implication for cancer progression.

Figure 10.90 Advances in Digital image analysis

Left *Screenshot of nucleotyping on 4 micron sections superimposed into the H&E slide image* ***right*** *3D nuclear reconstruction*

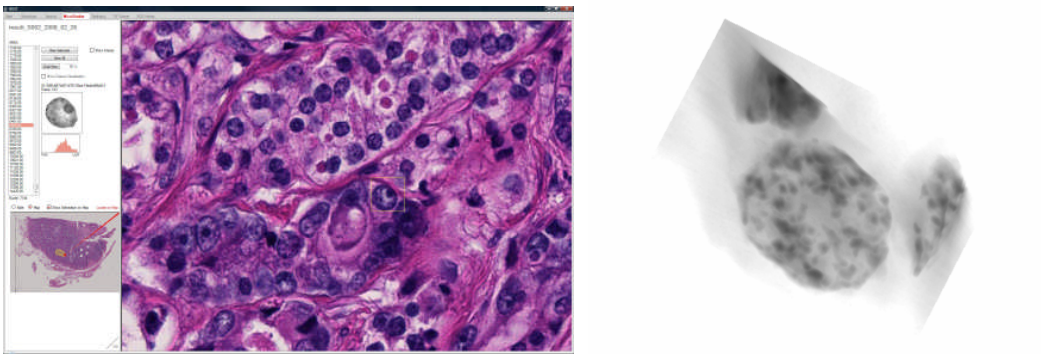

10.1.3 PLK-1 is a novel surrogate marker of aneuploidy

Results from this thesis

The utility of the S-G2-M replication licensing factors as surrogate markers for DNA ploidy has been demonstrated by the work presented here. This work was strengthened by use of laser capture microdissection, which allows accurate co-registration of sites. PLK-1 is the most promising as it correlated most closely with aneuploidy and is upregulated in dysplastic BO and OAC, the first time this has been demonstrated. This is a major step forward in the development of a simple IHC stain for risk stratification in BO.

Limitations and future work

The major limitation is that all patients had cancer in this study. To truly evaluate the future cancer risk of PLK-1 positivity we must test on a NDBO cohort and follow prospectively, similar to the NIBR study for ICDA/NT. We are currently assessing the possibility of using spare thin sections from that study. This would allow internal validation against aneuploidy on thick sections and assess the use of PLK-1 as a biomarker, either in isolation or in combination with other biomarkers, for example p53 staining, in an IHC panel.

I would also like to evaluate PLK-1 in different types of cancer, and assess how this correlates with aneuploidy and prognosis. This should allow for better classification of the cut offs for positivity of staining, which were somewhat arbitrary in the current study. For example both colorectal cancer and prostate cancer have been shown to have high rates of aneuploidy by ICDA, and this finding correlates with prognosis.[Pretorius et al., 2009;Bondi et al., 2009] In order to facilitate widespread use an automated quantification system would be necessary, and is currently under development.

The importance of PLK-1, should it accurately define DNA ploidy and cancer risk, is not to be underestimated. Consider the impact of HER2 on breast cancer management, initially as a prognostic marker and the subsequent evolution into a targeted treatment strategy with Herceptin. A similar strategy could be attempted in Barrett's OAC. PLK-1 inhibitors have already been developed and demonstrated high efficacy with tolerability in mouse models. As approximately 90% of patients with OAC will be PLK-1 positive, the vast majority of patients could benefit if such a drug was shown to reduce mortality. More work in this exciting area is warranted.

10.1.4 ESS can detect aneuploidy in vivo and measures a field effect

Results from this thesis

The work presented here has demonstrated that ESS informs on the genomic instability of Barrett's mucosa, when analysis was undertaken retrospectively. Furthermore ESS was

utilized *in vivo* to target dysplasia, and a field effect was demonstrated for the first time in BO, independent of dysplasia or DNA ploidy abnormalities. ESS has, however, been a difficult optical diagnostic tool to develop. Stumbling blocks needed to be overcome to achieve real time *in vivo* diagnosis include; overcomplicated statistical analysis; correlation with dysplasia for algorithm generation, therefore hardwiring human error by the pathologist; difficulties in co-registration of sites; sampling error similar to random four-quadrant biopsy due to point based interrogation of tissue. Furthermore since the emergence of spectroscopy, competing optical tools have been developed which allow the clinician to visualise and interpret tissue morphology accurately in real time (pCLE, OCT).

Future work

Where now for ESS? I think this promising tool may have more far-reaching applications than confirming the pathologist's view of tissue morphology. As demonstrated by both ICDA and Nucleotyping studies, chromosomal instability has great potential as a marker of future cancer risk, and if ESS can be trained to accurately target these areas in vivo then this would reduce the need for random biopsy and reduce the number of biopsies analysed by ICDA/NT. Further studies that focus on the physical correlation of spectral and nuclear texture abnormalities would also be of value, and may go some way to explain the field effect that was seen in patients with normal histology and DNA ploidy status.

10.1.5 ALA-PDT is safer and more effective than Photofrin PDT in BO ≤ 6cm

Results from thesis

The completion of the RCT of ALA vs. Photofrin PDT has delivered surprising yet compelling answers to the debate on ablation of HGD. ALA PDT in BO ≤ 6cm had a significantly higher cure rate then photofrin PDT, with no patients progressing to cancer and no strictures or photosensitivity. The achieved CR-HGD of 78%, although lower than published cohort studies, is equivalent to the 81% achieved by HALO RFA in the only directly comparable RCT. The results of our study are further strengthened by the RCT study design and rigorous entry criteria of HGD on two separate endoscopies, compared

with only once for the HALO RFA RCT, which had a consequent spontaneous reversion rate for HGD in the placebo arm of 19%. This study also showed that the majority of patients that achieved CR-HGD with ALA-PDT did so after a single treatment. In comparison with RFA, which requires a median of 3.5 treatment sessions, ALA-PDT may be a cheaper option resulting in substantial financial savings. The patients that failed in the short arm group all had residual HGD that was successfully treated with RFA, and those that needed multiple treatments had only a single focus of HGD, which may have been treated as effectively by EMR. Therefore for BO $\leq$ 6cm a single treatment with ALA PDT plus RFA/EMR for residual visible BO is a possible treatment strategy that needs further evaluation. For BO >6cm neither treatment strategy was effective, and PDT cannot be recommended for future use. HALO RFA was shown to be effective and safe rescue treatment for patients that failed either type of PDT.

The importance of the segment length for PDT is a novel finding, although it has been consistently shown to convey increased cancer risk in multivariate analysis from epidemiological studies. It may be due to the size of the aneuploidy population, as the length of aneuploid or tetraploid clones through a Barrett's segment has been shown to increase risk.[Maley et al., 2004] Importantly in our study the proportion of patients that achieved aneuploidy eradication was significantly higher in the short segment than long segment group.

Limitations and future work

The overarching limitation of the RCT is that it was carried out at a single centre. We have 15 years experience with ALA-PDT and there are many hurdles to overcome to successfully treat a patient. These include the optimisation of drug and light parameters, ward staff able to deal with the precise timing of drug administration and after treatment light precautions, a skilled medical physicist to oversee use of the lasers, and anaesthetist and nursing staff during the procedure and an endoscopist with the skill set required to treat these patients. A further limitation of ALA is that the drug is not licensed for use for BO in the UK, although it has recently received orphan drug status in the US for this indication. In comparison the RFA device is CE marked, FDA and NICE approved, can

be carried out as a day case under conscious sedation and there is no need for drug administration or technical staff. It is however expensive and associated with lacerations and perforations, due to automated insufflation of the sizing or treatment balloon in the oesophagus which is not under human control. A RCT of the two treatment strategies in BO < 7cm may be of value.

10.2 Future directions

Biomarkers

Two areas of biomarker development in BO may be close to realisation. The first, screening using a capsule sponge and evaluation of biomarkers on cytology brushings is soon to undergo a phase III study. It may be of value to add PLK-1 to the immunocytochemical panel to see how well it correlated with BO. If this study was successful it could pave the way for a non-endoscopic screening tool that could be undertaken in an outpatient clinic. Whether this will impact on oesophageal cancer rates, or merely increase the pool of patients with NDBO undergoing endoscopic surveillance, can only be answered if such a strategy were to be rolled out nationwide, in a similar fashion to faecal occult blood testing for colorectal cancer screening.

The second area of future development is the wider use of DNA ploidy/NT as a prognostic marker on surveillance cohorts. There is increasing evidence from our work that this biomarker is of real value in the clinical decision making process for BO patients. We are already using DNA ploidy at UCLH to identify at risk groups, and we shorten the surveillance intervals from 2 years to 1 year if NDBO displays aneuploidy. Anecdotally several patients with LGD and aneuploidy that have gone on to develop HGD have been identified. Ideally we should test our panel on patients enrolled in the BOSS study, which itself may create a clinical risk profile that would enhance detection of at risk groups in BO.

Imaging

With the introduction of OCT and CLE real time endomicroscopy is now a reality. We have started using pCLE as part of the CLEAN BE study, a multi centre RCT that is

evaluating CLE in the residual BO post HALO RFA or EMR to determine in real time whether repeat treatment is necessary. The results of this study may have an impact on how ablation is carried out.

With regards to surveillance, despite many attempts no study has shown that an advanced imaging technique is better than random four quadrant biopsy for detection of dysplasia. After the ESS pilot study described here, the next step is an RCT of HD WLE + i-scan + ESS vs. HD WLE alone. This study should tell us the incremental diagnostic yield for each technique and may allow for identification of DNA ploidy abnormalities *in vivo.*

Ultimately if there is a field effect in Barrett's carcinogenesis, which could be measured by ESS as demonstrated in this thesis, then this may be utilised to identify cancer risk by interrogating the buccal mucosa. A discovery study would be needed to evaluate buccal ESS measurements from patients with a spectrum of oesophageal disease including oesophagitis, non dysplastic BO, dysplasia, OAC as well as normal controls. If a spectroscopic signature was seen in these different groups then this may pave the way for a larger multicentre trial evaluating ESS as a non invasive optical biomarker.

Treatment

The efficacy and safety of HALO RFA for the treatment of HGD in BO, combined with the increased uptake of EMR for staging HGD and IMC, has led to a fundamental change in BO management. I believe this will continue and the first point of referral will be to a GI specialist rather than surgeon for HGD. Areas of continued research will be the combination of EMR + RFA, when to ablate the residual non dysplastic BO and what surveillance intervals to introduce post ablation. Furthermore it is likely that LGD will be treated by RFA, although in my view this is rather clumsy use of precious facilities – an unknown cancer risk treated with a device with a not insignificant side effect profile.

It would be much better to risk stratify patients with NDBO or LGD with a biomarker first, and then treat those at high risk whilst monitoring those at moderate or low risk. The work presented in this thesis suggests that for patients with LGD, DNA ploidy

abnormalities measured by ICDA would be a suitable biomarker that serves as an end point of ablative therapy. In NDBO it is likely a biomarker panel would be necessary, as the risk of DNA ploidy alone, whilst significant, is still low and therefore large numbers of patients would be necessary to generate statistical power.

A multi centre RCT would be needed to convince UK health providers of the benefit of such a strategy. Treatment would need to be carried out in centres displaying excellence for the RFA technique, and in the UK we have already set up a 12 centre HALO registry in order to facilitate this.[Dunn et al., 2010] We would then randomise into four groups according to future cancer risk –

a) Low risk LGD (Diploid and PLK-1 negative) surveillance or HALO RFA

b) High risk LGD (DNA ploidy positive or PLK-1 positive) surveillance or HALO RFA.

Ethical approval for such a study has been obtained by our centre. This would be the first phase V biomarker study of BO and could make a big impact on the management of this condition.

Barrett's oesophagus research has been an exciting area to be involved in over the last three years. There have been huge technical advances in endoscopic imaging and therapy, driven by both clinicians and corporations, and these will no doubt continue. I am sure these advances will be mirrored by continued efforts to understand the histogenesis of Barrett's oesophagus at a genomic level. This will be necessary to halt the inexorable rise of Barrett's associated oesophageal adenocarcinoma.

Appendix A Image cytometry monolayer preparation methodology

The Liberation of Nuclei form paraffin embedded tissue:

1. A 40 micrometre section was cut from paraffin block
2. Paraffin removed from embedded tissue with 1.5mls of xylene (VWR, Dorset, UK) for 10minutes),
3. Centrifuge for 1 minute 13,000 rpm, remove supernatant with pipette,
4. Add 100% Ethanol 1.5mls, vortex (Vortex Genie 2, Scientific Ind, New York, USA) for 5 seconds then stand in ethanol for 5 minutes.
5. Repeat centrifuge and removal of supernatant as described above
6. Add 1.5mls of distilled water, vortex, stand for 2minutes, centrifuge and remove supernatant (settings as above),
7. Mix 1 tablet (Sigma-Aldrich, Dorset, UK) of phosphate buffer to 200mls distilled water to create phosphate buffered saline (PBS, pH 7.4, Phosphate buffer 0.01M, 0.0027M KCl, 0.137M NaCl). Add 1.5mls vortex (5s) and the stand for 2 minutes. Centrifuge and remove supernatant as above,
8. Add 200 microlitres of proteinase XXIV (Sigma-Aldrich, Dorset, UK) at concentration 5mg/ml (0.05g in 10mls PBS) at temperature 37^0C, for varying times (1, 2, 2.5, 3hrs) described above,
9. Add 1.4mls PBS chilled to 4ºC. Pipette entire sample and filter though 40micrometre nylon mesh cell strainer (BD Biosciences, California, USA)
10. Centrifuge for 10minutes at 1600rpm. Remove supernatant,
11. Re-suspended in PBS 200microlitres, vortex (5s),
12. Cytospin (Shandon Cytospin 4 at 1500rpm for 5minutes) using a Shandon single use cytofunnel (Thermo Scientific, Basingstoke, UK) onto Superfrost Plus (blue) microscope slide (electrostatically permanently positive charge, VWR, Dorset, UK)
13. Air dry at room temperature for 1 hour in slide holder for 12 or 24 slides.

Feulgen-Schiff Staining Process:

14. Place slide holder in 200mls of 4% Formalin to fix overnight,
15. Wash slide in slide holder with 200mls of distilled water in large glass trough.
16. Transfer slide holder into glass trough containing 200mls HCL 5mol/litre for 1 hour,
17. Rinse in distilled water (200mls in glass though)for 2 minutes by transferring slide holder,
18. Place 200mls Feulgen stain (Schiff's reagent, Raymond A Lamb, Sussex, UK) in a glass through and transfer slide holder. Leave for 2 hours in the dark at room temperature,
19. Rinse in cool running tap water 5 minutes,
20. Place slide holder into 200mls of graduated ethanol (50%, 75%, and 100%) in glass troughs for 2 minutes each.
21. Place slide holder in 200mls xylene for 2 minutes, repeat.
22. Mount with DPX mounting medium (Lamb, Sussex, UK) and add microscope glass clover slip (24x32mm, VWR, Dorset, UK).

Appendix B Comparison of FC versus ICDA (raw data)

D = Diploid, A = Aneuploid, T = tetraploid, AT = Aneuploid and tetraploid, H= Hypodiploid, S = suspicious

Cases 1-16 = EMR specimens, 17-48 = oesophagectomy specimens. Discordant cases are highlighted in red. CV = Coefficient of variance, DI = DNA Index.

Specimen ID	Histology	DNA ploidy ICDA	Nuclei in G1 peak	CV	Peak DI	DNA ploidy Flow Cytometry	Nuclei in G1 peak	CV	Peak DI
1	IMC	A	1864	6.45	1.36	1 aneuploid cycle	14339	5.22	1.34
3	HGD	A (near diploid)	851	4.02	1.17	aneuploid (bimodal)	10987	7.58	1.19
4	IMC	A	360	11.50	1.56	1 aneuploid cycle	11769	9.17	1.58
5	HGD	A	1406	6.30	1.43	1 aneuploid cycle	11816	5.74	1.36
6	HGD	Diploid	222	5.82		diploid (with shoulder, high debris)	9025	7.45	
7	IMC	A	366	5.35	1.85	2 interpretations : 1 aneuploid cycle ; aneuploid cycle + bimodal aneuploid	10901	6.7	1.64
8	HGD	A&T	1777	8.44	1.52 & 2.05	aneuploid cycle + elevated 4N	11160	7.28	1.41
10	HGD	T	248	9.07		diploid (high debris)	10015	9.71	
11	CIS	A	1042	4.66	5CER 3.36%	1 aneuploid cycle (high D.I.)	11743	4.1	3.02
12	HGD	D	460	5.77		diploid	13397	4.47	
13	CIS	D	133	13.20		diploid	10358	9.84	
15	CIS	D	166	10.36		borderline quality, probably diploid	5559	8.49	
16	HGD	A	269	6.35	1.44	1 aneuploid cycle	9687	6.06	1.41
17	Squamous	D	606	6.46		diploid	13667	4.94	
18	OAC	A	529	7.82	1.28	1 aneuploid cycle	10952	3.83	1.25
19	Squamous	D	1010	5.20		diploid	10981	4.67	
20	OAC	D	329	5.01		diploid (shoulder present but too small to call, and not quite bimodal)	11390	5.15	
21	Squamous	D	848	4.90		diploid	12195	5.33	
22	OAC	D	241	4.48		1 aneuploid cycle	14003	4.81	1.44
23	Squamous	D	167	13.29		diploid	10284	4.47	

24	OAC	A x2	299	6.09	1.34 + 1.51	2 aneuploid cycles	11503	4.8	1.31 + 1.51
25	Squamous	D	205	7.44		diploid	10678	6.41	
26	OAC	A x2	798	5.30	1.44 + 5CER	2 aneuploid cycles	9917	7.88	1.36
27	Squamous	D	269	5.78		diploid	13263	6.81	
28	OAC	D	236	4.98		1 aneuploid cycle	13942	4.48	1.16
29	Barrett's IM	D	264	4.69		diploid	14439	4.94	
30	IMC	A	609	6.75	1.53	1 aneuploid cycle	15413	5.85	1.51
31	OAC	A x2	204	9.58	1.76 & 2.20	2 aneuploid cycles, diploid G2 D.I. is high. Alternatively, could be 3rd aneuploid.	12560	5.83	1.48 + 1.78
32	OAC	D	350	7.92		diploid	12858	4.78	
33	OAC	D	1350	7.04		diploid	11952	4.91	
34	OAC	A	279	6.20	1.61	1 aneuploid cycle (aneuploid may be bimodal)	13693	5.91	1.60
35	OAC	T	268	6.60		elevated 4N	14634	4.64	
36	OAC	A	486	9.55	1.79	1 aneuploid cycle	13263	6.01	1.73
37	OAC	A x2	327	3.95	1.52 + 5CER	2 aneuploid cycles	13987	4.54	1.20 + 1.42
38	OAC	A	383	4.85	1.31	1 aneuploid cycle	15839	4.54	1.53
39	OAC	A	230	3.84	1.59	1 aneuploid cycle	14572	4.05	1.56
40	OAC	T	508	6.68		elevated 4N	11258	4.47	
41	OAC	A	228	4.18	5CER	1 aneuploid cycle (tiny)	16392	4.17	1.77
42	OAC	A	777	6.37	1.73	1 aneuploid cycle	14100	5.37	1.74
43	OAC	A x2	413	5.37	1.40 + 2.53	2 interpretations: 1 aneuploid cycle; 2 aneuploid cycles	11720	6.98	1.41
44	OAC	A&T	650	15.34	1.44	1 aneuploid cycle, elevated 4N	8624	5.12	1.27
45	OAC	A	216	6.98	1.52 + 1.9	2 aneuploid cycles	7531	4.83	1.47 + 1.72
46	OAC	D	310	10.54		diploid	13872	10.64	
48	OAC	A	348	7.56	1.67	1 aneuploid cycle	10116	5.68	1.58

Appendix C ICDA using three different proteolysis methods (raw data)

ID	Result	Total nuc	Diploid (G0) Peak			Aneuploid Peak			>5c	Comments
			nuc	DI	CV	nuc	DI	CV		
1A-C	All D	535/467/667	527/456/641	1/0.99/1.01	2.1/1.65/2.55				0	
2A	D	753	712	0.99	3.43				0.13	
2B	S	189	147	0.94	10.1	23	1.51	6.31	3.72	
2C	S	135	101	1.01	8.09	23	1.38	5.09	5.19	
3 A-C	All D	701/358/409	646/337/395	1.02/0.98/1.04	3.11/5.81/8.49				0	
4A	D	798	739	1.01	2.52				0	
4B&C	Failed									>120 mins
5A	A	654	587	0.99	2.55	19	1.37	1.81	0	tiny 2.9% peak
5B&C	Failed									>120 mins)
6A	AT	289	230	1.04	2.87	9	1.81, 1.97	1.3, 1.97	1.04	9% tetraploid peak
6B	AT	276	156	0.96	3.21	51	1.80, 1.97	3.24, 1.28	3.62	10% tetraploid peak
6C	AT	245	164	1	4.17	24	1.78,2	3.17, 2.27	2.45	10% tetraploid peak
7A	A	643	159	1	2.05	95, 206, 29	1.4, 1.62, 1.77	2.44, 2.31, 1.33	11.2	3 aneuploid cycles
7B	A	520	191	1	4.77	115, 62, 30	1.47, 1.61, 1.85	2.73, 1.42, 1.54	12.3	3 aneuploid cycles
7C	A	303	129	1.01	5.62	74, 25, 23	1.49, 1.66, 1.84	2.8, 1.8, 1.74	7.6	3 aneuploid cycles
8 A- C	All D	670/471/413	580/417/372	1.01/0.99/0.98	2.45/2.51/4.25				0.15,0,0	
9A	A	542	331	0.99	1.6	163	1.67	3.69	2.58	30% aneuploid peak
9B	A	285	154	0.99	3.19	110	1.65	4.94	1.4	39% aneuploid peak
9C	A	222	128	1.01	3.76	78	1.66	5.06	3.6	35% aneuploid peak
10A	D	380	368	1.01	1.96					
10B&C	Failed									>120 mins

Appendix D ICDA post ALA PDT (raw data)

i) Cases of progression to HGD or Adenocarcinoma

Corresponding histology and raw ICDA data at 3 time points are shown

Study ID	Length BO (cm)	DNA ploidy status at baseline	Levels DNA ploidy	No of levels of HGD	Peak DI	Mean CV	Mean n in G1 peak	5c	DNA ploidy status at 4 months	No of levels DNA ploidy	Histology	Peak DI	Mean CV	Mean n in G1 peak	5c	DNA ploidy status at 12 months	Levels DNA ploidy	Histology	Peak DI	Mean CV	Mean n in G1 peak	5c
1	6	A	1	1	1.51	7.2	744	2.13	H	1	IM	0.73	8	777	0	D	0	LGD	1.01	6.8	852	0
2	6	A&T	1	1	1.32/ 2.02	10.9	1018	0.54	A	2	IND	1.52	9.2	557	0.74	A	1	IM	1.26	10.5	985	0.17
3	7	A,T	2	1	1.76/ 1.97	7.7	863	0.99	A&T	2	IM	1.29/ 1.99	10.7	363	0.23	A,T	1	LGD	0.5/ 2.05	6.8	576	0
4	3	A	1	1	1.69	9.6	907	1.20	A	1	CLO	1.65	10.2	807	0.41	A	1	IM	1.88	9.5	510	0.4
5	11	A&T	3	2	1.48/ 1.97	6.7	503	1.07	A	2	IND	1.75	6.0	681	0.29	n/a		IM				
6	3	A	1	1	1.89	15.1	986	0.76	A	2	IM	1.63	9.0	525	0.14	A	1	IND	1.38	5.0	923	0.15
7	5	A	2	1	1.56	9.3	725	0.37	D	0	IND	1.00	4.4	1103	0	H,T	1	IM	0.50 /1.97	10.1	392	0
8	4	A	1	1	1.83	10.4	648	0	D	0	CLO	1.01	5.9	916	0	A	3	CLO	1.85	11.6	224	1.50
9	13	A,T	6	3	1.74/ 2.05	9.43	708	1.79	A	1	IM	1.79	6.3	680	0.11	A	1	IM	1.87	7.4	773	0.26
10	3	A	1	1	1.31	8.6	626	0.78	A	3	Mixed	1.83	6.4	745	0.21	D	0	Mixed	1.00	4.6	1051	0
11	5	D	0	1	0.99	5.7	888	0	D	0	CLO	1.0	4.2	903	0	A	1	CLO	1.40	13	399	0.83
12	4	D	0	1	1.01	6.7	1194	0	D	0	IM	1.02	6.3	1064	0	D	0	IM	1.03	11.1	809	0
13	2	D	0	1	1.03	9.4	1274	0	D	0	IND	0.99	7.1	1059	0	D	0	IND	1.01	8.5	945	0

ii) Controls with no relapse

Corresponding histology and raw ICDA data at 3 time points are shown

Study ID	Length BO (cm)	DNA ploidy status at baseline	Levels DNA ploidy	No of levels of HGD	Peak DI	Mean CV	Mean n in G1 peak	Peak 5c	DNA ploidy status at 4 months	No of levels DNA ploidy	Histology	Peak DI at 4/12	Mean CV	Mean n in G1 peak	Peak 5c	DNA ploidy status at 12 months	Levels DNA ploidy	Histology	Peak DI	Mean CV	Mean n in G1 peak	Peak 5c
1	8	A	3	2	1.66	10.1	695	0.33	A	2	IM	1.61	11.1	650	0.12	A	2	IM	1.56	7.8	288	0.63
2	5	A	3	1	1.61	6.6	419	0.69	A	2	CLO	1.64	12.2	572	0.40	D	0	CLO	1.03	10.0	223	0
3	11	A	3	1	1.81	11.5	737	0.90	D	0	IM	1.01	7.0	1040	0	D	0	IM	1.02	4.0	852	0
4	5	A	1	1	1.27	6.8	783	0.30	D	0	IND	1.01	7.8	433	0	D	0	IM	1.00	8.2	425	0
5	4	A	2	1	1.77	10.5	448	0.23	D	0	CLO	1.01	7.0	1184	0	D	0	CLO	1.01	4.5	925	0
6	7	A	2	2	1.81	7.2	661	2.57	D	0	CLO	1.01	7.9	708	0	D	0	IM	1.01	6.8	455	0
7	6	A	1	1	1.21	7.8	761	0.09	D	0	IM	1.03	4.8	991	0	D	0	IM	0.99	4.3	850	0
8	5	A	1	1	1.45	9.7	881	0	D	0	LGD	1.02	8.6	1066	0	D	0	LGD	1.03	4.0	888	0
9	3	A	1	1	1.81	8.5	1071	0.09	D	0	IM	1.03	6.2	953	0	D	0	IM	1.03	9.9	885	0
10	4	A	2	2	1.34	6.2	338	2.30	D	0	CLO	1.01	4.3	1051	0	D	0	IM	1.01	9.2	402	0
11	5	A	1	1	1.83	6.5	1152	0.1	D	0	IM	1.04	8.8	1197	0	D	0	CLO	1.02	9.1	355	0
12	4	A	2	1	1.89	7.0	921	1.49	D	0	CLO	1.00	7.5	482	0	D	0	Mixed	1.00	7.9	1200	0
13	4	A	2	1	1.89	7.1	423	4.04	D	0	CLO	1.00	5.7	1000	0	D	0	CLO	0.99	5.8	859	0
14	4	A	1	1	1.85	11.2	905	2.68	D	0	CLO	0.99	6.7	923	0	D	0	CLO	0.99	5.2	890	0
15	8	A	1	1	1.56	8.3	587	0.74	D	0	IM	1.00	4.1	1182	0	D	0	IM	1.01	5.8	903	0
16	6	D	0	1	1.02	4.9	769	0.20	D	0	Mixed	1.01	9.7	1098	0	A	4	Mixed	1.85	7.9	235	0.12
17	3	D	0	1	1.01	6.0	408	0	D	0	CLO	1.01	6.6	752	0	D	0	CLO	1.04	10.3	1175	0

Study ID	Area	Histology	Date of LCM	DNA ploidy	Nuclei	CV	Peak DI	5CER	cdc 7	geminin	Ki67	mcm2	PLK1
1	Area 1	Cancer	04/02/2010	Aneuploid	119	2.28	1.59	5.88	52	35	74	48	31
1	Area 3	Cancer	04/02/2010	Aneuploid	458	2.43	1.57	7.86	71	38	78	56	48
2	All	IMC	27/05/2010	suspicious	311	6.98	1.64	0.00	44	9	57	27	13
3	Area 1	LGD	27/05/2010	Diploid	398	2.42	0.99	0.00	47	8	49	45	9
3	Area 2	LGD	27/05/2010	Diploid	358	3.29	0.98	0.00	27	4	36	34	6
3	Area 3	LGD	27/05/2010	Diploid	256	2.64	1.01	0.00	21	3	32	28	4
3	Area 4	IMC	27/05/2010	Diploid	270	2.74	0.99	0.00	26	3	35	49	9
3	Area 5	LGD	27/05/2010	Diploid	356	2.43	0.99	0.00	37	3	41	21	8
4	Area 1	LGD	27/05/2010	Diploid	355	3.11	1.00	0.00	28	7	34	35	4
5	Area 1	HGD	25/05/2010	Diploid	418	2.75	0.99	0.00	53	43	96	93	25
6	Area 1	Cancer	27/05/2010	Aneuploid	340-65	2.56	1.89	0.70	51	48	90	88	38
6	Area 2	LGD + HGD	11/02/2010	Diploid	213	2.94	0.98	0.47	36	22	92	83	22
7	All	HGD/Cancer	16/02/2010	Diploid	267	2.99	1.00	0.00	34	8	78	79	6
8	Area 1	IM	18/05/2010	Diploid	167	3.21	1.01	0.00	15	12	64	60	7
8	Area 2	Cancer	18/05/2010	Aneuploid	148-268	4.30	1.78	4.56	44	36	60	78	34
9	Area 1	HGD	18/05/2010	Diploid	212	3.80	1.00	0.44	16	18	88	82	2
9	Area 2	Cancer	18/05/2010	Aneuploid	170-204	2.82	1.40	2.40	35	30	78	84	38
9	Area 3	LGD	18/05/2010	Diploid	214	3.82	0.97	0.78	19	28	88	87	10
10	Area 5	Cancer	20/05/2010	Aneuploid	52-35	3.71	1.80	6.93	46	36	73	74	39
12	Area 1	IMC	18/05/2010	Diploid	368	4.06	1.00	0.00	17	25	80	65	7
12	Area 2	Cancer	18/05/2010	Aneuploid	457-67	4.62	1.78	1.46	33	47	80	90	34
12	Area 3	Cancer	18/05/2010	Aneuploid	181-239	2.99	1.43	1.09	49	48	86	96	36
13	All	IMC	18/05/2010	Aneuploid	106-16-54	3.62	1.41	37.92	63	41	78	89	37
14	Area 1	IM	18/05/2010	Diploid	202	3.04	0.97	0.00	11	6	34	54	3
14	Area 2	HGD	18/05/2010	Aneuploid	110-184	3.47	1.35	2.19	31	32	93	86	31
14	Area 3	Cancer	18/05/2010	Aneuploid	126-190	3.17	1.42	2.29	46	34	69	69	39
15	Area 1	Cancer	11/02/2010	Aneuploid	33-41	4.50	1.49	3.57	26	28	80	87	14
16	Area 1	Gastric mucosa	25/05/2010	Diploid	343	3.81	0.97	0.00	4	5	45	30	3
16	Area 2	Cancer	25/05/2010	Aneuploid & Tetraploid	213-132	2.82	1.71	3.48	51	30	60	84	43
17	Area 1	HGD	18/02/2010	Aneuploid	14-19	2.94	1.70	8.77	75	40	77	85	31
17	Area 2	IM	18/02/2010	Diploid	152	2.46	1.00	0.66	25	16	81	92	8
18	Area 1	IM	25/05/2010	Diploid	226	2.94	1.00	0.00	25	22	74	80	10
18	Area 2	HGD	25/05/2010	Aneuploid	69-209	3.76	1.55	5.72	41	28	70	81	33
18	Area 3	IM	25/05/2010	Diploid	279	3.91	1.00	0.00	23	16	78	88	7
19	All	IM	25/05/2010	Diploid	258	2.68	1.00	0.00	29	27	89	82	6
22	Area 1	IM	04/03/2010	Diploid	373	2.53	0.99	0.00	46	17	88	89	2
22	Area 2	LGD	04/03/2010	Diploid	87	4.50	0.99	0.00	40	20	73	78	23
23	Area 1	HGD	09/03/2010	Aneuploid	246-34-25	1.87	1.39	0.31	71	43	95	95	59
23	Area 2	LGD	09/03/2010	Aneuploid (near dip)	99-13	2.41	1.22	0.00	43	37	91	92	26
24	Area 1	HGD	27/05/2010	Aneuploid	424	5.31	1.82	0.00	65	47	92	95	34
24	Area 2	IM	27/05/2010	Diploid	335	4.76	1.00	0.45	51	20	64	69	17
24	Area 3	IM	27/05/2010	Diploid	337-17-21	7.35	0.99	0.00	10	3	29	71	1
24	Area 4	LGD	27/05/2010	Diploid	300	3.50	1.00	0.00	33	21	56	74	18
25	Area 1	HGD	27/05/2010	Diploid	132	3.72	0.98	0.00	56	30	86	91	23
25	Area 2	IM	27/05/2010	Diploid	461	3.21	1.00	0.00	44	53	67	78	24
27	Area 1	Cancer	20/05/2010	Diploid	85	5.18	1.01	0.00	30	11	81	89	7
28	Area 1	IM	20/05/2010	Diploid	61	6.06	1.00	0.00	23	25	64	68	9
28	Area 2	HGD	20/05/2010	Diploid	91	4.46	0.98	0.00	18	17	80	76	19
29	All	IM	20/05/2010	Diploid	404	4.33	1.01	0.00	46	21	93	93	9
30	Area 1	LGD	20/05/2010	Diploid	61	5.10	1.03	0.00	22	9	58	87	11
30	Area 2	Cancer	20/05/2010	Aneuploid (5CER)	52	6.66	0.96	1.82	56	40	92	90	40
31	Area 1	Cancer	25/05/2010	Aneuploid	64-57	2.61	1.60	2.19	63	53	92	92	48
31	Area 2	HGD	25/05/2010	Aneuploid	146-249	2.71	1.59	2.56	60	51	86	91	49
31	Area 3	LGD	25/05/2010	Diploid	223	2.82	0.99	0.00	4	18	58	59	5

Appendix E Replication licensing factor study (raw data)

Appendix F Inclusion and Exclusion Criteria ALA vs Photofrin PDT RCT

Inclusion Criteria

1. Patients will be recruited from those referred for management of HGD in BO.
2. Patients with biopsy proven Barrett's Columnar Lined Oesophagus and high-grade dysplasia confirmed by 2 independent pathologists, and no evidence of invasive cancer.
3. Patients with a visible distinct nodule of HGD will be eligible for inclusion following endoscopic mucosal resection or other ablative therapy to this nodule provided residual HGD remains in the patient's Barrett's segment.
4. Patients may have an endoscopic ultrasound to confirm non-invasive disease as clinically indicated.
5. Patients to be double stratified into:
   (a) Short or Long Segment BO: Short segment defined as 6 cm or less (single length treatment) and Long segment defined as >6cm but up to 13cm (double length treatment)
   (b) Single or Multiple sites of high grade dysplasia.

5 The maximum length of Barrett's oesophagus eligible for inclusion into the study will be 13cm.
6 Patients must have no contraindications to endoscopy.
7 Males and non-pregnant females over the age of 21 years. Female patients who are pre-menopausal must practice a medically acceptable form of contraception.
8 Patients must sign an informed consent form.

Exclusion criteria

1 Presence of invasive carcinoma of the oesophagus.
2 History of severe cardiovascular disease, severe angina, congestive heart failure, or recent syncope of cardiovascular origin.
3 Patients presenting with abnormal cardiac signs or symptoms and signs of congestive heart failure on physical examination.
4 Patients with orthostatic hypotension resistant to hydration.
5 Patients in whom endoscopy is contraindicated.
6 Patients who have a history of porphyria, or hypersensitivity to porphyrins.
7 Patients taking depot preparations of psychotropic medication
8 Patients with a WBC $<2x10^9$/L.
9 Patients with a platelet count $<50x10^9$/L.
10 Patients with a prothrombin time >1.5 times the upper limit of normal.

11 Patients with impaired renal and/or hepatic function at time of entry into the study (total serum bilirubin >50 μmol/L, serum creatinine >200 mcmol/L, alkaline phosphatase (of hepatic origin) and/or ALT >2 times upper limit of normal).
12 Patients are not allowed to receive concurrent chemotherapy, or radiation therapy or chemotherapy within 4 weeks of entry into this study.
13 Patients with prior PDT for Barrett's Columnar Lined Oesophagus.
14 Barrett's Oesophagus greater than 13cm in length.
15 Patients unable to sign an informed consent form.

Appendix G Outcome data for case series of HALO RFA post failed PDT

Corresponding histology and raw ICDA data at 2 time points are shown. DI = DNA Index. Patients that failed treatment are highlighted in red

Study ID	Length BO (cm)	Failed PDT Rx	No of levels of residual HGD	DNA ploidy status pre RFA	Peak DI	No of treatments (360/90)	Histology 3 months post HALO RFA	Additional Rx	DNA ploidy status at 3 months post combined therapy	Peak DI	Outcome histology at last endoscopy	Total follow up (months)
1	C3M7	Photofrin	2	Tetraploid	1.97	1/1	IM	None	Diploid	1.00	IM	17
2	C1M6	ALA	2	Aneuploid, tetraploid	1.67/1.95	0/1	Squamous	None	Diploid	1.00	Squamous	17
3	C1M10	ALA	3	Aneuploid & Tetraploid	1.76/1.96	3/0	IM	2 HALO 90	Diploid	0.99	IM	38
4	C4M9	ALA	3	Tetraploid	1.98	2/2	LGD	1 HALO 360, 1 HALO90	Aneuploid	1.84	HGD	27
5	C5M6	ALA	1	Hypodiploid & Tetraploid	0.5/1.97	2/1	IM	1 EMR, 1 HALO 360	Diploid	1.00	IM	20
6	C0M1	ALA	1	Aneuploid	1.85	1/1	Squamous	None	Tetraploid	2.01	Squamous	26
7	C0M4	Photofrin	1	Hypodiploid	0.71/1.0	0/2	Squamous	None	Diploid	1.00	Squamous	26
8	C4M6	ALA	1	Tetraploid	1.99	1/2	IM	None	Diploid	0.99	IM	36
9	C1M2	ALA	1	Tetraploid	1.96	0/2	HGD	1 x EMR	Aneuploid	1.62	Submucosal adenocarcinoma	15
10	C1M2	Photofrin	1	Aneuploid	1.59	0/1	HGD	1X EMR	Diploid	0.99	Glandular, no IM	18
11	C1M3	ALA	1	Aneuploid	1.83	1/2	Glandular	1 HALO 360, 1 HALO90	Diploid	0.99	Squamous	38
12	C0M8	ALA	1	Aneuploid	1.70	0/3	IM	None	Diploid	1.00	IM	12
13	C1M4	Photofrin	1	Tetraploid	1.96	1/2	HGD	1 x EMR	Diploid	1.00	IM	18
14	C0M2	Photofrin	1	Tetraploid	1.96	0/3	Squamous	None	Diploid	1.00	Squamous	12

Appendix H Publications arising from this thesis

Original articles

Dunn JM, Mackenzie GD *et al.* Image cytometry accurately detects DNA ploidy abnormalities and predicts late relapse to high grade dysplasia and adenocarcinoma in Barrett's oesophagus following photodynamic therapy. *Br J Cancer* 2010;**102**:1608-1617.

Dunn JM, Banks MR, Oukrif D *et al.* Radiofrequency ablation is an effective treatment for high grade dysplasia in Barrett's esophagus after failed Photodynamic therapy - a case series. *Endoscopy* In press

Invited reviews

Dunn J, Lovat L Photodynamic therapy using 5-aminolaevulinic acid for the treatment of dysplasia in Barrett's oesophagus. *Expert Opin Pharmacother* 2008;**9**:851-858.

Dunn J, Lovat L. The role of endoscopic ultrasonography in Barrett's esophagus and early esophageal cancer. *Techniques in Gastrointestinal Endoscopy* 2010;**12**(1):12-7.

Book Chapters

Dunn JM, Bown SG, Lovat LB. Barrett's oesophagus and gastroesophageal reflux disease - diagnosis and therapy In Popp J (Ed.). *Handbook of Biophotonics: Vol. 2*. Wiley Press

Selected abstracts

Dunn JM, Mackenzie GD, Oukrif D *et al*. DNA Ploidy as a prognostic biomarker after ALA Photodynamic Therapy for high grade dysplasia in Barrett's Esophagus. *Oral presentation* Digestive Disease Week May 30th -June 4th 2009, Chicago, US

Dunn JM, Mackenzie GD, Mosse CA *et al.* ALA PDT for High Grade Dysplasia in Barrett's Esophagus – review of a decade's experience. *Oral presentation* 12th World congress of the International Photodynamic Association, 11-15th June 2009, Seattle, US

Dunn JM, Fullarton GM, Thorpe S *et al*. Radiofrequency Ablation of High Grade Dysplasia in Barrett's Oesophagus Is Safe and Effective After Failed Photodynamic Therapy - First Results of the UK HALO RFA Registry. *Oral presentation* GASTRO 2009 UEGW/WCOG, November 21st-25th 2009, London, UK

Dunn JM, Lovat LB, Pretorius M *et al*. Combination of nuclear texture analysis and image cytometric DNA ploidy analsysis (ICDA) is more accurate then ICDA alone for risk stratification in Barrett's esophagus. *Oral Presenation* Digestive Disease Week May 1st - 5th 2010, New Orleans, US

Reference List

Abdalla SI, Lao-Sirieix P, Novelli MR, Lovat LB, Sanderson IR, Fitzgerald RC (2004) Gastrin-induced cyclooxygenase-2 expression in Barrett's carcinogenesis. *Clin Cancer Res* **10**: 4784-4792

Abela JE, Going JJ, Mackenzie JF, McKernan M, O'Mahoney S, Stuart RC (2008) Systematic four-quadrant biopsy detects Barrett's dysplasia in more patients than nonsystematic biopsy. *Am J Gastroenterol* **103**: 850-855

Abnet CC, Freedman ND, Kamangar F, Leitzmann MF, Hollenbeck AR, Schatzkin A (2009) Non-steroidal anti-inflammatory drugs and risk of gastric and oesophageal adenocarcinomas: results from a cohort study and a meta-analysis. *Br J Cancer* **100**: 551-557

Abrams JA, Kapel RC, Lindberg GM, Saboorian MH, Genta RM, Neugut AI, Lightdale CJ (2009) Adherence to biopsy guidelines for Barrett's esophagus surveillance in the community setting in the United States. *Clin Gastroenterol Hepatol* **7**: 736-742

Ackroyd R, Brown NJ, Davis MF, Stephenson TJ, Marcus SL, Stoddard CJ, Johnson AG, Reed MW (2000) Photodynamic therapy for dysplastic Barrett's oesophagus: a prospective, double blind, randomised, placebo controlled trial. *Gut* **47**: 612-617

Adler A, Pohl H, Papanikolaou IS, bou-Rebyeh H, Schachschal G, Veltzke-Schlieker W, Khalifa AC, Setka E, Koch M, Wiedenmann B, Rosch T (2008) A prospective randomised study on narrow-band imaging versus conventional colonoscopy for adenoma detection: does narrow-band imaging induce a learning effect? *Gut* **57**: 59-64

Adrain AL, Ter HC, Cassidy MJ, Schiano TD, Liu JB, Miller LS (1997) High-resolution endoluminal sonography is a sensitive modality for the identification of Barrett's metaplasia. *Gastrointest Endosc* **46**: 147-151

Ai H, Barrera JE, Meyers AD, Shroyer KR, Varella-Garcia M (2001) Chromosomal aneuploidy precedes morphological changes and supports multifocality in head and neck lesions. *Laryngoscope* **111**: 1853-1858

Alanen KA, Joensuu H, Klemi PJ (1989) Autolysis is a potential source of false aneuploid peaks in flow cytometric DNA histograms. *Cytometry* **10**: 417-425

Albregtsen F, Nielsen B, Danielsen HE (2000) Adaptive gray level run length features from class distance matrices. *Proceedings 15th International Conference on Pattern Recognition* **3**: 738-741

Allison PR, Johnstone AS (1953) The oesophagus lined with gastric mucous membrane. *Thorax* **8**: 87-101

Alsner J, Jensen V, Kyndi M, Offersen BV, Vu P, Borresen-Dale AL, Overgaard J (2008) A comparison between p53 accumulation determined by immunohistochemistry and TP53 mutations as prognostic variables in tumours from breast cancer patients. *Acta Oncol* **47**: 600-607

Amano Y, Kushiyama Y, Ishihara S, Yuki T, Miyaoka Y, Yoshino N, Ishimura N, Fujishiro H, Adachi K, Maruyama R, Rumi MA, Kinoshita Y (2005) Crystal violet chromoendoscopy with mucosal pit pattern diagnosis is useful for surveillance of short-segment Barrett's esophagus. *Am J Gastroenterol* **100**: 21-26

Amano Y, Komazawa Y, Ishimura N, Ohara S, Aimi M, Fujishiro H, Ishihara S, Adachi K, Kinoshita Y (2004) Two cases of superficial cancer in Barrett's esophagus detected by chromoendoscopy with crystal violet. *Gastrointestinal Endoscopy* **59**: 143-146

Anderson LA, Johnston BT, Watson RG, Murphy SJ, Ferguson HR, Comber H, McGuigan J, Reynolds JV, Murray LJ (2006) Nonsteroidal anti-inflammatory drugs and the esophageal inflammation-metaplasia-adenocarcinoma sequence. *Cancer Res* **66**: 4975-4982

Anderson LA, Murray LJ, Murphy SJ, Fitzpatrick DA, Johnston BT, Watson RGP, McCarron P, Gavin AT (2003) Mortality in Barrett's oesophagus: results from a population based study. *Gut* **52**: 1081-1084

Andersson J, Sjogren H, Meis-Kindblom JM, Stenman G, Aman P, Kindblom LG (2002) The complexity of KIT gene mutations and chromosome rearrangements and their clinical correlation in gastrointestinal stromal (pacemaker cell) tumors. *Am J Pathol* **160**: 15-22

Ando K, Ozaki T, Yamamoto H, Furuya K, Hosoda M, Hayashi S, Fukuzawa M, Nakagawara A (2004) Polo-like kinase 1 (Plk1) inhibits p53 function by physical interaction and phosphorylation. *J Biol Chem* **279**: 25549-25561

Atkinson M, Das A, Faulx A, Kinnard M, Falck-Ytter Y, Chak A (2008) Ultrathin Esophagoscopy in Screening for Barrett's Esophagus at a Veterans Administration Hospital: Easy Access Does Not Lead to Referrals. *Am J Gastroenterol* **103**: 92-97

Attwood SE, Lewis CJ, Caplin S, Hemming K, Armstrong G (2003) Argon beam plasma coagulation as therapy for high-grade dysplasia in Barrett's esophagus. *Clin Gastroenterol Hepatol* **1**: 258-263

Austwick MR, Clark B, Mosse CA, Johnson K, Chicken DW, Somasundaram SK, Calabro KW, Zhu Y, Falzon M, Kocjan G, Fearn T, Bown SG, Bigio IJ, Keshtgar MRS (2010) Scanning elastic scattering spectroscopy detects metastatic breast cancer in sentinel lymph nodes. *Journal of Biomedical Optics* **15**: 047001-047008

Backman V, Wallace MB, Perelman LT, Arendt JT, Gurjar R, Muller MG, Zhang Q, Zonios G, Kline E, McGilligan JA, Shapshay S, Valdez T, Badizadegan K, Crawford JM, Fitzmaurice M, Kabani S, Levin HS, Seiler M, Dasari RR, Itzkan I, Van Dam J, Feld MS (2000) Detection of preinvasive cancer cells. *Nature* **406**: 35-36

Bajbouj M, Vieth M, Rosch T, Miehlke S, Becker V, Anders M, Pohl H, Madisch A, Schuster T, Schmid RM, Meining A (2010) Probe-based confocal laser endomicroscopy compared with standard four-quadrant biopsy for evaluation of neoplasia in Barrett's esophagus. *Endoscopy* **42**: 435-440

Baldetorp B, Ferno M, Fallenius A, Fallenius-Vecchi G, Idvall I, Olsson H, Sigurdsson H, Akerman M, Killander D (1992) Image cytometric DNA analysis in human breast cancer analysis may add prognostic information in diploid cases with low S-phase fraction by flow cytometry. *Cytometry* **13**: 577-585

Bang YJ, Van CE, Feyereislova A, Chung HC, Shen L, Sawaki A, Lordick F, Ohtsu A, Omuro Y, Satoh T, Aprile G, Kulikov E, Hill J, Lehle M, Ruschoff J, Kang YK (2010) Trastuzumab in combination with chemotherapy versus chemotherapy alone for treatment of HER2-positive advanced gastric or gastro-oesophageal junction cancer (ToGA): a phase 3, open-label, randomised controlled trial. *Lancet* **376**: 687-697

Barr H, Shepherd NA, Dix A, Roberts DJ, Tan WC, Krasner N (1996) Eradication of high-grade dysplasia in columnar-lined (Barrett's) oesophagus by photodynamic therapy with endogenously generated protoporphyrin IX. *Lancet* **348**: 584-585

Barrett NR (1957) The lower esophagus lined by columnar epithelium. *Surgery* **41**: 881-894

Basu KK, Pick B, Bale R, West KP, de Caestecker JS (2002) Efficacy and one year follow up of argon plasma coagulation therapy for ablation of Barrett's oesophagus: factors determining persistence and recurrence of Barrett's epithelium. *Gut* **51**: 776-780

Battifora H, Kopinski M (1986) The influence of protease digestion and duration of fixation on the immunostaining of keratins. A comparison of formalin and ethanol fixation. *J Histochem Cytochem* **34**: 1095-1100

Bauer TW, Tubbs RR, Edinger MG, Suit PF, Gephardt GN, Levin HS (1990) A prospective comparison of DNA quantitation by image and flow cytometry. *Am J Clin Pathol* **93**: 322-326

Bektas N (2000) Allelic loss involving the tumor suppressor genes APC and MCC and expression of the APC protein in the development of dysplasia and carcinoma in Barrett esophagus. *Am J Clin Pathol* **114**: 890-895

Bell SP, Dutta A (2002) DNA replication in eukaryotic cells. *Annu Rev Biochem* **71**: 333-374

Bellizzi AM, Odze RD (2010) Histopathology of Barrett's esophagus: A review for the practicing gastroenterologist. *Techniques in Gastrointestinal Endoscopy* **12**: 69-81

Bergman JJ, Sondermeijer C, Peters FP, Ten Kate FJ, Fockens P (2006) Circumferential Balloon-Based Radiofrequency Ablation of Barrett's Esophagus Using the HALO 360 Ablation System Preserves the Inner Diameter of the Esophagus and Prevents Subsequent Narrowing and Compliance Reduction. *Gastrointestinal Endoscopy* **63**: AB138

Bertagnolli MM, Eagle CJ, Zauber AG, Redston M, Solomon SD, Kim K, Tang J, Rosenstein RB, Wittes J, Corle D, Hess TM, Woloj GM, Boisserie F, Anderson WF, Viner JL, Bagheri D, Burn J, Chung DC, Dewar T, Foley TR, Hoffman N, Macrae F, Pruitt RE, Saltzman JR, Salzberg B, Sylwestrowicz T, Gordon GB, Hawk ET (2006)

Celecoxib for the prevention of sporadic colorectal adenomas. *N Engl J Med* **355**: 873-884

Berthomieu C, Hienerwadel R (2009) Fourier transform infrared (FTIR) spectroscopy. *Photosynthesis Research* **101**: 157-170

Bhardwaj A, Hollenbeak CS, Pooran N, Mathew A (2009) A Meta-Analysis of the Diagnostic Accuracy of Esophageal Capsule Endoscopy for Barrett's Esophagus in Patients With Gastroesophageal Reflux Disease. *Am J Gastroenterol* **104**: 1533-1539

Bibbo M, Galera-Davidson H, Dytch HE, Gonzalez de CJ, Lopez-Garrido J, Bartels PH, Wied GL (1987) Karyometry and histometry of renal-cell carcinoma. *Anal Quant Cytol Histol* **9**: 182-187

Blant SA, Ballini JP, Caron CT, Fontolliet C, Monnier P, Laurini NR (2001) Evolution of DNA ploidy during squamous cell carcinogenesis in the esophagus. *Dis Esophagus* **14**: 178-184

Blount PL, Galipeau PC, Sanchez CA, Neshat K, Levine DS, Yin J, Suzuki H, Abraham JM, Meltzer SJ, Reid BJ (1994) 17p allelic losses in diploid cells of patients with Barrett's esophagus who develop aneuploidy. *Cancer Res* **54**: 2292-2295

Blow JJ, Hodgson B (2002) Replication licensing--defining the proliferative state? *Trends Cell Biol* **12**: 72-78

Boberg KM, Jebsen P, Clausen OP, Foss A, Aabakken L, Schrumpf E (2006) Diagnostic benefit of biliary brush cytology in cholangiocarcinoma in primary sclerosing cholangitis. *Journal of Hepatology* **45**: 568-574

Bocking A, Giroud F, Reith A (1995) ESACP DNA Consensus in Image Cytometry. *Anal Cell Pathol* **8**: 67-74

Bondi J, Pretorius M, Bukholm I, Danielsen H (2009) Large-scale genomic instability in colon adenocarcinomas and correlation with patient outcome. *APMIS* **117**: 730-736

Borrie J, Goldwater L (1976) Columnar cell-lined esophagus: assessment of etiology and treatment. A 22 year experience. *J Thorac Cardiovasc Surg* **71**: 825-834

Bosher LH, Taylor FH (1951) Heterotopic gastric mucosa in the esophagus with ulceration and stricture formation. *Journal of Thoracic Surgery* **21**: 306-312

Bourg-Heckly G, Blais J, Padilla JJ, Bourdon O, Etienne J, Guillemin F, Lafay L (2000) Endoscopic ultraviolet-induced autofluorescence spectroscopy of the esophagus: tissue characterization and potential for early cancer diagnosis. *Endoscopy* **32**: 756-765

Boustany NN, Boppart SA, Backman V (2010) Microscopic imaging and spectroscopy with scattered light. *Annu Rev Biomed Eng* **12**: 285-314

Boveri T (2008) Concerning the origin of malignant tumours by Theodor Boveri. Translated and annotated by Henry Harris. *J Cell Sci* **121 Suppl 1**: 1-84

Bown SG, Lovat LB (2000) The biology of photodynamic therapy in the gastrointestinal tract. *Gastrointest Endosc Clin N Am* **10**: 533-550

Bozzo PD, Vaught LC, Alberts DS, Thompson D, Bartels PH (1998) Nuclear morphometry in solar keratosis. *Anal Quant Cytol Histol* **20**: 21-28

Brand S, Wang TD, Schomacker KT, Poneros JM, Lauwers GY, Compton CC, Pedrosa MC, Nishioka NS (2002) Detection of high-grade dysplasia in Barrett's esophagus by spectroscopy measurement of 5-aminolevulinic acid-induced protoporphyrin IX fluorescence. *Gastrointest Endosc* **56**: 479-487

Brandt LJ, Kauvar DR (1992) Laser-induced transient regression of Barrett's epithelium. *Gastrointest Endosc* **38**: 619-622

Brenner RM, Slayden OD, Rodgers WH, Critchley HO, Carroll R, Nie XJ, Mah K (2003) Immunocytochemical assessment of mitotic activity with an antibody to phosphorylated histone H3 in the macaque and human endometrium. *Hum Reprod* **18**: 1185-1193

Brewster DH, Fraser LA, McKinney PA, Black RJ (2000) Socioeconomic status and risk of adenocarcinoma of the oesophagus and cancer of the gastric cardia in Scotland. *Br J Cancer* **83**: 387-390

Bronner MP, Overholt BF, Taylor SL, Haggitt RC, Wang KK, Burdick JS, Lightdale CJ, Kimmey M, Nava HR, Sivak MV, Nishioka N, Barr H, Canto MI, Marcon N, Pedrosa M, Grace M, Depot M (2009) Squamous overgrowth is not a safety concern for photodynamic therapy for Barrett's esophagus with high-grade dysplasia. *Gastroenterology* **136**: 56-64

Brumm C, Schulze C, Charels K, Morohoshi T, Kloppel G (1989) The significance of alpha-fetoprotein and other tumour markers in differential immunocytochemistry of primary liver tumours. *Histopathology* **14**: 503-513

Burnett RA, Brown IL, Findlay J (1987) Cresyl fast violet staining method for Campylobacter like organisms. *Journal of Clinical Pathology* **40**: 353

Buttar NS, Wang KK, Lutzke LS, Krishnadath KK, Anderson MA (2001a) Combined endoscopic mucosal resection and photodynamic therapy for esophageal neoplasia within Barrett's esophagus. *Gastrointest Endosc* **54**: 682-688

Buttar NS, Wang KK, Sebo TJ, Riehle DM, Krishnadath KK, Lutzke LS, Anderson MA, Petterson TM, Burgart LJ (2001b) Extent of high-grade dysplasia in Barrett's esophagus correlates with risk of adenocarcinoma. *Gastroenterology* **120**: 1630-1639

Caldwell MT, Lawlor P, Byrne PJ, Walsh TN, Hennessy TP (1995) Ambulatory oesophageal bile reflux monitoring in Barrett's oesophagus. *Br J Surg* **82**: 657-660

Cameron AJ, Lomboy CT, Pera M, Carpenter HA (1995) Adenocarcinoma of the esophagogastric junction and Barrett's esophagus. *Gastroenterology* **109**: 1541-1546

Canto MI (1999) Staining in gastrointestinal endoscopy: the basics. *Endoscopy* **31**: 479-486

Canto MI, Setrakian S, Petras RE, Blades E, Chak A, Sivak MV, Jr. (1996) Methylene blue selectively stains intestinal metaplasia in Barrett's esophagus. *Gastrointest Endosc* **44**: 1-7

Canto MI, Setrakian S, Willis J, Chak A, Petras R, Powe NR, Sivak MV, Jr. (2000) Methylene blue-directed biopsies improve detection of intestinal metaplasia and dysplasia in Barrett's esophagus. *Gastrointest Endosc* **51**: 560-568

Cardoso J, Molenaar L, de Menezes RX, van Leerdam M, Rosenberg C, M+Âslein G, Sampson J, Morreau H, Boer JM, Fodde R (2006) Chromosomal Instability in MYH- and APC-Mutant Adenomatous Polyps. *Cancer Res* **66**: 2514-2519

Casson AG, Tammemagi M, Eskandarian S, Redston M, McLaughlin J, Ozcelik H (1998) p53 alterations in oesophageal cancer: association with clinicopathological features, risk factors, and survival. *Mol Pathol* **51**: 71-79

Caygill CP, Watson A, Lao-Sirieix P, Fitzgerald RC (2004) Barrett's oesophagus and adenocarcinoma. *World J Surg Oncol* **2**: 12

Cestari R, Villanacci V, Rossi E, Della CD, Missale G, Conio M, Grigolato P, Bassotti G (2007) Fluorescence in situ hybridization to evaluate dysplasia in Barrett's esophagus: a pilot study. *Cancer Lett* **251**: 278-287

Chao DL, Sanchez CA, Galipeau PC, Blount PL, Paulson TG, Cowan DS, Ayub K, Odze RD, Rabinovitch PS, Reid BJ (2008) Cell proliferation, cell cycle abnormalities, and cancer outcome in patients with Barrett's esophagus: a long-term prospective study. *Clin Cancer Res* **14**: 6988-6995

Chaves DM, Sakai P, Mester M, Spinosa SR, Tomishige T, Ishioka S (1994) A new endoscopic technique for the resection of flat polypoid lesions. *Gastrointest Endosc* **40**: 224-226

Chaves P, Crespo M, Ribeiro C, Laranjeira C, Pereira AD, Suspiro A, Cardoso P, Leitao CN, Soares J (2007) Chromosomal analysis of Barrett's cells: demonstration of instability and detection of the metaplastic lineage involved. *Mod Pathol* **20**: 788-796

Chen TL, Luo I, Mikhail N, Raskova J, Raska K (1995) Comparison of Flow and Image Cytometry for Dna Content-Analysis of Fresh and Formalin-Fixed, Paraffin-Embedded Tissue in Breast-Carcinoma. *Cytometry* **22**: 181-189

Chen Y, Aguirre AD, Hsiung PL, Desai S, Herz PR, Pedrosa M, Huang Q, Figueiredo M, Huang SW, Koski A, Schmitt JM, Fujimoto JG, Mashimo H (2007) Ultrahigh resolution optical coherence tomography of Barrett's esophagus: preliminary descriptive clinical study correlating images with histology. *Endoscopy* **39**: 599-605

Chennat J, Konda VJ, Ross AS, de Tejada AH, Noffsinger A, Hart J, Lin S, Ferguson MK, Posner MC, Waxman I (2009) Complete Barrett's eradication endoscopic mucosal resection: an effective treatment modality for high-grade dysplasia and intramucosal carcinoma--an American single-center experience. *Am J Gastroenterol* **104**: 2684-2692

Chobanian SJ, Cattau EL, Jr., Winters C, Jr., Johnson DA, Van Ness MM, Miremadi A, Horwitz SL, Colcher H (1987) In vivo staining with toluidine blue as an adjunct to the endoscopic detection of Barrett's esophagus. *Gastrointest Endosc* **33**: 99-101

Chow WH, Blot WJ, Vaughan TL, Risch HA, Gammon MD, Stanford JL, Dubrow R, Schoenberg JB, Mayne ST, Farrow DC, Ahsan H, West AB, Rotterdam H, Niwa S, Fraumeni JF, Jr. (1998) Body mass index and risk of adenocarcinomas of the esophagus and gastric cardia. *J Natl Cancer Inst* **90**: 150-155

Clay FJ, McEwen SJ, Bertoncello I, Wilks AF, Dunn AR (1993) Identification and cloning of a protein kinase-encoding mouse gene, Plk, related to the polo gene of Drosophila. *Proc Natl Acad Sci U S A* **90**: 4882-4886

Comay D, Blackhouse G, Goeree R, Armstrong D, Marshall JK (2007) Photodynamic therapy for Barrett's esophagus with high-grade dysplasia: a cost-effectiveness analysis. *Can J Gastroenterol* **21**: 217-222

Cook MB, Wild CP, Everett SM, Hardie LJ, Bani-Hani KE, Martin IG, Forman D (2007) Risk of Mortality and Cancer Incidence in Barrett's Esophagus. *Cancer Epidemiol Biomarkers Prev* **16**: 2090-2096

Corley DA, Kerlikowske K, Verma R (2003) Protective association of aspirin/NSAIDs and esophageal cancer: a systematic review and meta-analysis. *Gastroenterology* **124**: 47-56

Corley DA, Levin TR, Habel LA (2002) Surveillance and survival in Barrett's adenocarcinomas: a population-based study. *Gastroenterology* **122**: 633-640

Corley DA, Kubo A, Levin TR, Block G, Habel L, Zhao W, Leighton P, Quesenberry C, Rumore GJ, Buffler PA (2007) Abdominal Obesity and Body Mass Index as Risk Factors for Barrett's Esophagus. *Gastroenterology* **133**: 34-41

Csendes A, Smok G, Quiroz J, Burdiles P, Rojas J, Castro C, Henriquez A (2002) Clinical, endoscopic, and functional studies in 408 patients with Barrett's esophagus, compared to 174 cases of intestinal metaplasia of the cardia. *Am J Gastroenterol* **97**: 554-560

Curvers WL, Bohmer CJ, Mallant-Hent RC, Naber AH, Ponsioen CIJ, Ragunath K, Singh R, Wallace MB, Wolfsen HC, Wong Kee Song LM, Lindeboom R, Fockens P, Bergman JJ (2008a) Mucosal morphology in Barrett's esophagus: interobserver agreement and role of narrow band imaging. *Endoscopy* **40**: 799-805

Curvers WL, Singh R, Song LM, Wolfsen HC, Ragunath K, Wang K, Wallace MB, Fockens P, Bergman JJ (2008b) Endoscopic tri-modal imaging for detection of early neoplasia in Barrett's oesophagus: a multi-centre feasibility study using high-resolution endoscopy, autofluorescence imaging and narrow band imaging incorporated in one endoscopy system. *Gut* **57**: 167-172

Curvers WL, ten Kate FJ, Krishnadath KK, Visser M, Elzer B, Baak LC, Bohmer C, Mallant-Hent RC, van OA, Naber AH, Scholten P, Busch OR, Blaauwgeers HG, Meijer GA, Bergman JJ (2010) Low-grade dysplasia in Barrett's esophagus: overdiagnosed and underestimated. *Am J Gastroenterol* **105**: 1523-1530

Curvers W, Baak L, Kiesslich R, Van Oijen A, Rabenstein T, Ragunath K, Rey JF, Scholten P, Seitz U, Ten Kate F, Fockens P, Bergman J (2008c) Chromoendoscopy and Narrow-Band Imaging Compared With High-Resolution Magnification Endoscopy in Barrett's Esophagus. *Gastroenterology* **134**: 670-679

Danielsen, H. E. Premalignant changes in DNA organization in mouse liver after diethylnitrosamine treatment. 1991. Univerity of Oslo.

Dawsey SM, Fleischer DE, Wang GQ, Zhou B, Kidwell JA, Lu N, Lewin KJ, Roth MJ, Tio TL, Taylor PR (1998) Mucosal iodine staining improves endoscopic visualization of squamous dysplasia and squamous cell carcinoma of the esophagus in Linxian, China. *Cancer* **83**: 220-231

Degenhardt Y, Greshock J, Laquerre S, Gilmartin AG, Jing J, Richter M, Zhang X, Bleam M, Halsey W, Hughes A, Moy C, Liu-Sullivan N, Powers S, Bachman K, Jackson J, Weber B, Wooster R (2010) Sensitivity of Cancer Cells to Plk1 Inhibitor GSK461364A Is Associated with Loss of p53 Function and Chromosome Instability. *Molecular Cancer Therapeutics* **9**: 2079-2089

Derakhshan MH, Liptrot S, Paul J, Brown IL, Morrison D, McColl KE (2009) Oesophageal and gastric intestinal-type adenocarcinomas show the same male predominance due to a 17 year delayed development in females. *Gut* **58**: 16-23

Devesa SS, Blot WJ, Fraumeni JF, Jr. (1998) Changing patterns in the incidence of esophageal and gastric carcinoma in the United States. *Cancer* **83**: 2049-2053

Dial S, Delaney JA, Barkun AN, Suissa S (2005) Use of gastric acid-suppressive agents and the risk of community-acquired Clostridium difficile-associated disease. *JAMA* **294**: 2989-2995

DiMagno EP, Buxton JL, Regan PT, Hattery RR, Wilson DA, Suarez JR, Green PS (1980) Ultrasonic endoscope. *Lancet* **1**: 629-631

Dimitrova DS, Prokhorova TA, Blow JJ, Todorov IT, Gilbert DM (2002) Mammalian nuclei become licensed for DNA replication during late telophase. *J Cell Sci* **115**: 51-59

Doak SH, Jenkins GJ, Parry EM, D'Souza FR, Griffiths AP, Toffazal N, Shah V, Baxter JN, Parry JM (2003) Chromosome 4 hyperploidy represents an early genetic aberration in premalignant Barrett's oesophagus. *Gut* **52**: 623-628

Doak SH, Jenkins GJS, Parry EM, Griffiths AP, Baxter JN, Parry JM (2004) Differential expression of the MAD2, BUB1 and HSP27 genes in Barrett's oesophagus--their association with aneuploidy and neoplastic progression. *Mutation Research/Fundamental and Molecular Mechanisms of Mutagenesis* **547**: 133-144

Dreyer T, Knoblauch I, Doudkine A, MacAulay CE, Garner D, Palcic B, Popella C (2001) Nuclear texture features for classifying benign vs. dysplastic or malignant squamous epithelium of the larynx. *Anal Quant Cytol Histol* **23**: 193-200

Duan L, Wu AH, Sullivan-Halley J, Bernstein L (2008) Nonsteroidal anti-inflammatory drugs and risk of esophageal and gastric adenocarcinomas in Los Angeles County. *Cancer Epidemiol Biomarkers Prev* **17**: 126-134

Dudderidge TJ, Stoeber K, Loddo M, Atkinson G, Fanshawe T, Griffiths DF, Williams GH (2005) Mcm2, Geminin, and KI67 define proliferative state and are prognostic markers in renal cell carcinoma. *Clin Cancer Res* **11**: 2510-2517

Dulai GS (2002) Surveying the case for surveillance. *Gastroenterology* **122**: 820-823

Dulai GS, Jensen DM, Cortina G, Fontana L, Ippoliti A (2005) Randomized trial of argon plasma coagulation vs. multipolar electrocoagulation for ablation of Barrett's esophagus. *Gastrointest Endosc* **61**: 232-240

Dumot JA, Greenwald BD (2008) Argon plasma coagulation, bipolar cautery, and cryotherapy: ABC's of ablative techniques. *Endoscopy* **40**: 1026-1032

Dumot JA, Vargo JJ, Zuccaro G, Rice TW (2007) Preliminary results of cryotherapy ablation for esophageal high grade dysplasia (HGD) or intra-mucosal cancer (IMC) in high risk non-surgical patients. *Gastrointestinal Endoscopy* **65**: AB110

Dunbar KB, Okolo III P, Montgomery E, Canto MI (2009) Confocal laser endomicroscopy in Barrett's esophagus and endoscopically inapparent Barrett's neoplasia: a prospective, randomized, double-blind, controlled, crossover trial. *Gastrointestinal Endoscopy* **70**: 645-654

Dunkin B, Martinez J, Bejarano P, Smith C, Chang K, Livingstone A, Melvin W (2006) Thin-layer ablation of human esophageal epithelium using a bipolar radiofrequency balloon device. *Surgical Endoscopy* **20**: 125-130

Dunn JM, Thorpe S, Fullarton GM, Smart H, Penman ID, Patel P, Willert RP, Novelli M, Banks MR, Lovat L (2010) Endoscopic Radiofrequency Ablation for HGD or IMC in Barrett's Esophagus - Results From the First 100 Patients Enrolled in the UK RFA Registry. *Gastrointestinal Endoscopy* **71**: AB176

Eckardt VF, Kanzler G, Bernhard G (2001) Life expectancy and cancer risk in patients with Barrett's esophagus: a prospective controlled investigation. *Am J Med* **111**: 33-37

Eckerdt F, Strebhardt K (2006) Polo-like kinase 1: target and regulator of anaphase-promoting complex/cyclosome-dependent proteolysis. *Cancer Res* **66**: 6895-6898

El-Serag HB, Aguirre TV, Davis S (2004) Proton pump inhibitors are associated with reduced incidence of dysplasia in Barrett's esophagus. *Am J Gastroenterol* **99**: 1877-1883

El-Serag HB, Nurgalieva Z, Souza RF, Shaw C, Darlington G (2006) Is genomic evaluation feasible in endoscopic studies of Barrett's esophagus? A pilot study. *Gastrointestinal Endoscopy* **64**: 17-26

Ell C, May A, Gossner L, Pech O, Gunter E, Mayer G, Henrich R, Vieth M, Muller H, Seitz G, Stolte M (2000) Endoscopic mucosal resection of early cancer and high-grade dysplasia in Barrett's esophagus. *Gastroenterology* **118**: 670-677

Ellis IO, Bartlett J, Dowsett M, Humphreys S, Jasani B, Miller K, Pinder SE, Rhodes A, Walker R (2004) Best Practice No 176: Updated recommendations for HER2 testing in the UK. *J Clin Pathol* **57**: 233-237

Emmert-Buck MR, Bonner RF, Smith PD, Chuaqui RF, Zhuang Z, Goldstein SR, Weiss RA, Liotta LA (1996) Laser capture microdissection. *Science* **274**: 998-1001

Esposito MJ, Fuchs A (1994) Computerized image analysis and flow cytometric evaluation of ovarian borderline tumors: a study of 24 cases. *Cytometry* **18**: 218-222

Etienne J, Dorme N, Bourg-Heckly G, Raimbert P, Flejou JF (2004) Photodynamic therapy with green light and m-tetrahydroxyphenyl chlorin for intramucosal adenocarcinoma and high-grade dysplasia in Barrett's esophagus. *Gastrointest Endosc* **59**: 880-889

Evans JA, Bouma BE, Bressner J, Shishkov M, Lauwers GY, Mino-Kenudson M, Nishioka NS, Tearney GJ (2007) Identifying intestinal metaplasia at the squamocolumnar junction by using optical coherence tomography. *Gastrointest Endosc* **65**: 50-56

Evans JA, Nishioka NS (2005) Endoscopic confocal microscopy. *Curr Opin Gastroenterol* **21**: 578-584

Evans JA, Poneros JM, Bouma BE, Bressner J, Halpern EF, Shishkov M, Lauwers GY, Mino-Kenudson M, Nishioka NS, Tearney GJ (2006) Optical coherence tomography to identify intramucosal carcinoma and high-grade dysplasia in Barrett's esophagus. *Clin Gastroenterol Hepatol* **4**: 38-43

Falk GW, Rice TW, Goldblum JR, Richter JE (1999) Jumbo biopsy forceps protocol still misses unsuspected cancer in Barrett's esophagus with high-grade dysplasia. *Gastrointest Endosc* **49**: 170-176

Farrow DC, Vaughan TL, Hansten PD, Stanford JL, Risch HA, Gammon MD, Chow WH, Dubrow R, Ahsan H, Mayne ST, Schoenberg JB, West AB, Rotterdam H, Fraumeni JF, Jr., Blot WJ (1998) Use of aspirin and other nonsteroidal anti-inflammatory drugs and risk of esophageal and gastric cancer. *Cancer Epidemiol Biomarkers Prev* **7**: 97-102

Ferguson HR, Wild CP, Anderson LA, Murphy SJ, Johnston BT, Murray LJ, Watson RG, McGuigan J, Reynolds JV, Hardie LJ (2008) Cyclooxygenase-2 and inducible nitric oxide synthase gene polymorphisms and risk of reflux esophagitis, Barrett's esophagus, and esophageal adenocarcinoma. *Cancer Epidemiol Biomarkers Prev* **17**: 727-731

Fernando HC, Luketich JD, Buenaventura PO, Perry Y, Christie NA (2002) Outcomes of minimally invasive esophagectomy (MIE) for high-grade dysplasia of the esophagus. *European Journal of Cardio-Thoracic Surgery* **22**: 1-6

Fleischer DE, Overholt BF, Sharma VK, Reymunde A, Kimmey MB, Chuttani R, Chang KJ, Muthasamy R, Lightdale CJ, Santiago N, Pleskow DK, Dean PJ, Wang KK (2010) Endoscopic radiofrequency ablation for Barrett's esophagus: 5-year outcomes from a prospective multicenter trial. *Endoscopy* **42**: 781-789

Fleischer DE, Wang GQ, Dawsey S, Tio TL, Newsome J, Kidwell J, Prifti S (1996) Tissue band ligation followed by snare resection (band and snare): a new technique for tissue acquisition in the esophagus. *Gastrointest Endosc* **44**: 68-72

Fleischer DE, Overholt BF, Sharma VK, Reymunde A, Kimmey MB, Chuttani R, Chang KJ, Lightdale CJ, Santiago N, Pleskow DK, Dean PJ, Wang KK (2008) Endoscopic ablation of Barrett's esophagus: a multicenter study with 2.5-year follow-up. *Gastrointestinal Endoscopy* **68**: 867-876

Flejou JF, Svrcek M (2007) Barrett's oesophagus--a pathologist's view. *Histopathology* **50**: 3-14

Fleming KA, Evans M, Ryley KC, Franklin D, Lovell-Badge RH, Morey AL (1992) Optimization of non-isotopic in situ hybridization on formalin-fixed, paraffin-embedded material using digoxigenin-labelled probes and transgenic tissues. *J Pathol* **167**: 9-17

Forcione DG, Hasan T, Ortel BJ, Nishioka NS (2004) Optimization of Aminolevulinic Acid-based Photodynamic Therapy of Barrett's Esophagus with High Grade Dysplasia. *Gastrointestinal Endoscopy* **59**: 251

Foultier MT, Vonarx-Coinsman V, de Brito LX, Morlet L, Robillard N, Patrice T (1994) DNA or cell kinetics flow cytometry analysis of 33 small gastrointestinal cancers treated by photodynamic therapy. *Cancer* **73**: 1595-1607

Fridolin I, Lindberg LG (2000) Optical non-invasive technique for vessel imaging: I. Experimental results. *Phys Med Biol* **45**: 3765-3778

Furuta Y, Kobori O, Shimazu H, Morioka Y, Okuyama Y (1985) A new in vivo staining method, cresyl violet staining, for fiberoptic magnified observation of carcinoma of the gastric mucosa. *Journal of Gastroenterology* **20**: 120-124

Galipeau PC, Li X, Blount PL, Maley CC, Sanchez CA, Odze RD, Ayub K, Rabinovitch PS, Vaughan TL, Reid BJ (2007) NSAIDs modulate CDKN2A, TP53, and DNA content risk for progression to esophageal adenocarcinoma. *PLoS Med* **4**: e67

Galipeau PC, Prevo LJ, Sanchez CA, Longton GM, Reid BJ (1999) Clonal expansion and loss of heterozygosity at chromosomes 9p and 17p in premalignant esophageal (Barrett's) tissue. *J Natl Cancer Inst* **91**: 2087-2095

Ganz RA, Overholt BF, Sharma VK, Fleischer DE, Shaheen NJ, Lightdale CJ, Freeman SR, Pruitt RE, Urayama SM, Gress F, Pavey DA, Branch MS, Savides TJ, Chang KJ, Muthusamy VR, Bohorfoush AG, Pace SC, DeMeester SR, Eysselein VE, Panjehpour M, Triadafilopoulos G (2008) Circumferential ablation of Barrett's esophagus that contains high-grade dysplasia: a U.S. Multicenter Registry. *Gastrointest Endosc* **68**: 35-40

Garcia Rodriguez LA, Ruigomez A, Panes J (2007) Use of acid-suppressing drugs and the risk of bacterial gastroenteritis. *Clin Gastroenterol Hepatol* **5**: 1418-1423

Gatenby P, Ramus J, Caygill C, Shepherd N, Winslet M, Watson A (2009) Routinely diagnosed low-grade dysplasia in Barrett's oesophagus: a population-based study of natural history. *Histopathology* **54**: 814-819

Georgakoudi I, Jacobson BC, Van Dam J, Backman V, Wallace MB, Muller MG, Zhang Q, Badizadegan K, Sun D, Thomas GA, Perelman LT, Feld MS (2001) Fluorescence, reflectance, and light-scattering spectroscopy for evaluating dysplasia in patients with Barrett's esophagus. *Gastroenterology* **120**: 1620-1629

Georgakoudi I, Van Dam J (2003) Characterization of dysplastic tissue morphology and biochemistry in Barrett's esophagus using diffuse reflectance and light scattering spectroscopy. *Gastrointest Endosc Clin N Am* **13**: 297-308

Gerdes J, Lemke H, Baisch H, Wacker HH, Schwab U, Stein H (1984) Cell cycle analysis of a cell proliferation-associated human nuclear antigen defined by the monoclonal antibody Ki-67. *J Immunol* **133**: 1710-1715

Glickman JN, Ormsby AH, Gramlich TL, Goldblum JR, Odze RD (2005) Interinstitutional variability and effect of tissue fixative on the interpretation of a Barrett cytokeratin 7/20 immunoreactivity pattern in Barrett esophagus. *Hum Pathol* **36**: 58-65

Glickman JN, Shahsafaei A, Odze RD (2003) Mucin core peptide expression can help differentiate Barrett's esophagus from intestinal metaplasia of the stomach. *Am J Surg Pathol* **27**: 1357-1365

Goetz M, Toermer T, Vieth M, Dunbar K, Hoffman A, Galle PR, Neurath MF, Delaney P, Kiesslich R (2009) Simultaneous confocal laser endomicroscopy and chromoendoscopy with topical cresyl violet. *Gastrointestinal Endoscopy* **70**: 959-968

Going JJ, Keith WN, Neilson L, Stoeber K, Stuart RC, Williams GH (2002) Aberrant expression of minichromosome maintenance proteins 2 and 5, and Ki-67 in dysplastic squamous oesophageal epithelium and Barrett's mucosa. *Gut* **50**: 373-377

Goldstein NS (2000) Gastric cardia intestinal metaplasia: biopsy follow-up of 85 patients. *Mod Pathol* **13**: 1072-1079

Golsteyn RM, Schultz SJ, Bartek J, Ziemiecki A, Ried T, Nigg EA (1994) Cell cycle analysis and chromosomal localization of human Plk1, a putative homologue of the mitotic kinases Drosophila polo and Saccharomyces cerevisiae Cdc5. *J Cell Sci* **107 (Pt 6)**: 1509-1517

Gomes AJ, Roy HK, Turzhitsky V, Kim Y, Rogers JD, Ruderman S, Stoyneva V, Goldberg MJ, Bianchi LK, Yen E, Kromine A, Jameel M, Backman V (2009) Rectal Mucosal Microvascular Blood Supply Increase Is Associated with Colonic Neoplasia. *Clin Cancer Res* **15**: 3110-3117

Gondrie JJ, Pouw RE, Sondermeijer CM, Peters FP, Curvers WL, Rosmolen WD, Krishnadath KK, Ten KF, Fockens P, Bergman JJ (2008) Stepwise circumferential and focal ablation of Barrett's esophagus with high-grade dysplasia: results of the first prospective series of 11 patients. *Endoscopy* **40**: 359-369

Gonzalez MA, Pinder SE, Callagy G, Vowler SL, Morris LS, Bird K, Bell JA, Laskey RA, Coleman N (2003) Minichromosome maintenance protein 2 is a strong independent prognostic marker in breast cancer. *J Clin Oncol* **21**: 4306-4313

Gossner L, Pech O, May A, Vieth M, Stolte M, Ell C (2006) Comparison of methylene blue-directed biopsies and four-quadrant biopsies in the detection of high-grade intraepithelial neoplasia and early cancer in Barrett's oesophagus. *Dig Liver Dis* **38**: 724-729

Gossner L, Stolte M, Sroka R, Rick K, May A, Hahn EG, Ell C (1998) Photodynamic ablation of high-grade dysplasia and early cancer in Barrett's esophagus by means of 5-aminolevulinic acid. *Gastroenterology* **114**: 448-455

Gray MR, Hall PA, Nash J, Ansari B, Lane DP, Kingsnorth AN (1992) Epithelial proliferation in Barrett's esophagus by proliferating cell nuclear antigen immunolocalization. *Gastroenterology* **103**: 1769-1776

Greenawalt DM, Duong C, Smyth GK, Ciavarella ML, Thompson NJ, Tiang T, Murray WK, Thomas RJ, Phillips WA (2007) Gene expression profiling of esophageal cancer: comparative analysis of Barrett's esophagus, adenocarcinoma, and squamous cell carcinoma. *Int J Cancer* **120**: 1914-1921

Guelrud M, Herrera I (1998) Acetic acid improves identification of remnant islands of Barrett's epithelium after endoscopic therapy. *Gastrointest Endosc* **47**: 512-515

Guelrud M, Herrera I, Essenfeld H, Castro J (2001) Enhanced magnification endoscopy: a new technique to identify specialized intestinal metaplasia in Barrett's esophagus. *Gastrointest Endosc* **53**: 559-565

Guillaud M, Cox D, dler-Storthz K, Malpica A, Staerkel G, Matisic J, van ND, Poulin N, Follen M, Macaulay C (2004) Exploratory analysis of quantitative histopathology of cervical intraepithelial neoplasia: objectivity, reproducibility, malignancy-associated changes, and human papillomavirus. *Cytometry A* **60**: 81-89

Guillaud M, dler-Storthz K, Malpica A, Staerkel G, Matisic J, Van ND, Cox D, Poulin N, Follen M, Macaulay C (2005) Subvisual chromatin changes in cervical epithelium measured by texture image analysis and correlated with HPV. *Gynecol Oncol* **99**: S16-S23

Gupta N, Abrams JA, Early DS, Wani SB, Hovis CE, Vaccaro BJ, Gaddam S, Bansal A, Rastogi A, Edmundowicz SA, Lightdale CJ, Sharma P (2010) Multimodality Endoscopic Therapy for Complete Eradication of Barrett's Esophagus. *Gastroenterology* **139**: e18

Gurjar RS, Backman V, Perelman LT, Georgakoudi I, Badizadegan K, Itzkan I, Dasari RR, Feld MS (2001) Imaging human epithelial properties with polarized light-scattering spectroscopy. *Nat Med* **7**: 1245-1248

Hage M, Siersema PD, Vissers KJ, Dinjens WN, Steyerberg EW, Haringsma J, Kuipers EJ, van Dekken H (2006) Genomic analysis of Barrett's esophagus after ablative therapy: persistence of genetic alterations at tumor suppressor loci. *Int J Cancer* **118**: 155-160

Haigh CR, Attwood SE, Thompson DG, Jankowski JA, Kirton CM, Pritchard DM, Varro A, Dimaline R (2003) Gastrin induces proliferation in Barrett's metaplasia through activation of the CCK2 receptor. *Gastroenterology* **124**: 615-625

Hale GM, Querry MR (1973) Optical-Constants of Water in 200-Nm to 200-Mum Wavelength Region. *Applied Optics* **12**: 555-563

Hamamoto Y, Endo T, Nosho K, Arimura Y, Sato M, Imai K (2004) Usefulness of narrow-band imaging endoscopy for diagnosis of Barrett's esophagus. *J Gastroenterol* **39**: 14-20

Hamilton SR, Smith RR, Cameron JL (1988) Prevalence and characteristics of Barrett esophagus in patients with adenocarcinoma of the esophagus or esophagogastric junction. *Hum Pathol* **19**: 942-948

Hampel H, Abraham NS, El-Serag HB (2005) Meta-analysis: Obesity and the risk for gastroesophageal reflux disease and its complications. *Annals of Internal Medicine* **143**: 199-211

Haralick RM (1979) Statistical and Structural Approaches to Texture. *Proceedings of the IEEE* **67**: 786-804

Haringsma J, Siersema PD, Kuipers EJ (2004) Endoscopic ablation of Barrett's neoplasia. Rotterdam results. *Gastrointestinal Endoscopy* **59**: AB252

Haringsma J, Tytgat GN, Yano H, Iishi H, Tatsuta M, Ogihara T, Watanabe H, Sato N, Marcon N, Wilson BC, Cline RW (2001) Autofluorescence endoscopy: feasibility of detection of GI neoplasms unapparent to white light endoscopy with an evolving technology. *Gastrointest Endosc* **53**: 642-650

Harris JC, Clarke PA, Awan A, Jankowski J, Watson SA (2004) An antiapoptotic role for gastrin and the gastrin/CCK-2 receptor in Barrett's esophagus. *Cancer Res* **64**: 1915-1919

Harrison R, Perry I, Haddadin W (2007) Detection of intestinal metaplasia in Barrett's esophagus: an observational comparator study suggests the need for a minimum of eight biopsies. *Am J Gastro* **102**: 1154-1161

Heath EI, Canto MI, Piantadosi S (2007) Secondary chemoprevention of Barrett's esophagus with celecoxib: results of a randomized trial. *J Natl Cancer Inst* **99**: 545-557

Hedley DW, Friedlander ML, Taylor IW, Rugg CA, Musgrove EA (1983) Method for Analysis of Cellular Dna Content of Paraffin-Embedded Pathological Material Using Flow-Cytometry. *Journal of Histochemistry & Cytochemistry* **31**: 1333-1335

Herrero LA, Pouw RE, Van Vilsteren FG, Sondermeijer C, Kate FJT, Fockens P, Weusten BL, Bergman J (2009) What Are the Outcomes of Endoscopic Radiofrequency Ablation for Very Long Segments of Barrett Esophagus Containing Neoplasia? *Gastrointestinal Endoscopy* **69**: AB116

Herz P, Chen Y, Aguirre A, Fujimoto J, Mashimo H, Schmitt J, Koski A, Goodnow J, Petersen C (2004) Ultrahigh resolution optical biopsy with endoscopic optical coherence tomography. *Opt Express* **12**: 3532-3542

Hillman LC, Chiragakis L, Shadbolt B (2004) Proton-pump inhibitor therapy and the development of dysplasia in patients with Barrett's oesophagus. *Med J Aust* **180**: 387-391

Hillman LC, Chiragakis L, Shadbolt B, Kaye GL, Clarke AC (2008) Effect of proton pump inhibitors on markers of risk for high-grade dysplasia and oesophageal cancer in Barrett's oesophagus. *Aliment Pharmacol Ther* **27**: 321-326

Hirota WK, Loughney TM, Lazas DJ, Maydonovitch CL, Rholl V, Wong RK (1999) Specialized intestinal metaplasia, dysplasia, and cancer of the esophagus and esophagogastric junction: prevalence and clinical data. *Gastroenterology* **116**: 277-285

Hoffman A, Kiesslich R, Bender A, Neurath MF, Nafe B, Herrmann G, Jung M (2006) Acetic acid-guided biopsies after magnifying endoscopy compared with random

biopsies in the detection of Barrett's esophagus: a prospective randomized trial with crossover design. *Gastrointestinal Endoscopy* **64**: 1-8

Hofmann M, Stoss O, Shi D, Buttner R, van d, V, Kim W, Ochiai A, Ruschoff J, Henkel T (2008) Assessment of a HER2 scoring system for gastric cancer: results from a validation study. *Histopathology* **52**: 797-805

Hong MK, Laskin WB, Herman BE, Johnston MH, Vargo JJ, Steinberg SM, Allegra CJ, Johnston PG (1995) Expansion of the Ki-67 proliferative compartment correlates with degree of dysplasia in Barrett's esophagus. *Cancer* **75**: 423-429

Hormi-Carver K, Zhang X, Zhang HY, Whitehead RH, Terada LS, Spechler SJ, Souza RF (2009) Unlike esophageal squamous cells, Barrett's epithelial cells resist apoptosis by activating the nuclear factor-kappaB pathway. *Cancer Res* **69**: 672-677

Hornick JL, Blount PL, Sanchez CA, Cowan DS, Ayub K, Maley CC, Reid BJ, Odze RD (2005) Biologic properties of columnar epithelium underneath reepithelialized squamous mucosa in Barrett's esophagus. *Am J Surg Pathol* **29**: 372-380

Hornick JL, Mino-Kenudson M, Lauwers GY, Liu W, Goyal R, Odze RD (2008) Buried Barrett's epithelium following photodynamic therapy shows reduced crypt proliferation and absence of DNA content abnormalities. *Am J Gastroenterol* **103**: 38-47

Howell MD, Novack V, Grgurich P, Soulliard D, Novack L, Pencina M, Talmor D (2010) Iatrogenic gastric acid suppression and the risk of nosocomial Clostridium difficile infection. *Arch Intern Med* **170**: 784-790

Huang Q, Yu C, Zhang X, Goyal RK (2008) Comparison of DNA histograms by standard flow cytometry and image cytometry on sections in Barrett's adenocarcinoma. *BMC Clin Pathol* **8**: 5

Huang Z (2005) A review of progress in clinical photodynamic therapy. *Technol Cancer Res Treat* **4**: 283-293

Hunt DP, Freeman A, Morris LS, Burnet NG, Bird K, Davies TW, Laskey RA, Coleman N (2002) Early recurrence of benign meningioma correlates with expression of mini-chromosome maintenance-2 protein. *Br J Neurosurg* **16**: 10-15

Inadomi JM, Sampliner R, Lagergren J, Lieberman D, Fendrick AM, Vakil N (2003) Screening and surveillance for Barrett esophagus in high-risk groups: a cost-utility analysis. *Ann Intern Med* **138**: 176-186

Inadomi JM, Somsouk M, Madanick RD, Thomas JP, Shaheen NJ (2009) A cost-utility analysis of ablative therapy for Barrett's esophagus. *Gastroenterology* **136**: 2101-2114

Incarbone R, Bonavina L, Saino G (2002) Outcome of esophageal adenocarcinoma detected during endoscopic biopsy surveillance for Barrett's esophagus. *Surg Endosc* **16**: 263-266

Inoue H, Noguchi O, Saito N, Takeshita K, Endo M (1994) Endoscopic mucosectomy for early cancer using a pre-looped plastic cap. *Gastrointest Endosc* **40**: 263-264

Isenberg G, Sivak MV, Jr., Chak A, Wong RC, Willis JE, Wolf B, Rowland DY, Das A, Rollins A (2005) Accuracy of endoscopic optical coherence tomography in the detection of dysplasia in Barrett's esophagus: a prospective, double-blinded study. *Gastrointest Endosc* **62**: 825-831

Ito Y, Miyoshi E, Sasaki N, Kakudo K, Yoshida H, Tomoda C, Uruno T, Takamura Y, Miya A, Kobayashi K, Matsuzuka F, Matsuura N, Kuma K, Miyauchi A (2004) Polo-like kinase 1 overexpression is an early event in the progression of papillary carcinoma. *Br J Cancer* **90**: 414-418

Jacobson BC, Chan AT, Giovannucci EL, Fuchs CS (2009) Body mass index and Barrett's oesophagus in women. *Gut* **58**: 1460-1466

Jagoe R, Sowter C, Slavin G (1984) Shape and texture analysis of liver cell nuclei in hepatomas by computer aided microscopy. *J Clin Pathol* **37**: 755-762

Jankowski J, Graham T, Harrison R (2010) Authors' response. *Gut* **59**: 1158

Jansen JB, Klinkenberg-Knol EC, Meuwissen SG, De Bruijne JW, Festen HP, Snel P, Luckers AE, Biemond I, Lamers CB (1990) Effect of long-term treatment with omeprazole on serum gastrin and serum group A and C pepsinogens in patients with reflux esophagitis. *Gastroenterology* **99**: 621-628

Jaskiewicz K, Venter FS, Marasas WF (1987) Cytopathology of the esophagus in Transkei. *Journal of the National Cancer Institute* **79**: 961-967

Javaid B, Watt P, Krasner N (2002) Photodynamic therapy (PDT) for oesophageal dysplasia and early carcinoma with mTHPC (m-tetrahydroxyphenyl chlorin): a preliminary study. *Lasers Med Sci* **17**: 51-56

Jenkins GJ, Cronin J, Alhamdani A, Rawat N, D'Souza F, Thomas T, Eltahir Z, Griffiths AP, Baxter JN (2008) The bile acid deoxycholic acid has a non-linear dose response for DNA damage and possibly NF-kappaB activation in oesophageal cells, with a mechanism of action involving ROS. *Mutagenesis* **23**: 399-405

Jenkins GJ, D'Souza FR, Suzen SH, Eltahir ZS, James SA, Parry JM, Griffiths PA, Baxter JN (2007) Deoxycholic acid at neutral and acid pH, is genotoxic to oesophageal cells through the induction of ROS: The potential role of anti-oxidants in Barrett's oesophagus. *Carcinogenesis* **28**: 136-142

Jin Z, Cheng Y, Gu W, Zheng Y, Sato F, Mori Y, Olaru AV, Paun BC, Yang J, Kan T, Ito T, Hamilton JP, Selaru FM, Agarwal R, David S, Abraham JM, Wolfsen HC, Wallace MB, Shaheen NJ, Washington K, Wang J, Canto MI, Bhattacharyya A, Nelson MA, Wagner PD, Romero Y, Wang KK, Feng Z, Sampliner RE, Meltzer SJ (2009) A multicenter, double-blinded validation study of methylation biomarkers for progression prediction in Barrett's esophagus. *Cancer Res* **69**: 4112-4115

Johnston MH, Eastone JA, Horwhat JD, Cartledge J, Mathews JS, Foggy JR (2005) Cryoablation of Barrett's esophagus: a pilot study. *Gastrointest Endosc* **62**: 842-848

Jorgensen T, Yogesan K, Tveter KJ, Skjorten F, Danielsen HE (1996) Nuclear texture analysis: A new prognostic tool in metastatic prostate cancer. *Cytometry* **24**: 277-283

Kadri SR, Lao-Sirieix P, O'Donovan M, Debiram I, Das M, Blazeby JM, Emery J, Boussioutas A, Morris H, Walter FM, Pharoah P, Hardwick RH, Fitzgerald RC (2010) Acceptability and accuracy of a non-endoscopic screening test for Barrett's oesophagus in primary care: cohort study. *BMJ* **341**: c4372

Kaern J, Wetteland J, Trope CG, Farrants GW, Juhng SW, Pettersen EO, Reith A, Danielsen HE (1992) Comparison between flow cytometry and image cytometry in ploidy distribution assessments in gynecologic cancer. *Cytometry* **13**: 314-321

Kakeji Y, Yamaguchi S, Yoshida D, Tanoue K, Ueda M, Masunari A, Utsunomiya T, Imamura M, Honda H, Maehara Y, Hashizume M (2006) Development and assessment

of morphologic criteria for diagnosing gastric cancer using confocal endomicroscopy: an ex vivo and in vivo study. *Endoscopy* **38**: 886-890

Kaptain S, Tan LK, Chen B (2001) Her-2/neu and breast cancer. *Diagn Mol Pathol* **10**: 139-152

Kara MA, Bergman JJ (2006) Autofluorescence Imaging and Narrow-Band Imaging for the Detection of Early Neoplasia in Patients with Barrett's Esophagus. *Endoscopy* **38**: 627-631

Kara MA, Peters FP, Rosmolen WD, Krishnadath KK, ten Kate FJ, Fockens P, Bergman JJ (2005a) High-resolution endoscopy plus chromoendoscopy or narrow-band imaging in Barrett's esophagus: a prospective randomized crossover study. *Endoscopy* **37**: 929-936

Kara MA, Peters FP, ten Kate FJ, Van Deventer SJ, Fockens P, Bergman JJ (2005b) Endoscopic video autofluorescence imaging may improve the detection of early neoplasia in patients with Barrett's esophagus. *Gastrointest Endosc* **61**: 679-685

Kara MA, Smits ME, Rosmolen WD, Bultje AC, ten Kate FJ, Fockens P, Tytgat GN, Bergman JJ (2005c) A randomized crossover study comparing light-induced fluorescence endoscopy with standard videoendoscopy for the detection of early neoplasia in Barrett's esophagus. *Gastrointest Endosc* **61**: 671-678

Kaur BS, Ouatu-Lascar R, Omary MB, Triadafilopoulos G (2000) Bile salts induce or blunt cell proliferation in Barrett's esophagus in an acid-dependent fashion. *Am J Physiol Gastrointest Liver Physiol* **278**: G1000-G1009

Kaur BS, Triadafilopoulos G (2002) Acid- and bile-induced PGE(2) release and hyperproliferation in Barrett's esophagus are COX-2 and PKC-epsilon dependent. *Am J Physiol Gastrointest Liver Physiol* **283**: G327-G334

Kayes OJ, Loddo M, Patel N, Patel P, Minhas S, Ambler G, Freeman A, Wollenschlaeger A, Ralph DJ, Stoeber K, Williams GH (2009) DNA Replication Licensing Factors and Aneuploidy Are Linked to Tumor Cell Cycle State and Clinical Outcome in Penile Carcinoma. *Clin Cancer Res* **15**: 7335-7344

Kearney PM, Baigent C, Godwin J, Halls H, Emberson JR, Patrono C (2006) Do selective cyclo-oxygenase-2 inhibitors and traditional non-steroidal anti-inflammatory

drugs increase the risk of atherothrombosis? Meta-analysis of randomised trials. *BMJ* **332**: 1302-1308

Kelsen DP, Winter KA, Gunderson LL, Mortimer J, Estes NC, Haller DG, Ajani JA, Kocha W, Minsky BD, Roth JA, Willett CG (2007) Long-term results of RTOG trial 8911 (USA Intergroup 113): a random assignment trial comparison of chemotherapy followed by surgery compared with surgery alone for esophageal cancer. *J Clin Oncol* **25**: 3719-3725

Kelty CJ, Ackroyd R, Brown NJ, Brown SB, Reed MW (2004a) Comparison of high- vs low-dose 5-aminolevulinic acid for photodynamic therapy of Barrett's esophagus. *Surg Endosc* **18**: 452-458

Kelty CJ, Ackroyd R, Brown NJ, Stephenson TJ, Stoddard CJ, Reed MW (2004b) Endoscopic ablation of Barrett's oesophagus: a randomized-controlled trial of photodynamic therapy vs. argon plasma coagulation. *Aliment Pharmacol Ther* **20**: 1289-1296

Kelty CJ, Gough MD, Van Wyk Q, Stephenson TJ, Ackroyd R (2007) Barrett's oesophagus: Intestinal metaplasia is not essential for cancer risk. *Scand J Gastroenterol* 1-4

Kendall C, Stone N, Shepherd N, Geboes K, Warren B, Bennett R, Barr H (2003) Raman spectroscopy, a potential tool for the objective identification and classification of neoplasia in Barrett's oesophagus. *J Pathol* **200**: 602-609

Kerkhof M, van Dekken H, Steyerberg EW, Meijer GA, Mulder AH, de Bruine A, Driessen A, ten Kate FJ, Kusters JG, Kuipers EJ, Siersema PD (2007) Grading of dysplasia in Barrett's oesophagus: substantial interobserver variation between general and gastrointestinal pathologists. *Histopathology* **50**: 920-927

Kiesslich R, Burg J, Vieth M, Gnaendiger J, Enders M, Delaney P, Polglase A, McLaren W, Janell D, Thomas S, Nafe B, Galle PR, Neurath MF (2004) Confocal laser endoscopy for diagnosing intraepithelial neoplasias and colorectal cancer in vivo. *Gastroenterology* **127**: 706-713

Kiesslich R, Gossner L, Goetz M, Dahlmann A, Vieth M, Stolte M, Hoffman A, Jung M, Nafe B, Galle PR, Neurath MF (2006) In vivo histology of Barrett's esophagus and

associated neoplasia by confocal laser endomicroscopy. *Clin Gastroenterol Hepatol* **4**: 979-987

Kiesslich R, Hahn M, Herrmann G, Jung M (2001) Screening for specialized columnar epithelium with methylene blue: Chromoendoscopy in patients with Barrett's esophagus and a normal control group. *Gastrointestinal Endoscopy* **53**: 47-52

Kim JM, Yamada M, Masai H (2003) Functions of mammalian Cdc7 kinase in initiation/monitoring of DNA replication and development. *Mutat Res* **532**: 29-40

Knecht R, Elez R, Oechler M, Solbach C, Ilberg Cv, Strebhardt K (1999) Prognostic Significance of Polo-like Kinase (PLK) Expression in Squamous Cell Carcinomas of the Head and Neck. *Cancer Res* **59**: 2794-2797

Ko MA, Rosario CO, Hudson JW, Kulkarni S, Pollett A, Dennis JW, Swallow CJ (2005) Plk4 haploinsufficiency causes mitotic infidelity and carcinogenesis. *Nat Genet* **37**: 883-888

Kopelovich L, Henson DE, Gazdar AF, Dunn B, Srivastava S, Kelloff GJ, Greenwald P (1999) Surrogate anatomic/functional sites for evaluating cancer risk: an extension of the field effect. *Clin Cancer Res* **5**: 3899-3905

Kovacs BJ, Chen YK, Lewis TD, DeGuzman LJ, Thompson KS (1999) Successful reversal of Barrett's esophagus with multipolar electrocoagulation despite inadequate acid suppression. *Gastrointest Endosc* **49**: 547-553

Kreitz S, Fackelmayer FO, Gerdes J, Knippers R (2000) The proliferation-specific human Ki-67 protein is a constituent of compact chromatin. *Exp Cell Res* **261**: 284-292

Kriete A, Schaffer R, Harms H, Aus HM (1987) On-line transmission electron microscopic image analysis of chromatin texture for differentiation of thyroid gland tumors. *Anal Quant Cytol Histol* **9**: 268-272

Kuester D, Dar AA, Moskaluk CC, Krueger S, Meyer F, Hartig R, Stolte M, Malfertheiner P, Lippert H, Roessner A, El-Rifai W, Schneider-Stock R (2007) Early involvement of death-associated protein kinase promoter hypermethylation in the carcinogenesis of Barrett's esophageal adenocarcinoma and its association with clinical progression. *Neoplasia* **9**: 236-245

Kulkarni AA, Loddo M, Leo E, Rashid M, Eward KL, Fanshawe TR, Butcher J, Frost A, Ledermann JA, Williams GH, Stoeber K (2007) DNA replication licensing factors and aurora kinases are linked to aneuploidy and clinical outcome in epithelial ovarian carcinoma. *Clin Cancer Res* **13**: 6153-6161

Kulkarni AA, Kingsbury SR, Tudzarova S, Hong HK, Loddo M, Rashid M, Rodriguez-Acebes S, Prevost AT, Ledermann JA, Stoeber K, Williams GH (2009) Cdc7 Kinase Is a Predictor of Survival and a Novel Therapeutic Target in Epithelial Ovarian Carcinoma. *Clin Cancer Res* **15**: 2417-2425

Lagergren J (2005) Adenocarcinoma of oesophagus: what exactly is the size of the problem and who is at risk? *Gut* **54 Suppl 1**: i1-i5

Lagergren J, Bergstrom R, Lindgren A, Nyren O (1999a) Symptomatic gastroesophageal reflux as a risk factor for esophageal adenocarcinoma. *N Engl J Med* **340**: 825-831

Lagergren J, Bergstrom R, Nyren O (1999b) Association between body mass and adenocarcinoma of the esophagus and gastric cardia. *Ann Intern Med* **130**: 883-890

Laitakari R, Laippala P, Isolauri J (1995) Barrett's oesophagus is not a risk factor for colonic neoplasia: a case-control study. *Ann Med* **27**: 499-502

Lake RJ, Jelinek WR (1993) Cell cycle- and terminal differentiation-associated regulation of the mouse mRNA encoding a conserved mitotic protein kinase. *Mol Cell Biol* **13**: 7793-7801

Lambert R, Rey JF, Sankaranarayanan R (2003) Magnification and Chromoscopy with the Acetic Acid Test. *Endoscopy* **35**: 437-445

Lane DP (1992) Cancer. p53, guardian of the genome. *Nature* **358**: 15-16

Lantz H, Vakil N (2003) Barrett's esophagus and argon plasma coagulation: buried trouble? *Am J Gastroenterol* **98**: 1647-1649

Lanza G, Gafa R, Santini A, Maestri I, Dubini A, Gilli G, Cavazzini L (1998) Prognostic significance of DNA ploidy in patients with stage II and stage III colon carcinoma: a prospective flow cytometric study. *Cancer* **82**: 49-59

Lao-Sirieix P, Boussioutas A, Kadri SR, O'Donovan M, Debiram I, Das M, Harihar L, Fitzgerald RC (2009) Non-endoscopic screening biomarkers for Barrett's oesophagus: from microarray analysis to the clinic. *Gut* **58**: 1451-1459

Lao-Sirieix P, Rous B, O'Donovan M, Hardwick RH, Debiram I, Fitzgerald RC (2007) Non-endoscopic immunocytological screening test for Barrett's oesophagus. *Gut* **56**: 1033-1034

Lauwers GY, Forcione DG, Nishioka NS, Deshpande V, Lisovsky MY, Brugge WR, Mino-Kenudson M (2009) Novel endoscopic therapeutic modalities for superficial neoplasms arising in Barrett's esophagus: a primer for surgical pathologists. *Mod Pathol* **22**: 489-498

Lee AKC, Dugan J, Hamilton WM, Cook L, Heatley G, Kamat B, Silverman ML (1991) Quantitative Dna Analysis in Breast Carcinomas - A Comparison Between Image-Analysis and Flow-Cytometry. *Mod Pathol* **4**: 178-182

Lee JH, Kim JW, Cho YK, Sohn CI, Jeon WK, Kim BI, Cho EY (2003) Detection of colorectal adenomas by routine chromoendoscopy with indigocarmine. *Am J Gastroenterol* **98**: 1284-1288

Leedham SJ, Preston SL, McDonald SA, Elia G, Bhandari P, Poller D, Harrison R, Novelli MR, Jankowski JA, Wright NA (2008) Individual crypt genetic heterogeneity and the origin of metaplastic glandular epithelium in human Barrett's oesophagus. *Gut* **57**: 1041-1048

Lei M, Tye BK (2001) Initiating DNA synthesis: from recruiting to activating the MCM complex. *J Cell Sci* **114**: 1447-1454

Leung KK, Maru D, Abraham S, Hofstetter WL, Mehran R, Anandasabapathy S (2009) Optical EMR: confocal endomicroscopy-targeted EMR of focal high-grade dysplasia in Barrett's esophagus. *Gastrointest Endosc* **69**: 170-172

Levine DS, Haggitt RC, Blount PL, Rabinovitch PS, Rusch VW, Reid BJ (1993) An endoscopic biopsy protocol can differentiate high-grade dysplasia from early adenocarcinoma in Barrett's esophagus. *Gastroenterology* **105**: 40-50

Levine DS, Reid BJ, Haggitt RC, Rubin CE, Rabinovitch PS (1989) Correlation of ultrastructural aberrations with dysplasia and flow cytometric abnormalities in Barrett's epithelium. *Gastroenterology* **96**: 355-367

Lim CH, Treanor D, Dixon MF, Axon AT (2007) Low-grade dysplasia in Barrett's esophagus has a high risk of progression. *Endoscopy* **39**: 581-587

Lin O, Schembre DB, KM (2007) Blinded comparison of esophageal capsule endoscopy versus conventional endoscopy for diagnosis of Barrett's esophagus in patients with chronic gastroesophageal reflux. *Gastrointest Endosc* **65**: 577-583

Lindahl B, Ranstam J, Willen R (1994) Five year survival rate in endometrial carcinoma stages I--II: influence of degree of tumour differentiation, age, myometrial invasion and DNA content. *Br J Obstet Gynaecol* **101**: 621-625

Linsky A, Gupta K, Lawler EV, Fonda JR, Hermos JA (2010) Proton pump inhibitors and risk for recurrent Clostridium difficile infection. *Arch Intern Med* **170**: 772-778

Liu H, Li YQ, Yu T, Zhao YA, Zhang JP, Zuo XL, Li CQ, Guo YT, Zhang TG (2009a) Confocal laser endomicroscopy for superficial esophageal squamous cell carcinoma. *Endoscopy* **41**: 99-106

Liu W, Hahn H, Odze RD, Goyal RK (2009b) Metaplastic esophageal columnar epithelium without goblet cells shows DNA content abnormalities similar to goblet cell-containing epithelium. *Am J Gastroenterol* **104**: 816-824

Liu Y, Brand RE, Turzhitsky V, Kim YL, Roy HK, Hasabou N, Sturgis C, Shah D, Hall C, Backman V (2007) Optical Markers in Duodenal Mucosa Predict the Presence of Pancreatic Cancer. *Clin Cancer Res* **13**: 4392-4399

Loddo M, Kingsbury SR, Rashid M, Proctor I, Holt C, Young J, El-Sheikh S, Falzon M, Eward KL, Prevost T, Sainsbury R, Stoeber K, Williams GH (2009) Cell-cycle-phase progression analysis identifies unique phenotypes of major prognostic and predictive significance in breast cancer. *Br J Cancer* **100**: 959-970

Lofgren LA, Ronn AM, Nouri M, Lee CJ, Yoo D, Steinberg BM (1995) Efficacy of intravenous delta-aminolaevulinic acid photodynamic therapy on rabbit papillomas. *Br J Cancer* **72**: 857-864

Loh CS, MacRobert AJ, Buonaccorsi G, Krasner N, Bown SG (1996) Mucosal ablation using photodynamic therapy for the treatment of dysplasia: an experimental study in the normal rat stomach. *Gut* **38**: 71-78

Loughney T, Maydonovitch CL, Wong RK (1998) Esophageal manometry and ambulatory 24-hour pH monitoring in patients with short and long segment Barrett's esophagus. *Am J Gastroenterol* **93**: 916-919

Lovat LB, Jamieson NF, Novelli MR, Mosse CA, Selvasekar C, Mackenzie GD, Thorpe SM, Bown SG (2005) Photodynamic therapy with m-tetrahydroxyphenyl chlorin for high-grade dysplasia and early cancer in Barrett's columnar lined esophagus. *Gastrointest Endosc* **62**: 617-623

Lovat LB, Johnson K, Mackenzie GD, Clark BR, Novelli MR, Davies S, O'Donovan M, Selvasekar C, Thorpe SM, Pickard D, Fitzgerald RC, Fearn T, Bigio I, Bown SG (2006) Elastic scattering spectroscopy accurately detects high grade dysplasia and cancer in Barrett's oesophagus. *Gut* **55**: 1078-1083

MacInnis RJ, English DR, Hopper JL, Giles GG (2006) Body size and composition and the risk of gastric and oesophageal adenocarcinoma. *Int J Cancer* **118**: 2628-2631

Mackenzie, G. D. Novel technologies for the diagnosis and treatment of high risk patients in Barrett's oesophagus. 2008. University College London, UK.

Mackenzie GD, Dunn JM, Novelli MR, Mosse S, Thorpe SM, Bown SG, Lovat LB (2008) Preliminary results of a randomised controlled trial into the safety and efficacy of ala versus photofrin photodynamic therapy for high grade dysplasia in Barrett's oesophagus. *Gut* **57**: A14

Mackenzie GD, Dunn JM, Selvasekar CR, Mosse CA, Thorpe SM, Novelli MR, Bown SG, Lovat LB (2009) Optimal conditions for successful ablation of high-grade dysplasia in Barrett's oesophagus using aminolaevulinic acid photodynamic therapy. *Lasers Med Sci* **24**: 729-734

Mackenzie GD, Jamieson NF, Novelli MR, Mosse CA, Clark BR, Thorpe SM, Bown SG, Lovat LB (2007a) How light dosimetry influences the efficacy of photodynamic therapy with 5-aminolaevulinic acid for ablation of high-grade dysplasia in Barrett's esophagus. *Lasers Med Sci* **23**: 203-210

Mackenzie GD, Oukrif D, Green S, Novelli MR, Bown SG, Lovat LB (2007b) Elastic scattering spectroscopy for the detection of aneuploidy in Barrett's oesophagus. *Gut* **56**: A71

Madisch A, Miehlke S, Bayerdorffer E, Wiedemann B, Antos D, Sievert A, Vieth M, Stolte M, Schulz H (2005) Long-term follow-up after complete ablation of Barrett's esophagus with argon plasma coagulation. *World J Gastroenterol* **11**: 1182-1186

Maley CC, Galipeau PC, Li X, Sanchez CA, Paulson TG, Blount PL, Reid BJ (2004) The combination of genetic instability and clonal expansion predicts progression to esophageal adenocarcinoma. *Cancer Res* **64**: 7629-7633

Marcus SL, Sobel RS, Golub AL, Carroll RL, Lundahl S, Shulman DG (1996) Photodynamic therapy (PDT) and photodiagnosis (PD) using endogenous photosensitization induced by 5-aminolevulinic acid (ALA): current clinical and development status. *J Clin Laser Med Surg* **14**: 59-66

Martin FL, Fullwood NJ (2007) Raman vs. Fourier transform spectroscopy in diagnostic medicine. *Proc Natl Acad Sci U S A* **104**: E1

May A, Gossner L, Pech O, Fritz A, Gunter E, Mayer G, Muller H, Seitz G, Vieth M, Stolte M, Ell C (2002) Local endoscopic therapy for intraepithelial high-grade neoplasia and early adenocarcinoma in Barrett's oesophagus: acute-phase and intermediate results of a new treatment approach. *Eur J Gastroenterol Hepatol* **14**: 1085-1091

McGarry TJ, Kirschner MW (1998) Geminin, an inhibitor of DNA replication, is degraded during mitosis. *Cell* **93**: 1043-1053

Meining A, Rosch T, Kiesslich R, Muders M, Sax F, Heldwein W (2004) Inter- and Intra-Observer Variability of Magnification Chromoendoscopy for Detecting Specialized Intestinal Metaplasia at the Gastroesophageal Junction. *Endoscopy* **36**: 160-164

Meining A, Saur D, Bajbouj M, Becker V, Peltier E, Hofler H, von Weyhern CH, Schmid RM, Prinz C (2007) In vivo histopathology for detection of gastrointestinal neoplasia with a portable, confocal miniprobe: an examiner blinded analysis. *Clin Gastroenterol Hepatol* **5**: 1261-1267

Mendez J, Stillman B (2000) Chromatin association of human origin recognition complex, cdc6, and minichromosome maintenance proteins during the cell cycle: assembly of prereplication complexes in late mitosis. *Mol Cell Biol* **20**: 8602-8612

Merry AHH, Schouten LJ, Goldbohm RA, van den Brandt PA (2007) Body mass index, height and risk of adenocarcinoma of the oesophagus and gastric cardia: a prospective cohort study. *Gut* **56**: 1503-1511

Minami S, Gotoda T, Ono H, Oda I, Hamanaka H (2006) Complete endoscopic closure of gastric perforation induced by endoscopic resection of early gastric cancer using endoclips can prevent surgery (with video). *Gastrointestinal Endoscopy* **63**: 596-601

Mino-Kenudson M, Ban S, Ohana M, Puricelli W, Deshpande V, Shimizu M, Nishioka NS, Lauwers GY (2007a) Buried dysplasia and early adenocarcinoma arising in barrett esophagus after porfimer-photodynamic therapy. *Am J Surg Pathol* **31**: 403-409

Mino-Kenudson M, Hull MJ, Brown I, Muzikansky A, Srivastava A, Glickman J, Park DY, Zuckerberg L, Misdraji J, Odze RD, Lauwers GY (2007b) EMR for Barrett's esophagus-related superficial neoplasms offers better diagnostic reproducibility than mucosal biopsy. *Gastrointest Endosc* **66**: 660-666

Mlkvy P, Messmann H, Regula J, Conio M, Pauer M, Millson CE, MacRobert AJ, Bown SG (1998) Photodynamic therapy for gastrointestinal tumors using three photosensitizers - ALA induced PPIX, Photofrin(R) and MTHPC. A pilot study. *Neoplasma* **45**: 157-161

Modiano N, Gerson L (2009) Risk factors for the detection of Barrett's esophagus in patients with erosive esophagitis. *Gastrointestinal Endoscopy* **69[6]**: 1014-1020.

Mohammed IA, Streutker CJ, Riddell RH (2002) Utilization of cytokeratins 7 and 20 does not differentiate between Barrett's esophagus and gastric cardiac intestinal metaplasia. *Mod Pathol* **15**: 611-616

Moll R, Mitze M, Frixen UH, Birchmeier W (1993) Differential loss of E-cadherin expression in infiltrating ductal and lobular breast carcinomas. *Am J Pathol* **143**: 1731-1742

Montgomery E, Goldblum JR, Greenson JK, Haber MM, Lamps LW, Lauwers GY, Lazenby AJ, Lewin DN, Robert ME, Washington K, Zahurak ML, Hart J (2001)

Dysplasia as a predictive marker for invasive carcinoma in Barrett esophagus: a follow-up study based on 138 cases from a diagnostic variability study. *Hum Pathol* **32**: 379-388

Moons LM, Kuipers EJ, Rygiel AM, Groothuismink AZ, Geldof H, Bode WA, Krishnadath KK, Bergman JJ, van Vliet AH, Siersema PD, Kusters JG (2007) COX-2 CA-haplotype is a risk factor for the development of esophageal adenocarcinoma. *Am J Gastroenterol* **102**: 2373-2379

Morales TG, Camargo E, Bhattacharyya A, Sampliner RE (2000) Long-term follow-up of intestinal metaplasia of the gastric cardia. *Am J Gastroenterol* **95**: 1677-1680

Morgan J, Petrucci CM (2009) The effect of ALA/PpIX PDT on putative cancer stem cells in tumor side populations. *Proceedings of SPIE*. Ed Kessel, David H. **7380[1]**: 738011-738019.

Mork H, Al Taie O, Berlin F, Kraus MR, Scheurlen M (2007) High recurrence rate of Barrett's epithelium during long-term follow-up after argon plasma coagulation. *Scand J Gastroenterol* **42**: 23-27

Morris CD, Byrne JP, Armstrong GR, Attwood SE (2001) Prevention of the neoplastic progression of Barrett's oesophagus by endoscopic argon beam plasma ablation. *Br J Surg* **88**: 1357-1362

Mourant JR, Canpolat M, Brocker C, Esponda-Ramos O, Johnson TM, Matanock A, Stetter K, Freyer JP (2000) Light scattering from cells: the contribution of the nucleus and the effects of proliferative status. *J Biomed Opt* **5**: 131-137

Mourant JR, Hielscher AH, Eick AA, Johnson TM, Freyer JP (1998) Evidence of intrinsic differences in the light scattering properties of tumorigenic and nontumorigenic cells. *Cancer Cytopathology* **84**: 366-374

Muller MG, Valdez TA, Georgakoudi I, Backman V, Fuentes C, Kabani S, Laver N, Wang Z, Boone CW, Dasari RR, Shapshay SM, Feld MS (2003) Spectroscopic detection and evaluation of morphologic and biochemical changes in early human oral carcinoma. *Cancer* **97**: 1681-1692

Murata A, Akahoshi K, Sumida Y, Yamamoto H, Nakamura K, Nawata H (2007) Prospective randomized trial of transnasal versus peroral endoscopy using an ultrathin videoendoscope in unsedated patients. *J Gastroenterol Hepatol* **22**: 482-485

Murray L, Sedo A, Scott M, McManus D, Sloan JM, Hardie LJ, Forman D, Wild CP (2006) TP53 and progression from Barrett's metaplasia to oesophageal adenocarcinoma in a UK population cohort. *Gut* **55(10)**: 1390–1397

Murray L, Watson P, Johnston B, Sloan J, Mainie IML, Gavin A (2003) Risk of adenocarcinoma in Barrett's oesophagus: population based study. *BMJ* **327**: 534-535

Mycek MA, Schomacker KT, Nishioka NS (1998) Colonic polyp differentiation using time-resolved autofluorescence spectroscopy. *Gastrointest Endosc* **48**: 390-394

Naef AP, Savary M, Ozzello L (1975) Columnar-lined lower esophagus: an acquired lesion with malignant predisposition. Report on 140 cases of Barrett's esophagus with 12 adenocarcinomas. *J Thorac Cardiovasc Surg* **70**: 826-835

Nehra D, Howell P, Williams CP, Pye JK, Beynon J (1999) Toxic bile acids in gastro-oesophageal reflux disease: influence of gastric acidity. *Gut* **44**: 598-602

Newnham A, Quinn MJ, Babb P, Kang JY, Majeed A (2003) Trends in oesophageal and gastric cancer incidence, mortality and survival in England and Wales 1971-1998/1999. *Alimentary Pharmacology & Therapeutics* **17**: 655-664

Ngamruengphong S, Sharma VK, Das A (2009) Diagnostic yield of methylene blue chromoendoscopy for detecting specialized intestinal metaplasia and dysplasia in Barrett's esophagus: a meta-analysis. *Gastrointestinal Endoscopy* **69**: 1021-1028

Nielsen B, Albregtsen F, Danielsen HE (2004) Low dimensional adaptive texture feature vectors from class distance and class difference matrices. *IEEE Trans Med Imaging* **23**: 73-84

Nielsen B, Albregtsen F, Danielsen HE (2008) Statistical nuclear texture analysis in cancer research: a review of methods and applications. *Crit Rev Oncog* **14**: 89-164

Nielsen B, Danielsen HE (2006) Prognostic value of adaptive textural features--the effect of standardizing nuclear first-order gray level statistics and mixing information from nuclei having different area. *Cell Oncol* **28**: 85-95

Niepsuj K, Niepsuj G, Cebula W, Zieleznik W, Adamek M, Sielanczyk A, Adamczyk J, Kurek J, Sieron A (2003) Autofluorescence endoscopy for detection of high-grade dysplasia in short-segment Barrett's esophagus. *Gastrointest Endosc* **58**: 715-719

Nigro JJ, Hagen JA, Demeester TR (1999) Occult esophageal adenocarcinoma. Extent of disease and implications for effective therapy. *Ann Surg* **230**: 433-440

Nilsson M, Johnsen R, Ye W, Hveem K, Lagergren J (2003) Obesity and Estrogen as Risk Factors for Gastroesophageal Reflux Symptoms. *JAMA* **290**: 66-72

Oberg S, Demeester TR, Peters JH, Hagen JA, Nigro JJ, DeMeester SR, Theisen J, Campos GM, Crookes PF (1999) The extent of Barrett's esophagus depends on the status of the lower esophageal sphincter and the degree of esophageal acid exposure. *J Thorac Cardiovasc Surg* **117**: 572-580

Obszynska JA, Atherfold PA, Nanji M, Glancy D, Santander S, Graham TA, Otto WR, West K, Harrison RF, Jankowski JA (2010) Long-term proton pump induced hypergastrinaemia does induce lineage-specific restitution but not clonal expansion in benign Barrett's oesophagus in vivo. *Gut* **59**: 156-163

Olliver JR, Wild CP, Sahay P, Dexter S, Hardie LJ (2003) Chromoendoscopy with methylene blue and associated DNA damage in Barrett's oesophagus. *Lancet* **362**: 373-374

Ormsby AH, Vaezi MF, Richter JE, Goldblum JR, Rice TW, Falk GW, Gramlich TL (2000) Cytokeratin immunoreactivity patterns in the diagnosis of short-segment Barrett's esophagus. *Gastroenterology* **119**: 683-690

Ortner MA, Ebert B, Hein E, Zumbusch K, Nolte D, Sukowski U, Weber-Eibel J, Fleige B, Dietel M, Stolte M, Oberhuber G, Porschen R, Klump B, Hortnagl H, Lochs H, Rinneberg H (2003) Time gated fluorescence spectroscopy in Barrett's oesophagus. *Gut* **52**: 28-33

Ottesen GL, Christensen IJ, Larsen JK, Larsen J, Baldetorp B, Linden T, Hansen B, Andersen J (2000) Carcinoma in situ of the breast: correlation of histopathology to immunohistochemical markers and DNA ploidy. *Breast Cancer Res Treat* **60**: 219-226

Ouatu-Lascar R, Fitzgerald RC, Triadafilopoulos G (1999) Differentiation and proliferation in Barrett's esophagus and the effects of acid suppression. *Gastroenterology* **117**: 327-335

Overholt BF, Lightdale CJ, Wang KK, Canto MI, Burdick S, Haggitt RC, Bronner MP, Taylor SL, Grace MG, Depot M (2005) Photodynamic therapy with porfimer sodium for ablation of high-grade dysplasia in Barrett's esophagus: international, partially blinded, randomized phase III trial. *Gastrointest Endosc* **62**: 488-498

Overholt BF, Panjehpour M, Ayres M (1997) Photodynamic therapy for Barrett's esophagus: cardiac effects. *Lasers Surg Med* **21**: 317-320

Overholt BF, Panjehpour M, Halberg DL (2003) Photodynamic therapy for Barrett's esophagus with dysplasia and/or early stage carcinoma: long-term results. *Gastrointest Endosc* **58**: 183-188

Overholt BF, Panjehpour M, Haydek JM (1999) Photodynamic therapy for Barrett's esophagus: follow-up in 100 patients. *Gastrointest Endosc* **49**: 1-7

Overholt BF, Wang KK, Burdick JS, Lightdale CJ, Kimmey M, Nava HR, Sivak MV, Jr., Nishioka N, Barr H, Marcon N, Pedrosa M, Bronner MP, Grace M, Depot M (2007) Five-year efficacy and safety of photodynamic therapy with Photofrin in Barrett's high-grade dysplasia. *Gastrointest Endosc* **66**: 460-468

Pacifico RJ, Wang KK, Wongkeesong LM, Buttar NS, Lutzke LS (2003) Combined endoscopic mucosal resection and photodynamic therapy versus esophagectomy for management of early adenocarcinoma in Barrett's esophagus. *Clin Gastroenterol Hepatol* **1**: 252-257

Panjehpour M, Overholt BF (2006) Porfimer sodium photodynamic therapy for management of Barrett's esophagus with high-grade dysplasia. *Lasers Surg Med* **38**: 390-395

Panjehpour M, Overholt BF, Haydek JM (2000a) Light sources and delivery devices for photodynamic therapy in the gastrointestinal tract. *Gastrointest Endosc Clin N Am* **10**: 513-532

Panjehpour M, Overholt BF, Haydek JM, Lee SG (2000b) Results of photodynamic therapy for ablation of dysplasia and early cancer in Barrett's esophagus and effect of oral steroids on stricture formation. *Am J Gastroenterol* **95**: 2177-2184

Panjehpour M, Overholt BF, Vo-Dinh T, Haggitt RC, Edwards DH, Buckley FP, III (1996) Endoscopic fluorescence detection of high-grade dysplasia in Barrett's esophagus. *Gastroenterology* **111**: 93-101

Pasricha PJ, Hill S, Wadwa KS, Gislason GT, Okolo PI, III, Magee CA, Canto MI, Kuo WH, Baust JG, Kalloo AN (1999) Endoscopic cryotherapy: experimental results and first clinical use. *Gastrointest Endosc* **49**: 627-631

Paulson TG, Maley CC, Li X, Li H, Sanchez CA, Chao DL, Odze RD, Vaughan TL, Blount PL, Reid BJ (2009) Chromosomal Instability and Copy Number Alterations in Barrett's Esophagus and Esophageal Adenocarcinoma. *Clin Cancer Res* **15**: 3305-3314

Pech O, Behrens A, May A, Nachbar L, Gossner L, Rabenstein T, Manner H, Guenter E, Huijsmans J, Vieth M, Stolte M, Ell C (2008) Long-term results and risk factor analysis for recurrence after curative endoscopic therapy in 349 patients with high-grade intraepithelial neoplasia and mucosal adenocarcinoma in BarrettΓÇÖs oesophagus. *Gut* **57**: 1200-1206

Pech O, Gossner L, May A, Rabenstein T, Vieth M, Stolte M, Berres M, Ell C (2005) Long-term results of photodynamic therapy with 5-aminolevulinic acid for superficial Barrett's cancer and high-grade intraepithelial neoplasia. *Gastrointest Endosc* **62**: 24-30

Pech O, May A, Rabenstein T, Ell C (2007) Endoscopic resection of early oesophageal cancer. *Gut* **56**: 1625-1634

Peitz U, Malfertheiner P (2002) Chromoendoscopy: From a Research Tool to Clinical Progress. *Digestive Diseases* **20**: 111-119

Peng DF, Razvi M, Chen H, Washington K, Roessner A, Schneider-Stock R, El-Rifai W (2009) DNA hypermethylation regulates the expression of members of the Mu-class glutathione S-transferases and glutathione peroxidases in Barrett's adenocarcinoma. *Gut* **58**: 5-15

Pepe MS, Etzioni R, Feng Z, Potter JD, Thompson ML, Thornquist M, Winget M, Yasui Y (2001) Phases of biomarker development for early detection of cancer. *J Natl Cancer Inst* **93**: 1054-1061

Pereira-Lima JC, Busnello JV, Saul C, Toneloto EB, Lopes CV, Rynkowski CB, Blaya C (2000) High power setting argon plasma coagulation for the eradication of Barrett's esophagus. *Am J Gastroenterol* **95**: 1661-1668

Peters F, Kara M, Rosmolen W, Aalders M, Ten Kate F, Krishnadath K, van Lanschot J, Fockens P, Bergman J (2005) Poor results of 5-aminolevulinic acid-photodynamic therapy for residual high-grade dysplasia and early cancer in barrett esophagus after endoscopic resection. *Endoscopy* **37**: 418-424

Peters FP, Kara MA, Curvers WL, Rosmolen WD, Fockens P, Krishnadath KK, ten Kate FJ, Bergman JJ (2007) Multiband mucosectomy for endoscopic resection of Barrett's esophagus: feasibility study with matched historical controls. *Eur J Gastroenterol Hepatol* **19**: 311-315

Pfefer TJ, Paithankar DY, Poneros JM, Schomacker KT, Nishioka NS (2003) Temporally and spectrally resolved fluorescence spectroscopy for the detection of high grade dysplasia in Barrett's esophagus. *Lasers Surg Med* **32**: 10-16

Pino MS, Chung DC (2010) The Chromosomal Instability Pathway in Colon Cancer. *Gastroenterology* **138**: 2059-2072

Playford RJ (2006) New British Society of Gastroenterology (BSG) guidelines for the diagnosis and management of Barrett's oesophagus. *Gut* **55**: 442

Poh-Fitzpatrick MB (1986) Molecular and cellular mechanisms of porphyrin photosensitization. *Photodermatol* **3**: 148-157

Pohl H, Rosch T, Vieth M, Koch M, Becker V, Anders M, Khalifa AC, Meining A (2008) Miniprobe confocal laser microscopy for the detection of invisible neoplasia in patients with Barrett's oesophagus. *Gut* **57**: 1648-1653

Polednak AP (2003) Trends in survival for both histologic types of esophageal cancer in US surveillance, epidemiology and end results areas. *Int J Cancer* **105**: 98-100

Poneros JM, Brand S, Bouma BE, Tearney GJ, Compton CC, Nishioka NS (2001) Diagnosis of specialized intestinal metaplasia by optical coherence tomography. *Gastroenterology* **120**: 7-12

Pouw RE, Gondrie JJ, Rygiel AM, Sondermeijer CM, ten Kate FJ, Odze RD, Vieth M, Krishnadath KK, Bergman JJ (2009) Properties of the neosquamous epithelium after radiofrequency ablation of Barrett's esophagus containing neoplasia. *Am J Gastroenterol* **104**: 1366-1373

Pouw RE, Seewald S, Gondrie JJ, Deprez PH, Piessevaux H, Pohl H, Rosch T, Soehendra N, Bergman JJ (2010a) Stepwise radical endoscopic resection for eradication of Barrett's oesophagus with early neoplasia in a cohort of 169 patients. *Gut* **59**: 1169-1177

Pouw RE, Wirths K, Eisendrath P, Sondermeijer CM, Ten Kate FJ, Fockens P, Deviere J, Neuhaus H, Bergman JJ (2010b) Efficacy of Radiofrequency Ablation Combined With Endoscopic Resection for Barrett's Esophagus With Early Neoplasia. *Clinical Gastroenterology and Hepatology* **8**: 23-29

Prasad GA, Buttar NS, Wongkeesong LM, Lewis JT, Sanderson SO, Lutzke LS, Borkenhagen LS, Wang KK (2007a) Significance of neoplastic involvement of margins obtained by endoscopic mucosal resection in Barrett's esophagus. *Am J Gastroenterol* **102**: 2380-2386

Prasad GA, Wang KK, Halling KC, Buttar NS, Wongkeesong LM, Zinsmeister AR, Brankley SM, Westra WM, Lutzke LS, Borkenhagen LS, Dunagan K (2008) Correlation of histology with biomarker status after photodynamic therapy in Barrett esophagus. *Cancer* **113**: 470-476

Prasad GA, Wu TT, Wigle DA, Buttar NS, Wongkeesong LM, Dunagan KT, Lutzke LS, Borkenhagen LS, Wang KK (2009) Endoscopic and surgical treatment of mucosal (T1a) esophageal adenocarcinoma in Barrett's esophagus. *Gastroenterology* **137**: 815-823

Prasad GA, Wang KK, Buttar NS, Wongkeesong L, Krishnadath KK, Nichols III FC, Lutzke LS, Borkenhagen LS (2007b) Long-Term Survival Following Endoscopic and Surgical Treatment of High-Grade Dysplasia in Barrett's Esophagus. *Gastroenterology* **132**: 1226-1233

Pressman NJ (1976) Markovian analysis of cervical cell images. *J Histochem Cytochem* **24**: 138-144

Pretorius ME, Waehre H, Abeler VM, Davidson B, Vlatkovic L, Lothe RA, Giercksky KE, Danielsen HE (2009) Large scale genomic instability as an additive prognostic marker in early prostate cancer. *Cell Oncol* **31**: 251-259

Pyhtila JW, Chalut KJ, Boyer JD, Keener J, D'Amico T, Gottfried M, Gress F, Wax A (2007) In situ detection of nuclear atypia in Barrett's esophagus by using angle-resolved low-coherence interferometry. *Gastrointest Endosc* **65**: 487-491

Qiu L, Pleskow DK, Chuttani R, Vitkin E, Leyden J, Ozden N, Itani S, Guo L, Sacks A, Goldsmith JD, Modell MD, Hanlon EB, Itzkan I, Perelman LT (2010) Multispectral scanning during endoscopy guides biopsy of dysplasia in Barrett's esophagus. *Nat Med* **16**: 603-6

Rabinovitch PS (1994) DNA content histogram and cell-cycle analysis. *Methods Cell Biol* **41**: 263-296

Rabinovitch PS, Longton G, Blount PL, Levine DS, Reid BJ (2001) Predictors of progression in Barrett's esophagus III: baseline flow cytometric variables. *Am J Gastroenterol* **96**: 3071-3083

Ragunath K, Krasner N, Raman VS, Haqqani MT, Phillips CJ, Cheung I (2005) Endoscopic ablation of dysplastic Barrett's oesophagus comparing argon plasma coagulation and photodynamic therapy: a randomized prospective trial assessing efficacy and cost-effectiveness. *Scand J Gastroenterol* **40**: 750-758

Rajab NF, McKenna DJ, Diamond J, Williamson K, Hamilton PW, Kelvey-Martin VJ (2006) Prediction of radiosensitivity in human bladder cell lines using nuclear chromatin phenotype. *Cytometry A* **69**: 1077-1085

Rajagopalan H, Nowak MA, Vogelstein B, Lengauer C (2003) The significance of unstable chromosomes in colorectal cancer. *Nat Rev Cancer* **3**: 695-701

Raju GS, Ahmed I, Xiao SY, Brining D, Bhutani MS, Pasricha PJ (2005) Graded esophageal mucosal ablation with cryotherapy, and the protective effects of submucosal saline. *Endoscopy* **37**: 523-526

Raman CV, Krishnan KS (1998) A new type of secondary radiation (Reprinted from Nature, vol 121, pg 501-502, 1928). *Current Science* **74**: 381

Ramirez FC, Akins R, Shaukat M (2008) Screening of Barrett's esophagus with string-capsule endoscopy: a prospective blinded study of 100 consecutive patients using histology as the criterion standard. *Gastrointestinal Endoscopy* **68**: 25-31

Ramirez FC, Shaukat MS, Young MA, Johnson DA, Akins R (2005) Feasibility and safety of string, wireless capsule endoscopy in the diagnosis of Barrett's esophagus. *Gastrointestinal Endoscopy* **61**: 741-746

Ramus JR, Gatenby PA, Caygill CP, Winslet MC, Watson A (2009) Surveillance of Barrett's columnar-lined oesophagus in the UK: endoscopic intervals and frequency of detection of dysplasia. *Eur J Gastroenterol Hepatol* **21**: 636-641

Reaud S, Croue A, Boyer J (2006) Diagnostic accuracy of magnifying chromoendoscopy with detection of intestinal metaplasia and dysplasia using acetic acid in Barrett's esophagus. *Gastroenterol Clin Biol* **30**: 217-223

Reed PI (1991) Changing Pattern of Esophageal Cancer. *Lancet* **338**: 178

Regula J, MacRobert AJ, Gorchein A, Buonaccorsi GA, Thorpe SM, Spencer GM, Hatfield AR, Bown SG (1995) Photosensitisation and photodynamic therapy of oesophageal, duodenal, and colorectal tumours using 5 aminolaevulinic acid induced protoporphyrin IX--a pilot study. *Gut* **36**: 67-75

Reid BJ, Blount PL, Feng Z, Levine DS (2000a) Optimizing endoscopic biopsy detection of early cancers in Barrett's high-grade dysplasia. *Am J Gastroenterol* **95**: 3089-3096

Reid BJ, Blount PL, Rabinovitch PS (2003) Biomarkers in Barrett's esophagus. *Gastrointest Endosc Clin N Am* **13**: 369-397

Reid BJ, Blount PL, Rubin CE, Levine DS, Haggitt RC, Rabinovitch PS (1992) Flow-cytometric and histological progression to malignancy in Barrett's esophagus: prospective endoscopic surveillance of a cohort. *Gastroenterology* **102**: 1212-1219

Reid BJ, Levine DS, Longton G, Blount PL, Rabinovitch PS (2000b) Predictors of progression to cancer in Barrett's esophagus: baseline histology and flow cytometry identify low- and high-risk patient subsets. *Am J Gastroenterol* **95**: 1669-1676

Reid BJ, Li X, Galipeau PC, Vaughan TL (2010) Barrett's oesophagus and oesophageal adenocarcinoma: time for a new synthesis. *Nat Rev Cancer* **10**: 87-101

Reid BJ, Prevo LJ, Galipeau PC, Sanchez CA, Longton G, Levine DS, Blount PL, Rabinovitch PS (2001) Predictors of progression in Barrett's esophagus II: baseline 17p (p53) loss of heterozygosity identifies a patient subset at increased risk for neoplastic progression. *Am J Gastroenterol* **96**: 2839-2848

Reid BJ, Weinstein WM, Lewin KJ, Haggitt RC, VanDeventer G, DenBesten L, Rubin CE (1988) Endoscopic biopsy can detect high-grade dysplasia or early adenocarcinoma in Barrett's esophagus without grossly recognizable neoplastic lesions. *Gastroenterology* **94**: 81-90

Ribeiro U, Jr., Finkelstein SD, Safatle-Ribeiro AV, Landreneau RJ, Clarke MR, Bakker A, Swalsky PA, Gooding WE, Posner MC (1998) p53 sequence analysis predicts treatment response and outcome of patients with esophageal carcinoma. *Cancer* **83**: 7-18

Rice TW, Zuccaro G, Jr., Adelstein DJ, Rybicki LA, Blackstone EH, Goldblum JR (1998) Esophageal carcinoma: depth of tumor invasion is predictive of regional lymph node status. *Ann Thorac Surg* **65**: 787-792

Riddell RH, Goldman H, Ransohoff DF, Appelman HD, Fenoglio CM, Haggitt RC, Ahren C, Correa P, Hamilton SR, Morson BC, . (1983) Dysplasia in inflammatory bowel disease: standardized classification with provisional clinical applications. *Hum Pathol* **14**: 931-968

Ried T, Heselmeyer-Haddad K, Blegen H, Schrock E, Auer G (1999) Genomic changes defining the genesis, progression, and malignancy potential in solid human tumors: a phenotype/genotype correlation. *Genes Chromosomes Cancer* **25**: 195-204

Rodins K, Cheale M, Coleman N, Fox SB (2002) Minichromosome maintenance protein 2 expression in normal kidney and renal cell carcinomas: relationship to tumor dormancy and potential clinical utility. *Clin Cancer Res* **8**: 1075-1081

Rodriguez, E, Lee, T. M, Bigio, I. J., and Singh, S. K. Optical Sensing of Field Carcinogenesis in Colonic Mucosa Using Elastic-Scattering Spectroscopy. Gastroenterology 138[5], S-96. 1-5-2010.
Ref Type: Abstract

Rodriguez-Acebes S, Proctor I, Loddo M, Wollenschlaeger A, Falzon M, Prevost AT, Sainsbury R, Stoeber K, Williams GH (2010) Targeting DNA Replication before it Starts. Cdc7 as a Therapeutic Target in p53-Mutant Breast Cancers. *Am J Pathol* **177**:1-12

Ronkainen J, Aro P, Storskrubb T, Johansson SE, Lind T, Bolling-Sternevald E, Vieth M, Stolte M, Talley NJ, Agreus L (2005) Prevalence of Barrett's esophagus in the general population: an endoscopic study. *Gastroenterology* **129**: 1825-1831

Roorda AK, Marcus SN, Triadafilopoulos G (2007) Early experience with radiofrequency energy ablation therapy for Barrett's esophagus with and without dysplasia. *Diseases of the Esophagus* **20**: 516-522

Rothstein RI, Chang K, Overholt BF, Bergman JJ, Shaheen NJ (2007) Focal Ablation for Treatment of Dysplastic and Non-Dysplastic Barrett Esophagus: Safety Profile and Initial Experience with the Halo90 Device in 508 Cases. *Gastrointestinal Endoscopy* **65**: AB147

Roy HK, Kim YL, Liu Y, Wali RK, Goldberg MJ, Turzhitsky V, Horwitz J, Backman V (2006) Risk stratification of colon carcinogenesis through enhanced backscattering spectroscopy analysis of the uninvolved colonic mucosa. *Clin Cancer Res* **12**: 961-968

Roy HK, Liu Y, Wali RK, Kim YL, Kromine AK, Goldberg MJ, Backman V (2004) Four-dimensional elastic light-scattering fingerprints as preneoplastic markers in the rat model of colon carcinogenesis. *Gastroenterology* **126**: 1071-1081

Roy HK, Turzhitsky V, Kim Y, Goldberg MJ, Watson P, Rogers JD, Gomes AJ, Kromine A, Brand RE, Jameel M, Bogovejic A, Pradhan P, Backman V (2009) Association between Rectal Optical Signatures and Colonic Neoplasia: Potential Applications for Screening. *Cancer Res* **69**: 4476-4483

Russack V (1994) Image cytometry: current applications and future trends. *Crit Rev Clin Lab Sci* **31**: 1-34

Rutter MD, Saunders BP, Schofield G, Forbes A, Price AB, Talbot IC (2004) Pancolonic indigo carmine dye spraying for the detection of dysplasia in ulcerative colitis. *Gut* **53**: 256-260

Saad RS, Mahood LK, Clary KM, Liu Y, Silverman JF, Raab SS (2003) Role of cytology in the diagnosis of Barrett's esophagus and associated neoplasia. *Diagn Cytopathol* **29**: 130-135

Sadeghi S, Bain CJ, Pandeya N, Webb PM, Green AC, Whiteman DC (2008) Aspirin, nonsteroidal anti-inflammatory drugs, and the risks of cancers of the esophagus. *Cancer Epidemiol Biomarkers Prev* **17**: 1169-1178

Saeian K, Staff DM, Vasilopoulos S, Townsend WF, Almagro UA, Komorowski RA, Choi H, Shaker R (2002) Unsedated transnasal endoscopy accurately detects Barrett's metaplasia and dysplasia. *Gastrointest Endosc* **56**: 472-478

Sampliner RE, Fennerty MB, Garewal HS (1996) Reversal of Barrett's esophagus with acid suppression and multipolar electrocoagulation: preliminary results. *Gastrointest Endosc* **44**: 532-535

Santamaria A, Neef R, Eberspacher U, Eis K, Husemann M, Mumberg D, Prechtl S, Schulze V, Siemeister G, Wortmann L, Barr FA, Nigg EA (2007) Use of the Novel Plk1 Inhibitor ZK-Thiazolidinone to Elucidate Functions of Plk1 in Early and Late Stages of Mitosis. *Mol Biol Cell* **18**: 4024-4036

Sarna T, Menon IA, Sealy RC (1984) Photoinduced Oxygen-Consumption in Melanin Systems .2. Action Spectra and Quantum Yields for Pheomelanins. *Photochemistry and Photobiology* **39**: 805-809

Sato F, Meltzer SJ (2005) CpG island hypermethylation in progression of esophageal and gastric cancer. *Cancer* **106**: 483-493

Sauter ER, Klein-Szanto A, Ehya H, MacGibbon B (2004) Ductoscopic cytology and image analysis to detect breast carcinoma. *Cancer* **101**: 1283-1292

Scarpelli M, Montironi R, Mazzucchelli R, Thompson D, Bartels PH (1999) Distinguishing cortical adrenal gland adenomas from carcinomas by their quantitative nuclear features. *Anal Quant Cytol Histol* **21**: 131-138

Schlemper RJ, Kato Y, Stolte M (2000a) Diagnostic criteria for gastrointestinal carcinomas in Japan and Western countries: proposal for a new classification system of gastrointestinal epithelial neoplasia. *J Gastroenterol Hepatol* **15 Suppl**: G49-G57

Schlemper RJ, Riddell RH, Kato Y, Borchard F, Cooper HS, Dawsey SM, Dixon MF, Fenoglio-Preiser CM, Flejou JF, Geboes K, Hattori T, Hirota T, Itabashi M, Iwafuchi M, Iwashita A, Kim YI, Kirchner T, Klimpfinger M, Koike M, Lauwers GY, Lewin KJ, Oberhuber G, Offner F, Price AB, Rubio CA, Shimizu M, Shimoda T, Sipponen P, Solcia E, Stolte M, Watanabe H, Yamabe H (2000b) The Vienna classification of gastrointestinal epithelial neoplasia. *Gut* **47**: 251-255

Schluter C, Duchrow M, Wohlenberg C, Becker MH, Key G, Flad HD, Gerdes J (1993) The cell proliferation-associated antigen of antibody Ki-67: a very large, ubiquitous nuclear protein with numerous repeated elements, representing a new kind of cell cycle-maintaining proteins. *J Cell Biol* **123**: 513-522

Schmidt HG, Riddell RH, Walther B, Skinner DB, Riemann JF (1985) Dysplasia in Barrett's esophagus. *J Cancer Res Clin Oncol* **110**: 145-152

Schnell TG, Sontag SJ, Chejfec G, Aranha G, Metz A, O'Connell S, Seidel UJ, Sonnenberg A (2001) Long-term nonsurgical management of Barrett's esophagus with high-grade dysplasia. *Gastroenterology* **120**: 1607-1619

Schulerud H, Kristensen GB, Liestol K, Vlatkovic L, Reith A, Danielsen H (1998) A review of caveats in statistical nuclear image analysis. *Analytical Cellular Pathology* **16**: 63-82

Schulmann K, Sterian A, Berki A, Yin J, Sato F, Xu Y, Olaru A, Wang S, Mori Y, Deacu E, Hamilton J, Kan T, Krasna MJ, Beer DG, Pepe MS, Abraham JM, Feng Z, Schmiegel W, Greenwald BD, Meltzer SJ (2005) Inactivation of p16, RUNX3, and HPP1 occurs early in Barrett's-associated neoplastic progression and predicts progression risk. *Oncogene* **24**: 4138-4148

Schulz H, Miehlke S, Antos D, Schentke KU, Vieth M, Stolte M, Bayerdorffer E (2000) Ablation of Barrett's epithelium by endoscopic argon plasma coagulation in combination with high-dose omeprazole. *Gastrointest Endosc* **51**: 659-663

Scott BB, Jenkins D (1982) Gastro-Esophageal Candidiasis. *Gut* **23**: 137-139

Sears RJ, Duckworth CW, Decaestecker C, Bourgeois N, Ledent T, Deviere J, Salmon I, Kiss R, Yeaton P (1998) Image cytometry as a discriminatory tool for cytologic specimens obtained by endoscopic retrograde cholangiopancreatography. *Cancer* **84**: 119-126

Seewald S, Ang TL, Gotoda T, Soehendra N (2008) Total endoscopic resection of Barrett esophagus. *Endoscopy* **40**: 1016-1020

Shaheen NJ, Inadomi JM, Overholt BF, Sharma P (2004) What is the best management strategy for high grade dysplasia in Barrett's oesophagus? A cost effectiveness analysis. *Gut* **53**: 1736-1744

Shaheen NJ, Sharma P, Overholt BF, Wolfsen HC, Sampliner RE, Wang KK, Galanko JA, Bronner MP, Goldblum JR, Bennett AE, Jobe BA, Eisen GM, Fennerty MB, Hunter JG, Fleischer DE, Sharma VK, Hawes RH, Hoffman BJ, Rothstein RI, Gordon SR, Mashimo H, Chang KJ, Muthusamy VR, Edmundowicz SA, Spechler SJ, Siddiqui AA, Souza RF, Infantolino A, Falk GW, Kimmey MB, Madanick RD, Chak A, Lightdale CJ (2009a) Radiofrequency ablation in Barrett's esophagus with dysplasia. *N Engl J Med* **360**: 2277-2288

Shaheen NJ, Fleischer DE, Eisen GM, Wang KK, Peery AF, Infantolino A, Chak A, Wolfsen HC, Falk GW, Muthusamy VR, Lightdale CJ (2010) 92 Durability of Epithelial Reversion After Radiofrequency Ablation: Follow-up of the AIM Dysplasia Trial. *Gastroenterology* **138**: S

Shaheen NJ, Greenwald BD, Dumot JA, Wolfsen HC, Abrams JA, Burdick SJ, Barthel JS, Wang KK, Johnston MH, Nishioka NS, Mallat DB, Zfass AM, Smith JO, Lightdale CJ (2009b) Safety and Efficacy of Endoscopic Spray Cryotherapy for Barrett's Esophagus with High-Grade Dysplasia. *Gastrointestinal Endoscopy* **69**: AB357

Shand A, Dallal H, Palmer K, Ghosh S, MacIntyre M (2001) Adenocarcinoma arising in columnar lined oesophagus following treatment with argon plasma coagulation. *Gut* **48**: 580-581

Sharma P, Bansal A (2006) Toward better imaging of Barrett's esophagus--see more, biopsy less! *Gastrointest Endosc* **64**: 188-192

Sharma P, Bansal A, Mathur S, Wani S, Cherian R, McGregor D, Higbee A, Hall S, Weston A (2006a) The utility of a novel narrow band imaging endoscopy system in patients with Barrett's esophagus. *Gastrointest Endosc* **64**: 167-175

Sharma P, Falk GW, Sampliner R, Jon SS, Wang K (2009a) Management of nondysplastic Barrett's esophagus: where are we now? *Am J Gastroenterol* **104**: 805-808

Sharma P, Falk GW, Weston AP, Reker D, Johnston M, Sampliner RE (2006b) Dysplasia and cancer in a large multicenter cohort of patients with Barrett's esophagus. *Clin Gastroenterol Hepatol* **4**: 566-572

Sharma P, Weston AP, Morales T, Topalovski M, Mayo MS, Sampliner RE (2000) Relative risk of dysplasia for patients with intestinal metaplasia in the distal oesophagus and in the gastric cardia. *Gut* **46**: 9-13

Sharma P, Weston AP, Topalovski M, Cherian R, Bhattacharyya A, Sampliner RE (2003) Magnification chromoendoscopy for the detection of intestinal metaplasia and dysplasia in Barrett's oesophagus. *Gut* **52**: 24-27

Sharma P, Dent J, Armstrong D, Bergman JJGH, Gossner L, Hoshihara Y, Jankowski JA, Junghard O, Lundell L, Tytgat GNJ, Vieth M (2006c) The Development and Validation of an Endoscopic Grading System for Barrett's Esophagus: The Prague C & M Criteria. *Gastroenterology* **131**: 1392-1399

Sharma P, Meining A, Coron E, Lightdale CJ, Wolfsen HC, Bansal A, Bajbouj M, Galmiche JP, Abrams JA, Lauwers GY, Wallace MB (2010) 1071 Detection of Neoplastic Tissue in Barrett's Esophagus With In Vivo Probe-Based Confocal Endomicroscopy (DONT BIOPCE). Final Results of a Prospective International RCT: Image Guided Versus 4 Quadrant Random Biopsies? *Gastroenterology* **138**: S-155

Sharma P, Wani S, Rastogi A, Bansal A, Higbee A, Mathur S, Esquivel R, Camargo L, Sampliner RE (2008) The Diagnostic Accuracy of Esophageal Capsule Endoscopy in Patients With Gastroesophageal Reflux Disease and Barrett's Esophagus: A Blinded, Prospective Study. *Am J Gastroenterol* **103**: 525-532

Sharma VK, Jae KH, Das A, Wells CD, Nguyen CC, Fleischer DE (2009b) Circumferential and focal ablation of Barrett's esophagus containing dysplasia. *Am J Gastroenterol* **104**: 310-317

Sharma VK, Wang KK, Overholt BF, Lightdale CJ, Fennerty MB, Dean PJ, Pleskow DK, Chuttani R, Reymunde A, Santiago N, Chang KJ, Kimmey MB, Fleischer DE (2007) Balloon-based, circumferential, endoscopic radiofrequency ablation of Barrett's esophagus: 1-year follow-up of 100 patients. *Gastrointest Endosc* **65**: 185-195

Sharma VK (2009) The Future Is Wireless: Advances in Wireless Diagnostic and Therapeutic Technologies in Gastroenterology. *Gastroenterology* **137**: 434-439

Shetty A, Loddo M, Fanshawe T, Prevost AT, Sainsbury R, Williams GH, Stoeber K (2005) DNA replication licensing and cell cycle kinetics of normal and neoplastic breast. *Br J Cancer* **93**: 1295-1300

Shetty G, Kendall C, Shepherd N, Stone N, Barr H (2006) Raman spectroscopy: elucidation of biochemical changes in carcinogenesis of oesophagus. *Br J Cancer* **94**: 1460-1464

Sikkema M, Kerkhof M, Steyerberg EW, Kusters JG, van Strien PM, Looman CW, van DH, Siersema PD, Kuipers EJ (2009) Aneuploidy and overexpression of Ki67 and p53 as markers for neoplastic progression in Barrett's esophagus: a case-control study. *Am J Gastroenterol* **104**: 2673-2680

Sirieix PS, O'Donovan M, Brown J, Save V, Coleman N, Fitzgerald RC (2003) Surface expression of minichromosome maintenance proteins provides a novel method for detecting patients at risk for developing adenocarcinoma in Barrett's esophagus. *Clin Cancer Res* **9**: 2560-2566

Skacel M, Petras RE, Gramlich TL, Sigel JE, Richter JE, Goldblum JR (2000) The diagnosis of low-grade dysplasia in Barrett's esophagus and its implications for disease progression. *Am J Gastroenterol* **95**: 3383-3387

Skinner DB, Walther BC, Riddell RH, Schmidt H, Iascone C, Demeester TR (1983) Barrett's esophagus. Comparison of benign and malignant cases. *Ann Surg* **198**: 554-565

Slack JM (1986) Epithelial metaplasia and the second anatomy. *Lancet* **2**: 268-271

Slamon DJ, Clark GM, Wong SG, Levin WJ, Ullrich A, McGuire WL (1987) Human breast cancer: correlation of relapse and survival with amplification of the HER-2/neu oncogene. *Science* **235**: 177-182

Slamon DJ, Leyland-Jones B, Shak S, Fuchs H, Paton V, Bajamonde A, Fleming T, Eiermann W, Wolter J, Pegram M, Baselga J, Norton L (2001) Use of chemotherapy plus a monoclonal antibody against HER2 for metastatic breast cancer that overexpresses HER2. *N Engl J Med* **344**: 783-792

Smith I, Procter M, Gelber RD, Guillaume S, Feyereislova A, Dowsett M, Goldhirsch A, Untch M, Mariani G, Baselga J, Kaufmann M, Cameron D, Bell R, Bergh J,

Coleman R, Wardley A, Harbeck N, Lopez RI, Mallmann P, Gelmon K, Wilcken N, Wist E, Sanchez RP, Piccart-Gebhart MJ (2007) 2-year follow-up of trastuzumab after adjuvant chemotherapy in HER2-positive breast cancer: a randomised controlled trial. *Lancet* **369**: 29-36

Soehendra N, Seewald S, Groth S, Omar S, Seitz U, Zhong Y, de WA, Thonke F, Schroeder S (2006) Use of modified multiband ligator facilitates circumferential EMR in Barrett's esophagus (with video). *Gastrointest Endosc* **63**: 847-852

Solaymani-Dodaran M, Logan RF, West J, Card T (2005) Mortality associated with Barrett's esophagus and gastroesophageal reflux disease diagnoses-a population-based cohort study. *Am J Gastroenterol* **100**: 2616-2621

Solonenko M, Cheung R, Busch TM, Kachur A, Griffin GM, Vulcan T, Zhu TC, Wang HW, Hahn SM, Yodh AG (2002) In vivo reflectance measurement of optical properties, blood oxygenation and motexafin lutetium uptake in canine large bowels, kidneys and prostates. *Phys Med Biol* **47**: 857-873

Somerville M, Garside R, Pitt M, Stein K (2008) Surveillance of Barrett's oesophagus: is it worthwhile? *Eur J Cancer* **44**: 588-599

Song LMWK, Molckovsky A, Wang K, Burgart L, Buttar N, Papenfuss S, Lutzke L, Wilson B, Dolenko B, Somorjai R (2005) Diagnostic performance of near-infrared Raman spectroscopy in Barrett's esophagus. *Gastroenterology* **128**: A51

Sonnenberg A, Soni A, Sampliner RE (2002) Medical decision analysis of endoscopic surveillance of Barrett's oesophagus to prevent oesophageal adenocarcinoma. *Aliment Pharmacol Ther* **16**: 41-50

Sontag SJ (1990) The medical management of reflux esophagitis. Role of antacids and acid inhibition. *Gastroenterol Clin North Am* **19**: 683-712

Sontag SJ, Schnell TG, Chejfec G, O'Connell S, Stanley MM, Best W, Chintam R, Nemchausky B, Wanner J, Moroni B (1985) Barrett's oesophagus and colonic tumours. *Lancet* **1**: 946-949

Spechler SJ, Fitzgerald RC, Prasad GA, Wang KK (2010) History, Molecular Mechanisms, and Endoscopic Treatment of Barrett's Esophagus. *Gastroenterology* **138(3)**:854-69

Spechler SJ, Zeroogian JM, Antonioli DA, Wang HH, Goyal RK (1994) Prevalence of metaplasia at the gastro-oesophageal junction. *Lancet* **344**: 1533-1536

Srivastava AK, Vanagunas A, Kamel P, Cooper R (1994) Endoscopic ultrasound in the evaluation of Barrett's esophagus: a preliminary report. *Am J Gastroenterol* **89**: 2192-2195

Steegmaier M, Hoffmann M, Baum A, Lθnβrt P, Petronczki M, Krssβk M, G³rtler U, Garin-Chesa P, Lieb S, Quant J, Grauert M, Adolf GR, Kraut N, Peters JM, Rettig WJ (2007) BI 2536, a Potent and Selective Inhibitor of Polo-like Kinase 1, Inhibits Tumor Growth In Vivo. *Current Biology* **17**: 316-322

Steevens J, Botterweck AAM, Dirx MJM, van den Brandt PA, Schouten LJ (2010) Trends in incidence of oesophageal and stomach cancer subtypes in Europe. *European Journal of Gastroenterology & Hepatology* **22**:669-678

Stoltey J, Reeba H, Ullah N, Sabhaie P, Gerson L (2007) Does Barrett's oesophagus develop over time in patients with chronic gastro-oesophageal reflux disease? *Alimentary Pharmacology and Therapeutics* **25**: 83-91

Stone N, Kendall C, Smith J, Crow P, Barr H (2004) Raman spectroscopy for identification of epithelial cancers. *Faraday Discuss* **126**: 141-157

Strebhardt K, Ullrich A (2006) Targeting polo-like kinase 1 for cancer therapy. *Nat Rev Cancer* **6**: 321-330

Suter MJ, Vakoc BJ, Yachimski PS, Shishkov M, Lauwers GY, Mino-Kenudson M, Bouma BE, Nishioka NS, Tearney GJ (2008) Comprehensive microscopy of the esophagus in human patients with optical frequency domain imaging. *Gastrointest Endosc* **68**: 745-753

Sylantiev C, Schoenfeld N, Mamet R, Groozman GB, Drory VE (2005) Acute neuropathy mimicking porphyria induced by aminolevulinic acid during photodynamic therapy. *Muscle Nerve* **31**: 390-393

Tachibana KE, Gonzalez MA, Guarguaglini G, Nigg EA, Laskey RA (2005) Depletion of licensing inhibitor geminin causes centrosome overduplication and mitotic defects. *EMBO Rep* **6**: 1052-1057

Tada M, Karita M, Yanai H, Takemoto T (1988) [Endoscopic therapy of early gastric cancer by strip biopsy]. *Gan To Kagaku Ryoho* **15**: 1460-1465

Tada M, Katoh S, Kohli Y, Kawai K (1977) On the dye spraying method in colonofiberscopy. *Endoscopy* **8**: 70-74

Tada S, Li A, Maiorano D, Mechali M, Blow JJ (2001) Repression of origin assembly in metaphase depends on inhibition of RLF-B/Cdt1 by geminin. *Nat Cell Biol* **3**: 107-113

Tagawa Y, Nakazaki T, Yasutake T, Matsuo S, Tomita M (1993) Comparison of pepsin and trypsin digestion on paraffin-embedded tissue preparation for DNA flow cytometry. *Cytometry* **14**: 541-549

Takai N, Miyazaki T, Fujisawa K, Nasu K, Hamanaka R, Miyakawa I (2001) Expression of polo-like kinase in ovarian cancer is associated with histological grade and clinical stage. *Cancer Letters* **164**: 41-49

Tanner M, Hollmen M, Junttila TT, Kapanen AI, Tommola S, Soini Y, Helin H, Salo J, Joensuu H, Sihvo E, Elenius K, Isola J (2005) Amplification of HER-2 in gastric carcinoma: association with Topoisomerase IIalpha gene amplification, intestinal type, poor prognosis and sensitivity to trastuzumab. *Ann Oncol* **16**: 273-278

Targownik LE, Lix LM, Leung S, Leslie WD (2010) Proton-pump inhibitor use is not associated with osteoporosis or accelerated bone mineral density loss. *Gastroenterology* **138**: 896-904

Targownik LE, Lix LM, Metge CJ, Prior HJ, Leung S, Leslie WD (2008) Use of proton pump inhibitors and risk of osteoporosis-related fractures. *CMAJ* **179**: 319-326

Tatsumi Y, Harada A, Matsumoto T, Tani T, Nishida H (2008) Feasibility and tolerance of 2-way and 4-way angulation videoscopes for unsedated patients undergoing transnasal EGD in GI cancer screening. *Gastrointest Endosc* **67**: 1021-1027

Tengs T, Hveem TS, Danielsen H (2008) Correlation between textural analyses of cell nuclei and genecopy number variations. *Cellular Oncology* **30**: 121

Theisen J, Nehra D, Citron D, Johansson J, Hagen JA, Crookes PF, DeMeester SR, Bremner CG, Demeester TR, Peters JH (2000) Suppression of gastric acid secretion in

patients with gastroesophageal reflux disease results in gastric bacterial overgrowth and deconjugation of bile acids. *J Gastrointest Surg* **4**: 50-54

Tileston W (1906) Peptic ulcer of the oesophagus. *Am J Med Sci* **132**: 240-265

Tokumitsu Y, Mori M, Tanaka S, Akazawa K, Nakano S, Niho Y (1999) Prognostic significance of polo-like kinase expression in esophageal carcinoma. *Int J Oncol* **15**: 687-692

Toyoda H, Rubio C, Befrits R, Hamamoto N, Adachi Y, Jaramillo E (2004) Detection of intestinal metaplasia in distal esophagus and esophagogastric junction by enhanced-magnification endoscopy. *Gastrointest Endosc* **59**: 15-21

Umansky M, Yasui W, Hallak A, Brill S, Shapira I, Halpern Z, Hibshoosh H, Rattan J, Meltzer S, Tahara E, Arber N (2001) Proton pump inhibitors reduce cell cycle abnormalities in Barrett's esophagus. *Oncogene* **20**: 7987-7991

Vakoc BJ, Shishko M, Yun SH, Oh WY, Suter MJ, Desjardins AE, Evans JA, Nishioka NS, Tearney GJ, Bouma BE (2007) Comprehensive esophageal microscopy by using optical frequency-domain imaging (with video). *Gastrointest Endosc* **65**: 898-905

van der BA, Dees J, Hop WC, Van BM (1996) Oesophageal cancer is an uncommon cause of death in patients with Barrett's oesophagus. *Gut* **39**: 5-8

Van Laethem JL, Peny MO, Salmon I, Cremer M, Deviere J (2000) Intramucosal adenocarcinoma arising under squamous re-epithelialisation of Barrett's oesophagus. *Gut* **46**: 574-577

Van Vilsteren FG, Pouw RE, Seewald S, Herrero LA, Sondermeijer C, Kate FJT, Fockens P, Teng KCY, Rosch T, Soehendra N, Weusten BL, Bergman J (2009) A Multi-Center Randomized Trial Comparing Stepwise Radical Endoscopic Resection Versus Radiofrequency Ablation for Barrett Esophagus Containing High-Grade Dysplasia and/or Early Cancer. *Gastrointest Endosc* **69**: AB133-AB134

Van d, V, Dees J, Blankensteijn JD, Van BM (1989) Adenocarcinoma in Barrett's oesophagus: an overrated risk. *Gut* **30**: 14-18

VandenBerg TJTP, Spekreijse H (1997) Near infrared light absorption in the human eye media. *Vision Research* **37**: 249-253

Vij R, Triadafilopoulos G, Owens DK, Kunz P, Sanders GD (2004) Cost-effectiveness of photodynamic therapy for high-grade dysplasia in Barrett's esophagus. *Gastrointest Endosc* **60**: 739-756

von Rahden BH, Stein HJ (2008) Endoscopic mucosal resection as curative therapy for esophageal cancer is inappropriate and should be discouraged. *Endoscopy* **40**: 169

Wagnieres GA, Star WM, Wilson BC (1998) In vivo fluorescence spectroscopy and imaging for oncological applications. *Photochemistry and Photobiology* **68**: 603-632

Wali RK, Roy HK, Kim YL, Liu Y, Koetsier JL, Kunte DP, Goldberg MJ, Turzhitsky V, Backman V (2005) Increased microvascular blood content is an early event in colon carcinogenesis. *Gut* **54**: 654-660

Wallace MB, Perelman LT, Backman V, Crawford JM, Fitzmaurice M, Seiler M, Badizadegan K, Shields SJ, Itzkan I, Dasari RR, Van Dam J, Feld MS (2000) Endoscopic detection of dysplasia in patients with Barrett's esophagus using light-scattering spectroscopy. *Gastroenterology* **119**: 677-682

Wang GQ, Abnet CC, Shen Q, Lewin KJ, Sun XD, Roth MJ, Qiao YL, Mark SD, Dong ZW, Taylor PR, Dawsey SM (2005) Histological precursors of oesophageal squamous cell carcinoma: results from a 13 year prospective follow up study in a high risk population. *Gut* **54**: 187-192

Wang HH, Doria MI, Jr., Purohit-Buch S, Schnell T, Sontag S, Chejfec G (1992) Barrett's esophagus. The cytology of dysplasia in comparison to benign and malignant lesions. *Acta Cytol* **36**: 60-64

Wang JS, Varro A, Lightdale CJ, Lertkowit N, Slack KN, Fingerhood ML, Tsai WY, Wang TC, Abrams JA (2010) Elevated serum gastrin is associated with a history of advanced neoplasia in Barrett's esophagus. *Am J Gastroenterol* **105**: 1039-1045

Wang KK (2000) Photodynamic therapy of Barrett's esophagus. *Gastrointest Endosc Clin N Am* **10**: 409-419

Wang KK, Sampliner RE (2008) Updated Guidelines 2008 for the Diagnosis, Surveillance and Therapy of Barrett's Esophagus. *Am J Gastroenterol* **103**: 788-797

Wang S, Zhan M, Yin J, Abraham JM, Mori Y, Sato F, Xu Y, Olaru A, Berki AT, Li H, Schulmann K, Kan T, Hamilton JP, Paun B, Yu MM, Jin Z, Cheng Y, Ito T, Mantzur

C, Greenwald BD, Meltzer SJ (2006) Transcriptional profiling suggests that Barrett's metaplasia is an early intermediate stage in esophageal adenocarcinogenesis. *Oncogene* **25**: 3346-3356

Wang TD, Triadafilopoulos G, Crawford JM, Dixon LR, Bhandari T, Sahbaie P, Friedland S, Soetikno R, Contag CH (2007) Detection of endogenous biomolecules in Barrett's esophagus by Fourier transform infrared spectroscopy. *Proc Natl Acad Sci U S A* **104**: 15864-15869

Wang VS, Hornick JL, Sepulveda JA, Mauer R, Poneros JM (2009) Low prevalence of submucosal invasive carcinoma at esophagectomy for high-grade dysplasia or intramucosal adenocarcinoma in Barrett's esophagus: a 20-year experience. *Gastrointest Endosc* **69**: 777-783

Wani S, Mathur SC, Curvers WL, Singh V, Herrero LA, Hall SB, Ulusarac O, Cherian R, McGregor DH, Bansal A, Rastogi A, Ahmed B, Singh M, Gaddam S, ten Kate FJ, Bergman J, Sharma P (2010) Greater Interobserver Agreement by Endoscopic Mucosal Resection Than Biopsy Samples in Barrett's Dysplasia. *Clin Gastroenterol Hepatol* **8(9)**:783-8

Wani S, Puli SR, Shaheen NJ, Westhoff B, Slehria S, Bansal A, Rastogi A, Sayana H, Sharma P (2009) Esophageal adenocarcinoma in Barrett's esophagus after endoscopic ablative therapy: a meta-analysis and systematic review. *Am J Gastroenterol* **104**: 502-513

Ward EM, Wolfsen HC, Achem SR, Loeb DS, Krishna M, Hemminger LL, Devault KR (2006) Barrett's esophagus is common in older men and women undergoing screening colonoscopy regardless of reflux symptoms. *Am J Gastroenterol* **101**: 12-17

Watson, A., Heading, RC, and Shepherd, N. BSG guidelines for the diagnosis and management of Barrett's Columnar-linde oesophagus (CLO): Principle recommendations. British Society of Gastroenterology Guidelines , 1-2. 2007.

Weaver BA, Cleveland DW (2006) Does aneuploidy cause cancer? *Curr Opin Cell Biol* **18**: 658-667

Weston AP, Banerjee SK, Sharma P, Tran TM, Richards R, Cherian R (2001) p53 protein overexpression in low grade dysplasia (LGD) in Barrett's esophagus:

immunohistochemical marker predictive of progression. *Am J Gastroenterol* **96**: 1355-1362

Weston AP, Krmpotich PT, Cherian R, Dixon A, Topalosvki M (1997) Prospective long-term endoscopic and histological follow-up of short segment Barrett's esophagus: comparison with traditional long segment Barrett's esophagus. *Am J Gastroenterol* **92**: 407-413

Weyn B, Jacob W, da S, V, Montironi R, Hamilton PW, Thompson D, Bartels HG, Van DA, Dillon K, Bartels PH (2000) Data representation and reduction for chromatin texture in nuclei from premalignant prostatic, esophageal, and colonic lesions. *Cytometry* **41**: 133-138

Wharton SB, Hibberd S, Eward KL, Crimmins D, Jellinek DA, Levy D, Stoeber K, Williams GH (2004) DNA replication licensing and cell cycle kinetics of oligodendroglial tumours. *Br J Cancer* **91**: 262-269

Williams BR, Prabhu VR, Hunter KE, Glazier CM, Whittaker CA, Housman DE, Amon A (2008) Aneuploidy affects proliferation and spontaneous immortalization in mammalian cells. *Science* **322**: 703-709

Williams L, Somasekar A, Davies DJ, Cronin J, Doak SH, Alcolado R, Williams JG, Griffiths AP, Baxter JN, Jenkins GJ (2009) Aneuploidy involving chromosome 1 may be an early predictive marker of intestinal type gastric cancer. *Mutat Res* **669**: 104-111

Witt H, Watanabe M, Slezak P, Rubio C (1994) The significance of mucosal staining for the endoscopic diagnosis of chronic esophagitis as assessed in biopsy findings. *Hepatogastroenterology* **41**: 564-567

Wohlschlegel JA, Dwyer BT, Dhar SK, Cvetic C, Walter JC, Dutta A (2000) Inhibition of eukaryotic DNA replication by geminin binding to Cdt1. *Science* **290**: 2309-2312

Wolfsen HC, Crook JE, Krishna M, Achem SR, Devault KR, Bouras EP, Loeb DS, Stark ME, Woodward TA, Hemminger LL, Cayer FK, Wallace MB (2008) Prospective, controlled tandem endoscopy study of narrow band imaging for dysplasia detection in Barrett's Esophagus. *Gastroenterology* **135**: 24-31

Wongsurawat VJ, Finley JC, Galipeau PC, Sanchez CA, Maley CC, Li X, Blount PL, Odze RD, Rabinovitch PS, Reid BJ (2006) Genetic mechanisms of TP53 loss of

heterozygosity in Barrett's esophagus: implications for biomarker validation. *Cancer Epidemiol Biomarkers Prev* **15**: 509-516

Wright TA, Gray MR, Morris AI, Gilmore IT, Ellis A, Smart HL, Myskow M, Nash J, Donnelly RJ, Kingsnorth AN (1996) Cost effectiveness of detecting Barrett's cancer. *Gut* **39**: 574-579

Yang YX, Lewis JD, Epstein S, Metz DC (2006) Long-term proton pump inhibitor therapy and risk of hip fracture. *JAMA* **296**: 2947-2953

Yogesan K, Jorgensen T, Albregtsen F, Tveter KJ, Danielsen HE (1996) Entropy-based texture analysis of chromatin structure in advanced prostate cancer. *Cytometry* **24**: 268-276

Yoshinaga S, Gotoda T, Kusano C, Oda I, Nakamura K, Takayanagi R (2008) Clinical impact of endoscopic submucosal dissection for superficial adenocarcinoma located at the esophagogastric junction. *Gastrointest Endosc* **67**: 202-209

Yousef F, Cardwell C, Cantwell MM, Galway K, Johnston BT, Murray L (2008) The incidence of esophageal cancer and high-grade dysplasia in Barrett's esophagus: a systematic review and meta-analysis. *Am J Epidemiol* **168**: 237-249

Yuki T, Amano Y, Kushiyama Y, Takahashi Y, Ose T, Moriyama I, Fukuhara H, Ishimura N, Koshino K, Furuta K, Ishihara S, Adachi K, Kinoshita Y (2006) Evaluation of modified crystal violet chromoendoscopy procedure using new mucosal pit pattern classification for detection of Barrett's dysplastic lesions. *Dig Liver Dis* **38**: 296-300

Yun SH, Tearney GJ, Vakoc BJ, Shishkov M, Oh WY, Desjardins AE, Suter MJ, Chan RC, Evans JA, Jang IK, Nishioka NS, de Boer JF, Bouma BE (2006) Comprehensive volumetric optical microscopy in vivo. *Nat Med* **12**: 1429-1433

Zhu W, Depamphilis ML (2009) Selective killing of cancer cells by suppression of geminin activity. *Cancer Res* **69**: 4870-4877

Zhu Y, Fearn T, Mackenzie G, Clark B, Dunn JM, Bigio IJ, Bown SG, Lovat LB (2009) Elastic scattering spectroscopy for detection of cancer risk in Barrett's esophagus: experimental and clinical validation of error removal by orthogonal subtraction for increasing accuracy. *J Biomed Opt* **14**: 044022

Zijlistra W, Buursma A, Van Assendelft O (2000) Visible and near infrared absorption spectra of human and animal haemoglobin: determination and application. VSP International Science Publishers, Netherlands.